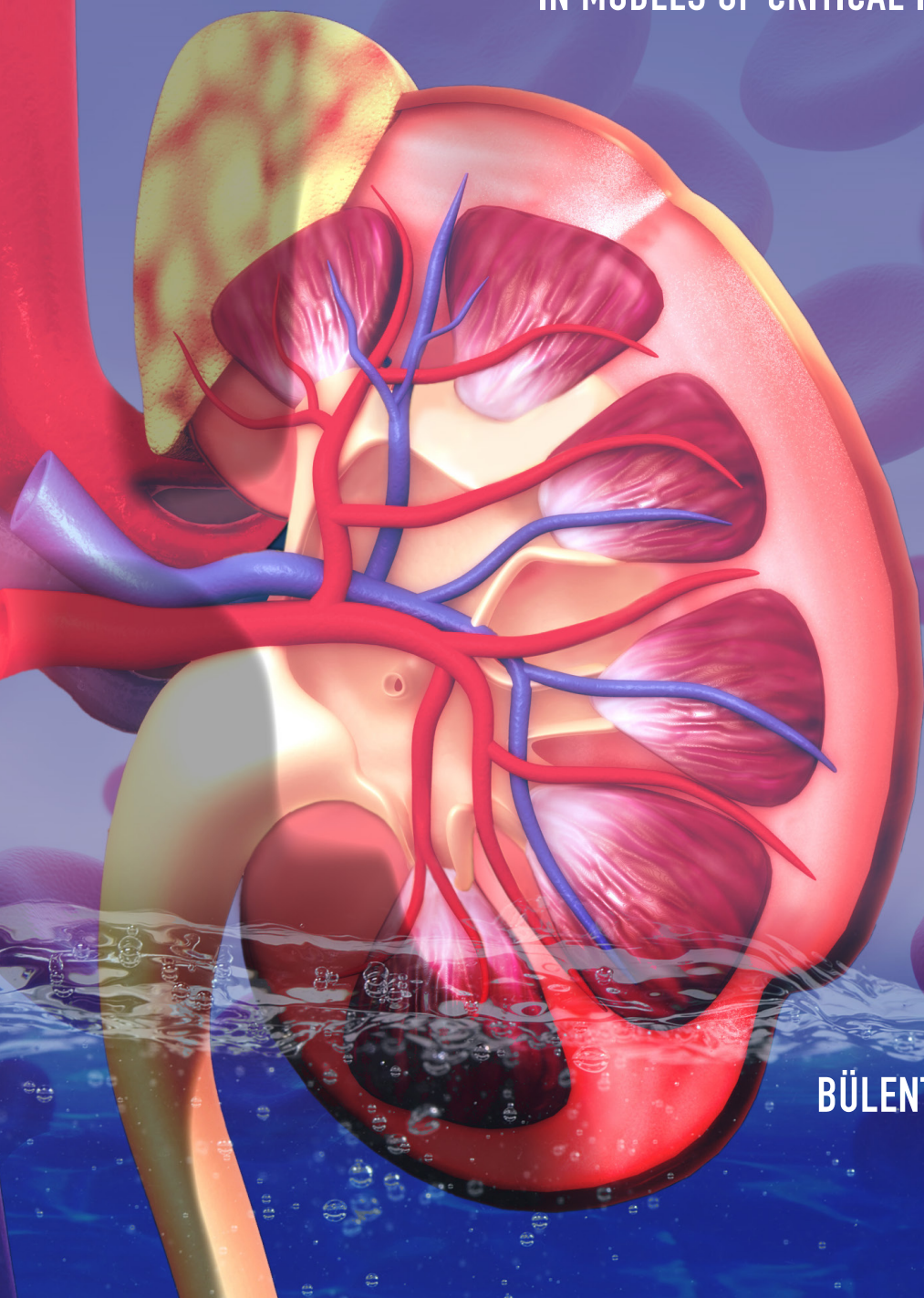


THE RENAL MICROCIRCULATION

AS A TARGET FOR THE TREATMENT OF ACUTE KIDNEY INJURY
IN MODELS OF CRITICAL ILLNESS



BÜLENT ERGİN

The Renal Microcirculation as a Target for the Treatment of Acute Kidney Injury
in Models of Critical Illness

© Bülent Ergin, 2018

ISBN: 978-94-6380-051-8

Cover and lay-out: wenz iD || Wendy Schoneveld

Printed by: ProefschriftMaken || Proefschriftmaken.nl

Financial support by Department of Intensive Care Adult, Erasmus MC; Department of Translational Physiology, Amsterdam UMC; Research Foundation Oxygen Transport to Tissue

THE RENAL MICROCIRCULATION

AS A TARGET FOR THE TREATMENT OF ACUTE KIDNEY INJURY
IN MODELS OF CRITICAL ILLNESS

DE RENALE MICROCIRCULATIE ALS DOELWIT VOOR DE BEHANDELING
VAN ACUTE NIERSCHADE BIJ MODELLEN VAN KRITISCHE ZIEKTEN

Proefschrift

ter verkrijging van de graad van doctor aan de
Erasmus Universiteit Rotterdam
op gezag van de
rector magnificus

Prof.dr. R.C.M.E. Engels
en volgens besluit van het College voor Promoties.
De openbare verdediging zal plaatsvinden op

donderdag 20 december 2018 om 9:30 uur

door

Bülent Ergin
geboren te Istanbul, Turkije

PROMOTIECOMMISSIE

Promotor(en): Prof.dr. D.A.M.P.J. Gommers
Prof.dr. C. Ince

Overige leden: Prof.dr. R.J. Stolker
Prof.dr. D. Tibboel
Dr. D. Merkus

Copromotor: Dr. C.J. Zuurbier

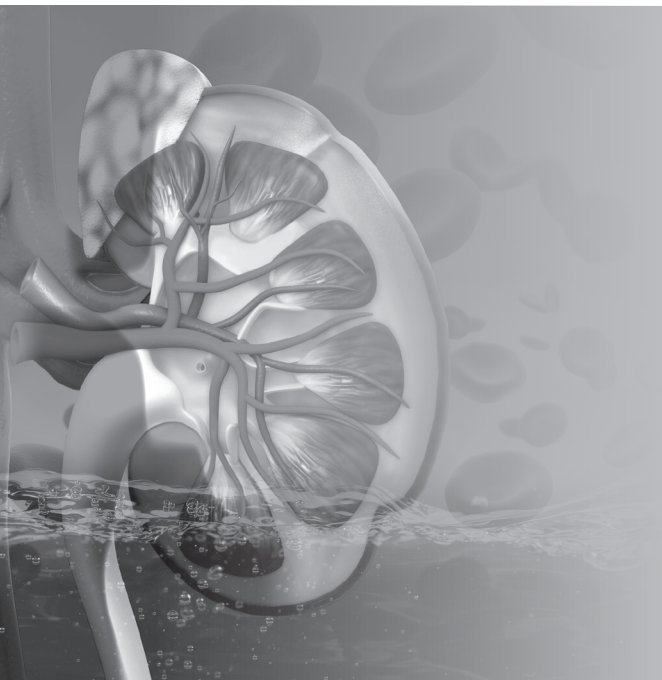
TABLE OF CONTENTS

CHAPTER 1	Introduction and outline of the thesis	9
CHAPTER 2	The renal microcirculation in sepsis	15
CHAPTER 3	Ascorbic acid improves renal microcirculatory oxygenation in a rat model of renal I/R injury	35
CHAPTER 4	TEMPOL has limited protective effects on renal oxygenation and hemodynamics but reduces kidney damage and inflammation in a rat model of renal ischemia/reperfusion by aortic clamping	53
CHAPTER 5	Mycophenolate mofetil improves renal hemodynamics, renal microvascular oxygenation, and inflammation in a rat model of renal ischemia reperfusion injury	79
CHAPTER 6	Divergent effects of hypertonic fluid resuscitation on renal pathophysiological and structural parameters in a rat model of lower body ischemia/reperfusion-induced sterile inflammation	99
CHAPTER 7	Fully Balanced Fluids do not Improve Microvascular Oxygenation, Acidosis and Renal Function in a Rat Model of Endotoxemia	121
CHAPTER 8	Human recombinant alkaline phosphatase modulates renal inflammation and injury in two rat models of acute kidney injury	143
CHAPTER 9	Effects of supplementing resuscitation fluids with N-acetylcysteine (NAC) on renal microcirculatory oxygenation, inflammation, and function in a rat model of septic shock	165
CHAPTER 10	Blood transfusion improves renal oxygenation and renal outcome in sepsis induced acute kidney injury in rats	187
CHAPTER 11	The role of bicarbonate precursors in balanced fluids during hemorrhagic shock with and without compromised liver function	207

CHAPTER 12	The effect of anemia on intra-renal microcirculation in a pig model of acute normovolemic hemodilution	229
CHAPTER 13	General discussion and future directions	251
CHAPTER 14	Summary and conclusion	257
CHAPTER 15	Samenvatting en conclusie	263

APPENDICES

Dankwoord	270
List of publications and presentations	271
PhD portfolio	277
Curriculum vitae	279



CHAPTER 1

Introduction and outline of the thesis

INTRODUCTION

Acute kidney injury (AKI) is a major problem that accompanies several clinical conditions, such as sepsis, supra-aortic ischemia/reperfusion and hemorrhage (1,2,3). Despite practical and technical advances, the mortality and morbidity rates among patients with AKI remain unacceptably high. Additionally, microcirculation plays a unique role in cell survival and the maintenance of organ function, providing adequate oxygen, nutrients, hormones, vasoactive agents, electrolytes and immune cells to tissues while removing the waste products of cells, such as ammonia, CO₂ and bilirubin. Macrocirculation is thought to be a main determinate in the effectiveness of microcirculation. However, increasing evidence has shown that microcirculation involves different mechanisms. These microcirculation mechanisms regulate the efficiency of blood supply in tissues by altering the diameter or number of vessels in microcirculatory regions; they also regulate the heterogeneity of oxygen distribution and blood flow by modulating adhesion molecule expression or local inflammation based on the oxygen demand of the tissue or organ. The etiologies of AKI are complex (4) and involve both the morphological and physiological complexity of the kidney and the impact of underlying diseases. Maintenance of adequate organ function requires an adequate supply and effective utilization of oxygen at the microcirculatory and cellular level. In addition to the complex architecture of the renal microvasculature and tubular system, the functional workload leads to a high energy demand in the kidney; therefore, the kidney is vulnerable to ischemic or hyper-hypoxemic injury. Under steady-state conditions, the oxygen (O₂) supply to renal tissues is well regulated; however, under pathological conditions, the delicate balance of oxygen supply versus demand is disturbed due to renal microvascular dysfunction. Hypovolemia, systemic hypotension, ischemia/reperfusion (I/R), anemia, cardiac dysfunction and tissue edema can also impair renal microcirculatory function and oxygenation.

Ischemia/reperfusion is a condition that is associated with sterile inflammation. Clinical aortic cross clamping-induced I/R injury is not limited to only the lower body; damages can also occur in remote organs and tissues, such as the lung, kidney, heart, and liver (5,6), after reperfusion. After removal of the aortic clamp, hyperoxemia leads to the generation of oxygen-derived free radicals, release of systemic vasoconstrictors, and activation of neutrophils (7). Reactive oxygen species (ROS) can damage proteins, lipids, mitochondria, and DNA (8,9). In addition, ROS causes endothelial cell injury and local inflammation, which lead to microvascular dysfunction and consequent tissue hypoxia (10-12).

In addition to systemic hypotension, hypovolemia and low systemic vascular resistance, several studies have reported that sepsis-induced AKI can also lead to renal perfusion defects, hypoxemia and imbalance between pro- and anti-inflammatory cytokines (1,13). Activation of the immune cells, overproduction of reactive oxygen and nitrogen species, infiltration of predominantly mononuclear immune cells, some degree of tubular cell vacuolization, loss of brush border and polarity and apoptosis (14,15) as well as dysfunction of the intracellular junction and basal membrane with the consequent detachment of cells into the tubular lumen are also emphasized as additional pathophysiological mechanisms of AKI (16).

Hypovolemia and hypoxia may be induced by hemorrhagic shock (HS) and lead to perfusion defects as well as the possible development of systemic inflammatory response syndrome and subsequently multiple organ failure, including AKI. In patients with multiple organ failure, inflammatory cytokines and ROS are mobilized into the systemic circulation and localize to organs, causing direct local cytotoxic cellular effects (3).

As an example of an anemia model, acute normovolemic hemodilution (ANH) may cause microcirculatory disturbance associated with reduced oxygen-carrying capacity in blood, impairs tissue oxygenation and increases flow heterogeneity and subsequent tissue injury (17). It was previously reported that during ANH, the kidney might be more vulnerable to hypoxic organ damage than the heart, brain and spinal cord (18).

The aim of this thesis was to investigate the underlying mechanism associated with the alteration of renal microvascular oxygenation under different pathophysiological conditions, such as hemodilution, sepsis, I/R and hemorrhage, in conjunction with acute kidney injury. Additionally, the influences of certain microcirculatory pathways that are manipulated by the administration of fluids, blood transfusion, ROS scavenging, detoxification and immune suppression on acute kidney injury were evaluated.

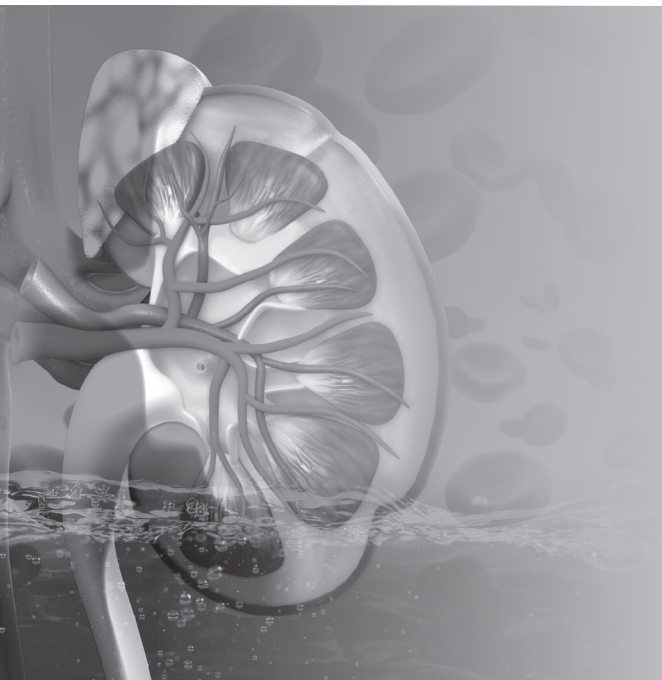
REFERENCES

1. Wan L, Bagshaw SM, Langenberg C, *et al.* Pathophysiology of septic acute kidney injury: what do we really know? *Crit. Care Med.* 36(4): S198- S203, 2008.
2. Rabb H, Wang Z, Nemoto T, *et al.* Acute renal failure leads to dysregulation of lung salt and water channels. *Kidney Int.* 63:600–606, 2003.
3. Dewar D, Moore FA, Moore EE, *et al.* Postinjury multiple organ failure. *Injury* 40:912–8, 2009.
4. Uchino S, Kellum JA, Bellomo R, *et al.* Acute renal failure in critically ill patients: a multinational, multicenter study. *JAMA* 294: 813-818, 2005.
5. Parrino PE, Laubach VE, Gaughen JR, *et al.* Inhibition of inducible nitric oxide synthase after myocardial ischemia increases coronary flow. *Ann. Thorac. Surg.* 66:733, 1998.
6. Koksels O, Ozdulger A, Aytacoglu B, *et al.* The influence of iloprost on acute lung injury induced by hind limb ischemia-reperfusion in rats. *Pulm. Pharmacol. Ther.* 18(4):235-41, 2005.
7. Grace PA. Ischemia-reperfusion injury. *Br. J. Surg.* 81:637, 1994.
8. Noiri E, Nakao A, Uchida K, *et al.* Oxidative and nitrosative stress in acute renal ischemia. *Am. J. Physiol. Renal Physiol.* 281:F948, 2001.
9. Versteilen AM, Di Maggio F, Leemreis JR, *et al.* Molecular mechanisms of acute renal failure following ischemia/reperfusion. *Int. J. Artif. Organs* 27:1019, 2004.
10. Lum H, Roebuck KA. Oxidant stress and endothelial cell dysfunction. *Am. J. Physiol. Cell Physiol.* 280:C719, 2001.
11. Bonventre JV, Weinberg JM. Recent advances in the pathophysiology of ischemic acute renal failure. *J. Am. Soc. Nephrol.* 14: 2199, 2003.
12. Legrand M, Ince C, Mik E, *et al.* Renal hypoxia and dysoxia following reperfusion of the ischemic kidney. *Mol. Med.* 14:502–516, 2008.
13. Zarjou A, Agarwal A. Sepsis and acute kidney injury. *J. Am. Soc. Nephro.* 22:999-1006, 2011.
14. Lerolle N, Nochy D, Guerot E, *et al.* Histopathology of septic shock induced acute kidney injury: apoptosis and leukocytic infiltration. *Intensive Care Med.* 36:471-8, 2010.
15. Doi K, Leelahavanichkul A, Yuen PS, *et al.* Animal models of sepsis and sepsis-induced kidney injury. *J. Clin. Invest* 119:2868-78, 2009.
16. Fink MP, Delude RL. Epithelial barrier dysfunction: a unifying theme to explain the pathogenesis of multiple organ dysfunction at the cellular level. *Crit. Care Clin* 21:177-96, 2005.
17. Koning NJ, de Lange F, Vonk ABA, *et al.* Impaired microcirculatory perfusion in a rat model of cardiopulmonary bypass: the role of hemodilution. *Am. J. Physiol. Heart Circ. Physiol.* 310:H550-558, 2016.
18. Crystal GJ. Regional tolerance to acute normovolemic hemodilution: evidence that the kidney may be at greatest risk. *J. Cardiothorac. Vasc. Anesth.* 29:320–327, 2015.

OUTLINE OF THE THESIS

The studies included in this thesis have been carried out in the Department of Translational Physiology in the Academic Medical Center of the University of Amsterdam. The Laboratory of Translational Physiology possesses special equipment that has been setup to produce a fully functional rodent intensive care unit capable of supporting different types of rodent experiments for the necessary duration of the experimental time. It is well-known that the microcirculation has a vital role in delivering oxygen, nutrients and electrolytes in tissue whilst removing waste products from cells. Therefore, all our research is focused on investigating the renal microcirculation, oxygenation and renal function in several clinically relevant models such as ischemia/reperfusion, sepsis, hemodilution and hemorrhagic shock.

This thesis is comprised of 14 Chapters: **Chapter 1** includes the introduction and outline of this thesis, **Chapter 2** introduces the structural and functional mechanisms of the renal microcirculation in both states of healthy and sepsis; **Chapter 3** demonstrates the potential effect of vitamin c on renal oxygenation and function in ischemia/reperfusion-induced Acute Kidney Injury (AKI); **Chapter 4** describes the effects of tempol as metal-independent SOD mimetic on renal oxygenation in I/R induced AKI; **Chapter 5** determines the potential role of using immunosuppressant on renal microvascular oxygenation in I/R-induced AKI; in **Chapter 6** It was tested whether or not the treatment of hypertonic saline may cause any improvement on renal oxygenation and inflammation following I/R; **Chapter 7** demonstrates insufficient effects of different fluids on microvascular oxygenation, acidosis and renal function in endotoxemic shock; **Chapter 8** shows results of human recombinant alkaline phosphatase administration on renal hemodynamics, oxygenation and inflammation in ischemia/reperfusion- and endotoxemia-induced acute kidney injury; **Chapter 9** introduced the effects of supplementing resuscitation fluids with N-acetylcysteine (NAC) on renal microcirculatory oxygenation, inflammation, and function in a rat model of septic shock; **Chapter 10** elaborates the effects of an increased blood oxygen carrying capacity by blood transfusion renal oxygenation and renal outcome in sepsis induced AKI; **Chapter 11** describes the role of bicarbonate precursors in balanced fluids during hemorrhagic shock with and without compromised liver function and **Chapter 12** sought to investigate the effect of severe hemodilution on kidney; **Chapter 13** is the discussion and future direction and **Chapter 14** contains the summary and conclusion.



CHAPTER 2

The Renal Microcirculation in Sepsis

Adapted from *Nephrol. Dial. Transplant.* 2015 Feb;30(2):169-77

Bulent Ergin ¹, Aysegul Kapucu ^{1,2}, Cihan Demirci ² and Can Ince ¹

¹ Department of Translational Physiology, Academic Medical Center, Amsterdam, The Netherlands

² Department of Biology and Zoology Division, University of Istanbul, Istanbul, Turkey

ABSTRACT

Despite the identification of several cellular mechanisms being thought to underlie the development of septic acute kidney injury (AKI), the pathophysiology of the occurrence of AKI is still ill-understood. It is clear however that instead of single mechanism being responsible for its etiology, an orchestra of cellular mechanisms failing is associated with AKI. The integrative physiological compartment where these mechanisms come together and exert their integrative deleterious action is the renal microcirculation. This is why it is opportune to review the response of the renal microcirculation to sepsis and discuss the determinants of its (dys)function and how it contributes to the pathogenesis of renal failure. A main determinant of adequate organ function is the adequate supply and utilization of oxygen at the microcirculatory and cellular level to perform organ function. The highly complex architecture of the renal microvasculature, the need to meet a high-energy demand and the fact that the kidney is borderline ischemic makes the kidney a highly vulnerable organ to hypoxemic injury. Under normal, steady state conditions, the oxygen (O_2) supply to the renal tissues is well regulated, however, under septic conditions, the delicate balance of oxygen supply versus demand is disturbed due to renal microvasculature dysfunction. This dysfunction is largely due to the interaction of renal oxygen handling, nitric oxide metabolism and radical formation. Renal tissue oxygenation is highly heterogeneous not only between the cortex and medulla but also within these renal compartments. Integrative evaluation of the different determinants of tissue oxygen in sepsis models has identified the deterioration of microcirculatory oxygenation as a key component in the development of AKI. It is becoming clear that resuscitation of the failing kidney needs to integratively correct the homeostasis between oxygen, and reactive oxygen and nitrogen species. Several experimental therapeutic modalities have been found to be effective in restoring microcirculatory oxygenation in parallel to improving renal function following septic AKI. However, these have to be verified in clinical studies. The development of clinical physiological biomarkers of AKI specifically aimed at the microcirculation should form a valuable contribution to monitoring such new therapeutic modalities.

Keywords: AKI, microcirculation, nitric oxide, oxygen radicals, oxygenation.

INTRODUCTION

Sepsis is a condition characterized by progressive systemic hemodynamic deterioration and a massive increase in inflammatory mediators and activated leukocytes, which together cause severe microcirculatory dysfunction and disrupt oxygen homeostasis, leading to oxidative stress and hypoxemia (1). One of the most frequent and serious complications for septic patients is acute kidney injury (AKI), a disorder characterized by a rapid failure of the kidneys to adequately filter the blood, regulate the ion and water balance, and generate urine (2). Although there is appropriate supportive therapy for the treatment of sepsis associated with AKI, the underlying mechanisms are poorly understood and the mortality rate remains considerably high. Recently, a multinational prospective observational study including 29,269 critically ill patients revealed that the most frequent contributing factor to AKI was sepsis (50%) (3). Other reports have shown that between 45% and 70% of all AKI is associated with sepsis (4,5). Many studies have indicated that the pathogenesis of sepsis induced AKI is initiated by renal microcirculatory dysfunction (6,7).

There are two specialized microcirculatory structures in the kidney, the glomerulus and peritubular microcirculatory networks located in the renal cortex and renal medulla, which play a key role in the homeostasis of the hemodynamic regulation and function of the kidney. Several different pathophysiological mechanisms have been proposed for sepsis-induced AKI, such as vasodilatation-induced glomerular hypoperfusion, dysregulation of the circulation within the peritubular capillary network, inflammatory reactions by systemic cytokines or local cytokine production (8), and tubular dysfunction by oxidative stress (9). These effects on the cellular functions affect the renal microcirculation (MC) and impair the main function of the renal MC of transporting oxygen to the respiring renal cells.

The oxygen requirement of the kidney is mainly determined by the ATP production needed for the Na/K pump function (10). Microcirculatory dysfunction can severely limit the ability of the circulation to provide adequate oxygen for fuelling oxidative phosphorylation for the production of ATP and can directly impair the function of the Na/K ATPase pump. However, inflammation and oxidative stress can also severely alter the delicate balance between the oxygen supply and consumption in the kidney (11,12). In addition, a disturbance in the homeostasis between reactive oxygen species (ROS), nitric oxide (NO) and renal oxygenation fuelled by renal inflammation may contribute to kidney dysfunction and lead to renal failure (6). Many other studies on renal injury have also reported that the common pathway to renal failure includes microcirculatory failure (13). The success of microcirculatory function involves the successful interaction of many cellular and subcellular systems matched to the needs for renal function.

Septic insults have been shown to influence almost all the cellular and subcellular compartments needed to achieve adequate renal microcirculatory function for renal function. Different pathogenic factors are associated with sepsis, which can result in renal dysfunction. In this paper, we review the renal microcirculation and its response to sepsis as well as potential therapeutic strategies that may protect vulnerable renal microcirculation in sepsis.

The Pathophysiology of Sepsis

Sepsis is characterized by a number of circulatory disorders, including decreased systemic vascular resistance, hypotension, impaired oxygen utilization, lactic acidosis, and misdistribution of blood flow in microcirculation (14-16). Importantly, sepsis is commonly caused by stimulating the host immune system cells and leads to the production of many types of important mediators such as cytokines, eicosanoids, complement and coagulation components, kinins, platelet activating factor, NO, and oxygen radicals that can have profound effects on the vascular tone and permeability, resulting in microcirculatory disturbances, cell damage, shock and organ dysfunction (17,18). Furthermore, endothelial \ platelet-derived ROS enhance platelet activation and adhesion and promote coagulation during inflammation (19). Another important aspect of sepsis is the alteration of the procoagulant-anticoagulant balance (20), stimulating endothelial cells to up-regulate tissue factor and activating coagulation factors such as fibrin, which leads to the formation of microvascular thrombi. These effects might contribute to the renal microcirculatory injury.

Numerous studies have shown that sepsis attenuates the arteriolar diameter response to vasoconstrictors (21-23) and vasodilators (24,25). In the case of the sepsis, the pooling of the blood in the venous system also promote capillary leak, which can lead to the progression of tissue edema and compromise the tissue oxygenation and microvascular barrier caused by inflammatory and oxidative insult associated with sepsis.

Several studies have indicated that inflammatory mediators also alter the barrier function of the microcirculation, including junctions between cells and possibly the endothelial glycocalyx, leading to tissue edema and further oxygen extraction deficiency (26,27). Endothelial glycocalyx components such as Syndecan-1 and glycosaminoglycans levels also increase in septic shock patients. The increase of these components in the blood has been found to correlate with albuminuria and mortality (28). The best-described effects of endothelial glycocalyx degradation have included increased vascular permeability, interstitial edema formation, increased rolling and adhesion of leucocytes and increased platelet adhesion (29). Red blood cells (RBC) also play an important role in the regulation of microcirculatory blood flow by their ability to release NO in the presence of hypoxia

and, thus, cause vasodilatation (30,31). Studies had shown evidence that RBC's become less deformable and aggregate during sepsis (32,33) promoting microcirculatory dysfunction.

These described sequel of events lead to massive microcirculatory collapse, which specifically influences the renal function, whereby the physiological vascular mechanism responsible for the vasotone regulation necessary for meeting oxygen needs is no longer functional and microcirculatory patency becomes impaired.

Renal Microvascular Structures

The functional morphology of the microcirculatory networks in the different organs systems is highly heterogeneous, having adapted itself the metabolic demand and function of each organ type (34) as illustrated in Fig 1. In the kidney, the renal artery branches continue to the inter-lobar artery, arcuate artery and interlobular artery, which supply blood to the afferent artery. A unique arteriolar capillary network in the present glomerulus is fed by the afferent arteriole in both the cortex and medulla. The nephron, consisting of the glomerulus, Bowman capsules and tubules, maintains the excretion, reabsorption and secretion functions of the kidney. In addition to the glomerular arteriolar structure, the renal cortex has a peri-tubular capillary network arising from efferent arterioles surrounding the proximal and distal convoluted tubules to maintain large reabsorption of glomerular filtrate. In contrast, the vasa recta is located specifically in the medulla and is fed by efferent arterioles and peri-glomerular shunt pathways located at juxta-medullary glomeruli follows to the loops of Henle' and collecting ducts deep into the medulla. The parallel arrangement of descending vasa recta (DVR) and ascending vasa recta (AVR) with descending (DL) and ascending limbs (AL) gives rise to a counter-current exchange system that maintains the cortico-medullary osmotic gradient established from counter-current multiplication by the loops of Henle crucial for concentrating the urine (35-37) while maintaining adequate oxygen and nutrient delivery as well as metabolic clearance (38). Moreover, this parallel arrangement has a key role in regulating regional perfusion between the outer versus inner medulla (35). Contraction of the DVR results in the redirection of blood to the outer medullary inter-bundle capillaries (36) (Figure 1). A consequence of this structural arrangement is that there is a low oxygen tension in the medulla with medullary partial pressure of oxygen between 30 and 40 mmHg compared of the 40-60 mmHg in the cortex (39). Renal blood flow is also regionally specific, and tightly regulated by tubuloglomerular feedback mechanism in the cortex. Although only a small fraction (~10%) of the total renal blood flow enters the renal medulla, the regulation of medullar flow is important because renal blood flow seems to play a key role in the regulation of tubular function, sodium excretion, fluid volume control, and ultimately blood pressure regulation (40) which is locally

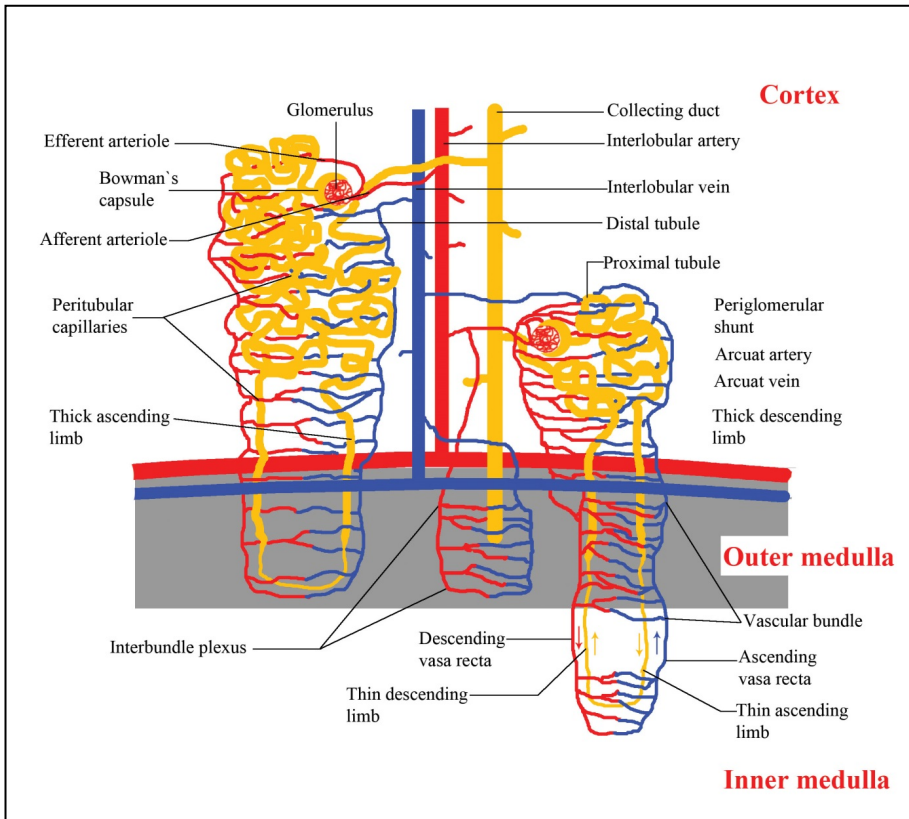


Figure 1. Renal tubules and its microvascular organization in kidney (Not shown are lateral microvascular connections where post glomerular arterioles can also supply neighboring nephrons).

adjusted by renin secretion from juxtaglomerular cells (Figure 2). Proper reabsorption of water and electrolytes is dependent on optimal blood flow through specific regions of the kidney. Consequently, blood flow is regulated differently in the cortex and medulla (41). Additionally, the afferent and efferent arteriole tone is regulated by complex interactions between vasodilators such as nitric oxide (NO) and prostaglandin E2 (PGE2) and vasoconstrictors such as endothelin, angiotensin II, and adenosine (42-45). Importantly, the altered tonicity of both afferent and efferent arterioles including the vasa recta can directly affect both the renal function and distribution of oxygen transport in the kidney (Figure 1).

Renal Histopathology and Ultrastructural Changes in Sepsis

Histopathological studies have shown that sepsis or septic shock can lead to ischemic necrosis of tubular cells (46) or acute tubular necrosis (ATN) in the renal cortex and

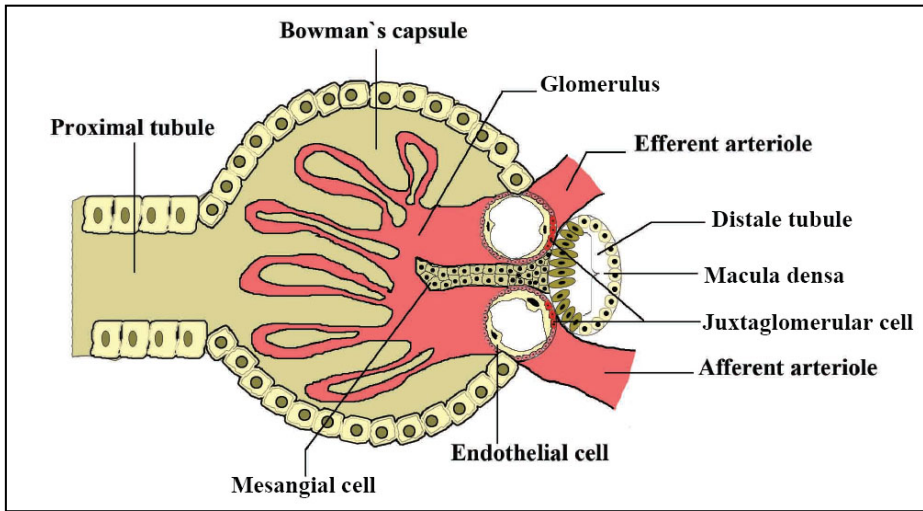


Figure 2. Structure of the renal corpuscle consisting of the afferent, efferent arterioles and distal tubule.

medulla (47) because of hypoxia and the overproduction of reactive oxygen and nitrogen species and cytokines (6,12). The consequences of ATN can be tubular obstruction and back-leak of the ultra-filtrate proximal from the obstruction by an increase in the intra-tubular pressure and loss of part of the anatomical barrier between the tubular lumen and the post-glomerular efferent capillaries surrounding the tubules (48). Other studies have described that the alterations of sepsis-induced AKI consist of the predominantly mononuclear immune cell infiltration, some degree of tubular cell vacuolization, loss of brush border and polarity, apoptosis (47,49), and dysfunction of the intracellular junction and basal membrane with the consequent detachment of cells into the tubular lumen (50). Additionally, LPS and cytokines also increase the expression of P-selectin at the endothelial cell surface and initiate platelet adhesion in sepsis (51). Thus, platelet activation, aggregation, and platelet-endothelial adhesion in sepsis could contribute to microthrombi formation and cause plugging of the capillaries.

Under normal conditions, the blood plasma is filtered from the capillaries of the glomerulus into the Bowman capsule's lumen and vascular permeability is regulated by glomerular hydrostatic pressure, oncotic pressure and the glomerular filtration barrier (GFB). The latter consists of fenestrated glomerular endothelial cells, podocytes and the glomerular basement membrane. GFB is selectively permeable, allowing the passage of water and small solutes but not the passage of macromolecules such as albumin. The permselectivity of GFB is achieved by the contribution of the glycocalyx (52). The microvascular endothelium is covered by a glycocalyx layer, which consists of

proteoglycans (syndecan and glypican), negatively charged glycosaminoglycans (hyaluronan, heparan sulphate and chondroitin sulphate) and soluble constituents. Under normal physiological conditions, the endothelial glycocalyx plays an active role in maintaining vascular homeostasis by inducing endothelial cells to synthesize shear-induced NO and preventing the adhesion of platelets and leukocytes as well as regulating vascular permeability and tone (53). Adembri *et al.* reported that sepsis is also associated with a significant alteration in the composition of the GFB associated glycocalyx. The authors observed a decrease in the expression of syndecan-I, the hyaluronan content and the total amount of sialic acid in the kidney tissue; they also observed an increase in the plasma TNF- α levels and urinary albumin level with loss of GFB permselectivity in an experimental rat model of polymicrobial sepsis (52).

Consequently, all these physiological and structural changes contribute to renal microvascular deterioration and dysfunction in sepsis-induced AKI. It is clear that the physiological function of the kidney relies on a delicate balance between oxygen transport and utilization, reactive oxygen and nitrogen metabolism and that this balance results in effective renal microcirculation that is essential for renal function (Figure 3)(6).

Impaired Renal Microvascular Perfusion during Sepsis

Microcirculatory dysfunction in sepsis is characterized by heterogeneous abnormalities in renal blood flow (RBF) in which some capillaries are under-perfused, while others have normal or abnormally high blood flow (11,54,55). Langenberg and co-workers had shown that hyperdynamic sepsis may cause an increase of renal blood flow in a sheep model of sepsis and have suggested (56), in contrast to the general belief (8,13), that renal ischemia may not play a central role in sepsis induced-AKI (57). However, in a rat model of sepsis induced-AKI with maintained constant renal arterial blood flow, we identified using speckle imaging of the cortex, microcirculatory perfusion alterations. We then showed that the origin of the ischemic component of AKI was indeed located at the cortex microcirculatory level. Chojvka and co-workers in a porcine model of septic AKI using micro-laser probe showed similar results (58). The ischemic component is not found in global renal arterial blood flow but rather in a defect in the distribution of renal cortex microcirculation with patchy areas of micro-ischemia (11). Indeed, these heterogeneous conditions can occur during the septic shock but also can be the result of therapy such as the administration of fluids. Additionally, Faivre and co-workers showed that whereas arginine vasopressin consistently reduced renal medullary blood flow with or without pretreatment with levosimendan as a calcium sensitizing agent and saline, neither arginine vasopressin or norepinephrine changed cortical renal blood flow after pretreatment with levosimendan and saline challenge in septic rabbits (59). Thus, although fluid resuscitation can normalize the renal arterial flow, it can cause

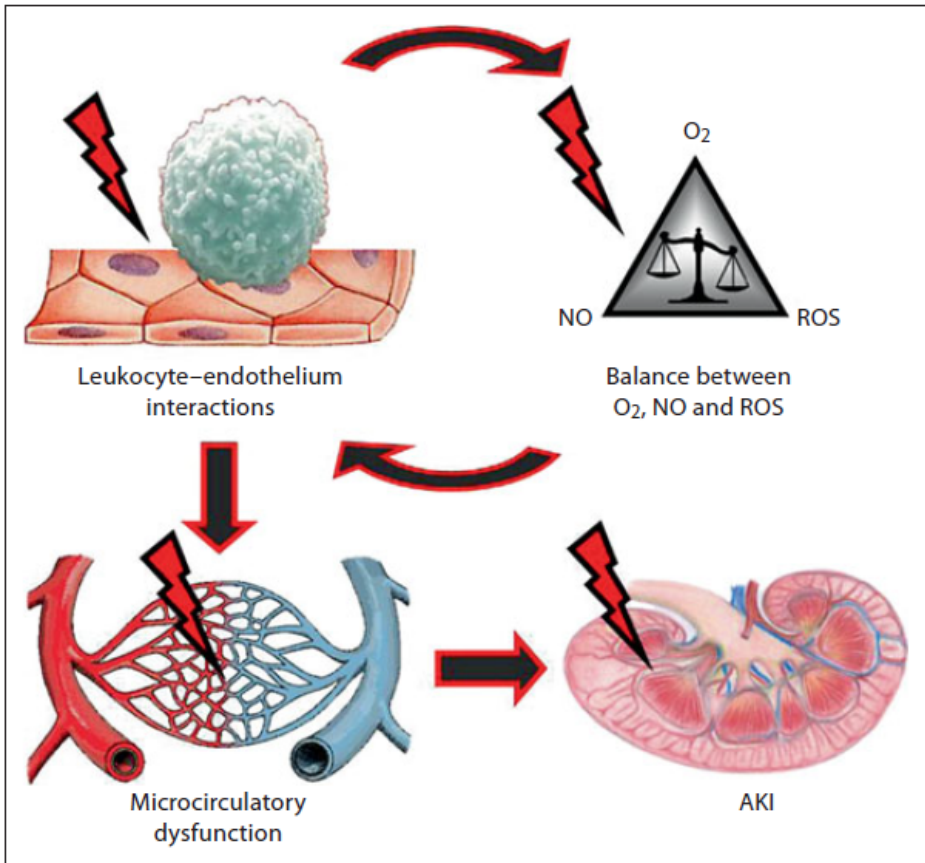


Figure 3. The toxic triangle of oxygen, nitric oxide and reactive oxygen species. An integrated hypothesis of the pathogenesis of AKI. Inflammation-induced leukocyte-endothelium interactions lead to a distortion of the homeostatic balance between O_2 , NO and ROS. It is hypothesized that, taken together, the imbalances in these factors fuel microcirculatory dysfunction, which leads to AKI and, ultimately, renal failure. Reproduced by permission from reference 6.

heterogeneous microcirculatory flow in the renal cortex, resulting in heterogeneous hypoxic areas that contribute to renal oxygen extraction dysfunction (11).

Impaired Renal Microvascular Oxygenation During Sepsis

Fluid administration can contribute to renal dysfunction by reducing the renal microcirculatory oxygenation causing an imbalance between the renal oxygen consumption and sodium reabsorption, which is indicative of a loss of tubular polarity (60). These insights have been gained by our introduction of the non-invasive quenching of palladium (Pd) porphyrin phosphorescence technique. This technique allows *in vivo*

quantitative measurement of microcirculatory oxygen pressure in rat kidneys (61,62). The heterogeneous nature of oxygen pressure distribution, measured in the cortex and medulla, as well as the noninvasive assessment of oxygen levels in the renal vein to determine renal O_2 consumption (VO_2) allowing the calculation of the important functional parameter of the kidney mainly oxygen consumption per tubular Na^+ reabsorption (VO_2/TNa^+) were studied with this technique (63-65).

Johannes *et al.* showed in an endotoxemia model that the rat cortex microcirculatory μPO_2 was preserved despite endotoxemia causing hypotension and a drop in renal arterial flow. Interestingly, fluid resuscitation in this model resulted in a correction of blood pressure and the restoration of renal blood flow, but paradoxically at the expense of decrease in cortex μPO_2 (61). Recently, Leong *et al.* determined that RBF could be reduced or increased by $\sim 30\%$ without detectable changes in tissue PO_2 in the cortex or medulla under normoxic, hypoxic, and hyperoxic conditions. Changes in RBF induced by renal arterial infusion of angiotensin II (ang II) and acetylcholine were accompanied by changes in renal O_2 delivery and efflux but not in renal O_2 consumption. Thus, arterial-to-venous (AV) shunting may be a contributor factor in the regulation of renal oxygenation and bioavailability of microcirculation (66). Moreover, Johannes *et al.* found that renal cortical tissue PO_2 fell during normovolemic hemodilution to a much greater extent than the PO_2 of renal venous blood. The authors reasoned that the increased “gap” between the tissue and venous PO_2 during hemodilution indicated increased arterial-to-venous (AV) oxygen shunting (62). Evans *et al.* suggested that AV shunting is an adaptation to prevent hyperoxia and the overproduction of ROS due to the high renal perfusion needed to sustain GFR (67). Nonetheless, a decrease in renal blood flow either at the renal arterial level and/or at the microcirculatory level in the kidney cortex can be regarded as central to the pathogenesis of septic AKI.

The highly complex structure of the renal microvasculature, its high-energy demand and borderline hypoxemic nature of renal medulla make the kidney highly vulnerable to injury, and adequate microcirculatory oxygenation is important (68). Under normal conditions, approximately 80% of renal oxygen consumption (VO_2) is used to drive Na/K ATPase in the proximal tubules, which is responsible for Na reabsorption. Approximately two-thirds of NaCl is reabsorbed by the proximal tubule as a result glomerular filtration (GFR) (69). Thus, renal oxygen consumption is dominated by the requirements of Na/K ATPase, which, in turn, drives most active and passive reabsorptive processes in the kidney (10). Na/K ATPase leads not only the active transport of sodium but also the dependent transport processes of glucose, amino acids, and other solutes (69). The loss of tubular polarity associated with sepsis-induced AKI can result in an increase VO_2/TNa^+ with Na/K pump being ineffective in achieving Na^+ reabsorption (13). The

heterogeneous nature of microcirculatory oxygenation and hypoxia may then result in an inactivation of the Na/K ATPase pump due to reduced ATP levels.

The medullary thick ascending limb (mTAL) has higher Na/K ATPase activity than the proximal tubules, and the metabolic energy is mostly used by TAL in addition to the proximal tubules and is further increased in the distal tubule (60). Increased Na⁺ transport in the TAL without an increase in oxygen delivery through the vasa recta can exacerbate medullary hypoxia. Brezis *et al.* clearly demonstrated that inhibition of Na⁺ transport in the TAL and proximal tubule by diuretics elevates PO₂ in the renal medulla and cortex (70). Apparently, there is a positive correlation between renal oxygen consumption (VO₂), oxygen delivery (DO₂), tubular sodium reabsorption and GFR.

Impact of Renin Angiotensin Aldosterone System on Renal Microcirculation

Activation of the renin-angiotensin-aldosterone system (RAAS) with elevated levels of angiotensin II (Ang II) and a rise in vasopressin levels is often part of host response (71). Even if these mechanisms are largely responsible for the systemic vasoconstriction and hyperdynamic circulation, the local production of Ang II also takes place in the kidneys (72), which leads to a reduction in the GFR because of the vasoconstriction of the glomerular afferent and efferent arterioles. Thus, RAAS activation gives rise to a greater increase in the vascular resistance and the transglomerular hydraulic pressure (73). Importantly, Patzak *et al.* have shown the relationship between angiotensin II and NO in which intraluminal perfusion of angiotensin II decreased dose dependence in isolated afferent arteriolar diameters and simultaneously enhanced nitric oxide fluorescence in mice (74). Additionally, low doses of aldosterone induces both afferent and especially efferent arteriolar constriction (75), elevating the glomerular capillary pressure and renal vascular resistance (RVR) contributing to glomerular dysfunction and glomerular structural damage in renal diseases (76).

The afferent and efferent arteriolar vasoconstriction induced by RAAS causes regional microischemia resulting in reduced cortical μPO_2 , medullary μPO_2 and oxygen delivery (DO₂) in the kidney. This condition might be an important contributing factor to AV shunting (12).

Effects of Reactive Oxygen and Nitrogen Species on the Renal Microcirculation in Sepsis

NO is a major regulator of the microvascular oxygen supply and VO₂ and increases the RBF via vasodilation, which in turn increases the oxygen delivery. Non-specific NO synthase (NOS) blockade reduces the GFR and TNa⁺ and enhances the renal VO₂ in dogs (77). In contrast to many other organs, inducible nitric oxide synthase (iNOS) is

constitutively expressed in both mouse and human renal tubule cells (78,79) and contributes to subsequent renal hemodynamic changes and reduction in the GFR during the first stage of sepsis-induced AKI. However, the overexpression of iNOS and excessive production of nitrogen species can induce nitrosative stress, resulting in pathological shunting of flow (80,81), arteriolar responsiveness (22), impairment of capillary blood flow (82) and cell function during sepsis. However, constitutive NOS isoforms are susceptible to inhibition by elevated levels of NO. For this reason, some studies have suggested that an elevated value of iNOS might actually inhibit endothelial NOS (eNOS) activity, which results in impaired microvascular homeostasis and renal function in sepsis (83,84). Recently, Langenberg and co-workers demonstrated that production of all NOS isoforms are increased during sepsis in the renal cortex but not in the renal medulla. Thus, they hypothesized that overexpression of the NOS isoforms in cortex may lead to intrarenal shunting. Indeed, blood is carried away from the medulla and induces medullar hypoxia during sepsis (85). We demonstrated the elevated NOS isoforms in a rat model of sepsis induced-AKI as well (86,87). Thus, excessive NO produced by cells can besides causing nitrosative damage inhibit mitochondrial respiration by competing with oxygen for binding mitochondrial cytochrome oxidase in a dose-dependent manner (88). NO reacts immediately with elevated levels of superoxide ions and can generate peroxynitrite radicals. Peroxynitrite is a powerful oxidant, capable of oxidizing thiol groups and DNA bases and modifying protein and lipids by nitration. As a result, peroxynitrite leads to direct inhibition of the mitochondrial respiratory chain enzyme, DNA damage, inhibition of membrane Na/K-ATPase activity, and activation of apoptotic enzymes (89). Interestingly, Lowes and co-workers demonstrated that treatments with antioxidants in order to preserve mitochondrial function and structure, such as MitoQ, MitoE and melatonin are able to reduce mitochondrial damage, organ dysfunction and attenuate inflammatory responses in a rat model of sepsis (90).

Oxidative stress is an imbalance between oxidants and antioxidants that favors oxidants and causes a disruption in redox signaling and control, leading to damage of the cellular molecular structures (67,91). Under normal circumstances, ROS are released at low concentrations and are neutralized by endogenous antioxidant compounds. Both high and low levels of oxygen tension however promote oxidative stress, making it necessary to keep the levels of tissue oxygen tensions at physiological levels to avoid the detrimental effects of oxidative stress (89). The dependency of ROS activity on oxygen availability was recently demonstrated in a model of oxidative stress in spontaneously hypertensive rats wherein a loss of bioactive NO by high ROS production interfered with normal oxygen usage in the kidney. In addition, superoxide produced by NADPH oxidase is inhibited when oxygen tensions drop below 20 mm Hg (92).

Consequently, the close relationship between the NO and ROS, the inhibition of membrane Na/K ATPase by peroxynitrite, mitochondrial damage and shunting seem to play a critical role on the microcirculatory process by reducing the oxygen consumption and delivery as well as tubular sodium reabsorption in the septic kidney.

Therapeutic Approaches

AKI develops within the first 24 hours in 64% of patients with sepsis with hypotension (93). Protecting the kidney during sepsis could significantly reduce morbidity and mortality in patients with severe sepsis. Treatment of sepsis and especially sepsis-induced AKI has advanced little in recent decades (94). Our working hypothesis states that in order for a microcirculatory therapy to be effective in protecting the kidney from AKI, an integrative therapeutic improvement of all the factors shown in Figure 3 would need to be targeted including an antiinflammatory agent in combination with effects for restoring the homeostasis between oxygen and oxygen and nitrogen reactive species (6). Fluid resuscitation is a cornerstone of the treatment of sepsis because it is considered crucial for the preservation of adequate intravascular volume, the maintenance of blood pressure with the ultimate aim of promoting tissue perfusion and oxygenation (95). However, the extent to which fluid therapy is effective in promoting renal oxygenation has recently been questioned (96,97). The limited effects of fluids in this respect are caused not only by the poor oxygen solubility in fluids but also the hemodilution it causes which reduces renal capillary density due to reduced viscosity (98). Fluid resuscitation can have severe deleterious effects on microcirculation (61) and hemodilution may contribute to AKI (99). In sepsis excessive fluid administration has been found associated with renal failure (100), although restrictions in fluid use can on the other hand lead to hypovolemia, which equally can contribute to renal failure. Therefore, determining the optimal fluid volume to administer during sepsis to treat hypovolemia remains a source of uncertainty.

Recently, Legrand *et al.* have shown that endotoxemia could induce alterations in the microvascular perfusion distribution and reduce oxygenation in the renal cortex in rats, and these alterations appear to be weakly dependent on systemic and renal macrohemodynamics. Importantly, prevention of endotoxemia-induced hypotension and reduction of RBF by immediate colloidal fluid resuscitation did not prevent systemic inflammation activation but did reduce renal inflammation such as the iNOS level in the kidney (11). Other studies showed that treatment with low-dose dexamethasone (DEX) having iNOS inhibitory and anti-inflammatory properties in combination with fluid (hydroxyethyl starch, HES) resuscitation therapy significantly improved the reduced value of the systemic and renal hemodynamic and oxygenation parameters compared to standard fluid resuscitation in LPS-induced sepsis rats. Although the average microvascular oxygen levels were unaffected by treatment with DEX the

appearance of the microcirculatory hypoxic areas in the cortical oxygen histogram was reversed after treatment with DEX in parallel with improved renal function as demonstrated by restoration of the creatinine clearance and normalization of the tubular sodium reabsorption (87). Indeed in an ischemia-reperfusion model, a specific inhibitor of iNOS, L-N6-iminoethyllysine (L-NIL) was found to be effective in restoring renal oxygenation, nitrosative homeostasis and renal functional markers (86). Moreover, Choi and co-workers have shown that glucocorticoids induce a decrease in proinflammatory cytokines, apoptosis and mitochondrial damage in a cecal ligation and puncture model of sepsis (101).

Finally, compounds that have an anti-inflammatory effect in combination with vasoactive properties promoting tissue perfusion may be beneficial in correcting the various pathogenic mechanisms involved in microcirculatory dysfunction. Indeed two compounds we found to be highly effective in this respect for the septic kidney were iloprost and activated protein C both having such multiple actions (102,103).

CONCLUSION

Renal oxygen consumption usually changes in response to altered arterial pressure, RBF, GFR and sodium balance. The oxygen supply to the renal tissues is well regulated and utilized not only for the mitochondrial production of ATP to maintain the Na/K ATPase activation needed for Na-reabsorption but also for the production of nitric oxide and the reactive oxygen species needed for the physiological control of renal function. In sepsis the balance between these physiological determinants of renal function becomes disturbed mainly due to the inflammatory insult resulting in abnormal levels of these compounds, which then exert pathogenic effects, such as hypoxemia, oxidative and nitrosative stress. This sequel of events results in a deterioration of the renal microcirculation function and oxygenation leading to acute renal failure. Although there is experimental evidence for effective therapeutic procedures for prevention of sepsis induced-AKI further clinical investigations are needed. Fluid resuscitation therapy supplemented with antioxidants or other vasoactive and anti-inflammatory substances may provide an integrative therapeutic platform to prevent renal microcirculatory dysfunction and sepsis-induced AKI.

REFERENCES

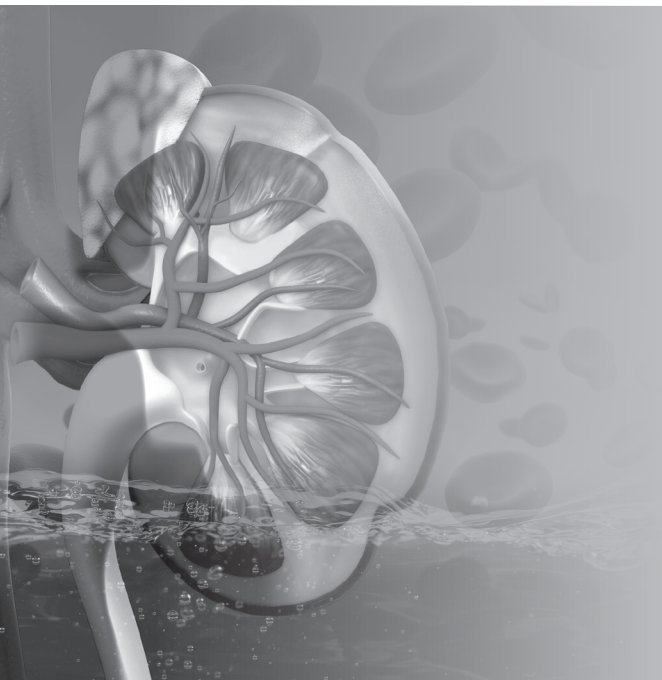
1. Wan L, Bagshaw SM, Langenberg C, *et al.* Pathophysiology of septic acute kidney injury: what do we really know? *Crit. Care Med.* 36(4):S198- S203, 2008.
2. Zarjou A, Agarwal A. Sepsis and acute kidney injury. *J. Am. Soc. Nephro.* 22:999-1006, 2011.
3. Uchino S, Kellum JA, Bellomo R, *et al.* Acute renal failure in critically ill patients: a multinational, multicenter study. *JAMA* 294:813-818, 2005.
4. Bagshaw SM, Laupland KB, Doig CJ, *et al.* Prognosis for long-term survival and renal recovery in critically ill patients with severe acute renal failure: a population-based study. *Crit. Care* 9:R700-R709, 2005.
5. Silvester W, Bellomo R, Cole L. Epidemiology, management, and outcome of severe acute renal failure of critical illness in Australia. *Crit. Care Med.* 29:1910-1915, 2001.
6. Aksu U, Demirci C, Ince C. The Pathogenesis of Acute Kidney Injury and the Toxic Triangle of Oxygen, Reactive Oxygen Species and Nitric Oxide. In: *Controversies in Acute Kidney Injury, Contrib. Nephrol. Karger Basel.* CH: 174: pp 119-128, 2011.
7. Le Dorze M, Legrand M, Payen D, *et al.* The role of the microcirculation in acute kidney injury. *Curr. Opin. Crit. Care* 15(6):503-8. 2009. Review
8. Schrier RW and Wang W. Acute renal failure and sepsis. *N. Engl. J. Med.* 351:159-169, 2004.
9. Wu L, Gokden N, Mayeux P.R. Evidence for the role of reactive nitrogen species in polymicrobial sepsis-induced renal peritubular capillary dysfunction and tubular injury. *J. Am. Soc. Nephrol.* 18:1807-1815, 2007.
10. Welch WJ. Intrarenal oxygen and hypertension. *Clin. Exp. Pharmacol. Physiol.* 33(10):1002-5. 2006. Review
11. Legrand M, Bezemer R, Kandil A, *et al.* The role of renal hypoperfusion in development of renal microcirculatory dysfunction in endotoxemic rats. *Intensive Care Med.* 37(9):1534-42, 2011.
12. Evans RG, Ince C, Joles JA, *et al.* Haemodynamic influences on kidney oxygenation: clinical implications of integrative physiology. *Clin. Exp. Pharmacol. Physiol.* 40(2):106-22, 2013.
13. Bonventre JV, Yang L. Cellular pathophysiology of ischemic acute kidney injury. *J. Clin. Invest.* 121(11):4210-21, 2011.
14. Bone RC. Gram-negative sepsis. Background, clinical features, and intervention. *Chest* 100:802-808, 1991.
15. Nguyen HB, Rivers EP, Knoblich BP, *et al.* Early lactate clearance is associated with improved outcome in severe sepsis and septic shock. *Crit. Care Med.* 32: 1637-1642, 2004.
16. Vincent JL, Martinez EO, Silva E. Evolving concepts in sepsis definitions. *Crit. Care Clin.* 25:665-675, 2009.
17. Koch T. Origin and mediators involved in sepsis and SIRS. *Kidney Int.* 53 (64):S66-S69, 1998.
18. Kamal F Badr. Novel mediators of sepsis - associated renal failure. *Seminars in Nephrology* 14 (1):3-7, 1994.
19. Levi M, van der Poll T, Buller HR. Bidirectional relation between inflammation and coagulation. *Circulation* 109:2698-2704, 2004.
20. Creasey AA, Reinhart K. Tissue factor pathway inhibitor activity in severe sepsis. *Crit. Care Med.* 29(7):S126-9, 2001.
21. Baker CH, Wilmoth FR. Microvascular responses to E. coli endotoxin with altered adrenergic activity. *Circ. Shock* 12:165-176, 1984.
22. Wu F, Wilson JX, Tyml K. Ascorbate inhibits iNOS expression and preserves vasoconstrictor responsiveness in skeletal muscle of septic mice. *Am. J. Physiol. Regul. Integr. Comp. Physiol.* 285: R50-R56, 2003.
23. Wu F, Wilson JX, Tyml K. Ascorbate protects against impaired arteriolar constriction in sepsis by inhibiting inducible nitric oxide synthase expression. *Free Radic. Biol. Med.* 37:1282-1289, 2004.
24. Baker CH, Sutton ET. Arteriolar endothelium- dependent vasodilation occurs during endotoxin shock. *Am. J. Physiol.* 264:H1118-H1123, 1993.
25. Gocan NC, Scott JA, Tyml K. Nitric oxide produced via neuronal NOS may impair vasodilatation in septic rat skeletal muscle. *Am. J. Physiol. Heart Circ. Physiol.* 278:H1480-H1489, 2000.

26. Fink MP. Intestinal epithelial hyperpermeability: update on the pathogenesis of gut mucosal barrier dysfunction in critical illness. *Curr. Opin. Crit. Care* 9:143-151, 2003.
27. Van den Berg BM, Vink H, Spaan JA. The endothelial glycocalyx protects against myocardial edema. *Circ. Res.* 92:592- 594, 2003.
28. Nelson A, Berkestedt I, Schmidtchen A, *et al.* Increased Levels of Glycosaminoglycans During Septic Shock: Relation to Mortality and the Antibacterial Actions of Plasma. *Shock* 30- 6:623-627, 2008.
29. Vlahu C A, Lemkes B A, Struijk D G, *et al.* Damage of the Endothelial Glycocalyx in Dialysis Patients. *Am. Soc. Nephrol.* 23:1900-1908, 2012.
30. Cosby K, Partovi KS, Crawford JH, *et al.* Nitrite reduction to nitric oxide by deoxyhemoglobin vasodilates the human circulation. *Nat. Med.* 9:1498-1505, 2003.
31. Singel DJ, Stamler JS. Chemical physiology of blood flow regulation by red blood cells: the role of nitric oxide and S-nitrosohemoglobin. *Annu. Rev. Physiol.* 67:99-14, 2005.
32. Siegemund M, Hardeman MR, van Bommel J, *et al.* Red blood cell deformability in two different doses of LPS in a porcine model of endotoxemia. *Intensive Care Med.* 25: S21, 1999.
33. Baskurt OK, Temiz A, Meiselman HJ. Red blood cell aggregation in experimental sepsis. *J. Lab. Clin. Med.* 130:183-190, 1997.
34. Klijn E, Den Uil CA, Bakker J, *et al.* The heterogeneity of the microcirculation in critical illness. *Clin. Chest Med.* 29(4):643-54, 2009.
35. Cowley AW Jr. Role of the renal medulla in volume and arterial pressure regulation. *Am. J. Physiol.* 273(1 Pt 2):R1-15, 1997. Review
36. Pallone TL, Silldorff EP, Turner MR. Intrarenal blood flow: microvascular anatomy and the regulation of medullary perfusion. *Clin. Exp. Pharmacol. Physiol.* 25(6):383-92, 1998. Review
37. Pallone TL, Turner MR, Edwards A, *et al.* Countercurrent exchange in the renal medulla. *Am. J. Physiol. Regul. Integr. Comp. Physiol.* 284(5):R1153-75, 2003. Review
38. Kennedy-Lydon TM, Crawford C, Wildman SS, *et al.* Renal pericytes: regulators of medullary blood flow. *Acta. Physiol. (Oxf)* 207(2):212-25, 2013. Review
39. Mik EG, van Leeuwen TG, Raat NJ, *et al.* Quantitative determination of localized tissue oxygen concentration in vivo by two-photon excitation phosphorescence lifetime measurements. *J. Appl. Physiol.* 97(5):1962-9, 2004.
40. Bergstrom G, Evans RG. Mechanisms underlying the antihypertensive functions of the renal medulla. *Acta. Physiol. Scand.* 181: 475-486, 2004.
41. Damkjaer M, Vafaee M, Moller ML, *et al.* Renal cortical and medullary blood flow responses to altered NO availability in humans. *Am. J. Physiol. Regul. Integr. Comp. Physiol.* 299:R1449-R1455, 2010.
42. Hansen PB, Schnermann J. Vasoconstrictor and vasodilator effects of adenosine in the kidney. *Am. J. Physiol. Renal Physiol.* 285:F590-F599, 2003.
43. Pallone TL, Zhang Z, Rhinehart K. Physiology of the renal medullary microcirculation. *Am. J. Physiol. Renal Physiol.* 284:F253-F266, 2003.
44. Guan Z, Osmond DA, Inscho EW. P2X receptors as regulators of the renal microvasculature. *Trends. Pharmacol. Sci.* 28:646-652, 2007.
45. Bauerle JD, Grenz A, Kim JH, *et al.* Adenosine generation and signaling during acute kidney injury. *J. Am. Soc. Nephrol.* 22:14-20, 2011.
46. Jones DB. Ultrastructure of human acute renal failure. *Lab. Invest.* 46:254-264, 1982.
47. Lerolle N, Nochy D, Guerot E, *et al.* Histopathology of septic shock induced acute kidney injury: apoptosis and leukocytic infiltration. *Intensive Care Med.* 36:471-8, 2010.
48. Myers BD, Moran SM. Hemodynamically mediated acute renal failure. *N. Engl. J. Med.* 314:97-105, 1986.
49. Doi K, Leelahavanichkul A, Yuen PS, *et al.* Animal models of sepsis and sepsis-induced kidney injury. *J. Clin. Invest.* 119:2868-78, 2009.
50. Fink MP, Delude RL. Epithelial barrier dysfunction: a unifying theme to explain the pathogenesis of multiple organ dysfunction at the cellular level. *Crit. Care Clin.* 21:177-96, 2005.
51. Lindenblatt N, Menger MD, Klar E, *et al.* Systemic hypothermia increases PAI-1 expression and accelerates microvascular thrombus formation in endotoxemic mice. *Crit. Care* 10:R148, 2006.

52. Adembri C, Sgambati E, Vitali L, *et al.* Sepsis induces albuminuria and alterations in the glomerular filtration barrier: a morphofunctional study in the rat. *Crit. Care* 15(6):R277, 2011.
53. Chappell D, Westphal M and Jacob M. The impact of the glycocalyx on microcirculatory oxygen distribution in critical illness. *Curr. Opin. Anaesthesiol.* 22:155-162, 2009.
54. Bateman RM, Sharpe MD, Ellis CG. Bench-to-bedside review: Microvascular dysfunction in sepsis – hemodynamics, oxygen transport, and nitric oxide. *Crit. Care* 7:359-373, 2003.
55. Spronk PE, Ince C, Gardien MJ, *et al.* Nitroglycerin promotes microvascular recruitment in septic shock after intravascular volume resuscitation. *Lancet* 360:1395-1396, 2002.
56. Langenberg C, Wan L, Egi M, *et al.* Renal blood flow in experimental septic acute renal failure. *Kidney Int.* 69(11):1996-2002, 2006.
57. Kellum JA. Impaired renal blood flow and the 'spicy food' hypothesis of acute kidney injury. *Crit. Care Med.* 39(4):901-3, 2011.
58. Chvojka J, Sykora R, Krouzecky A, *et al.* Renal haemodynamic, microcirculatory, metabolic and histopathological responses to peritonitis-induced septic shock in pigs. *Crit. Care* 12(6):R164, 2008.
59. Faivre V, Kaskos H, Callebort J, *et al.* Cardiac and renal effects of levosimendan, arginine vasopressin, and norepinephrine in lipopolysaccharide-treated rabbits. *Anesthesiology* 103(3):514-21, 2005.
60. Mandel LJ. Primary active sodium transport, oxygen consumption, and ATP coupling and regulation. *Kidney Int.* 29:3-9, 1986.
61. Johannes T, Mik EG, Nohé B, *et al.* Influence of fluid resuscitation on renal microvascular PO₂ in a normotensive rat model of endotoxemia. *Crit. Care* 10(3):R88, 2006.
62. Johannes T, Mik EG, Nohe B, *et al.* Acute decrease in renal microvascular PO₂ during acute normovolemic hemodilution. *Am. J. Physiol. Renal Physiol.* 292:F796-F803, 2007.
63. Johannes T, Mik EG, Ince C. Dual-wavelength phosphorimetry for determination of cortical and subcortical microvascular oxygenation in rat kidney. *J. Appl. Physiol.* 100(4):1301-10, 2006.
64. Bezemer R, Faber DJ, Almac E, *et al.* Evaluation of multi-exponential curve fitting analysis of oxygen-quenched phosphorescence decay traces for recovering microvascular oxygen tension histograms. *Med. Biol. Eng. Comput.* 48(12):1233-42, 2010.
65. Mik EG, Johannes T, Ince C. Monitoring of renal venous PO₂ and kidney oxygen consumption in rats by a near-infrared phosphorescence lifetime technique. *Am. J. Physiol.* 294(3):F676-8, 2008.
66. Leong CL, Anderson WP, O'Connor PM, *et al.* Evidence that renal arterial-venous oxygen shunting contributes to dynamic regulation of renal oxygenation. *Am. J. Physiol. Renal Physiol.* 292(6):F1726-33, 2007.
67. Evans RG, Gardiner BS, Smith DW, *et al.* Intrarenal oxygenation: Unique challenges and the biophysical basis of homeostasis. *Am. J. Physiol. Renal Physiol.* 295:F1259-70, 2008.
68. Legrand M, Klijn E, Payen D, *et al.* The response of the host microcirculation to bacterial sepsis: does the pathogen matter? *J. Mol. Med. (Berl)* 88(2):127-33, 2010. Review
69. Gullans SR, Hebert SC. Metabolic basis of ion transport. In: *Brenner and Rector's The Kidney (5th ed.)*, edited by Brenner BM. Philadelphia, PA: WB Saunders 211-246, 1996.
70. Brezis M, Agmon Y, Epstein FH. Determinants of intrarenal oxygenation. I. Effects of diuretics. *Am. J. Physiol.* 267:F1059-62, 1994.
71. Cumming AD, Driedger AA, McDonald JW, *et al.* Vasoactive hormones in the renal response to systemic sepsis. *Am. J. Kidney Dis.* 11:23-32, 1988.
72. Zhuo JL, Li XC. Novel roles of intracrine angiotensin II and signalling mechanisms in kidney cells. *J. Renin Angiotensin Aldosterone Syst.* 8:23-33, 2007.
73. Denton KM, Fennessy PA, Alcorn D, *et al.* Morphometric analysis of the actions of angiotensin II on renal arterioles and glomeruli. *Am. J. Physiol.* 262:F367-72, 1992.
74. Patzak A, Persson AE. Angiotensin II-nitric oxide interaction in the kidney. *Curr. Opin. Nephrol. Hypertens.* 16(1):46-51, 2007.
75. Arima S. Aldosterone and the kidney: rapid regulation of renal microcirculation. *Steroids* 71(4):281-5, 2006.
76. Abe K. Physiopathology and therapy of hypertension. *Nihon Naika Gakkai Zasshi* 86(9):1545-55, 1997.

77. Deng A, Miracle CM, Suarez JM, *et al.* Oxygen consumption in the kidney: effects of nitric oxide synthase isoforms and angiotensin II. *Kidney Int.* 68(2):723-30, 2005.
78. Ortiz PA, Garvin JL. Cardiovascular and renal control in NOS-deficient mouse models. *Am. J. Physiol. Regul. Integr. Comp. Physiol.* 284(3):R628-38, 2003.
79. Kone BC. Nitric oxide in renal health and disease. *Am. J. Kidney Dis.* 30(3):311-33, 1997.
80. Morin MJ, Unno N, Hodin RA, *et al.* Differential expression of inducible nitric oxide synthase messenger RNA along the longitudinal and crypt-villus axes of the intestine in endotoxemic rats. *Crit. Care Med.* 26:1258-1264, 1998.
81. Revelly JP, Ayuse T, Brienza N, *et al.* Endotoxic shock alters distribution of blood flow within the intestinal wall. *Crit. Care Med.* 24:1345-1351, 1996.
82. Bateman RM, Jagger JE, Sharpe MD, *et al.* Erythrocyte deformability is a nitric oxide-mediated factor in decreased capillary density during sepsis. *Am. J. Physiol. Heart Circ. Physiol.* 280:H2848-H2856, 2001.
83. Schwartz D, Mendonca M, Schwartz I, *et al.* Inhibition of constitutive nitric oxide synthase (NOS) by nitric oxide generated by inducible NOS after lipopolysaccharide administration provokes renal dysfunction in rats. *J. Clin. Invest.* 100(2):439-48, 1997.
84. Chauhan SD, Seggara G, Vo PA, *et al.* Protection against lipopolysaccharide-induced endothelial dysfunction in resistance and conduit vasculature of iNOS knockout mice. *FASEB J.* 17(6):773-5, 2003.
85. Langenberg C, Gobe G, Hood S, *et al.* Renal histopathology during experimental septic acute kidney injury and recovery. *Crit. Care Med.* 42(1):e58-67, 2014.
86. Legrand M, Almac E, Mik EG, *et al.* L-NIL prevents renal microvascular hypoxia and increase of renal oxygen consumption after ischemia-reperfusion in rats. *Am. J. Physiol. Renal Physiol.* 296(5):F1109-17, 2009.
87. Johannes T, Mik EG, Klingel K, *et al.* Low-dose dexamethasone-supplemented fluid resuscitation reverses endotoxin-induced acute renal failure and prevents cortical microvascular hypoxia. *Shock* 31(5):521-8, 2009.
88. Cooper CE, Giulivi C. Nitric oxide regulation of mitochondrial oxygen consumption II: molecular mechanism and tissue physiology. *Am. J. Physiol. Cell Physiol.* 292:C1993-C2003, 2007.
89. Szabó C, Módos K. Pathophysiological roles of peroxynitrite in circulatory shock. *Shock* 34(1):4-14, 2010.
90. Lowes DA, Webster NR, Murphy MP, *et al.* Antioxidants that protect mitochondria reduce interleukin-6 and oxidative stress, improve mitochondrial function, and reduce biochemical markers of organ dysfunction in a rat model of acutesepsis. *Br. J. Anaesth.* 110(3):472-80, 2013.
91. Clanton TL. Hypoxia- induced reactive oxygen species formation in skeletal muscle. *J. Appl. Physiol.* 102:2379-2388, 2007.
92. Adler S, Huang H. Oxidant stress in kidneys of spontaneously hypertensive rats involves both oxidase overexpression and loss of extracellular superoxide dismutase. *Am. J. Physiol. Renal Physiol.* 287:F907-F913, 2004.
93. Bagshaw SM, Lapinsky S, Dial S, *et al.* Acute kidney injury in septic shock: clinical outcomes and impact of duration of hypotension prior to initiation of antimicrobial therapy. *Intensive Care Med.* 35:871-881, 2009.
94. Ricci Z, Polito A, Ronco C. The implications and management of septic acute kidney injury. *Nat. Rev. Nephrol.* 7:218-225, 2011.
95. Vincent JL, Gerlach H. Fluid resuscitation in severe sepsis and septic shock: an evidence- based review. *Crit. Care Med.* 32(11):S451-S454, 2004.
96. Legrand M, Mik EG, Balestra GM, *et al.* Fluid resuscitation does not improve renal oxygenation during hemorrhagic shock in rats. *Anesthesiology* 112:119-127, 2010.
97. Aksu U, Bezemer R, Yavuz B, *et al.* Balanced vs unbalanced crystalloid resuscitation in a near-fatal model of hemorrhagic shock and the effects on renal oxygenation, oxidative stress, and inflammation. *Resuscitation* 83(6):767-73, 2012.
98. Vermeer H, Teerenstra S, de Sévaux RG, *et al.* The effect of hemodilution during normothermic cardiac surgery on renal physiology and function. *Perfusion* 23:329, 2008.

99. Habib RH, Zacharias A, Schwann TA, *et al.* Role of hemodilutional anemia and transfusion during cardiopulmonary bypass in renal injury after coronary revascularization: implications on operative outcome. *Crit. Care Med.* 33:1749-1756, 2005.
100. Payen D, de Pont AC, Sakr Y, *et al.* A positive fluid balance is associated with a worse outcome in patients with acute renal failure. *Crit. Care* 12:R74, 2008.
101. Choi HM, Jo SK, Kim SH, *et al.* Glucocorticoids attenuate septic acute kidney injury. *Biochem. Biophys. Res. Commun.* 435(4):678-84, 2013.
102. Almac E, Johannes T, Bezemer R, *et al.* Activated protein C ameliorates impaired renal microvascular oxygenation and sodium reabsorption in endotoxemic rats. *Intensive Care Med. Experimental* 1(1):24, 2013.
103. Johannes T, Ince C, Klingel K, *et al.* Iloprost preserves renal oxygenation and restores kidney function in endotoxemia-related acute renal failure in the rat. *Crit. Care Med.* 37(4):1423-32, 2009.



CHAPTER 3

The treatment of ascorbic acid improves renal microcirculatory oxygenation in a rat model of renal I/R injury

Adapted from *J. Transl. Int. Med.* 2015 Jun-Sep;3(3):116-125

Bulent Ergin¹, Coert J Zuurbier², Rick Bezemer¹, Asli Kandil³, Emre Almac⁴, Cihan Demirci³, Can Ince¹

¹ Department of Translational Physiology, Academic Medical Center, University of Amsterdam, Amsterdam, The Netherlands

² Laboratory of Experimental Anesthesiology and Intensive Care, Department of Anesthesiology, Academic Medical Center, University of Amsterdam, The Netherlands

³ Department of Biology, Faculty of Science, University of Istanbul, Istanbul, Turkey

⁴ Department of Anesthesiology, St. Antonius Hospital Nieuwegein, Nieuwegein, The Netherlands

ABSTRACT

Acute kidney injury (AKI) is a clinical condition associated with a high degree of morbidity and mortality despite supportive care, and ischemia/reperfusion injury (I/R) is one of the main causes of AKI. The pathophysiology of I/R injury is a complex cascade of events including the release of free oxygen radicals followed by damage to proteins, lipids, mitochondria and deranged tissue oxygenation. In this study, we investigated whether the antioxidant ascorbic acid would be able to largely prevent oxidative stress and consequently reduce I/R-related injury to the kidneys in terms of oxygenation, inflammation and renal failure. Rats were divided into 3 groups ($n = 6/\text{group}$): (1) a time control group; (2) a group subjected to renal ischemia for 60 min by high aortic occlusion followed by 2 h of reperfusion (I/R); and (3) a group subjected to I/R and treated with an i.v. 100 mg/kg bolus ascorbic acid 15 min before ischemia and continuous infusion of 50 mg/kg/hour for two hours during reperfusion (I/R+AA). We measured renal tissue oxidative stress, microvascular oxygenation, renal oxygen delivery and consumption, and renal expression of inflammatory and injury markers. We demonstrated that aortic clamping and release resulted in increased oxidative stress and inflammation that was associated with a significant fall in systemic and renal hemodynamics and oxygenation parameters. The treatment of ascorbic acid completely abrogated oxidative stress and inflammatory parameters. However, it only partly improved microcirculatory oxygenation and was without any effect on anuria. To conclude, the ascorbic acid treatment partly improved microcirculatory oxygenation and prevented oxidative stress without restoring urine output in a severe I/R model of AKI.

Keywords: I/R, ascorbic acid, AKI, oxygenation, oxidative stress.

INTRODUCTION

Acute kidney injury (AKI) is a critical clinical condition associated with a high degree of morbidity and mortality despite supportive care. Ischemia/reperfusion injury (I/R) is one of the main causes of AKI, which is a complex event encountered, for instance, during abdominal aortic surgery (1). Recently, an increasing body of evidence suggests that renal hypoxia contributes to the pathogenesis of AKI (2-4). It is known that most organs compensate against hypoxia through increases in blood flow or oxygen delivery (DO_2) (5). Therefore, an increased DO_2 may act to improve tissue oxygenation and so attenuates development of hypoxia and injury. The kidney has a unique system and complexity for regulation of blood flow, that is dominated by the functional requirements of extracellular fluid and electrolytes load, rather than by local metabolic needs (6). Another way to protect the organ against hypoxia is to reduce oxygen consumption (VO_2) in order to attenuate oxygen requirement. Such a strategy gives rise to decreases in tubular sodium reabsorption (5,7) and glomerular filtration rate (urine output) in kidney. Abdelkader *et al.* (2014) documented that even though I/R gave rise to reductions in $\text{VO}_{2\text{ren}}$ and $\text{DO}_{2\text{ren}}$, renal cortical and inner medullar PO_2 remained stable (8). Our earlier findings (9,10) indicated that renal $\text{DO}_{2\text{ren}}$ and $\text{VO}_{2\text{ren}}$ was reduced after removal of the aortic clamp, and correlated with depletion of the renal microcirculatory oxygenation. This decrease in oxygenation was associated with upregulation of inducible form of nitric oxide synthase (iNOS) and downregulation of endothelial form (eNOS). The relationship between $\text{DO}_{2\text{ren}}$, $\text{VO}_{2\text{ren}}$ and renal tissue PO_2 appears unclear and may vary according to different pathological condition.

The I/R injury with clinical aortic cross clamping is not limited to the lower extremities, but also causes damage to remote organs and tissues such as lungs, kidneys, heart, and liver (11,12). After the removal of aortic clamp, reperfusion leads to the generation of oxygen-derived free radicals, release of systemic vasoconstrictors, and activation of neutrophils (13). The reactive oxygen species (ROS) is able to damage proteins, lipids, mitochondria, and DNA (14,15). In addition, ROS cause endothelial cell injury and local inflammation that leads to disturbed microvascular function and consequent tissue hypoxia (16-18). The kidneys are especially sensitive to this type of injury due to their complex microvascular structure and high oxygen demand (17,19-22).

Several therapeutic agents have been examined to protect the kidneys from I/R injury, including allopurinol, superoxide dismutase, coenzyme Q, antioxidant vitamins, and n-acetylcysteine (23,24). L-ascorbic acid (vitamin C) and α -tocopherol (vitamin E) also play important roles in the endogenous antioxidant defense systems, and serum levels of these vitamins are significantly decreased in patients with ischemic heart disease (25).

In their systematic review Sadat and co-workers (2013) concluded that vitamin C provided effective nephroprotection in patients with contrast-induced acute kidney injury, suggesting that ascorbic acid may form part of an effective prophylactic pharmacological regimen (26). Based on the above it has as yet to be determined which precise mechanism manipulating oxidative stress by vitamin C affects the injured kidney and if reducing oxidative stress in this way can restore microcirculatory function in terms of oxygen transport and affect renal dysfunction following reperfusion injury. In the present study, therefore we investigated the hypothesis that using the antioxidant capacity of the ascorbic acid can also efficiently reduce I/R-induced impairment of the renal oxygenation and renal function following acute I/R in the rat kidney.

MATERIALS AND METHODS

Animals

All experiments in this study were approved by the institutional Animal Experimentation Committee of the Academic Medical Center of the University of Amsterdam (DFL 83). Care and handling of the animals were in accordance with the guidelines for Institutional and Animal Care and Use Committees. The study has been carried out in accordance with the Declaration of Helsinki. Experiments were performed on 18 *Wistar albino* rats (Harlan Netherlands BV, Horst, The Netherlands) with a mean \pm SD body weight of 325 ± 6 g.

Surgical Preparation

All animals were anesthetized with an intraperitoneal injection of a mixture of 90 mg/kg ketamine (Nimatek[®], Eurovet, Bladel, The Netherlands), 0.5 mg/kg dexmedetomidine (Dexdomitor, Pfizer Animal Health BV, Capelle aan den IJssel, The Netherlands), and 0.05 mg/kg atropine-sulfate (Centrafarm Pharmaceuticals BV, Etten-Leur, The Netherlands) (27). After preparing a tracheotomy the animals were mechanically ventilated with a FiO_2 of 0.4. Body temperature was maintained at 37 ± 0.5 °C during the entire experiment by an external thermal heating pad. Ventilator settings were adjusted to maintain end-tidal pCO_2 between 30 and 35 mmHg and arterial pCO_2 between 35 and 40 mmHg.

For drug and fluid administration and hemodynamic monitoring, vessels were cannulated with polyethylene catheters with an outer diameter of 0.9 mm (Braun, Melsungen, Germany). A catheter in the right carotid artery was connected to a pressure transducer to monitor mean arterial blood pressure (MAP) and heart rate. The right jugular vein was cannulated for continuous infusion of Ringer's Lactate (Baxter, Utrecht, The Netherlands) at a rate of 15 mL/kg/hour and maintenance of anesthesia. The right femoral artery was cannulated for drawing blood samples and the right femoral vein for drug

administration.

The left kidney was exposed, decapsulated, and immobilized in a Lucite kidney cup (K. Effenberger, Pfaffingen, Germany) via ~4 cm incision in the left flank in each animal. Renal vessels were carefully separated under preservation of nerves and the adrenal gland. A perivascular ultrasonic transient time flow probe was placed around the left renal artery (type 0.7 RB Transonic Systems Inc., Ithaca, NY, USA) and connected to a flow meter (T206, Transonic Systems Inc., Ithaca, NY, USA) to continuously measure renal blood flow (RBF). An estimation of the renal vascular resistance (RVR) was made as: $RVR \text{ (dynes.sec.cm}^{-5}\text{)} = (\text{MAP/RBF})$. The left ureter was isolated, ligated, and cannulated with a polyethylene catheter for urine collection.

After the surgical preparation one optical fiber was placed 1 mm above the decapsulated kidney and another optical fiber was placed 1 mm above the renal vein to measure renal microvascular and venous oxygenation using phosphorimetry (explained in more detail below). A small piece of aluminum foil was placed on the dorsal side of the renal vein to prevent contribution of the underlying tissues to the phosphorescence signal in the venous pO_2 measurements. Oxyphor G2, a two-layer glutamate dendrimer of tetra-(4-carboxy-phenyl) benzoporphyrin (Oxygen Enterprises Ltd., Philadelphia, PA, USA) was subsequently infused (i.e. 6 mg/kg IV over 5 min), followed by 30 min of stabilization time. The surgical field was covered with a humidified gauze compress throughout the entire experiment to prevent drying of the exposed tissues.

Experimental Protocol

The rats were divided into 3 groups ($n = 6/\text{group}$): (1) a sham-operated control group; (2) a group subjected to renal ischemia for 60 min, by high aortic occlusion with a custom-made vascular occluder placed on the abdominal aorta just above mesenteric artery, followed by 2 h of reperfusion (I/R); and (3) a group subjected to I/R and treated with ascorbic acid: at 15 min before ischemia an i.v. bolus (100 mg/kg dissolved in 1 ml 0.09% saline) was administered during 5 min, followed by continuous i.v. infusion (50 mg/kg/h dissolved in 0.5 ml 0.09% saline) for two hours during reperfusion (I/R+AA).

Blood variables

Arterial blood samples (0.5 ml) were taken from the carotid artery at three time points: 1) before aortic occlusion, (baseline, BL); 2) 15 min. after reperfusion (initial reperfusion phase, R15); and 3) 120 min. after reperfusion (late reperfusion phase, R120). The blood samples were replaced by the same volume of HES130/0.4 (Voluven, 6% HES 130/0.4; Fresenius Kabi Nederland, Schelle, Belgium). The samples were used for determination of blood gas values (ABL505 blood gas analyzer; Radiometer, Copenhagen, Denmark),

as well as for determination of the hemoglobin concentration, hemoglobin oxygen saturation (OSM 3; Radiometer).

Renal microvascular and venous oxygenation

Microvascular oxygen tension in the renal cortex ($C_{\mu}PO_2$), outer medulla ($M_{\mu}PO_2$), and renal venous oxygen tension ($P_{rv}O_2$) were measured by oxygen-dependent quenching of phosphorescence lifetimes of the systemically infused albumin-targeted (and therefore circulation-confined) phosphorescent dye Oxyphor G2 (28). Oxyphor G2 has two excitation peaks ($\lambda_{excitation1}=440\text{ nm}$, $\lambda_{excitation2}=632\text{ nm}$) and one emission peak ($\lambda_{emission}=800\text{ nm}$). These optical properties allow (near) simultaneous lifetime measurements in microcirculation of the kidney cortex and the outer medulla due to different optical penetration depths of the excitation light (28). For the measurement of renal venous PO_2 ($P_{rv}O_2$), a mono-wavelength phosphorimeter was used (29). Oxygen measurements based on phosphorescence lifetime techniques rely on the principle that phosphorescence can be quenched by energy transfer to oxygen resulting in shortening of the phosphorescence lifetime. A linear relationship between reciprocal phosphorescence lifetime and oxygen tension (i.e., the Stern-Volmer relation) allows quantitative measurement of PO_2 (30).

Renal oxygen delivery and consumption

Arterial oxygen content (AOC) was calculated by $(1.31 \times \text{hemoglobin} \times S_aO_2) + (0.003 \times P_aO_2)$, where S_aO_2 is arterial oxygen saturation and P_aO_2 is arterial partial pressure of oxygen. Renal venous oxygen content (RVOC) was calculated as $(1.31 \times \text{hemoglobin} \times S_{rv}O_2) + (0.003 \times P_{rv}O_2)$, where $S_{rv}O_2$ is venous oxygen saturation and $P_{rv}O_2$ is renal vein partial pressure of oxygen (measured using phosphorimetry). Renal oxygen delivery was calculated as $DO_{2ren} \text{ (mL/min)} = RBF \times AOC$. Renal oxygen consumption was calculated as $VO_{2ren} \text{ (mL/min)} = RBF \times (AOC - RVOC)$.

Renal function

Creatinine was determined in plasma at the end of the experiment. We aimed to collect urine samples from the left ureter, but due to the severity of our model no urine was produced after I/R.

Renal tissue oxidative stress

Renal tissue malondialdehyde (MDA) levels were determined to assess lipid peroxidation as a measure of renal oxidative stress. At the end of the experiment, the left kidney was cut in two, and one half was immediately frozen in liquid nitrogen and stored at -80°C . Frozen kidneys were homogenized in cold 5 mM sodium phosphate buffer. The homogenates were centrifuged at 12,000 g for 15 min at 4°C and supernatants were used

for MDA determination. The amount of MDA was quantified using a Quattro Premier XE tandem mass spectrometer (MS/MS) from Waters (Milford, MA, USA) with a Acquity sample manager and a Acquity binary solvent manager. MDA and MDA-d2 were separated on a Supelco LC-18DB column (250 mm-length x 4.6 mm-diameter, with 5 μ m particles), using a isocratic run from 50% acetonitrile, 50 % water and 0.2% Acetic acid; the flow rate was 1 ml/min with a total run time of 10 min. Both compounds were detected and quantified by MRM acquisition in positive electrospray ionisation mode, using the transitions m/z 235 >159 for MDA, and 237 >161 for MDA-d2.

Immunohistochemistry

At the end of the experiment, the other half of the left kidney was fixed in 4% formalin and embedded in paraffin. Kidney sections (4 μ m) were deparaffinized with xylene and rehydrated with decreasing percentages of ethanol and finally with water. Antigen retrieval was accomplished by microwaving slides in citrate buffer (pH 6.0) (Thermo Scientific, AP-9003-500) for 10 min. Slides were left to cool for 20 min at room temperature and then rinsed with distilled water. Surroundings of the sections were marked with a PAP pen. The endogenous peroxidase activity was blocked with 3% H_2O_2 for 15 min at room temperature and later rinsed with distilled water and PBS. Blocking reagent (Lab Vision, TA-125-UB) was applied to each slide followed by 5 min incubation at room temperature in a humid chamber. Kidney sections were incubated overnight at 4°C with rabbit polyclonal iNOS antibody (iNOS Ab-1, Rabbit PAb, RB-1605-P, NeoMarkers Fremont, CA) and IL-6 (Abcam, 6672), and incubated for 1 hour at room temperature with anti-myeloperoxidase (MPO) antibodies (Myeloperoxidase Ab-1, RB-373-A, NeoMarkers Fremont, CA), Lipocalin 2 antibody (NGAL) (abcam 41105), polyclonal antibody to rat L-FABP (Hycult Biotect HP8010). Antibodies were diluted in a large volume of UltrAb Diluent (Thermo Scientific, TA-125-UD). The sections were washed in PBS three times for 5 min each time and then incubated for 30 min at room temperature with biotinylated goat anti-rabbit antibodies (LabVision, TP-125-BN). After slides were washed in PBS, the streptavidin peroxidase label reagent (LabVision, TS-125-HR) was applied for 30 min at room temperature in a humid chamber. The colored product was developed by incubation with AEC (3-amino-9-ethylcarbazole). The slides were counterstained with Mayer's hematoxylin (LabVision, TA-125-MH) and mounted in vision mount (LabVision, TA-060-UG) after being washed in distilled water. Both the intensity and the distribution of iNOS, IL-6, L-FABP, NGAL staining were scored in 10 different areas for each samples under light microscope at magnification X400 in the kidney slices. For each sample, a histological score (HSCORE) value was derived by summing the percentages of cells that stained at each intensity multiplied by the weighted intensity of the staining ($HSCORE = \sum S_i P_i$), where i is the intensity score and P_i is the corresponding percentage of the cells). We evaluated MPO reaction in the glomerulus

from 250 selected glomeruli and in 250 selected peritubular areas under a light microscope at a magnification X400. We scored 1 if leukocytes could be seen in the glomerulus or peritubular areas and 0 if not (9,31).

Statistical Analysis

Data analysis and presentation were performed using GraphPad Prism (GraphPad Software, San Diego, CA, USA). Values are reported as the mean \pm SD. Two-way ANOVA for repeated measurements with a Bonferroni post hoc test were used for comparative analysis between different time points of the groups. The repeated-measures analysis of variance (one-way ANOVA with Bonferroni post hoc test) was used for comparative analysis between groups. p-value of <0.05 was considered statistically significant.

RESULTS

Systemic and renal hemodynamic

Systemic and renal hemodynamic parameters are reported in Table 1. High aortic clamping and release resulted in a significant fall in blood pressure and RBF at R15 and R120 ($p<0.05$ vs. time control), and a significant increase in RVR at R120 ($p<0.05$ vs. time control). Although AA treatment was associated with a non-significant trend for improved MAP and RBF, this only resulted in a significant improvement for RVR at R120 ($p<0.05$ vs. I/R+AA group). MAP and RBF remained significantly decreased in the I/R+AA group as compared to the time control group.

Renal oxygenation

Renal oxygenation parameters are reported in Figure 1 and 2. Briefly, renal $\text{DO}_{2\text{ren}}$, $\text{VO}_{2\text{ren}}$, $\text{C}\mu\text{PO}_2$ and $\text{M}\mu\text{PO}_2$ slightly reduced after releasing of the clamp at R15 and R120 ($p<0.05$ vs. Time control, respectively)(Figure 1). AA treatment improved $\text{C}\mu\text{PO}_2$ in I/R group at R15 and R120 ($p<0.05$ vs. I/R, respectively), whereas $\text{M}\mu\text{PO}_2$ was improved only at R120 ($p<0.05$ vs. I/R) (Figure 1C and 1D). Additionally, while $\text{C}\mu\text{PO}_2$ decreased by % ~ 23 in the control group, by ~ 75 in the I/R group ($p<0.05$ vs. time control) and by % ~ 51 in the I/R+AA group ($p<0.05$ vs. time control) which also indicated an improvement in I/R group treated with AA in comparison to I/R group ($p<0.05$) as a percentage from BL to R120. $\text{M}\mu\text{PO}_2$ decreased by % ~ 19 in Control group, by % ~ 80 in I/R group ($p<0.05$ vs. time Control) and % ~ 59 in I/R+AA group ($p<0.05$ vs. time control) resulted significant improvement in I/R group received AA compared with the I/R group ($p<0.05$) (Figure 2C, 2D). Overall, the data suggest that AA treatment can, at least partly, improve the I/R-induced hypo-oxygenation of the kidney.

Plasma lactate levels

Table 1. Systemic and renal hemodynamics variables.

	BL	R15	R120
MAP (mmHg)			
Time control	87±7	88±21	69±7
I/R	84±3	44±8 *	34±7 *
I/R+AA	93±14	48±14 *	46±14 *
RBF (mL/min)			
Time control	4.1±1.0	3.4±1.2	3.8±0.9
I/R	4.6±1.0	1.6±0.2 *	0.6±0.2 *
I/R+AA	4.6±0.8	1.4±0.4 *	1.2±0.4 *
RVR (dyn.s.cm⁻⁵)			
Time control	23±7	28±9	19±4
I/R	19±5	28±4	54±10 *
I/R+AA	21±4	35±10	34±6 *,†

Values are presented as Mean ± SD, *p<0.05 vs. Time control; †p<0.05 vs. I/R group.

Abbreviations: I/R; ischemia/reperfusion, AA; ascorbic acid, MAP; mean arterial pressure, RBF; renal blood flow, RVR; renal vascular resistance.

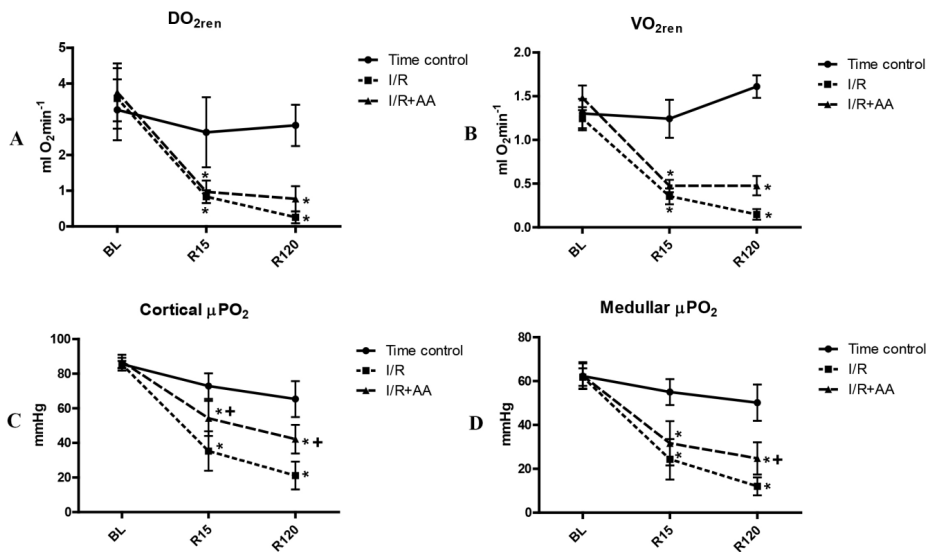


Figure 1. Renal oxygen delivery (DO_{2ren}) (Panel A), renal oxygen consumption (VO_{2ren}) (Panel B), cortical microvascular oxygen pressure (cortical μPO_2) (Panel C) and medullar microvascular oxygen pressure (medullar μPO_2) (Panel D) during experiments. I/R; ischemia/reperfusion, AA; ascorbic acid. Values are presented as Mean ± SD, *p<0.05 vs. Time control, †p<0.01 vs. I/R group.

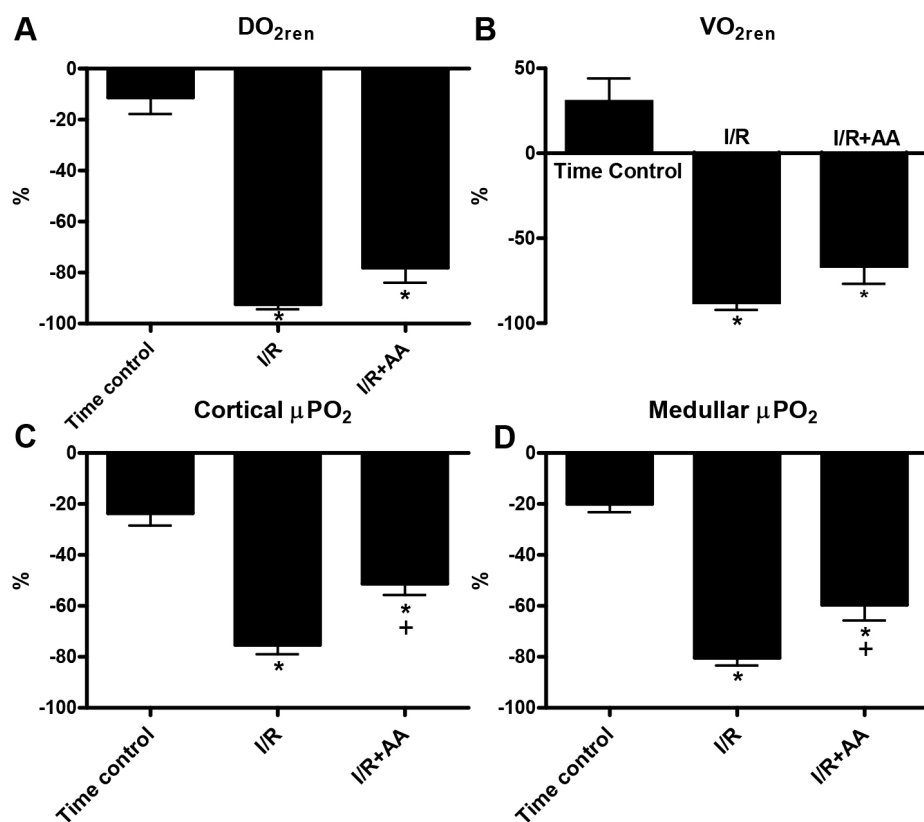


Figure 2. Changing values of renal oxygen delivery (DO_{2ren}) (Panel A), renal oxygen consumption (VO_{2ren}) (Panel B), cortical microvascular oxygen pressure (cortical μPO_2) (Panel C) and medullar microvascular oxygen pressure (medullar μPO_2) (Panel D) from BL to R120 between groups. I/R; ischemia/reperfusion, AA; ascorbic acid. Values are presented as Mean \pm SD, * $p < 0.05$ vs. Time control, + $p < 0.01$ vs. I/R group.

In accordance with the I/R-induced hypo-oxygenation of the kidney, untreated I/R was associated with large increases in plasma lactate levels, from 2 ± 1 mmol/L in the control group to 13 ± 4 mmol/L in the I/R group ($p < 0.05$). The rise in lactate levels was significantly reduced to 7 ± 4 mmol/L by AA administration with respect to I/R group ($p < 0.05$) (Figure 3).

Renal function parameters

We aimed to collect urine samples from the left ureter for analysis of urine volume, creatinine concentration, and sodium concentration at the end of the protocol, but due to the severity of our model (severe fall in MAP, RBF, and renal oxygenation and a significant rise in RVR) no urine was produced after I/R. AA treatment was unable to restore this blocked urine production. Plasma creatinine levels were higher after the I/R

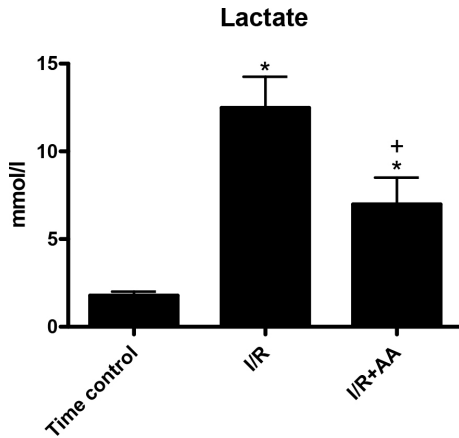


Figure 3. Plasma lactate levels at the end of the protocol (R120). I/R; ischemia/reperfusion, AA; ascorbic acid. Values are presented as Mean \pm SD, * p <0.05 vs. Time control and + p <0.05 vs. I/R group.

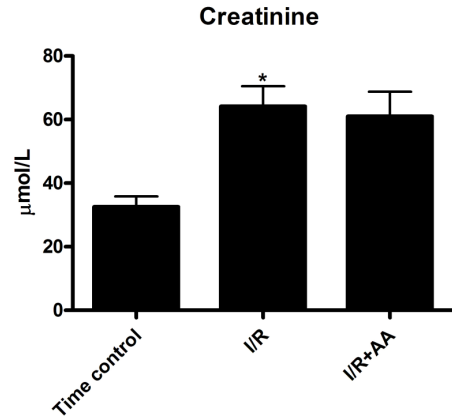


Figure 4. Plasma creatinine levels at the end of the protocol (R120). I/R; ischemia/reperfusion, AA; ascorbic acid. Values are presented as Mean \pm SD, * p <0.05 vs. Time control.

insult at the end of the experiment, suggesting decreased kidney function. However, AA treatment was also unable to attenuate the I/R-induced creatinine increase (Figure 4).

Immunohistochemistry

Next we examined whether the decreased oxidative stress by AA treatment resulted in attenuation of I/R-induced inflammation and kidney damage (Figure 5). In comparison to the Control group, I/R led to a significant rise in all immunohistochemistry parameters: iNOS, IL-6, NGAL, FABP, and MPO expression in the glomeruli (gMPO) and peritubular areas (ptMPO) (p <0.05, respectively). Ascorbic acid treatment was able to prevent the I/R-induced rise in all of these parameters (p <0.05) with respect to the I/R group.

Renal tissue oxidative stress

We first assessed whether oxidative stress developed and to what extent AA treatment was effective in reducing oxidative stress in our model. Renal tissue MDA levels were determined to assess lipid peroxidation as a measure of renal oxidative stress. I/R led to a significant increase in MDA levels from 4.9 ± 1.3 mmol/g in the time control group to 7.6 ± 1.3 mmol/g in the I/R group (p <0.05), which was decreased to control levels (5.3 ± 0.9 mmol/g) by ascorbic acid administration (p <0.05) (Figure 6).

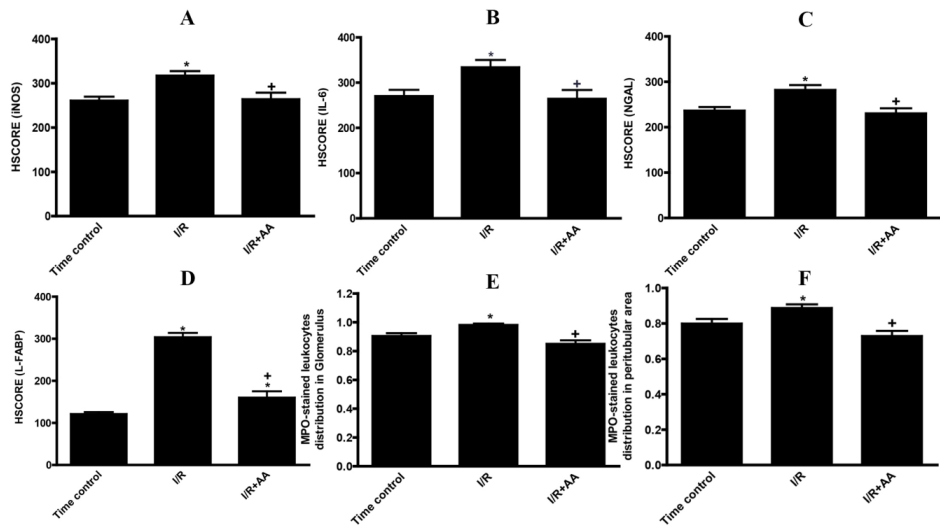


Figure 5. The immunohistochemistry results for expression of inducible nitric oxide (iNOS) (Panel A), interleukin 6 (IL-6) (Panel B), neutrophil gelatinase-associated lipocalin (NGAL) (Panel C), fatty acid binding protein (FABP) (Panel D), and myeloperoxidase (MPO) in the glomeruli (gMPO) (Panel E) and peritubular areas (ptMPO) (Panel F). I/R; ischemia/reperfusion, AA; ascorbic acid. Values are presented as Mean \pm SD, * p <0.05 vs. Time control; + p <0.05 vs. I/R group.

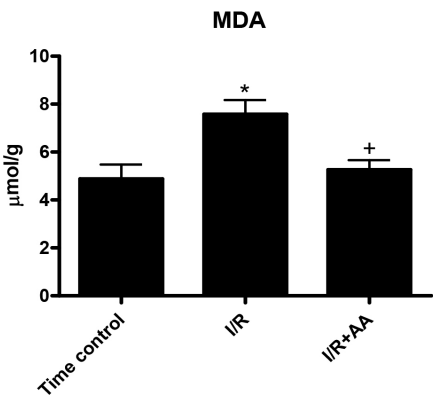


Figure 6. Renal tissue malondialdehyde levels at the end of the protocol (R120). I/R; ischemia/reperfusion, AA; ascorbic acid. Values are presented as Mean \pm SD, * p <0.05 vs. Time control and + p <0.05 vs. I/R group.

DISCUSSION AND CONCLUSION

In the present study we investigated whether the ascorbic acid (vitamin C) administration would be able to reduce I/R-related injury to the kidneys in terms of renal microvascular hypoxia, oxidative stress, inflammation and finally renal failure. The severe I/R intervention resulted in a fall in systemic and renal hemodynamics and oxygenation parameters, and significantly increased the expression of biomarkers of kidney injury and inflammation.

This was also associated with complete anuria and elevated plasma creatinine and lactate levels. However, treatment of ascorbic acid resulted in improvement on the renal cortical and medulla oxygenation and partially enhanced in renal oxygen delivery and consumption as a result of a decreased amount of oxygen using for the reactive oxygen species production. We demonstrated that ascorbic acid administration was able to completely prevent the burst in oxidative stress, inflammation and renal injury. However, the AA was unable to improved hemodynamics or urine function in this severe model of AKI.

Many regulatory factors contribute to the homeostasis of oxygen supply and consumption of the kidney (18), including the systemic and microvascular hemodynamic circumstances. To demonstrate complexity of the renal oxygenation and perfusion, O'Connor *et al.* reported that reductions in renal blood flow (RBF), instigated by direct injection of vasopressin into the renal artery, led to a selective reduction in medullar perfusion and PO_2 , without affecting cortical perfusion or tissue oxygenation. On the other hand, stimulation of the renal nerves caused renal cortical ischemia associated with reductions in renal flow, cortical perfusion and cortical PO_2 (32). In the present study, we documented that macrohemodynamic changes such as MAP and RBF are associated with alteration of the renal microvascular and oxygenation properties as reflected by a change in the renal vascular resistance. Recently, a few studies suggested that oxygen shunting may also contribute to renal microcirculatory disturbance and oxygen heterogeneity (10,33), which shunting possibly being an adaptation to prevent overproduction of the reactive oxygen species (ROS) (6). Legrand *et al.* suggested that the homeostasis of oxygen supply and utilization is severely impaired during ischemia/reperfusion in kidney (18). In this study, we found that I/R induced impairment of renal cortical and medullar microcirculatory oxygenation correlates with the deterioration of DO_{2ren} and VO_{2ren} . Legrand *et al.* also documented that microcirculatory oxygen disturbance and tissue hypoxia occurred during the first hours of the reperfusion, and correlated with the reduction of the DO_{2ren} and VO_{2ren} in both renal cortex and medulla. As an additional correlate of oxygen homeostasis disturbance, we also observed elevated plasma lactate levels after I/R. These microcirculatory disturbances were previously shown to be partly mediated through upregulation of iNOS and downregulation of eNOS (9,10). In fact, nitric oxide (NO) is of prime importance because of its central regulatory role in intrarenal microcirculation (34) and renal oxygen consumption regulation (35,36). In the present study we also demonstrate that severe hemodynamic alterations are associated with elevating iNOS activity.

In the present study, we used AA, which is one of the water-soluble vitamins and is well known as a strong antioxidant agent reacting with and scavenging superoxide, hydroxyl radicals and singlet oxygen (37). Tyml *et al.* (2005) have also demonstrated that an

intravenous bolus of ascorbate could protect against maldistribution of microvascular blood flow and reversed microcirculatory dysfunction in sepsis (38). In present study, we demonstrated that intravenous AA administration could improve the level of lactate in plasma as a result of its protective effect on the microvascular circulation and oxygenation.

It has been documented that AA also reduces peroxynitrite formation, which is a strong oxidant molecule and is mainly generated when overexpressed NO reacts with singlet oxygen. Recently, Wang P *et al.* (39) have also demonstrated that levels of the nuclear factor- κ B (NF- κ B) and iNOS mRNA were elevated in ischemia-reperfused kidney, resulting in an increased peroxynitrite formation and lipid peroxidation. Additionally, another study showed that peroxynitrite can lead to inhibition of mitochondrial respiratory chain activity and membrane Na/K-ATPase activity, and activation of apoptotic enzymes (40). Thus, it might be hypothesized that peroxynitrite is able to impair the renal microcirculatory oxygenation and utilization by inhibition of the Na/K-ATPase and mitochondrial respiratory chain enzymes. Indeed, under physiological conditions, approximately 80% of oxygen is used to drive the Na/K-ATPase in kidney (41). In the present study, we concluded that although ascorbic acid could restore renal cortical and medullar oxygenation, and marginally improved in the renal oxygen delivery and consumption. These oxygenation results also indicated that AA was able to prevent peroxynitrite formation and was effective on the oxygen utilization by decreased in iNOS levels and peroxynitrite formation in this study. However, this cortico-medullar microcirculatory effect of AA can be explained through inhibition of the A-V shunting process due to reduces in oxidative stress and supplying sufficient oxygen in the renal microvasculature by protecting the endothelium and reducing of the RVR by local vessel vasodilatation even though unimproved renal blood flow and arterial pressure because of consistent hypotension.

Several studies have demonstrated that I/R in the kidney is associated with lipid peroxidation, which is an autocatalytic mechanism leading to oxidative destruction of cellular membranes (42,43). In accordance renal MDA level was also significantly increased in our model, indicating the presence of enhanced lipid peroxidation due to I/R injury (44). In the present study we demonstrated that the ascorbic acid was able to completely prevent the I/R-induced increase in tissue MDA levels. However, kidney function was not completely restored, indicating that oxidative stress is not the only causal factor for the development of AKI. Furthermore, we showed that ascorbic acid also attenuates leukocyte activation and leukocyte adhesion to microvascular endothelium by assessment in renal tissue levels of MPO and IL-6. Previous studies demonstrated that inflammatory molecules are expressed in a few minutes of I/R injury, including platelet-

activating factor (PAF) and P-selectin, which associated with activation of the complement system, release of leukocyte chemotactic factors (45), and up-regulation of adhesion molecules on the cell surface, leading to adherence of circulating leukocytes to the vessel walls and their diapedesis into the tissues (46). Our results are in support of the findings by Lloberas *et al.* (47), showing AA-induced attenuation of PAF activation and leukocyte recruitment in kidney.

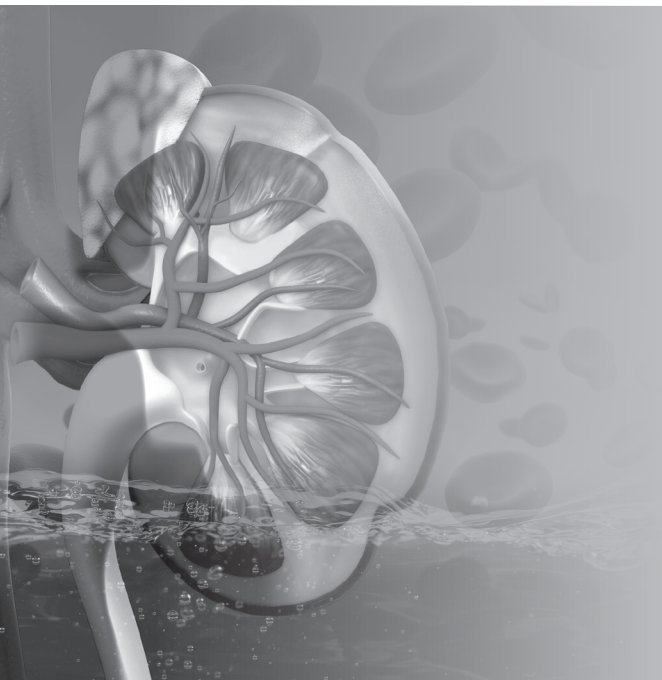
This study has several limitations. First of all, the two hours measurement period post-ischemia might be considered too short for assessment of the actual impact of I/R injury on kidney. However, the aim of this study was first to focus on renal hemodynamic and oxygenation changes in early stage of I/R. Furthermore, our results clearly demonstrate the initiation of renal dysfunction within this acute phase. A further important limitation of the study is that the procedure we chose resulted in acute hypotension and shock as indicated by the fall in MAP and rise of lactate. In fact simply administering AA was not able to restore macrohemodynamic parameters and this could also underlie our finding of the inability of only AA administration to restore kidney. Co-administering fluids with AA and targeting a blood pressure could have modulated this affect and maybe have had a more beneficial effect on renal function. However we did not want to mix these two therapies in present study. The severity of the I/R injury led to anuria, which is why we could not determine creatinine clearance and sodium reabsorption and instead focused our attention on biomarkers of renal injury such as NGAL and FABP.

In this study we have demonstrated that acute ischemia/reperfusion cause an impairment of kidney cortical and medullar oxygenation. These microcirculatory alterations are associated with decreases in renal oxygen supply and oxygen consumption, and increases in renal vascular resistance. At the same time, these changes were also correlated with systemic hypotension, tissue damage, inflammatory activation and oxidative stress. Finally, assuming oxidative stress and microcirculatory disturbance to be an important contributor to I/R-induced AKI, we examined whether the ascorbic acid can prevent oxidative stress and therefore I/R induce microcirculatory disturbance. We observed that the ascorbic acid was able to completely prevent the rise in oxidative stress, and partly improved renal microcirculatory oxygenation with reductions in kidney inflammation and tissue damage. However, the mitigation of oxidative stress was unable to restore kidney function in this rat model of severe ischemia/reperfusion. To conclude, we suggested that ascorbic acid might be used for prophylactic and therapeutic agent in order to prevent I/R induced oxidative stress and renal oxygenation disturbance along with the fluid replacement and vasoconstrictor therapy against to hypotension.

REFERENCES

1. Rabb H, Wang Z, Nemoto T, *et al.* Acute renal failure leads to dysregulation of lung salt and water channels. *Kidney Int.* 63:600–606, 2003.
2. Evans RG, Ince C, Joles JA, *et al.* Haemodynamic influences on kidney oxygenation: clinical implications of integrative physiology. *Clin. Exp. Pharmacol. Physiol.* 40(2):106–22, 2013.
3. Le Dorze M, Legrand M, Payen D, *et al.* The role of the microcirculation in acute kidney injury. *Curr. Opin. Crit. Care.* 15(6):503–8, 2009.
4. Singh P, Ricksten SE, Bragadottir G, *et al.* Renal oxygenation and haemodynamics in acute kidney injury and chronic kidney disease. *Clin. Exp. Pharmacol. Physiol.* 40(2):138–47, 2013.
5. Evans RG, Eppel GA, Michaels S, *et al.* Multiple mechanisms act to maintain kidney oxygenation during renal ischemia in anesthetized rabbits. *Am. J. Physiol. Renal Physiol.* 298: F1235–F1243, 2010.
6. Evans RG, Gardiner BS, Smith DW, *et al.* Intrarenal oxygenation: Unique challenges and the biophysical basis of homeostasis. *Am. J. Physiol. Renal Physiol.* 295:F1259–70, 2008.
7. Warner L, Gomez SI, Bolterman R, *et al.* Regional decreases in renal oxygenation during graded acute renal arterial stenosis: a case for renal ischemia. *Am. J. Physiol. Regul. Integr. Comp. Physiol.* 296(1):R67–71, 2009.
8. Abdelkader A, Ho J, Ow CP *et al.* Renal oxygenation in acute renal ischemia-reperfusion injury. *Am. J. Physiol. Renal Physiol.* 306(9):F1026–38, 2014.
9. Legrand M, Almac E, Mik EG, *et al.* L-NIL prevents renal microvascular hypoxia and increase of renal oxygen consumption after ischemia-reperfusion in rats. *Am. J. Physiol. Renal Physiol.* 296(5):F1109–17, 2009.
10. Legrand M, Kandil A, Payen D, *et al.* Effects of sepiapterin infusion on renal oxygenation and early acute renal injury after suprarenal aortic clamping in rats. *J. Cardiovasc. Pharmacol.* 58(2):192–8, 2011.
11. Parrino PE, Laubach VE, Gaughen JR, *et al.* Inhibition of inducible nitric oxide synthase after myocardial ischemia increases coronary flow. *Ann. Thorac. Surg.* 66:733, 1998.
12. Koksel O, Ozdulger A, Aytacoglu B, *et al.* The influence of iloprost on acute lung injury induced by hind limb ischemia-reperfusion in rats. *Pulm. Pharmacol. Ther.* 18(4):235–41, 2005.
13. Grace PA. Ischemia-reperfusion injury. *Br. J. Surg.* 81:637, 1994.
14. Noiri E, Nakao A, Uchida K, *et al.* Oxidative and nitrosative stress in acute renal ischemia. *Am. J. Physiol. Renal Physiol.* 281:F948, 2001.
15. Versteilen AM, Di Maggio F, Leemreis JR, *et al.* Molecular mechanisms of acute renal failure following ischemia/reperfusion. *Int. J. Artif. Organs* 27:1019, 2004.
16. Lum H, Roebuck KA. Oxidant stress and endothelial cell dysfunction. *Am. J. Physiol. Cell Physiol.* 280:C719, 2001.
17. Bonventre JV, Weinberg JM. Recent advances in the pathophysiology of ischemic acute renal failure. *J. Am. Soc. Nephrol.* 14:2199, 2003.
18. Legrand M, Ince C, Mik E, *et al.* Renal hypoxia and dysoxia following reperfusion of the ischemic kidney. *Mol. Med.* 14:502–516, 2008.
19. Basile DP, Donohoe D, Roethe K, *et al.* Renal ischemic injury results in permanent damage to peritubular capillaries and influences long-term function. *Am. J. Physiol. Renal Physiol.* 281: F887–F899, 2001.
20. Molitoris BA, Sandoval R, Sutton TA. Endothelial injury and dysfunction in ischemic acute renal failure. *Crit. Care Med.* 30:S235–240, 2002.
21. Brodsky SV, Yamamoto T, Tada T, *et al.* Endothelial dysfunction in ischemic acute renal failure: rescue by transplanted endothelial cells. *Am. J. Physiol. Renal Physiol.* 282:F1140–F1149, 2002.
22. Sutton TA, Mang HE, Campos SB, *et al.* Injury of the renal microvascular endothelium alters barrier function after ischemia. *Am. J. Physiol. Renal Physiol.* 285:F191–F198, 2003.
23. Goode HF, Webster NR, Howdle PD, *et al.* Reperfusion injury, antioxidants and hemodynamics during orthotopic liver transplantation. *Hepatology* 19:354, 1994.

24. Xia Y, Khatchikian G, Zweier JY. Adenosin deaminase inhibition prevents free radical mediated injury in the postischemic heart. *J. Biol. Chem.* 271:10096, 1996.
25. Cherubini A, Polidori MC, Bregnocchi M, *et al.* Antioxidant profile and early outcome in stroke patients. *Stroke* 31:2295, 2000.
26. Sadat U, Usman A, Gillard JH, *et al.* Does ascorbic acid protect against contrast induced- acute kidney injury in patients undergoing coronary angiography – a systematic review with meta-analysis of randomized controlled trials. *J. Am. Coll. Cardiol.* 62(23):2167-75, 2013.
27. Zuurbier CJ, Emons VM, Ince C. Hemodynamics of anesthetized ventilated mouse models: aspects of anesthetics, fluid support, and strain. *Am. J. Physiol. Heart Circ. Physiol.* 282: H2099-H2105, 2002.
28. Johannes T, Mik EG, Ince C. Dual-wavelength phosphorimetry for determination of cortical and subcortical microvascular oxygenation in rat kidney. *J. Appl. Physiol.* 100(4):1301-10, 2006.
29. Mik EG, Johannes T, Zuurbier CJ, *et al.* In vivo mitochondrial oxygen tension measured by a delayed fluorescence lifetime technique. *Biophys. J.* 95(8):3977-90, 2008.
30. Bezemer R, Faber DJ, Almac E, *et al.* Evaluation of multi-exponential curve fitting analysis of oxygen-quenched phosphorescence decay traces for recovering microvascular oxygen tension histograms. *Med. Biol. Eng. Comput.* 48(12):1233-42, 2010.
31. Demirci C, Gargili A, Kandil A, *et al.* Inhibition of inducible nitric oxide synthase in murine visceral larva migrans: effects on lung and liver damage. *Chin. J. Physiol.* 49:326–334, 2006.
32. O'Connor PM, Kett MM, Anderson WP, *et al.* Renal medullary tissue oxygenation is dependent on both cortical and medullary blood flow. *Am. J. Physiol. Renal. Physiol.* 290:F688–F694, 2006.
33. Johannes T, Mik EG, Nohe B, *et al.* Acute decrease in renal microvascular PO₂ during acute normovolemic hemodilution. *Am. J. Physiol. Renal Physiol.* 292:F796–F803, 2007.
34. Cowley AW Jr, Mori T, Mattson D, *et al.* Role of renal NO production in the regulation of medullary blood flow. *Am. J. Physiol. Regul. Integr. Comp. Physiol.* 284:R1355–R1369, 2003.
35. Adler S, Huang H, Loke KE *et al.* Endothelial nitric oxide synthase plays an essential role in regulation of renal oxygen consumption by NO. *Am. J. Physiol. Renal Physiol.* 280:F838 –F843, 2001.
36. Laycock SK, Vogel T, Forfia PR, *et al.* Role of nitric oxide in the control of renal oxygen consumption and the regulation of chemical work in the kidney. *Circ. Res.* 82:1263–1271, 1998.
37. Karaman A, Turkmen E, Gursul C, *et al.* Prevention of renal ischemia/reperfusion-induced injury in rats by leflunomide. *International Journal of Urology* 13:1434–1441, 2006.
38. Tyml K, Li F, Wilson JX. Delayed ascorbate bolus protects against maldistribution of microvascular blood flow in septic rat skeletal muscle. *Crit. Care Med.* 33(8):1823-8, 2005.
39. Wang P, Zhu Q, Wu N, *et al.* Tyrosol attenuates ischemia-reperfusion-induced kidney injury via inhibition of inducible nitric oxide synthase. *J. Agric. Food Chem.* 17;61(15):3669-75, 2013.
40. Szabó C, Módis K. Pathophysiological roles of peroxynitrite in circulatory shock. *Shock* 34(1):4-14, 2010.
41. Gullans SR, Hebert SC. Metabolic basis of ion transport. In: *Brenner and Rector's The Kidney (5th ed.)*, edited by Brenner BM. Philadelphia, PA: WB Saunders, p. 211–246, 1996.
42. Eschwege P, Paradis V, Conti M, *et al.* In situ detection of lipid peroxidation by-products as markers of renal ischemia injuries in rat kidneys. *J. Urol.* 162:553–557, 1999.
43. Sigh D, Chopra K. The effect of naringin, a bioflavonoid on ischemia-reperfusion-induced renal injury in rats. *Pharmacological Research* 50:187–193, 2004.
44. Baud L, Ardaillou R. Involvement of reactive oxygen species in kidney damage. *Br. Med. Bull.* 49:621–629, 1993.
45. Dreyer WJ, Smith CW, Michael LH *et al.* Canine neutrophil activation by cardiac lymph obtained during reperfusion of ischemic myocardium. *Circ. Res.* 65(6):1751-62, 1989.
46. Prescott SM, Zimmerman GA, Stafforini DM, *et al.* Platelet-activating factor and related lipid mediators. *Annu. Rev. Biochem.* 69:419-45, 2000. Review.
47. Lloberas N, Torras J, Herrero-Fresneda I, *et al.* Postischemic renal oxidative stress induces inflammatory response through PAF and oxidized phospholipids. Prevention by antioxidant treatment. *FASEB J.* 16(8):908-10, 2002.



CHAPTER 4

TEMPOL has limited protective effects on renal oxygenation and hemodynamics but reduces kidney damage and inflammation in a rat model of renal ischemia/reperfusion by aortic clamping

Adapted from *Journal of Clinical and Translational Research* 2015(2): 116-128

Bulent Ergin¹, Rick Bezemer¹, Asli Kandil², Cihan Demirci-Tansel², Can Ince¹

¹ Department of Translational Physiology, Academic Medical Center, University of Amsterdam, Amsterdam, The Netherlands

² Department of Biology, Faculty of Science, Istanbul University, Vezneciler, Istanbul, Turkey

ABSTRACT

Renal ischemia-reperfusion (I/R) is a common clinical complication in critically ill patients that is associated with considerable morbidity and mortality. Renal I/R is a major cause of acute kidney injury (AKI) resulting from I/R-induced oxidative stress, sterile inflammation, and microcirculatory perfusion defects, which can be ameliorated with the superoxide scavenger TEMPOL. The most common cause of AKI in the clinical setting is aortic surgery with suprarenal aortic clamping. The protective effect of TEMPOL in aortic clamping-induced renal I/R has not been studied before. To evaluate the protective effects of TEMPOL on oxidative stress, inflammation, tissue injury, and renal hemodynamics and oxygenation in a clinically representative rat model of I/R using aortic cross-clamping. Animals ($n = 24$) were either sham-operated or subjected to ischemia (30 min) and 90-min reperfusion, with or without TEMPOL treatment (15 min before ischemia and during entire reperfusion phase, 200 $\mu\text{mol/kg/h}$). Systemic and renal hemodynamics, renal oxygenation, and blood gas values were determined at 15 min and 90 min of reperfusion. At 90-min reperfusion, iNOS, inflammation (IL-6, MPO), oxidative stress (MPO), and tissue damage (NGAL, L-FABP) were determined in tissue biopsies. TEMPOL administration at a cumulative dose of 400 $\mu\text{mol/kg}$ conferred a protective effect on AKI in terms of reducing renal damage, inflammation, and iNOS activation. With respect to renal hemodynamics and oxygenation, TEMPOL only reduced renal vascular resistance to near-baseline levels at both reperfusion time points and partially ameliorated the I/R-induced drop microvascular partial tension of oxygen at 90 min reperfusion. Also, TEMPOL alleviated the I/R-induced metabolic acidosis. However, TEMPOL exerted no restorative effect in terms of the severely reduced mean arterial pressure, renal blood flow, and renal oxygen delivery and consumption. The renal oxygen extraction ratio remained unchanged during the 90-min reperfusion phase. Kidneys in all groups were anuric throughout the experiment. In conclusion, this clinically representative renal I/R model, which entails both renal I/R and hind limb I/R as opposed to the standardly used renal I/R model that employs renal artery clamping, resulted in relatively moderate direct AKI. The damage was exacerbated by the perturbed systemic hemodynamics and metabolic acidosis as a result of the hind limb I/R. TEMPOL partially intervened in the factors that lead to AKI as well as renal microvascular partial tension of oxygen and metabolic acidosis. However, more effective interventions should be devised for the mean arterial pressure drop (i.e., anuria) associated with aortic clamping and for restoring other critical renal hemodynamic and oxygenation parameters in order to improve post-I/R renal function.

Keywords: oxidative stress, antioxidants, acute kidney injury, cortical and medullar microcirculation, sterile immune response, systemic and renal hemodynamics, microvascular oxygenation

INTRODUCTION

Renal ischemia-reperfusion (I/R) is a common clinical complication in critically ill patients that leads to a high incidence of morbidity and mortality (1). Renal I/R is a major cause of acute kidney injury (AKI) (2). Although the etiology of AKI is multifarious (3), the most common cause of AKI in the clinical setting is a suprarenal aortic clamping (4), which is performed in procedures such as kidney transplantation (5), pancreas transplantation (6), and aortic aneurysm repair (7).

The general pathogenic mechanism underlying I/R-mediated AKI is summarized in Figure 1 (2,8-11). The development of AKI entails a vicious cycle involving reactive oxygen and nitrogen species (ROS and RNS, respectively), parenchymal cell death and structural damage, and sterile inflammation (Figure 1). In addition, ROS and RNS contribute to microvascular dysfunction and debilitated microvascular oxygenation in I/R-subjected kidneys (2,11). Rodent I/R AKI models revealed that I/R-mediated endothelial injury (12), characterized by e.g., glycocalyx degradation (13,14), microvascular thrombosis (15), and endothelial activation (8), affects the peritubular microcirculation (e.g., perfusion defects (16,17)) and culminates in organ dysfunction (18). These effects have also been reported for I/R AKI in patients (19,20). Moreover, perturbations in local oxygenation due to microvascular perfusion defects (16,17) translate to debilitated mitochondrial function and energy metabolism that in turn contribute to diminished kidney viability, function, and restorative capacity (8,21). Corroboratively, Funk *et al.* demonstrated that AKI causes mitochondrial dysfunction in the renal cortex and that this state correlates with sustained tubular damage (22). Taken altogether, oxygenation and oxidative stress are intricately related during renal I/R and lie at the basis of AKI (8).

The biological trigger of oxidative/nitrosative stress is superoxide, which is generated in mitochondria at low levels under normophysiological conditions (23) but hyperproduced following I/R in both endothelial cell (24) and renal mitochondria (25). Intravascular sources of superoxide during I/R include xanthine oxidase and NADPH oxidase (NOX) in endothelial cells, leukocytes, and platelets (10), whereby NOX1 (26), NOX2 (27), and NOX4 (28) have been implicated in renal I/R. Although relatively innocuous itself, superoxide gives rise to more toxic secondary and tertiary reactive intermediates (29) that form from the superoxide dismutase-catalyzed end product hydrogen peroxide (30-32). Superoxide also reacts with NO that is extensively produced during renal I/R (33) to form peroxynitrite (34,35), which oxidatively modifies proteins, DNA bases, and lipids by nitration, rendering the biomolecules dysfunction. The reaction between NO and superoxide operates at a diffusion-controlled rate and therefore predominates over

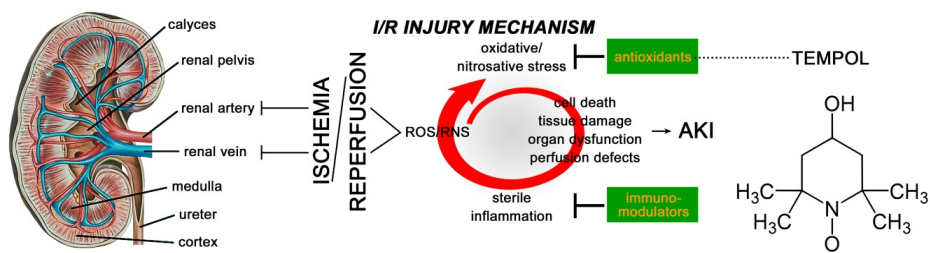


Figure 1. Gross anatomy of the kidney, the general mechanisms of renal ischemia/reperfusion (I/R) injury, and the most plausible pharmacological intervention sites for the amelioration of renal I/R injury. Cessation of blood supply to the kidney causes ischemia that, when ensued by reperfusion, results in the production of reactive oxygen and nitrogen species (ROS/RNS, respectively). The excessive generation of ROS/RNS leads to oxidative/nitrosative stress, the oxidative/nitrosative modification of biomolecules, and ultimately cell death, acute kidney injury (AKI), and renal (microvascular) dysfunction. Dead and dying cells release self-antigens called damage-associated molecular patterns (DAMPs) that chemotactically recruit and activate immune cells (neutrophils and monocytes/macrophages) in the injured kidney. In the absence of pathogens (i.e., sterile inflammation), the activated immune cells generate ROS/RNS that are directed at renal vascular and parenchymal cells, exacerbating the prevailing oxidative/nitrosative stress and corollary AKI. Accordingly, two plausible types of interventions entail (1) the administration of antioxidants (e.g., TEMPOL) or agonists of endogenous antioxidants to reduce the extent of oxidative stress and (2) immunomodulatory agents to downscale the pro-inflammatory response and associated ROS/RNS generation.

virtually all other competing reactions. Furthermore, peroxynitrite perturbs electron transport chain functionality (i.e., aerobic respiration), inhibits membrane Na/K ATPase activity, and activates pro-apoptotic enzymes (36). Superoxide therefore constitutes an important therapeutic target in I/R AKI (37).

Pharmacological interventions aimed at reducing the deleterious (downstream) effects of superoxide overproduction by the administration of antioxidants or agonists of endogenous antioxidants (38) (Figure 1) have proven beneficial and effective against I/R injury in the heart (39), liver (40), brain (41,42), intestines (43), lungs (44), skin (45), and kidney (46), albeit the protective effects are not always ubiquitous (47). With respect to the kidneys, experimental studies have demonstrated that membrane-permeable, low molecular weight SOD mimetics may improve post-I/R outcomes due to their beneficial effects on ROS scavenging and mitochondrial metabolism (48-50). TEMPOL (4-hydroxy-2,2,6,6-tetramethyl piperidinoxyl) is a membrane-permeable, metal-independent SOD mimetic with specific reactivity towards superoxide (51) and hence capable of intervening early in the injurious redox chain and renal pathogenesis (Figure 1). Also, TEMPOL has been shown to cause dilation of I/R-constricted (inflamed) coronary blood vessels (52) and retinal arterioles (53). Accordingly, numerous studies have shown that TEMPOL reduces I/R AKI in different species, including rats (54).

The antioxidant (55), immunosuppressive (56,57), and AKI-ameliorating effects of TEMPOL are well-established in I/R AKI. Conversely, relatively little information is available in terms of renal oxygenation, which is critical for renal function (8). In a study that was conducted in parallel to the work presented here (58), the protective effects of TEMPOL on (micro)vascular hemodynamics and oxygenation were demonstrated in a setting of renal I/R induced by renal artery clamping (30 min ischemia, 90 min reperfusion). However, this procedure is not representative for the clinical situation where AKI is mainly induced by aortic clamping (4), affecting more than just the kidneys. For example, the lower extremities are also implicated, which may confer ancillary sequelae on kidneys during reperfusion (59,60). The aim of this study was therefore to determine whether systemic TEMPOL administration in rats subjected to moderate renal I/R (30 min ischemia and 90 min reperfusion) induced by aortic clamping instead of suprarenal artery clamping also improves (micro)vascular hemodynamic and oxygenation parameters in the acute reperfusion phase (10). First, the renal I/R model was validated in terms of oxidative stress, tissue injury, and inflammation parameters, after which a panel of (micro)vascular hemodynamic and oxygenation parameters was assessed in real time following vehicle delivery or TEMPOL treatment. The main findings were that TEMPOL (1) reduced the extent of iNOS activation, tissue injury, and inflammation, (2) downmodulated renal vascular resistance to near-baseline levels in the early (15 min) and late (90 min) reperfusion phase, and (3) improved microvascular oxygen tension in the renal cortex and medulla at 90 min reperfusion but not renal oxygen delivery, consumption, and extraction ratio. Overall, the protective effects of TEMPOL were not as profound as was the case in AKI induced by renal artery clamping, which generally was associated with less sizeable alterations in the tested parameters compared to aortic clamping.

MATERIALS AND METHODS

Animals

The animal experiments were approved by the animal ethics committee of the Academic Medical Center of the University of Amsterdam (DFL 83) and animals were treated in accordance with the Guide for the Care and Use of Laboratory Animals (NRC 2011). The study was performed with 24 male *Wistar albino* rats (Harlan Laboratories, Horst, The Netherlands) with a mean body weight of 348 ± 41 g.

Anesthesia and surgical procedures

Rats were anesthetized by intraperitoneal injection of a mixture of 100 mg/kg ketamine (Nimatek, Eurovet, Bladel, The Netherlands), 0.5 mg/kg dexmedetomidine (Dexdomitor, Pfizer, New York, NY), and 0.05 mg/kg atropine-sulfate (Centrafarm, Etten-Leur, The

Netherlands). Following a tracheotomy the animals were mechanically ventilated at a FiO_2 of 0.4. The ventilator settings were adjusted to maintain an end-tidal partial pressure of carbon dioxide (pCO_2) between 30 and 35 mmHg and an arterial pCO_2 between 35 and 40 mmHg. Body temperature was maintained at $37 \pm 0.5^\circ\text{C}$ using a heating pad. The surgical field was covered with a humidified gauze compress throughout the entire experiment to prevent desiccation of the exposed tissues.

Blood vessels were cannulated with polyethylene catheters (outer $\text{Ø} = 0.9$ mm, B. Braun Melsungen, Melsungen, Germany). A catheter was inserted into the right carotid artery and connected to a pressure transducer to monitor mean arterial blood pressure (MAP). The right jugular vein was cannulated for continuous infusion of Ringer's lactate (Baxter

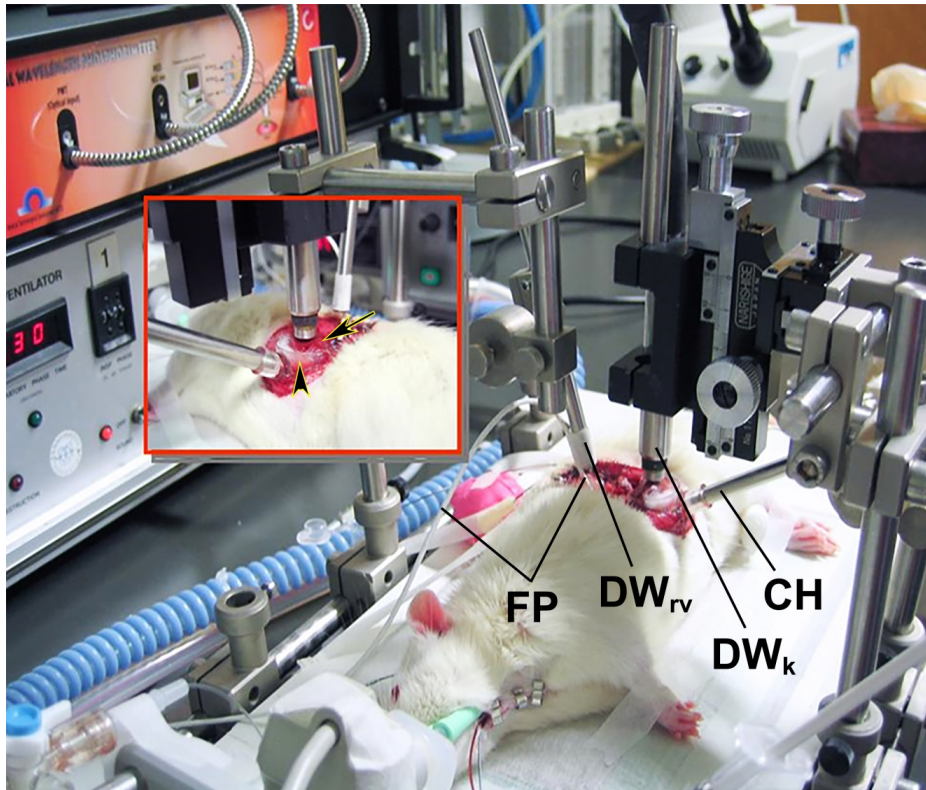


Figure 2. Rat anesthesia, ventilation, sampling, and monitoring setup. The DW_{rv} designates the dual wavelength phosphorimetry probe on the renal vein. The DW_k refers to the dual wavelength phosphorimetry probe placed on the kidney. CH signifies the kidney cup holder and FP refers to the ultrasonic flow probe. Insert: rear perspective view of the mobilized left kidney (arrow) positioned in the kidney cup (arrowhead) through the 4-cm dorsal incision.

Healthcare, Deerfield, IL) at a rate of 15 mL/kg/h and of maintenance anesthesia (50 mg/kg/h ketamine dissolved in Ringer's lactate, 5 mL/kg/h). The right femoral artery was cannulated for blood sampling and the right femoral vein was cannulated for TEMPOL (400 μ mol/kg, dissolved in 0.9 % NaCl) and Oxyphor G2 (6 mg/kg, dissolved in 0.9 % NaCl) administration and fluid resuscitation. The left ureter was isolated, ligated, and cannulated with a polyethylene catheter for urine collection and quantification of urine production.

The left kidney was exposed via a ~4-cm incision in the left dorsal flank, decapsulated, and immobilized in a custom-built 3D-printed kidney cup (Lucite International, Hampshire, UK, Figure 2). Renal vessels were carefully separated while preserving the nerves and adrenal gland.

Monitoring of renal blood flow and oxygenation

A perivascular ultrasonic transient time flow probe was placed around the left renal artery (model 0.7 RB, Transonic Systems, Ithaca, NY) and connected to a flow meter (model T206, Transonic Systems) (Figure 2) to continuously measure renal blood flow (RBF).

A detailed description of the phosphorimetry method can be found in (61). After the surgical procedure, one optical fiber was placed 1 mm above the decapsulated kidney and another optical fiber was placed 1 mm above the renal vein to measure renal microvascular and venous oxygenation, respectively (Figure 2). A small piece of aluminum foil was placed on the dorsal side of the renal vein to prevent phosphorescence signal spillover from underlying tissues during venous partial pressure of oxygen (pO_2) measurements.

Experimental protocol

The animals were randomly allocated to one of four groups ($n = 6$ /group). In the first group ('Ctrl'), animals were sham-operated but not subjected to I/R. In the second group ('Ctrl + TEMPOL'), rats underwent a sham operation and were administered TEMPOL at 200 μ mol/kg/h during 105 min. This dose was validated in our previous study (58). In the third group ('I/R'), the animals underwent a 30-min aortic cross-clamping (just below the superior mesenteric artery), rendering both kidneys ischemic, followed by 90 min of reperfusion. In the fourth group ('I/R + TEMPOL'), rats were given TEMPOL for 15 min prior to ischemia (200 μ mol/kg bolus) and during the entire reperfusion phase (200 μ mol/kg/h, total infusion time of 90 min). It should be noted that sham-operated animals underwent the same procedures as described in sections 2.2, 2.3, and above except for the cross-clamping of the aorta.

At the end of the experiment the animals were sacrificed by intravenous administration of 1 mL of 3 M potassium chloride. The I/R-subjected kidney was excised for oxidative stress assays (section 2.8) and histological analysis (section 2.9).

Phosphorimetric measurement of renal microvascular and venous PO₂

Systemically administered Oxyphor G2 (tetra-(4-carboxy-phenyl) benzoporphyrin, Oxygen Enterprises, Philadelphia, PA) was used for the measurement of renal oxygenation. Oxyphor G2 binds to albumin and therefore remains confined to the vasculature. The probe has two excitation peaks ($\lambda_{\text{ex1}} = 440 \text{ nm}$, $\lambda_{\text{ex2}} = 632 \text{ nm}$) and one emission peak ($\lambda_{\text{em}} = 800 \text{ nm}$). These optical properties allow near-simultaneous phosphorescence lifetime measurements in the microcirculation of the kidney cortex ($\text{C}\mu\text{PO}_2$) and the outer medulla ($\text{M}\mu\text{PO}_2$) due to different optical penetration depths of the excitation light. The local oxygen tension can be extrapolated from the degree of phosphorescence quenching (i.e., shortening of phosphorescence lifetime) by oxygen. The linear relationship between reciprocal phosphorescence lifetimes and oxygen tension, derived from the Stern-Volmer equation, allows quantitative analysis of μPO_2 (61).

Oxyphor G2 was infused (6 mg/kg during 5 min) 30 min before the start of phosphorimetry (i.e., before ischemia induction). Renal microvascular PO₂ (μPO_2) and renal venous PO₂ (rvPO_2) were measured at baseline, 15 min of reperfusion (R15), and 90 min of reperfusion (R90). In the non-I/R groups, these parameters were measured at 15 min and 90 min during continuous TEMPOL administration. For the measurement of μPO_2 and rvPO_2 , dual wavelength phosphorimeters ($\lambda_{\text{ex}} = 440$ and 632 nm) were used (Figure 2).

Calculation of derivative oxygenation parameters and renal vascular resistance

Renal oxygen delivery ($\text{DO}_{2\text{ren}}$, mL/min) was calculated by $\text{RBF} \times \text{arterial oxygen content}$ ($\text{C}_a\text{O}_2 = 1.31 \times \text{hemoglobin} \times \text{S}_a\text{O}_2 + (0.003 \times \text{P}_a\text{O}_2)$), where S_aO_2 is arterial oxygen saturation and P_aO_2 is arterial partial pressure of oxygen. Renal oxygen consumption ($\text{VO}_{2\text{ren}}$, mL·min⁻¹) was calculated as $\text{RBF} \times (\text{C}_a\text{O}_2 - \text{C}_v\text{O}_2)$, where renal venous oxygen content (C_vO_2) was calculated as $(1.31 \times \text{hemoglobin} \times \text{S}_{rv}\text{O}_2) + (0.003 \times \text{rvPO}_2)$. The S_{rv}O_2 was calculated using the Hill equation with $\text{P50} = 37 \text{ Torr}$ (4.9 kPa) and Hill coefficient = 2.7. The renal oxygen extraction ratio ($\text{ERO}_{2\text{ren}}$, %) was calculated as $\text{VO}_{2\text{ren}} / \text{DO}_{2\text{ren}} \times 100\%$. An estimation of the renal vascular resistance (RVR, dynes·s⁻¹·cm⁻²) was made according to $(\text{MAP} / \text{RBF}) \times 100$.

Blood gas, acid-base balance, and lactate analysis from blood samples

Arterial blood samples (0.5 mL) were drawn from the femoral artery at baseline, R15, and R90. The same volume of balanced colloid solution (VOLUVEN, Fresenius Kabi,

Bad Homburg, Germany), was infused to correct for the very mild transient hypovolemia. Blood gas values, hemoglobin concentration, hemoglobin oxygen saturation, and acid-base balance were determined directly after sampling (ABL 505 blood gas analyzer, Radiometer, Copenhagen, Denmark).

Plasma lactate levels were assayed in samples acquired at baseline and at R90 by an enzymatic colorimetric method (modular P800 automatic analyzer, Roche Diagnostics, Basel, Switzerland).

It should be noted that urine-based kidney function parameters (urine production, creatinine clearance rate / glomerular filtration rate, and renal sodium reabsorption (58)) could not be determined because of I/R-induced anuria in all groups.

Determination of renal oxidative stress

Tissue malondialdehyde (MDA) levels were used as a measure of lipid peroxidation to determine the extent of oxidative stress. Kidneys were homogenized in ice-cold 5 mM sodium phosphate buffer. The homogenates were centrifuged at 12,000 $\times g$ for 15 min at 4 °C and the supernatant was used for MDA determination by tandem mass spectrometry (62-64) in accordance with (65). The level of lipid peroxides was expressed as micromoles of MDA per milligram of protein (Bradford assay).

MDA was quantified using a Quattro Premier XE tandem mass spectrometer (Waters, Milford, MA) with an Acquity sample manager and an Acquity binary solvent manager. MDA and MDA-d2 were separated on a Supelco LC-18DB column (250-mm length, 4.6-mm diameter, 5- μm particles) using an isocratic run from 50% acetonitrile, 50 % water, and 0.2% acetic acid. The flow rate was set to 1 mL/min with a total run time of 10 min. Both compounds were detected and quantified by MRM acquisition in positive electrospray ionization mode, using the transitions m/z 235 > 159 for MDA and 237 > 161 for MDA-d2.

Immunohistochemistry

Kidney tissue was fixed in 10% formalin and embedded in paraffin. Kidney sections (5 μm) were deparaffinized with xylene and rehydrated with decreasing grades of ethanol and finally with water. Antigen retrieval was accomplished by microwaving the sections in citrate buffer (pH = 6.0) for 10 min at 800 W. Sections were cooled for 20 min at room temperature (RT) and rinsed with MilliQ. The section margins were marked with a PAP pen. Endogenous peroxidase activity was blocked with 3% H_2O_2 for 10 min at room temperature (RT), after which the sections were rinsed with MilliQ and PBS. Blocking reagent (TA-125-UB, Lab Vision, Fremont, CA) was applied to each slide for 5 min at

RT in a humidified chamber. The sections were incubated overnight at 4 °C with rabbit anti-mouse inducible nitric oxide synthase (iNOS) (iNOS rabbit Pab Neomarker, RB-1605-P, Lab Vision), interleukin (IL)-6 (product # 6672, Abcam, Cambridge, UK), myeloperoxidase (MPO) (MPO rabbit RB-373-A, Thermo Fisher Scientific, Waltham, MA), neutrophil gelatinase-associated lipocalin (NGAL) (product # 41105, Abcam), liver-type fatty acid binding protein (L-FABP) (product # HP8010, Hycult Biotech, Uden, The Netherlands). Antibodies were diluted in a large volume of UltraB Diluent (product # TA-125-UD, Lab Vision) at a 1:100 dilution. The sections were washed thrice in PBS (5 min per washing step) and incubated for 30 min at RT with biotinylated goat anti-rabbit secondary antibodies (product # TR-125-BN, Lab Vision) (66). Next, the streptavidin peroxidase label reagent (product # TS-125-HR, Lab Vision) was applied for 30 min at RT in a humidified chamber. The colored product was developed by incubation with AEC (product # TA-007-HAC, Lab Vision). The slides were counterstained with hematoxylin and mounted in glycerol gelatin after being washed in distilled water. Both the intensity and the distribution of antigens were scored.

For each sample, a histological score (HSCORE) value was derived by summing the percentages of cells that stained at each intensity multiplied by the weighted intensity of the staining ($HSCORE = \sum P_i (i+1)$, where i is the intensity score and P_i is the corresponding percentage of the cells (67)). MPO was scored in 30 selected glomeruli and peritubular areas (binary scoring system; 1 if leukocytes were observed in the glomerulus and 0 if not).

Statistical analysis

The decay curves of phosphorescence intensity were analyzed in LabVIEW (National Instruments, Austin, TX) as described in (61). Statistical analysis was performed using GraphPad Prism (GraphPad Software, San Diego, CA). Intragroup differences between ordinal variables were analyzed using a two-way ANOVA with a Bonferroni post-hoc test (different time points in the same group). Intergroup differences were analyzed with repeated measures ANOVA using a Tukey post-hoc test (same time points in different groups). A p -value of ≤ 0.05 was considered statistically significant. Data are reported as mean \pm standard deviation (SD).

RESULTS AND DISCUSSION

Characterization and validation of the ischemia/reperfusion acute kidney injury model

To validate our I/R AKI model and the pharmacodynamic effects of TEMPOL in juxtaposition to the results obtained in literature and our parallel study with renal artery occlusion (58), the degree of iNOS expression, oxidative stress, kidney damage, and

inflammation were analyzed first in rats subjected to 30 min of renal ischemia followed by 90 min of reperfusion. This I/R regimen has been standardly employed as a model for AKI (68,69). The renal hemodynamics and oxygenation parameters, which constituted the main focus of the study, are presented and discussed following the model validation.

TEMPOL reduces I/R-induced iNOS and IL-6 expression

Inducible nitric oxide synthase (iNOS), which produces NO from L-arginine upon activation, is replete in macrophages that have infiltrated the injured kidney as well as tubular epithelium (70) but not parenchymal cells (71). iNOS is activated under oxidative stress conditions via redox-sensitive nuclear factor kappa-light-chain-enhancer of activated B cells (NF- κ B) (72) and by pro-inflammatory cytokines such as tumor necrosis factor alpha (TNF- α), IL-1, -6, -12, and -18, as well as interferon- γ (73-75), all of which are released during renal I/R (73,76).

In the renal cortex, iNOS expression was increased in the I/R group compared to control (Figure 3A), which is consistent with earlier reports (77). This trend was mirrored by increased IL-6 immunostaining (Figure 3B), also occurring in accordance with previous findings (78) and thereby validating our I/R AKI model. The administration of TEMPOL before ischemia and during reperfusion ameliorated the extent of iNOS expression (Figure 3A) and decreased IL-6 levels at a similar rate relative to iNOS (Figure 3B). The same trend was observed in TEMPOL-treated rats that did not undergo I/R compared to baseline levels (Ctrl group, Figure 3A and B), most likely because the surgical procedures alone lead to a mild sterile immune response.

An iNOS-reductive effect has not been described before for TEMPOL. Although not confirmed experimentally, this effect is likely related to the superoxide scavenging properties of TEMPOL, as a result of which hydrogen peroxide production and corollary NF- κ B activation (79,80) and thus iNOS hyperactivation and NO overproduction are suppressed. Our parallel study with suprarenal artery clamping as a model for I/R AKI (58) demonstrated a considerable drop in renal NO levels at 90 min reperfusion (reflecting an increase in peroxynitrite formation). The intrarenal NO concentration was restored to pre-I/R levels by TEMPOL pretreatment in that model, implying that peroxynitrite formation was blocked due to reduced superoxide production. Although NO levels were not directly measured in this study, the post-ischemic increase in tissular iNOS (I/R group, Figure 3A) strongly suggests a burst in NO production that, in the absence of excessive superoxide and hence peroxynitrite generation (I/R + TEMPOL group) (29), conferred its well-established protective effects on kidney function and viability (81-86). Thus, inhibition of the pro-inflammatory response and the cell-protective effects by TEMPOL may translate to reduced NOS uncoupling and increased NO bioavailability.

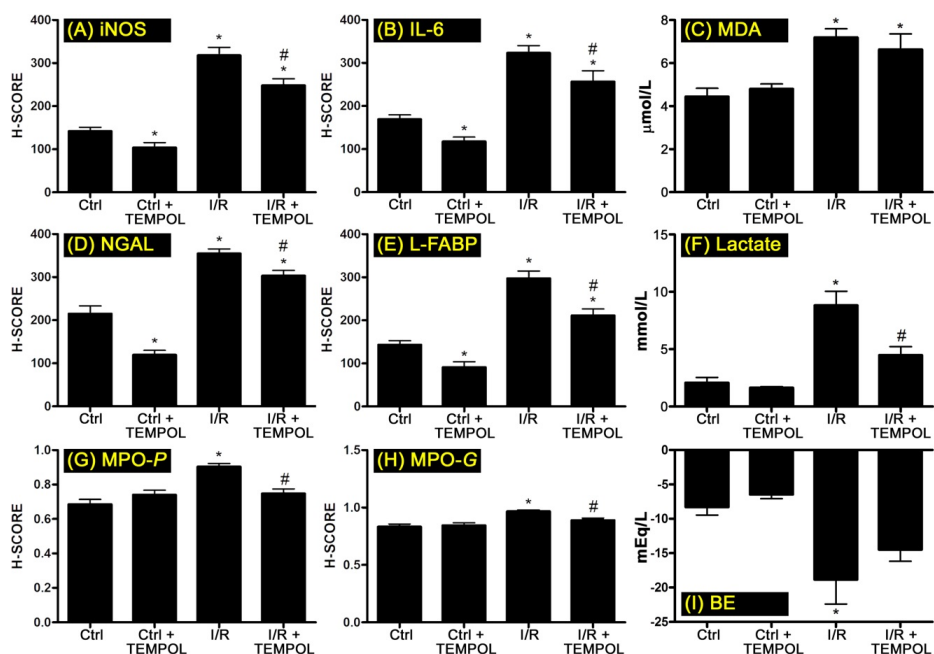


Figure 3. Summary of iNOS activation (A), oxidative stress (C), kidney damage (D-F), inflammation (B, G, H), and base excess (I) following sham operation or 30 min ischemia and 90 min reperfusion in rat kidneys. In the TEMPOL groups, rats received TEMPOL at 200 $\mu\text{mol/kg/h}$ during 105 min (in the I/R + TEMPOL group, 15 min before ischemia and during 90 min of reperfusion).

TEMPOL does not alleviate lipid peroxidation in renal tissue in the acute reperfusion phase following aortic clamping-induced renal I/R

At low concentrations, NO causes dilation of the renal (micro)circulation (87) that is associated with improved renal function after I/R (88). During all phases of I/R, however, superoxide is excessively produced intracellularly and extracellularly by different molecular and cellular sources (10) and reacts with NO to form peroxynitrite (34,35) and tertiary radical derivatives that induce oxidative damage in the cellular and vascular compartment (9,29). As shown in Figure 3C, lipid peroxidation (MDA) in renal tissue was exacerbated by I/R but not reduced by TEMPOL. A TEMPOL-mediated reduction in lipid peroxidation has been reported before in a rat renal I/R model employing 45 min ischemia and 6 h reperfusion (54), which is a more severe I/R model where sufficient time was provided for the manifestation of oxidative/nitrosative stress in the chronic reperfusion phase (10).

As recently advocated (89), pharmacological interventions should be tested in both mild and severe I/R injury models. When the aortic occlusion was performed more proximally to the kidney (i.e., suprarenal artery instead of the abdominal aorta just below the superior mesenteric artery), MDA levels were significantly reduced by prior TEMPOL administration (200 $\mu\text{mol/kg/k}$ for 15 min prior to ischemia but not during the reperfusion phase) (58). This difference in outcome implies that the concomitant manifestation of lower limb ischemia contributed to post-ischemic oxidative stress in the kidneys and abrogated the antioxidant efficacy of TEMPOL, at least at this administered dose.

It should further be noted that the chain propagating redox reaction that is characteristic of lipid peroxidation is mainly deterred by lipophilic antioxidants (29), whereas TEMPOL, with a computed logP of 0.9 (PubChem), is hydrophilic and may therefore not intercalate in cell- and subcellular membranes to prevent lipid peroxidation. Instead, TEMPOL may confer anti-oxidant protection in plasma and the cytosol and thereby prevent superoxide-derived secondary and tertiary ROS/RNS from attacking membrane constituents and reduce renal dysfunction and I/R injury through its superoxide scavenging activity (48,90).

TEMPOL reduces ischemia/reperfusion-mediated acute kidney injury

NGAL and L-FABP are biomarkers of acute kidney injury (91,92). After 90 min of reperfusion, both NGAL and L-FABP were increased in kidney tissue (Figure 3D and E). An increase in NGAL following I/R in rats is in agreement with literature (93,94). No studies could be retrieved for L-FABP in terms of renal I/R injury in rats, although urinary L-FABP levels were found to be predictive of the severity of AKI in mice (95). TEMPOL treatment resulted in decreased levels of these biomarkers in both control and I/R-subjected rats (Figure 3D and E).

Similar results were obtained in terms of plasma lactate (Figure 3F), although this biomarker may have confounding causes such as defects in blood supply (type A lactic acidosis) and perturbed aerobic respiration / electron transport chain functionality in mitochondria (type B lactic acidosis) (96). Both are pertinent to renal I/R AKI but do not reflect direct (histological) tissue injury, in which case lactate is liberated from dying and dead cells. Moreover, lactate is removed from the circulation via renal clearance (mainly under conditions of hyperlactatemia, Figure 3F) and metabolism (97). Renal contribution to lactate metabolism is influenced by renal mitochondrial metabolism (which seemed to be unperturbed based on the $\text{ERO}_{2\text{ren}}$ data) and glomerular filtration (which was absent). The lactate data may therefore also have been skewed by mainly the fact that the I/R-subjected kidneys were hypoperfused (section 3.2.1) and anuric in all

groups (data not shown). This would shift the lactate clearance to the liver (97), despite the fact that the prevailing acidosis during reperfusion (Supplemental Figure 1) generally improves renal removal of lactate and inhibits its hepatic clearance (97). Finally, the extent of contribution of the hind limb ischemia to lactate kinetics and disposition is elusive (98). TEMPOL was not able to restore urine production (i.e., primary kidney function), which was not the case in our parallel study employing a less severe I/R model with suprarenal artery clamping (58). The anuria was likely caused by the significantly reduced MAP (Table 1). TEMPOL did normalize the acidosis (Supplemental Figure 1), most likely due to its beneficial effects on microcirculatory oxygenation in the hind limb and on kidney function, which is related to the production of bicarbonate.

As alluded to previously, the renal damage- and function-ameliorating effects of TEMPOL are well-established. This is partly due to its inhibition of iNOS activation (Figure 3A) inasmuch as the extent of iNOS activation and NO production are proportional to the degree of apoptotic tubular and glomerular cell death (99) and AKI (84,85). Taken together, these data validate the AKI component of our I/R model and connect iNOS/NO to oxidative stress and AKI.

TEMPOL reduces peritubular and glomerular neutrophil influx and inflammation

TEMPOL has been shown to reduce post-ischemic inflammatory signaling in a rat (54) and mouse (57) model of renal I/R and a Guinea pig model of gallbladder I/R (56). Oxidative stress and cell death during I/R lead to highly pleiotropic immune signaling and sterile inflammation (9), which was confirmed in our model on the basis of the IL-6 (Figure 3B) and MPO data (Figure 3G, H). In addition to reducing tissular IL-6 levels following I/R (Figure 3B), TEMPOL treatment also reduced the degree of neutrophil influx into peritubular regions (Figure 3G) as well as glomeruli (Figure 3H), an effect that has been reported previously in the I/R AKI setting (54), albeit in a more rigorous damage model. As depicted in Figure 1 and described in section 1, a reduction in sterile inflammation has beneficial implications on the pathogenesis of AKI. Accordingly, amelioration of pro-inflammatory signaling by TEMPOL (Figure 3B, G, H) was associated with reduced AKI (Figure 3D-F).

Renal hemodynamic and oxygenation alterations in response to moderate ischemic injury

In terms of the parameters assessed in section 3.1, the increase in iNOS activation, oxidative stress, kidney damage, and inflammation during the acute reperfusion phase was generally moderate in our AKI model of 30 min ischemia and 90 min reperfusion compared to studies employing longer I/R durations. The present model was deliberately

employed because (a) it is more clinically representative than our previous work using renal artery clamping (58), (b) it has been standardized for I/R AKI in numerous other studies (e.g., (68,69)), and (c) we did not want to exceed the maximum damage threshold beyond which intervening with TEMPOL would no longer be useful (89). Moreover, as has been explained in detail in (8), iNOS hyperactivation, inflammation, and deleterious changes in mitochondrial metabolism and redox balance have a disproportionately detrimental effect on renal hemodynamics and oxygenation and consequently on primary kidney function (i.e., electrolyte homeostasis mediated by the electrolyte transporter Na^+/K^+ -ATPase, which is a heavy oxygen-consuming process in the kidney (8)) and viability, particularly in the outer medulla and corticomedullary junction (100). Kidneys are particularly sensitive to hypo-oxygenation (I/R) and oxidative/nitrosative stress for several reasons. First, the renal vascular anatomy and physiology (inherently low medullary blood flow and oxygen supply) precludes adequate management of hypoxic/anoxic conditions. Second, a large fraction of the available oxygen is used to produce ATP for the electrolyte transporter Na^+/K^+ -ATPase, as a result of which a relatively minor fraction of ATP is available to sustain cell viability. Third, excessive NO and ROS/RNS production during I/R causes mitochondrial dysfunction and an immediate reduction in renal oxygenation (8,36,58), further debilitating medullary and cortical oxygen availability (58) at the cellular level and therefore primary kidney function and viability. Accordingly, by implementing a moderately injurious ischemia time we could control the parameters addressed in section 3.1 so as to prevent disproportionately severe hypoxia and irreversible kidney damage, to which the hind limb I/R was also expected to contribute (59,60).

TEMPOL reduces increased renal vascular resistance following ischemia/reperfusion but has no effect on other systemic and local hemodynamic parameters

The hemodynamic parameters at baseline, R15, and R90 are listed in Table 1 and show that I/R was associated with a drop in MAP and RBF and an increased RVR. The values in the I/R group clearly demonstrate the more profound impact of aortic clamping on systemic and renal hemodynamic parameters compared to clamping of only the renal artery (58). Illustratively, the MAP in this study decreased by 38% and 47% at R15 and R90, respectively, versus a decrease of merely 7% and -2%, respectively, in case of renal artery clamping (58). These data might be explained by the suprarenal aortic occlusion, which also blocks the inferior mesenteric artery blood supply and may lead to sepsis-induced hypotension due to increased bacterial translocation into blood stream. The RBF declined by 76% (R15) and 78% (R90) after aortic occlusion, in line with previous reports (16), which occurred at approximately half these rates (39% and 37%, respectively) following renal artery occlusion (58). The RVR increased by 313% (R15) and 303% (R90) compared to 154% and 162%, respectively, following renal artery occlusion (58).

Table 1. Hemodynamic parameters at baseline and at 15 min (R15) and 90 min (R90) reperfusion.

	Baseline	R15	R90
MAP (mmHg)			
Ctrl	93.1 ± 10.7	86.1 ± 5.1	69.0 ± 6.6
Ctrl + TEMPOL	92.1 ± 8.1	87.6 ± 8.5	80.8 ± 3.6
I/R	99.0 ± 12.6	53.0 ± 18.7^C	36.5 ± 10.5^C
I/R + TEMPOL	86.3 ± 10.5	60.6 ± 16.9^C	44.3 ± 5.9^C
RBF (mL·min⁻¹)			
Ctrl	4.3 ± 0.7	3.8 ± 1.2	3.2 ± 0.4
Ctrl + TEMPOL	4.2 ± 0.7	3.6 ± 1.0	3.6 ± 1.3
I/R	4.7 ± 1.5	0.9 ± 0.7^C	0.7 ± 0.3^C
I/R + TEMPOL	3.9 ± 0.3	1.9 ± 0.7^C	1.4 ± 0.3^C
RVR (dyn·s·cm²)			
Ctrl	2217 ± 418	2390 ± 671	2169 ± 278
Ctrl + TEMPOL	2208 ± 447	2598 ± 835	2438 ± 800
I/R	2276 ± 801	7485 ± 4316^C	6581 ± 3404^C
I/R + TEMPOL	2238 ± 391	3399 ± 1540^I	3378 ± 928^I

Values are presented as Mean ± SD. A superscript 'C' indicates that $p \leq 0.05$ vs. the control group (Ctrl) and a superscript 'I' signifies that $p \leq 0.05$ vs. the ischemia/reperfusion group (I/R). Abbreviations: MAP; mean arterial pressure, RBF; renal blood flow, RVR; renal vascular resistance.

The increased RVR is attributable to constriction of renal microvasculature, which can have multiple causes such as an I/R-induced imbalance between vasodilatory and vasoconstrictive mediators and compression of peritubular capillaries due to interstitial edema (8). iNOS, which was considerably elevated during I/R (Figure 3A), plays an instrumental role in post-ischemic modulation of vascular tonicity (101,102). These data together attest to the fact that the clinically representative I/R model, which encompasses supraregional effectors (e.g., hind limb I/R), has a more deleterious impact on AKI than when only renal artery occlusion is applied.

The more prolific renal damage profile seemed to be inversely proportional to TEMPOL's pharmacodynamic efficacy, even when the cumulative administered dose was considerably higher compared to that used in the renal artery occlusion study (58) due to the continuous administration throughout the 90-min reperfusion phase. The MAP and RBF were not alleviated by TEMPOL (Table 1), at least not to a statistically significant degree. In the renal artery clamping study (58), TEMPOL evidently exerted no effect on the MAP (which was unimpaired by I/R) but normalized the RBF to Ctrl levels at both R15 and R90 (58). Inasmuch as glomerular filtration rate declines in concordance with declining RBF and the MAP (Table 1) (103-105), it can be inferred that I/R in the present model was associated with strongly deteriorated glomerular filtration (i.e., renal function), supported by the absence of urine production (section 3.1.3), most likely as a result of

systemic hemodynamics (MAP). However, we demonstrated that administration of TEMPOL resulted in a significant improvement in renal vascular resistance as a result of vasodilatation in the renal vascular bed and increased NO bioavailability. Following this line of reasoning, it can be concluded that TEMPOL was partially effective in safeguarding primary renal function after aortic occlusion-induced I/R.

TEMPOL improves cortical and medullary microvascular oxygenation but not renal oxygen delivery, renal oxygen consumption, and renal oxygen extraction ratio

The renal oxygenation parameters are summarized in Table 2. As with the systemic and hemodynamic variables (Table 1), a similar trend was observed in terms of the change amplitude of parameters in the aortic clamping group versus the renal artery clamping group (58). Whereas the DO_{2ren} was decreased by 36% (R15) and 41% (R90) after I/R (58) in the latter group, the decreases following aortic clamping were 76% (R15) and 83% (R90). The rate at which the DO_{2ren} decreased was very comparable to the rate at which the RBF decreased (Table 1 and (58)). Furthermore, the post-ischemic VO_{2ren} was unaffected by renal artery clamping (58) yet considerably compromised by aortic clamping (−79% at R15 and −82% at R90 compared to Ctrl). These events were accompanied by reduced $CuPO_2$ (26% at R15 and 52% at R90) and $MuPO_2$ (32% at R15 and 61% at R90), that, again, encompassed more profound changes in microvascular oxygenation than observed during renal artery occlusion-induced I/R ($CuPO_2$, 16% at R15 and 29% at R90; $MuPO_2$, 7% at R15 and 20% at R90) (58). TEMPOL treatment only partially restored the drop in $CuPO_2$ (↑ by 42%) and $MuPO_2$ (↑ by 68%) at R90, but had otherwise no significant effect on these parameters at R15 or on the DO_{2ren} and VO_{2ren} altogether, despite the fact that these values more than doubled at both reperfusion time points in the I/R + TEMPOL group compared to the I/R group.

Provided that a large fraction of oxygen is used to support the functionality of the Na^+/K^+ -ATPase (8), the observation that ERO_{2ren} remained unaltered following aortic clamping-induced I/R (Table 2) can be biochemically and physiologically accounted for, at least partially. The rise in intrarenal iNOS (Figure 3A) coincides with a burst in local NO production (33) that, in a milieu of concomitant superoxide hyperproduction (23-25,58), results in peroxynitrite formation (34,35) and consequent decrease in Na^+/K^+ -ATPase activity (36). The perturbed Na^+/K^+ -ATPase activity translates to lower oxygen demand in the kidneys (i.e., lowered demand for ATP) and hence a decrease in VO_{2ren} that, under conditions of reduced RBF (Table 1), $CuPO_2$, $MuPO_2$, and DO_{2ren} (Table 2), ultimately has no net effect on ERO_{2ren} .

The ERO_{2ren} is essentially a measure of how well metabolic demand (ATP) is aligned with metabolic supply (oxygen). Inasmuch as the DO_{2ren} reflects oxygen delivery to tissue

Table 2. Renal oxygenation parameters at baseline and at 15 min (R15) and 90 min (R90) reperfusion.

	Baseline	R15	R90
DO_{2ren} (mL O₂/min)			
Ctrl	3.55 ± 0.63	3.01 ± 1.12	2.46 ± 0.42
Ctrl + TEMPOL	3.68 ± 0.61	3.00 ± 0.85	2.98 ± 0.97
I/R	3.81 ± 1.23	0.72 ± 0.57^c	0.43 ± 0.32^c
I/R + TEMPOL	3.17 ± 0.40	1.56 ± 0.69^c	0.99 ± 0.28^c
VO_{2ren} (mL O₂/min/g)			
Ctrl	1.58 ± 0.28	1.47 ± 0.54	1.35 ± 0.26
Ctrl + TEMPOL	1.72 ± 0.28	1.52 ± 0.50	1.60 ± 0.56
I/R	1.36 ± 0.47	0.31 ± 0.23^c	0.24 ± 0.23^c
I/R + TEMPOL	1.31 ± 0.24	0.75 ± 0.40^c	0.58 ± 0.17^c
CμPO₂ (mmHg)			
Ctrl	81.6 ± 7.6	68.9 ± 14.4	70.3 ± 11.3
Ctrl + TEMPOL	89.5 ± 2.7	84.4 ± 6.1^c	69.1 ± 6.3
I/R	84.6 ± 3.2	50.9 ± 14.3^c	33.6 ± 7.6^c
I/R + TEMPOL	89.5 ± 9.4	55.3 ± 8.4^c	47.7 ± 5.4^{c,I}
MμPO₂ (mmHg)			
Ctrl	64.3 ± 8.0	59.8 ± 9.9	56.8 ± 8.2
Ctrl + TEMPOL	68.3 ± 9.0	62.3 ± 7.1	57.0 ± 6.8
I/R	65.8 ± 4.1	40.7 ± 10.8^c	21.9 ± 7.4^c
I/R + TEMPOL	59.7 ± 7.9	43.6 ± 5.4^c	36.7 ± 4.8^{c,I}
ERO_{2ren} (%)			
Ctrl	44.6 ± 3.6	49.3 ± 4.1	55.1 ± 6.7
Ctrl + TEMPOL	46.8 ± 3.2	50.1 ± 5.0	53.6 ± 3.5
I/R	36.2 ± 8.0	44.7 ± 7.9	50.0 ± 21.4
I/R + TEMPOL	40.9 ± 2.6	46.2 ± 7.3	58.5 ± 8.0

Values are presented as Mean ± SD, ^cp < 0.05 vs. Ctrl; ^Ip < 0.05 vs. I/R.

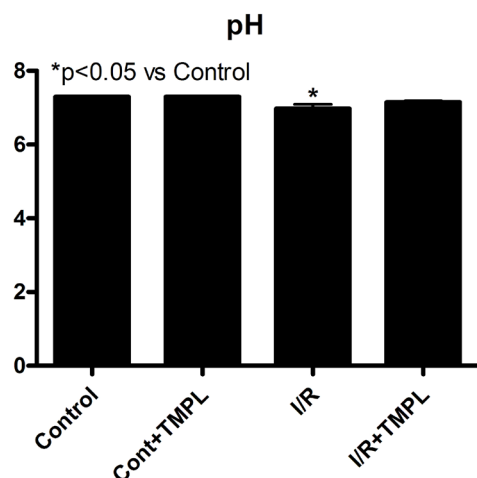
Abbreviations: Ctrl; Control, I/R; ischemia/reperfusion, DO_{2ren}; renal oxygen delivery, VO_{2ren}; renal oxygen consumption, CμPO₂; microvascular oxygen tension in the renal cortex, MμPO₂; microvascular oxygen tension in the renal medulla, ERO_{2ren}%; renal oxygen extraction ratio.

irrespective of the distribution of blood flow, the ERO_{2ren} signifies the degree to which oxygen is uncoupled from hemoglobin and used in aerobic respiration in cells that comprise the perfused tissue. Somewhat surprisingly, post-ischemic renal cells did not exhibit an increased predilection for oxygen (Table 2, ERO_{2ren}) under conditions of hypoperfusion (Table 1, RBF) and reduced μPO₂ (Table 2). It is not illogical to expect that the oxygen-driven metabolic rate in viable mitochondria (23) of hypoxia-subjected cells would be increased to compensate for the perturbed aerobic metabolism in oxidatively compromised mitochondria (46,106). Analogous compensatory effects have been described in other I/R settings, such as reactive hyperemia in upper extremities of human subjects (107) and post-ischemic NADH hyperoxidation in rat livers (21). However, in this case it seems that the metabolic demands of renal cells were met, even

at the clearly perturbed oxygenation parameters (Table 2). In that respect, it has been reported that kidneys are quite able to maintain a stable ERO_{2ren} over a wide range of conditions (108).

Two possible explanations are that, on the one hand, the damage to renal cells was not as profound as the degree of Na^+/K^+ -ATPase shutdown, which would account for the considerable reduction in VO_{2ren} without notable changes in ERO_{2ren} , especially since cessation of Na^+/K^+ -ATPase activity would reallocate the ATP to other vital cell metabolic processes (e.g., survival and damage repair). Such a scenario implies that the impact of the hind limb I/R was most profound on the manifestation of renal pathophysiology. On the other hand, the renal cells were damaged to such an extent (8) that aerobic respiration had mainly ceased in the kidney as a result of mitochondrial dys-/non-function (8,36,58). This is supported by the 79-82% drop in VO_{2ren} during the 90-min reperfusion phase (Table 2), and the prevailing metabolic acidosis, as evidenced by the combination of elevated plasma lactate levels (Figure 3F), reduced pH (Supp. Figure 1), relatively stable pCO_2 values (data not shown), and considerably lowered negative base excess ratio (Figure 3I).

Juxtaposition of our result to literature plead for the first scenario, namely that 30/90 min I/R was in itself not very injurious to the kidney but ultimately led to AKI due to the contribution of hind limb I/R. In a study by de Carvalho *et al.* (93), rats were subjected to 30-min renal artery clamping, after which NGAL and histological damage were determined in blood samples and by evaluation by a pathologist, respectively, at different reperfusion times. A moderate-to-severe damage profile, characterized by 25-50% tubular necrosis, was noted at 12-h reperfusion, which corresponded to a 3,636% increase in plasma NGAL compared to baseline after only renal artery occlusion (93). By deduction, the 167% increase in tissue NGAL (Figure 3D) reflects minimal histological damage. Moreover, a reduction in MAP was not observed after renal clamping (58), altogether pleading in favor of the hypothesis that the hind limb I/R and bacterial translocation conferred a more debilitating effect on kidney viability and function than I/R affecting the kidneys only. In that respect, the metabolic acidosis, as alluded to in the second abovementioned hypothesis, may very well have stemmed from chiefly the hind limb I/R and masked the relatively mild direct effects of this I/R regimen on the kidneys. However, additional studies are warranted to examine the efficacy of higher TEMPOL doses and the pathological contribution of separate anatomical compartments to post-ischemic kidney injury.



Supplemental Figure 1. Plasma pH following sham operation or 30 min ischemia and 90 min reperfusion in rat kidney. Values are presented as Mean ± SD, *p < 0.05 vs. Ctrl.

CONCLUSIONS

In the final analysis, TEMPOL administration at a cumulative dose of 400 $\mu\text{mol/kg}$ before aortic occlusion-induced ischemia and during the early reperfusion phase conferred a protective effect on AKI in terms of renal damage, inflammation, and iNOS production. The beneficial effects of TEMPOL on renal hemodynamics and oxygenation were limited, however, only manifesting themselves at the level of RVR and μPO_2 but not MAP, RBF, $\text{DO}_{2\text{ren}}$, $\text{VO}_{2\text{ren}}$, and $\text{ERO}_{2\text{ren}}$. The main overshadowing elements in the renal pathophysiology were the drop in MAP in consequence to the conjoint hind limb and gut I/R, which led to hypotension and abrogated glomerular filtration (i.e., anuria), and perhaps metabolic acidosis. Although TEMPOL alleviated the metabolic acidosis, the superoxide scavenger exerted no evident beneficial effects on the MAP, which should be accounted for by alternative interventions to ensure sustenance of renal function during clinical procedures that involve aortic (cross-)clamping. Our findings are particularly important for the renal transplantation setting, as these procedures entail aortic clamping as well as stimulation of innate and adaptive immunity following transplantation. A pharmacological role of TEMPOL may therefore be even more limited in this context, and other therapeutics in addition to immunosuppressive drugs should be studied to protect both donor (in case of living donor kidney transplantation) and recipient.

REFERENCES

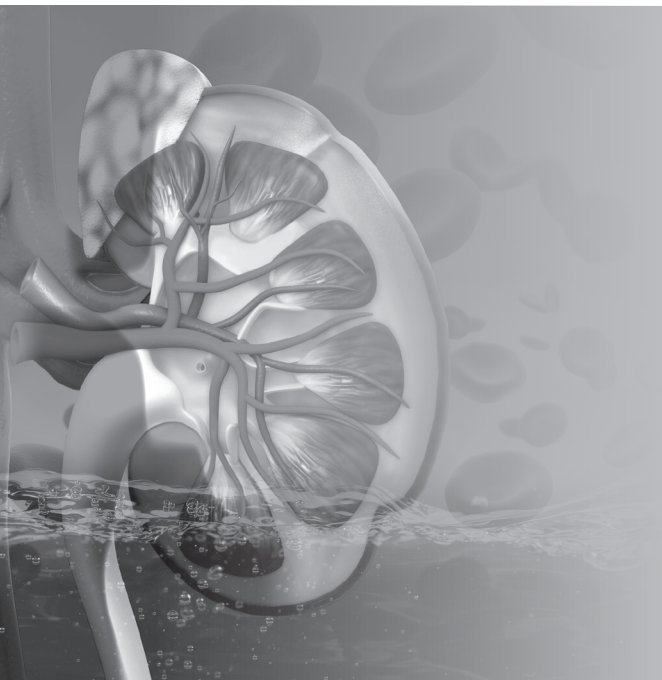
1. Thadhani R, Pascual M, Bonventre JV. Acute renal failure. *N. Engl. J. Med.* 334:1448-1460, 1996.
2. Legrand M, Almac E, Mik EG, *et al.* L-NIL prevents renal microvascular hypoxia and increase of renal oxygen consumption after ischemia-reperfusion in rats. *Am. J. Physiol. Renal Physiol.* 296:F1109-F1117, 2009.
3. Basile DP, Anderson MD, Sutton TA. Pathophysiology of acute kidney injury. *Compr. Physiol.* 2:1303-1353, 2012.
4. Schlosser FJ, Mojibian H, Verhagen HJ, *et al.* Open thoracic or thoracoabdominal aortic aneurysm repair after previous abdominal aortic aneurysm surgery. *J. Vasc. Surg.* 48:761-768, 2008.
5. Maeda T, Watanabe N, Muraki S. Abdominal aortic aneurysm repair in a renal transplant recipient using a femoral V-A bypass. *Ann. Thorac. Cardiovasc Surg.* 15:415-417, 2009.
6. Miranda MP, Genzini T, Noujaim H, *et al.* Aortic clamping in pancreas transplantation: is there any harm to the transplanted kidney graft? *Transplant. Proc.* 44:2397-2398, 2012.
7. Min EK, Kim YH, Han DJ, *et al.* Renal autotransplantation in open surgical repair of suprarenal abdominal aortic aneurysm. *Ann. Surg. Treat. Res.* 89:48-50, 2015.
8. Legrand M, Mik EG, Johannes T, *et al.* Renal hypoxia and dysoxia after reperfusion of the ischemic kidney. *Mol. Med.* 14:502-516, 2008.
9. van Golen RF, van Gulik TM, Heger M. The sterile immune response during hepatic ischemia/reperfusion. *Cytokine Growth Factor Rev.* 23:69-84, 2012.
10. van Golen RF, van Gulik TM, Heger M. Mechanistic overview of reactive species-induced degradation of the endothelial glycocalyx during hepatic ischemia/reperfusion injury. *Free Radic. Biol. Med.* 52:1382-1402, 2012.
11. Legrand M, Kandil A, Payen D, *et al.* Effects of sepiapterin infusion on renal oxygenation and early acute renal injury after suprarenal aortic clamping in rats. *J. Cardiovasc. Pharmacol.* 58:192-198, 2011.
12. Zhang JJ, Kelm RJ, Biswas P, *et al.* PECAM-1 modulates thrombin-induced tissue factor expression on endothelial cells. *J. Cell. Physiol.* 210:527-537, 2007.
13. Snoeijs MG, Vink H, Voesten N, *et al.* Acute ischemic injury to the renal microvasculature in human kidney transplantation. *Am. J. Physiol. Renal Physiol.* 299:F1134-F1140, 2010.
14. van Golen RF, Reiniers MJ, Vrisekoop N, *et al.* The mechanisms and physiological relevance of glycocalyx degradation in hepatic ischemia/reperfusion injury. *Antioxid. Redox Signal* 21:1098-1118, 2014.
15. De VE, Lubatti L, Beretta C, *et al.* Protection from renal ischemia-reperfusion injury by the 2-methylaminochroman U83836E. *Kidney Int.* 54:857-863, 1998.
16. Yamamoto T, Tada T, Brodsky SV, *et al.* Intravital videomicroscopy of peritubular capillaries in renal ischemia. *Am. J. Physiol. Renal Physiol.* 282:F1150-F1155, 2002.
17. Hu L, Chen J, Yang X, *et al.* Assessing intrarenal nonperfusion and vascular leakage in acute kidney injury with multinuclear (1) H/(19) F MRI and perfluorocarbon nanoparticles. *Magn. Reson. Med.* 71:2186-2196, 2014.
18. Brodsky SV, Yamamoto T, Tada T, *et al.* Endothelial dysfunction in ischemic acute renal failure: rescue by transplanted endothelial cells. *Am. J. Physiol. Renal Physiol.* 282:F1140-F1149, 2002.
19. Hattori R, Ono Y, Kato M, *et al.* Direct visualization of cortical peritubular capillary of transplanted human kidney with reperfusion injury using a magnifying endoscopy. *Transplantation* 79:1190-1194, 2005.
20. Kwon O, Wang WW, Miller S. Renal organic anion transporter 1 is maldistributed and diminishes in proximal tubule cells but increases in vasculature after ischemia and reperfusion. *Am. J. Physiol. Renal Physiol.* 295:F1807-F1816, 2008.
21. Kloek JJ, Marechal X, Roelofsen J, *et al.* Cholestasis is associated with hepatic microvascular dysfunction and aberrant energy metabolism before and during ischemia-reperfusion. *Antioxid. Redox Signal* 17:1109-1123, 2012.
22. Funk JA, Schnellmann RG. Persistent disruption of mitochondrial homeostasis after acute kidney injury. *Am. J. Physiol. Renal Physiol.* 302:F853-F864, 2012.

23. Turrens JF. Mitochondrial formation of reactive oxygen species. *J. Physiol.* 552:335-344, 2003.
24. Zulueta JJ, Sawhney R, Yu FS, *et al.* Intracellular generation of reactive oxygen species in endothelial cells exposed to anoxia-reoxygenation. *Am. J. Physiol.* 272:L897-L902, 1997.
25. Plotnikov EY, Kazachenko AV, Vyssokikh MY, *et al.* The role of mitochondria in oxidative and nitrosative stress during ischemia/reperfusion in the rat kidney. *Kidney Int.* 72:1493-1502, 2007.
26. Teruya R, Ikejiri AT, Somaio NF, *et al.* Expression of oxidative stress and antioxidant defense genes in the kidney of inbred mice after intestinal ischemia and reperfusion. *Acta. Cir. Bras.* 28:848-855, 2013.
27. Zhang G, Zou X, Miao S, *et al.* The anti-oxidative role of micro-vesicles derived from human Wharton-Jelly mesenchymal stromal cells through NOX2/gp91(phox) suppression in alleviating renal ischemia-reperfusion injury in rats. *PLoS One* 9:e92129, 2014.
28. Ben MS, Pedruzzi E, Werts C, *et al.* Heat shock protein gp96 and NAD(P)H oxidase 4 play key roles in Toll-like receptor 4-activated apoptosis during renal ischemia/reperfusion injury. *Cell Death Differ.* 17:1474-1485, 210.
29. Reiniers MJ, van Golen RF, van Gulik TM, *et al.* Reactive oxygen and nitrogen species in steatotic hepatocytes: a molecular perspective on the pathophysiology of ischemia-reperfusion injury in the fatty liver. *Antioxid. Redox Signal* 21:1119-1142, 2014.
30. Fridovich I. Superoxide dismutases: defence against endogenous superoxide radical. *Ciba. Found. Symp.* 77-93, 1978.
31. Fridovich I. Superoxide radical and superoxide dismutases. *Annu. Rev. Biochem.* 64:97-112, 1995.
32. Paller MS, Eaton JW. Hazards of antioxidant combinations containing superoxide dismutase. *Free Radic. Biol. Med.* 18:883-890, 1995.
33. Collins JL, Vodovotz Y, Hierholzer C, *et al.* Characterization of the expression of inducible nitric oxide synthase in rat and human liver during hemorrhagic shock. *Shock* 19:117-122, 2003.
34. Huie RE, Padmaja S. The reaction of NO with superoxide. *Free Radic. Res. Commun.* 18:195-199, 1993.
35. Radi R, Peluffo G, Alvarez MN, *et al.* Unraveling peroxynitrite formation in biological systems. *Free Radic. Biol. Med.* 30:463-488, 2001.
36. Szabo C, Modis K. Pathophysiological roles of peroxynitrite in circulatory shock. *Shock* 34 Suppl 1:4-14, 2010.
37. Huang L, Belousova T, Chen M, *et al.* Overexpression of stanniocalcin-1 inhibits reactive oxygen species and renal ischemia/reperfusion injury in mice. *Kidney Int.* 82:867-877, 2012.
38. Cuzzocrea S, Riley DP, Caputi AP, *et al.* Antioxidant therapy: a new pharmacological approach in shock, inflammation, and ischemia/reperfusion injury. *Pharmacol. Rev.* 53:135-159, 2001.
39. Li W, Wu M, Tang L, *et al.* Novel curcumin analogue 14p protects against myocardial ischemia reperfusion injury through Nrf2-activating anti-oxidative activity. *Toxicol. Appl. Pharmacol.* 282:175-183, 2015.
40. van Golen RF, Reiniers MJ, Olthof PB, *et al.* Sterile inflammation in hepatic ischemia/reperfusion injury: present concepts and potential therapeutics. *J. Gastroenterol. Hepatol.* 28:394-400, 2013.
41. Abd-Elsamea AA, Moustaf AA, Mohamed AM. Modulation of the oxidative stress by metformin in the cerebrum of rats exposed to global cerebral ischemia and ischemia/reperfusion. *Eur. Rev. Med. Pharmacol. Sci.* 18:2387-2392, 2014.
42. Li H, Wang Y, Feng D, *et al.* Alterations in the time course of expression of the Nox family in the brain in a rat experimental cerebral ischemia and reperfusion model: effects of melatonin. *J. Pineal Res.* 57:110-119, 2014.
43. Flessas I, Bramis I, Menenakos E, T *et al.* Effects of Iazaroid U-74389G on intestinal ischemia and reperfusion injury in porcine experimental model. *Int. J. Surg.* 13:42-48, 2015.
44. Yang B, Ni YF, Wang WC, *et al.* Melatonin attenuates intestinal ischemia--reperfusion-induced lung injury in rats by upregulating N-myc downstream-regulated gene 2. *J. Surg. Res.* 194:273-280, 2015.
45. Bozkurt M, Kapi E, Kulahci Y, *et al.* Antioxidant support in composite musculo-adipose-fasciocutaneous flap applications: an experimental study. *J. Plast. Surg. Hand Surg.* 48:44-50, 2014.

46. Dare AJ, Bolton EA, Pettigrew GJ, *et al.* Protection against renal ischemia-reperfusion injury in vivo by the mitochondria targeted antioxidant MitoQ. *Redox Biol.* 5:163-168, 2015.
47. Orban JC, Quintard H, Cassuto E, *et al.* Effect of N-acetylcysteine pretreatment of deceased organ donors on renal allograft function: a randomized controlled trial. *Transplantation* 99:746-753, 2015.
48. Fujii T, Takaoka M, Ohkita M, *et al.* Tempol protects against ischemic acute renal failure by inhibiting renal noradrenaline overflow and endothelin-1 overproduction. *Biol. Pharm. Bull.* 28:641-645, 2005.
49. Paller MS, Hoidal JR, Ferris TF. Oxygen free radicals in ischemic acute renal failure in the rat. *J. Clin. Invest.* 74:1156-1164, 1984.
50. Baker GL, Corry RJ, Autor AP. Oxygen free radical induced damage in kidneys subjected to warm ischemia and reperfusion. Protective effect of superoxide dismutase. *Ann. Surg.* 202:628-641, 1985.
51. Schnackenberg CG, Wilcox CS. The SOD mimetic tempol restores vasodilation in afferent arterioles of experimental diabetes. *Kidney Int.* 59:1859-1864, 2001.
52. Zhang C, Xu X, Potter BJ, *et al.* TNF-alpha contributes to endothelial dysfunction in ischemia/reperfusion injury. *Arterioscler. Thromb. Biol.* 26:475-480, 2006.
53. Hein TW, Ren Y, Potts LB, *et al.* Acute retinal ischemia inhibits endothelium-dependent nitric oxide-mediated dilation of retinal arterioles via enhanced superoxide production. *Invest Ophthalmol. Vis. Sci.* 53:30-36, 2012.
54. Chatterjee PK, Cuzzocrea S, Brown PA, Z *et al.* Tempol, a membrane-permeable radical scavenger, reduces oxidant stress-mediated renal dysfunction and injury in the rat. *Kidney Int.* 58:658-673, 2000.
55. Wilcox CS. Effects of tempol and redox-cycling nitroxides in models of oxidative stress. *Pharmacol. Ther.* 126:119-145, 2010.
56. Gomez-Pinilla PJ, Camello PJ, Tresguerres JA, *et al.* Tempol protects the gallbladder against ischemia/reperfusion. *J. Physiol. Biochem.* 66:161-172, 2010.
57. Knight SF, Kundu K, Joseph G, *et al.* Folate receptor-targeted antioxidant therapy ameliorates renal ischemia-reperfusion injury. *J. Am. Soc. Nephrol.* 23:793-800, 2012.
58. Aksu U, Ergin B, Bezemer R, *et al.* Scavenging reactive oxygen species using tempol in the acute phase of renal ischemia/reperfusion and its effects on kidney oxygenation and nitric oxide levels. *Intensive Care Med. Exp.* 3:21, 2015.
59. Awad RW, Barham WJ, Taylor DN, *et al.* The effect of infrarenal aortic reconstruction on glomerular filtration rate and effective renal plasma flow. *Eur. J. Vasc. Surg.* 6:362-367, 1992.
60. Yassin MM, Harkin DW, Barros D'Sa AA, *et al.* Lower limb ischemia-reperfusion injury triggers a systemic inflammatory response and multiple organ dysfunction. *World J. Surg.* 26:115-121, 2002.
61. Johannes T, Mik EG, Ince C. Dual-wavelength phosphorimetry for determination of cortical and subcortical microvascular oxygenation in rat kidney. *J. Appl. Physiol.* (1985) 100:1301-1310, 2006.
62. Andreoli R, Manini P, Corradi M, *et al.* Determination of patterns of biologically relevant aldehydes in exhaled breath condensate of healthy subjects by liquid chromatography/atmospheric chemical ionization tandem mass spectrometry. *Rapid Commun. Mass Spectrom.* 17:637-645, 2003.
63. Sim AS, Salonikas C, Naidoo D, *et al.* Improved method for plasma malondialdehyde measurement by high-performance liquid chromatography using methyl malondialdehyde as an internal standard. *J. Chromatogr. B. Analyt. Technol. Biomed. Life Sci.* 785:337-344, 2003.
64. Pilz J, Meineke I, Gleiter CH. Measurement of free and bound malondialdehyde in plasma by high-performance liquid chromatography as the 2,4-dinitrophenylhydrazine derivative. *J Chromatogr B Biomed Sci Appl.* 742:315-325, 2000.
65. Forman HJ, Augusto O, Brigelius-Flohe R, *et al.* Even free radicals should follow some rules: a guide to free radical research terminology and methodology. *Free Radic. Biol. Med.* 78:233-235, 2015.
66. Demirci C, Gargili A, Kandil A, C *et al.* Inhibition of inducible nitric oxide synthase in murine visceral larva migrans: effects on lung and liver damage. *Chin. J. Physiol.* 49:326-334, 2006.

67. Senturk LM, Seli E, Gutierrez LS, *et al.* Monocyte chemotactic protein-1 expression in human corpus luteum. *Mol. Hum. Reprod.* 5:697-702, 1999.
68. Szeto HH, Liu S, Soong Y, *et al.* Improving mitochondrial bioenergetics under ischemic conditions increases warm ischemia tolerance in the kidney. *Am. J. Physiol. Renal Physiol.* 308:F11-F21, 2015.
69. Zhang J, Zou YR, Zhong X, *et al.* Erythropoietin pretreatment ameliorates renal ischaemia-reperfusion injury by activating PI3K/Akt signalling. *Nephrology (Carlton)* 20:266-272, 2015.
70. Tojo A, Welch WJ, Bremer V, *et al.* Colocalization of demethylating enzymes and NOS and functional effects of methylarginines in rat kidney. *Kidney Int.* 52:1593-1601, 1997.
71. Cattell V, Smith J, Jansen A, *et al.* Localization of inducible nitric oxide synthase in acute renal allograft rejection in the rat. *Transplantation* 58:1399-1402, 1994.
72. Hur GM, Ryu YS, Yun HY, *et al.* Hepatic ischemia/reperfusion in rats induces iNOS gene transcription by activation of NF-kappaB. *Biochem. Biophys. Res. Commun.* 261:917-922, 1999.
73. Daemen MA, van't Veer C, Wolfs TG, *et al.* Ischemia/reperfusion-induced IFN-gamma up-regulation: involvement of IL-12 and IL-18. *J. Immunol.* 162:5506-5510, 1999.
74. Spink J, Cohen J, Evans TJ. The cytokine responsive vascular smooth muscle cell enhancer of inducible nitric oxide synthase. Activation by nuclear factor-kappa B. *J. Biol. Chem.* 270:29541-29547, 1995.
75. Yu X, Kennedy RH, Liu SJ. JAK2/STAT3, not ERK1/2, mediates interleukin-6-induced activation of inducible nitric-oxide synthase and decrease in contractility of adult ventricular myocytes. *J. Biol. Chem.* 278:16304-16309, 2003.
76. Freitas MC, Uchida Y, Lassman C, *et al.* Type I interferon pathway mediates renal ischemia/reperfusion injury. *Transplantation* 92:131-138, 2011.
77. Pararajasingam R, Weight SC, Bell PR, *et al.* Endogenous renal nitric oxide metabolism following experimental infrarenal aortic cross-clamp-induced ischaemia-reperfusion injury. *Br. J. Surg.* 86:795-799, 1999.
78. Kielar ML, John R, Bennett M, *et al.* Maladaptive role of IL-6 in ischemic acute renal failure. *J. Am. Soc. Nephrol.* 16:3315-3325, 2005.
79. Schmidt KN, Amstad P, Cerutti P, *et al.* The roles of hydrogen peroxide and superoxide as messengers in the activation of transcription factor NF-kappa B. *Chem. Biol.* 2:13-22, 1995.
80. Morgan MJ, Liu ZG. Crosstalk of reactive oxygen species and NF-kappaB signaling. *Cell Res.* 21:103-115, 2011.
81. Chatterjee PK. Novel pharmacological approaches to the treatment of renal ischemia-reperfusion injury: a comprehensive review. *Naunyn Schmiedebergs Arch. Pharmacol.* 376:1-43, 2007.
82. Kucuk HF, Kaptanoglu L, Ozalp F, *et al.* Role of glyceryl trinitrate, a nitric oxide donor, in the renal ischemia-reperfusion injury of rats. *Eur. Surg. Res.* 38:431-437, 2006.
83. Jeong GY, Chung KY, Lee WJ, *et al.* The effect of a nitric oxide donor on endogenous endothelin-1 expression in renal ischemia/reperfusion injury. *Transplant. Proc.* 36:1943-1945, 2004.
84. Noiri E, Peresleni T, Miller F, *et al.* In vivo targeting of inducible NO synthase with oligodeoxynucleotides protects rat kidney against ischemia. *J. Clin. Invest.* 97:2377-2383, 1996.
85. Chatterjee PK, Patel NS, Kvale EO, *et al.* Inhibition of inducible nitric oxide synthase reduces renal ischemia/reperfusion injury. *Kidney Int.* 61:862-871, 2002.
86. Vinas JL, Sola A, Genesca M, *et al.* NO and NOS isoforms in the development of apoptosis in renal ischemia/reperfusion. *Free Radic. Biol. Med.* 40:992-1003, 2006.
87. Zatz R, de NG. Effects of acute nitric oxide inhibition on rat glomerular microcirculation. *Am. J. Physiol.* 261:F360-F363, 1991.
88. Rhoden EL, Rhoden CR, Lucas ML, *et al.* The role of nitric oxide pathway in the renal ischemia-reperfusion injury in rats. *Transpl. Immunol.* 10:277-284, 2002.
89. van Golen RF, Reiniers MJ, Heger M, *et al.* Solutions to the discrepancies in the extent of liver damage following ischemia/reperfusion in standard mouse models. *J. Hepatol.* 62:975-977, 2015.
90. Chatterjee PK, Zacharowski K, Cuzzocrea S, *et al.* Inhibitors of poly (ADP-ribose) synthetase reduce renal ischemia-reperfusion injury in the anesthetized rat in vivo. *FASEB J.* 14:641-651, 2000.
91. Yamamoto T, Noiri E, Ono Y, *et al.* Renal L-type fatty acid--binding protein in acute ischemic injury. *J. Am. Soc. Nephrol.* 18:2894-2902, 2007.

92. Mishra J, Ma Q, Kelly C, *et al.* Kidney NGAL is a novel early marker of acute injury following transplantation. *Pediatr. Nephrol.* 21:856-863, 2006.
93. de Carvalho AL, Vital RB, Kakuda CM, *et al.* Dexmedetomidine on renal ischemia-reperfusion injury in rats: assessment by means of NGAL and histology. *Ren. Fail.* 37:526-530, 2015
94. Chen X, Liu X, Wan X, *et al.* Ischemic preconditioning attenuates renal ischemia-reperfusion injury by inhibiting activation of IKKbeta and inflammatory response. *Am. J. Nephrol.* 30:287-294, 2009.
95. Negishi K, Noiri E, Doi K, *et al.* Monitoring of urinary L-type fatty acid-binding protein predicts histological severity of acute kidney injury. *Am. J. Pathol.* 174:1154-1159, 2009.
96. Fall PJ, Szerlip HM. Lactic acidosis: from sour milk to septic shock. *J. Intensive Care Med.* 20:255-271, 2005.
97. Bellomo R. Bench-to-bedside review: lactate and the kidney. *Crit. Care* 6:322-326, 2002.
98. James JH, Luchette FA, McCarter FD, *et al.* Lactate is an unreliable indicator of tissue hypoxia in injury or sepsis. *Lancet* 354:505-508, 1999.
99. Hruby Z, Rosinski M, Tyran B. Parenchymal injury in remnant-kidney model may be linked to apoptosis of renal cells mediated by nitric oxide. *J. Nephrol.* 21:686-693, 2008.
100. Eckardt KU, Bernhardt WM, Weidemann A, *et al.* Role of hypoxia in the pathogenesis of renal disease. *Kidney Int. Suppl.* S46-S51, 2005.
101. Goligorsky MS, Brodsky SV, Noiri E. NO bioavailability, endothelial dysfunction, and acute renal failure: new insights into pathophysiology. *Semin. Nephrol.* 24:316-323, 2004.
102. Gunnnett CA, Lund DD, McDowell AK, *et al.* Mechanisms of inducible nitric oxide synthase-mediated vascular dysfunction. *Arterioscler. Tromb. Vasc. Biol.* 25:1617-1622, 2005.
103. Tanner GA. Kidney function; in Rhoades RA, Bell DR, (eds): *Medical Physiology: Principles for Clinical Medicine*. Baltimore, MD, Lippincott, Williams & Wilkins, pp 399-427, 2013.
104. Brezis M, Heyman SN, Epstein FH. Determinants of intrarenal oxygenation. II. Hemodynamic effects. *Am. J. Physiol.* 267:F1063-F1068, 1994.
105. Rosen S, Epstein FH, Brezis M. Determinants of intrarenal oxygenation: factors in acute renal failure. *Ren. Fail.* 14:321-325, 1992.
106. Saba H, Batinic-Haberle I, Munusamy S, *et al.* Manganese porphyrin reduces renal injury and mitochondrial damage during ischemia/reperfusion. *Free Radic. Biol. Med.* 2:1571-1578, 2007.
107. Bezemer R, Klijn E, Khalilzada M, *et al.* Validation of near-infrared laser speckle imaging for assessing microvascular (re)perfusion. *Microvasc. Res.* 79:139-143, 2010.
108. Levy MN. Effect of variations of blood flow on renal oxygen extraction. *Am. J. Physiol.* 199:13-18, 1960.



CHAPTER 5

Mycophenolate mofetil improves renal hemodynamics, renal microvascular oxygenation, and inflammation in a rat model of supra-aortic clamping mediated-renal ischemia reperfusion injury

Adapted from *Clin. Exp. Pharmacol. Physiol.* 2017 Feb;44(2):294-304

Bulent Ergin¹, Michal Heger², Asli Kandil³, Cihan Demirci-Tansel³, Can Ince^{1,4}

¹ Department of Translational Physiology, Academic Medical Center, University of Amsterdam, Amsterdam, The Netherlands

² Department of Experimental Surgery, Academic Medical Center, University of Amsterdam, Amsterdam, The Netherlands

³ Department of Biology, Faculty of Science, University of Istanbul, Istanbul, Turkey

⁴ Department of Intensive Care, Erasmus MC, University Medical Center, Rotterdam, The Netherlands

ABSTRACT

Ischemia/reperfusion (I/R) is one of the main causes of acute kidney injury (AKI), which is characterized by sterile inflammation and oxidative stress. Immune cell activation may provoke overproduction of the inflammatory mediators and reactive oxygen species (ROS) leading to perturbation of the microcirculation and tissue oxygenation associated with local and remote tissue injury. This study investigated whether the clinically employed immunosuppressant mycophenolate mofetil (MMF), is able to reduce I/R-induced renal oxygenation defects and oxidative stress by preventing sterile inflammation. Rats were divided into 3 groups (n = 6/group): (1) a sham-operated control group; (2) a group subjected to renal I/R alone (I/R); and (3) a group subjected to I/R and MMF treatment (20 mg/kg prior to I/R) (I/R + MMF). Ischemia was induced by vascular occluder placed on the abdominal aorta over 30min followed by 120 min. reperfusion. Renal I/R deteriorated renal oxygenation ($p < 0.001$) and oxygen delivery ($p < 0.01$), reduced creatinine clearance ($p < 0.01$) and tubular sodium reabsorption ($p < 0.001$), and increased iNOS, renal tissue injury markers ($p < 0.001$), and IL-6 ($p < 0.001$). Oral MMF administration prior to insult restored renal cortical oxygenation ($p < 0.05$) and iNOS, renal injury markers, and inflammation parameters ($p < 0.001$) to (near-)baseline levels without affecting renal function. MMF exerts a prophylactic effect on renal microvascular oxygenation and abrogates tissue inflammation and renal injury following lower body I/R-induced AKI. This may have clinical implications during major vascular or renal transplant surgery.

Keywords: ischemia/reperfusion, mycophenolate mofetil, microvascular oxygenation, inflammation, immunosuppression

INTRODUCTION

Acute kidney injury (AKI) (1) is a deleterious condition associated with a high degree of morbidity and mortality despite proper implementation of various critical care interventions. Presently, no effective treatment is available for AKI. Ischemia/reperfusion (I/R) injury is one of the main causes of AKI¹, and predominantly occurs after major abdominal vascular surgery (2).

Sterile inflammation is propagated through various mechanisms by I/R-subjected kidneys. First, hypoxia stimulates the production and release of pro-inflammatory cytokines and chemokines from parenchymal cells, including tumor necrosis factor alpha (TNF- α) and monocyte chemoattractant protein 1 (MCP-1) (3). Second, ROS cause oxidative degradation of the endothelial glycocalyx (4,5), in oxidatively stressed kidneys (6,7). Glycocalyx degradation products such as hyaluronan (8) and heparin sulfate (9) are potent inducers of sterile inflammation (4). Third, oxidatively stressed, dying, and dead cells release damage-associated molecular patterns (DAMPs) such as high mobility group box 1 (HMGB1) (10) that further fuel the sterile immune response (11). Fourth, I/R-induced endothelial damage causes thrombosis in the renal microcirculation (12). Consequently, post-ischemic kidneys constitute a preferred 'meeting place' for various types of chemoattracted immune cells (e.g., neutrophils and monocytes/macrophages (13)) that become stationary in the kidneys as a result of endothelial perturbations (14), and expression of leukocyte adhesion molecules (13,15,16). All of these interactions, activated molecules and cells finally play a detrimental role on the microcirculatory oxygenation and cell survival. Pharmacologically intervening in post-ischemic sterile inflammation and its effects on the microcirculatory oxygenation may therefore be a viable means to ameliorate I/R damage and hence AKI.

Mycophenolate mofetil (MMF), the prodrug of mycophenolic acid (MPA), is an immunosuppressant that is currently used in organ transplantation and under evaluation in immune-mediated inflammatory diseases (17,18). MPA depletes guanosine triphosphate pools in lymphocytes and monocytes and suppresses the de novo synthesis of purines, exerting a selective and reversible anti-proliferative activity on these cells. In addition, MPA inhibits production of cell-surface adhesion molecules, which is critical for the recruitment of leukocytes to sites of inflammation (19,20), and reduces infiltrating macrophages/lymphocytes and cell proliferation after ischemia (21). Several studies have demonstrated that blockade of leukocytes and adhesion molecules are protective against post-ischemic renal injury (22,23). Additionally, it has been reported that pre-treatment of MMF before the ischemic insult improve in renal blood flow and inulin clearances after 2 days of ischemia (21). Even though positive effect of the MMF

on renal function, inflammation and damage has been shown before (21,24,25), herein we tested the effect of immunosuppression on renal microcirculatory oxygenation. Therefore, we hypothesized that the factors responsible for renal microcirculatory dysfunction and alteration of oxygenation include a combination of inflammatory and/or hypoxemic insults. These cause the activation of all type of leucocytes and inflammatory mediators which adversely impact normal renal microcirculation and oxygenation essential for the renal function. Accordingly, the aim of this study was to determine whether a short term of controlled inflammatory activation by use of MMF improves renal microvascular oxygenation and function in a rat model of supra-aortic occlusion mediated lower body I/R.

MATERIAL AND METHODS

Animals

All animal experiments were approved by the Animal Experimentation Committee of Academic Medical Center (DFL 83). Animal care and handling were performed according to the Guide for the Care and Use of Laboratory Animals (NIH Publication 85-23, 1985). Experiments were performed on 18 male *Wistar albino* rats (Harlan, Horst, The Netherlands) with a mean \pm SD body weight of 325 ± 6 g. The animal protocol has been described in detail elsewhere (26).

Animal surgery and anesthesia

The rats were anesthetized by intraperitoneal administration of ketamine (90 mg/kg, Nimatek, Eurovet, Bladel, The Netherlands), medetomidine (0.5 mg/kg, Domitor, Pfizer, New York, NY), and atropine sulfate (0.05 mg/kg, Centrafarm, Etten-Leur, The Netherlands). The animals were intubated via a tracheotomy and mechanically ventilated with an inspired oxygen fraction of 0.4. Body temperature was maintained at 37 ± 0.5 °C during the entire experiment. The ventilator settings were adjusted to maintain an arterial partial carbon dioxide pressure (PCO_2) between 35 and 40 Torr.

For fluid administration and hemodynamic monitoring, vessels were cannulated with polyethylene catheters (outer diameter of 0.9 mm, B. Braun Melsungen, Melsungen, Germany). The catheter in the right carotid artery was connected to a pressure transducer to monitor arterial blood pressure and heart rate. The right jugular vein was cannulated for continuous infusion of Ringer's lactate (Baxter International, Deerfield, IL) at a rate of $15 \text{ mL} \cdot \text{kg}^{-1} \cdot \text{h}^{-1}$ and 50 mg/kg ketamine dissolved in Ringer's lactate at a rate of 5 mL/kg/h for the infusion of maintenance anesthesia. The right femoral artery was cannulated for drawing blood samples and the right femoral vein for Oxyphor G2, fluid and sodium pentobarbital administration.

The left kidney was exposed, decapsulated, and immobilized in a kidney cup via a 4-cm incision in the left flank. Renal vessels were carefully separated while preserving nerves and adrenal glands. A perivascular ultrasonic transient time flow probe (model 0.7 RB, Transonic Systems, Ithaca, NY) was placed around the left renal artery and connected to a flow meter (model T206, Transonic Systems) to allow continuous measurement of renal blood flow (RBF). The left ureter was isolated, ligated, and cannulated with a polyethylene catheter for urine collection.

After the surgical protocol (~60 min), one optical fiber was placed 1 mm above the decapsulated kidney and another optical fiber was placed 1 mm above the renal vein to measure oxygenation based on phosphorescence lifetimes as described in elsewhere.² Oxyphor G2 (Oxygen Enterprises, Philadelphia, PA) was dissolved in saline at a 6-mg/mL concentration and infused (6 mg/kg) as a bolus into the femoral vein. Before baseline measurement and ischemic insult, animals were kept over 30 min. of recovery period following surgery.

After the experiment, the kidney was removed, weighed, and sectioned longitudinally into two parts. One part was fixed in 10% buffered formalin for immunohistochemical analysis and the other part was snap frozen in liquid nitrogen and stored at -20 °C for analysis of lipid peroxidation. The animals were sacrificed by systemic administration of 1 mL/kg b.w. sodium pentobarbital through the femoral vein.

Experimental protocol

The animals were divided into 3 groups. The first group ($n = 6$) comprised a control group that was subjected to surgery but that did not undergo any interventions. In the I/R group ($n = 6$), animals were subjected to lower body ischemia for 30 min by supra renal aortic occlusion with a custom-made vascular occluder followed by 2 h of reperfusion. The vascular occluder was placed on the aorta beneath mesenteric artery and above the renal artery. Animals in the I/R + MMF group ($n = 6$) underwent the same procedure as the animals in the I/R group but received MMF (20 mg/kg) per gavage directly before the surgery.

Blood gas analysis

Arterial blood samples (0.5 mL) were taken from the femoral artery at three time points: before aortic occlusion (baseline, BL), 15 min after reperfusion (early reperfusion phase, R15), and 120 min after reperfusion (late reperfusion phase, R120). The blood samples were replaced by the same volume of hydroxyethyl starch solution (Voluven, 6% HES 130/0.4, Fresenius Kabi, Bad Homburg vor der Höhe, Germany) through the femoral vein. Blood gases were assayed on an ABL505 blood gas analyzer (Radiometer,

Copenhagen, Denmark). The hemoglobin concentration, hemoglobin oxygen saturation, and sodium and potassium concentration were determined on an OSM 3 blood gas analyzer (Radiometer).

Measurement of renal microvascular oxygenation and renal venous PO₂

Oxygen-quenched phosphorescence lifetimes of systemically infused Oxyphor G2, which conjugates to albumin and is therefore circulation-confined, were measured with a dual-wavelength time-domain phosphorimeter capable of measuring microvascular PO₂ (μPO_2) (27). Oxyphor G2 has two excitation peaks ($\lambda_{\text{excitation1}} = 440 \text{ nm}$, $\lambda_{\text{excitation2}} = 632 \text{ nm}$) and one emission peak ($\lambda_{\text{emission}} = 800 \text{ nm}$), which allows simultaneous lifetime measurements in the kidney cortex and the outer medulla because of different optical penetration depths of the excitation light (28). For the measurement of renal venous PO₂ (rvPO_2), a single-wavelength frequency-domain phosphorimeter was used (29).

Calculation of renal oxygen delivery, consumption, and renal vascular resistance

Renal oxygen delivery ($\text{DO}_{2\text{ren}}$) was calculated by $\text{RBF} \times \text{arterial O}_2 \text{ content}$ ($1.31 \times \text{Hb} \times \text{SaO}_2$) + $(0.003 \times \text{PaO}_2)$, where SaO_2 represents arterial oxygen saturation and PaO_2 represents arterial partial oxygen pressure. Renal venous O₂ content was calculated by $(1.31 \times \text{Hb} \times \text{rvSaO}_2) + (0.003 \times \text{rvPaO}_2)$, where rvSaO_2 represents renal vein oxygen saturation. The rvSaO_2 was calculated using the Hill equation with $\text{P50} = 37 \text{ Torr}$ (4.9 kPa) and Hill coefficient = 2.7. Renal oxygen consumption ($\text{VO}_{2\text{ren}}$) was calculated by $\text{RBF} \times (\text{arterial} - \text{renal venous O}_2 \text{ content})$. An estimation of the renal vascular resistance (RVR) was made on the basis of $\text{RVR} = \text{MAP} / \text{RBF}$.

Assessment of kidney function

Creatinine clearance ($\text{Clear}_{\text{crea}}$ (mL/min)) was measured as an index of the glomerular filtration rate. Creatinine clearance was calculated with the following formula: $\text{Clear}_{\text{crea}} = (\text{U}_{\text{crea}} \times \text{V}) / \text{P}_{\text{crea}}$, where U_{crea} was the concentration of creatinine in urine, V is the urine volume per unit time and P_{crea} was the concentration of creatinine in plasma. The total amount of sodium reabsorbed by kidney was calculated (TNa^+ , mmol/min) according to: $(\text{Clear}_{\text{crea}} \times \text{P}_{\text{Na}}) - \text{U}_{\text{Na}} \times \text{V}$, where P_{Na} was the plasma sodium concentration and U_{Na} was the urine sodium concentration. Fractional excretion of sodium (EFNa^+) was calculated with following formula: $(\text{U}_{\text{Na}} \times \text{P}_{\text{crea}}) / (\text{U}_{\text{crea}} \times \text{P}_{\text{Na}}) \times 100$. The renal oxygen consumption efficiency for sodium transport ($\text{VO}_{2\text{ren}} / \text{TNa}^+$) was assessed as the ratio of the renal VO_2 over the total amount of sodium reabsorbed (TNa^+ , (mmol/min)).

Determination of lipid peroxidation

Lipid peroxidation was determined by tissue malondialdehyde (MDA) levels as a measure of oxidative stress in the lipid compartment. Snap frozen kidney samples were

homogenized in ice-cold 5 mM sodium phosphate buffer. The homogenates were centrifuged at 12,000 $\times g$ for 15 min at 4 °C and supernatants were used for MDA determination. MDA was quantified using a Quattro Premier XE tandem mass spectrometer (MS/MS, Waters, Milford, MA) with an Acquity sample manager and an Acquity binary solvent manager in accordance with (26,30).

Immunohistochemistry

Formalin-fixed tissue samples were embedded in paraffin. Kidney sections (5 μm) were deparaffinized with xylene and rehydrated with decreasing percentages of ethanol and finally with water. Antigen retrieval was accomplished by microwaving the sections in citrate buffer (pH = 6.0) for 10 min at 800 W. Sections were left to cool for 20 min at room temperature (RT) and rinsed with distilled water. Endogenous peroxidase activity was blocked with 3% H₂O₂ for 10 min at RT and later rinsed with distilled water and PBS. Blocking reagent (TA-125-UB, Lab Vision, Fremont, CA) was applied to each section followed by 5-min incubation at RT in a humid chamber. Kidney sections were incubated overnight at 4 °C with rabbit polyclonal iNOS antibody (iNOS Ab-1, Rabbit PAb, RB-1605-P, NeoMarkers, Fremont, CA) and anti-IL-6 antibodies (Abcam, 6672). Additionally, the sections were incubated for 1 h at room temperature with anti-myeloperoxidase (MPO) antibodies (Myeloperoxidase Ab-1, RB-373-A, NeoMarkers), anti-lipocalin 2 antibodies (NGAL) (Abcam 41105), and polyclonal antibody to rat L-FABP (Hycult Biotech HP8010) described in detail elsewhere (31).

The staining intensity and the distribution of iNOS, NGAL, L-FABP and IL-6 were quantified in blinded tissue samples. For each sample, a histological score (HSCORE) value was derived by summing the percentages of cells that stained at each intensity multiplied by the weighted intensity of the staining ($HSCORE = \sum P_i (i+1)$, where i is the intensity score and P_i is the corresponding percentage of the cells, i.e., the distribution as a described in) in 10 randomly selected area of view (x200 magnification) in the renal cortex and medulla (32,33). MPO was scored in 30 selected glomeruli and peritubular areas (binary scoring system; 1 if leukocytes were observed in the glomerulus and 0 if not).

Data and statistical analysis

The decay curves of phosphorescence intensity were analyzed with dedicated software (LabVIEW 6.1, National Instruments, Austin, TX) as described elsewhere (27). Statistical analysis was performed in GraphPad Prism (GraphPad Software, San Diego, CA). Two-way analysis of variance (ANOVA) and Bonferroni post-hoc testing were used for repeated measurements to determine intergroup and intragroup differences. Intergroup comparisons for lactate, MDA, creatinine clearances and TNa⁺ were analyzed by one-way ANOVA with Tukey post-hoc test. A p-value of < 0.05 was considered statistically significant. Values are reported as mean \pm SD.

RESULTS

MMF improves systemic and renal hemodynamics following ischemia

The systemic and renal hemodynamic variables are presented in Table 1. Mean arterial pressure (MAP) and heart rate (HR) remained stable throughout the experiment in all groups. The RBF was constant in the control group at all stages of the experiment, whereas a significant decrease was observed in the I/R group at the R15 ($p < 0.001$) and R120 ($p < 0.001$) time points and I/R + MMF groups at R15 ($p < 0.05$) and R120 ($p < 0.001$). However, MMF treatment resulted in a significantly improved RBF relative to the I/R group at R120 ($p < 0.05$) and it was also substantially increased at BL compared to the control. The RVR was significantly increased in the I/R group at all reperfusion time points compared to the control group ($p < 0.001$). MMF treatment restored the RVR to near-baseline levels in ischemia-subjected kidneys at entire reperfusion ($p < 0.001$).

MMF improves renal oxygenation following ischemia

The calculation of DO_{2ren} and VO_{2ren} , and renal cortical and medullar oxygenation measurements are summarized in Table 2. The DO_{2ren} decreased significantly in the I/R group at R15 ($p < 0.001$) and R120 ($p < 0.01$) compared to control. MMF administration

Table 1. Results of systemic and renal hemodynamic variables.

	BL	R15	R120
MAP [mmHg]			
Control	84.6 ± 5.7	86.1 ± 9.2	72.3 ± 7.5
I/R	94.6 ± 10.8	96.8 ± 18.0	69.5 ± 12.2
I/R + MMF	88.6 ± 5.1	95.5 ± 14.6	70.0 ± 6.9
HR [bpm]			
Control	229 ± 30	233 ± 22	244 ± 24
I/R	207 ± 25	215 ± 17	226 ± 25
I/R + MMF	217 ± 15	232 ± 14	234 ± 19
RBF [mL/min]			
Control	4.3 ± 0.4	4.4 ± 1.2	4.6 ± 1.2
I/R	4.8 ± 1.1	2.6 ± 1.2***	1.6 ± 0.9***
I/R + MMF	5.7 ± 1.1	3.4 ± 1.2*	3.2 ± 1.2***,†
RVR [dyn•sec/cm²]			
Control	19.6 ± 3.4	20.7 ± 6.5	16.1 ± 3.1
I/R	21.2 ± 8.6	44.1 ± 19.8***	51.3 ± 21.6***
I/R + MMF	16.3 ± 4.4	29.7 ± 8.8***	23.9 ± 8.5***

Values are presented as Mean ± SD, * $p < 0.05$, *** $p < 0.001$ vs. Control group; † $p < 0.05$, *** $p < 0.001$ vs. I/R group. Abbreviations: BL; baseline, R15; reperfusion at 15 min, R120; reperfusion at 120 min, MAP; mean arterial pressure, HR; heart rate, RBF; renal blood flow, RVR; renal vascular resistance, I/R; ischemia/reperfusion, MMF; mycophenolate mofetil.

Table 2. Results of renal oxygenation variables.

	BL	R15	R120
DO_{2ren} [mL/min]			
Control	3.5 ± 0.4	3.6 ± 1.2	3.7 ± 1.0
I/R	4.0 ± 0.8	2.1 ± 1.1^{***}	1.2 ± 0.7^{**}
I/R + MMF	4.7 ± 0.9[*]	2.8 ± 1.0	2.5 ± 1.0^{***,*}
VO_{2ren} [mL/min]			
Control	1.5 ± 0.2	1.7 ± 0.7	2.1 ± 0.6
I/R	1.6 ± 0.3	0.9 ± 0.6	0.5 ± 0.3
I/R + MMF	1.9 ± 0.4	1.2 ± 0.5	1.2 ± 0.6
CuPO₂ [torr]			
Control	86.4 ± 3.2	80.7 ± 4.7	80.0 ± 6.3
I/R	84.4 ± 4.6	69.4 ± 6.6^{**}	59.4 ± 5.2^{***}
I/R + MMF	87.8 ± 6.8	77.2 ± 7.4⁺	66.8 ± 5.7^{***,*}
MuPO₂ [torr]			
Control	63.6 ± 5.6	60.5 ± 5.5	56.4 ± 5.9
I/R	60.5 ± 5.6	55.3 ± 3.5	47.1 ± 4.8^{***}
I/R + MMF	64.8 ± 1.8	55.4 ± 3.4	49.5 ± 2.2[*]

Values are presented as Mean ± SD, *p < 0.05, **p < 0.01 and ***p < 0.001 vs. Control group; +p < 0.05 vs. I/R group. Abbreviations: BL; baseline, R15; reperfusion at 15 min, R120; reperfusion at 120 min, DO_{2ren}; renal oxygen delivery, VO_{2ren}; renal oxygen consumption, CuPO₂; cortical microvascular oxygen pressure, MuPO₂; medullar microvascular oxygen pressure, I/R; ischemia/reperfusion, MMF; mycophenolate mofetil.

improved the DO_{2ren} at the BL and R120 compared to the control (p<0.05 and p<0.01, respectively). The DO_{2ren} at R120 was also improved by MMF with respect to I/R group (p<0.05). There were no significant differences with respect to VO_{2ren} in any of the groups at any of the time points. The cortical μPO₂ decreased in the I/R group at R15 (p<0.01) and R120 (p<0.001) compared to the control but was improved at 15 (p<0.05) and 120 min reperfusion (p<0.05) by MMF administration compared to the I/R group. Finally, medullar μPO₂ had significantly deteriorated at 120 min reperfusion and was not restored by MMF treatment.

Blood gas analysis, acid-base and electrolytes status

The complete blood gas analysis is summarized in Table 3. No differences were found in arterial partial pressure of oxygen (PaO₂), hemoglobin oxygen saturation (sO₂Hb), total hemoglobin (Hb) and hematocrit (Hct) between the groups. Arterial partial pressure of carbon dioxide (PaCO₂) was higher in I/R+MMF group at R120 than the control. Partial pressure of oxygen required to saturate %50 of hemoglobin (P50) was increased in I/R at R15 and R120, and in I/R+MMF group at R120 with respect to the control. Acid-base status and plasma electrolytes levels were reported in Table 4. While base excess (BE), plasma bicarbonate (HCO₃⁻) and Na⁺ levels were stable in all groups, decreased pH in I/R group at R120 and increased K⁺ level was found in both I/R and I/R+MMF group compared to the control.

Table 3. Blood gas measurements.

	BL	R15	R120
PaO₂ (torr)			
Control	191.3±11.4	198.5±14.7	194.6±12
I/R	190.5±17.9	193.6±8.8	182.3±12.1
I/R+MMF	176.4±19.3	187.7±23.7	176.7±26.6
PrvO₂ (torr)			
Control	78.5±5.8	69.1±7	58.3±5.2
I/R	82.1±6.1	77.1±13.8	65.6±5.4
I/R+MMF	81.6±6.6	72.5±8.2	62±6±3.5
PaCO₂ (torr)			
Control	39.5±6	37.5±5.3	37.8±4.5
I/R	41.3±2	39.2±4.5	42.4±1.7
I/R+MMF	41.7±4.3	39.3±4.3	45±4.1*
SaO₂ %			
Control	98±1	98±1	98±1
I/R	98±1	98±1	98±1
I/R+MMF	96±1	98±1	98±1
rvSaO₂ %c			
Control	88±2	84±4	77±5
I/R	89±2	86±7	82±4
I/R+MMF	89±2	85±5	80±3
tHb (g/dl)			
Control	20.8±0.9	19.1±1.5	18.5±1.5
I/R	21.7±0.9	20.4±3	18.8±2.4
I/R+MMF	21.6±1.4	21±1.8	19.7±1.2
Hct %			
Control	64.4±1.5	59.4±4.7	54.5±5.7
I/R	66.2±2.7	60.7±9.8	59.2±6.1
I/R+MMF	65.8±4.4	64.1±5.4	60.9±3.7
P50 (mmHg)			
Control	28.6±1.2	28.3±0.8	27.7±1.3
I/R	29.3±0.7	30.7±1**	29.8±0.7*
I/R+MMF	29.3±0.9	30±1.5	29.7±1.1*

Values are presented as Mean ± SD, *p < 0.05, **p < 0.01 vs. Control group.

Abbreviations: BL; baseline, R15; reperfusion at 15 min, R120; reperfusion at 120 min, I/R; ischemia/reperfusion, MMF; mycophenolate mofetil, PaO₂; arterial partial oxygen pressure, PrvO₂; venous partial oxygen pressure, PaCO₂; arterial partial carbonmonoxide pressure, SaO₂; hemoglobin oxygen saturation, rvSaO₂; renal vein hemoglobin oxygen saturation, Hct; hematocrit.

Table 4. Plasma acid-base and electrolytes levels between all the time points in experimental groups.

	BL	R15	R120
pH			
Control	7.30±0.04	7.31±0.03	7.33±0.04
I/R	7.29±0.03	7.25±0.05	7.26±0.02*
I/R+MMF	7.35±0.05	7.26±0.04	7.27±0.02
Base excess [mmol/L]			
Control	-6.5±2.7	-5.9±2.5	-6.0±2.1
I/R	-6.3±3.4	-9.9±3.2	-7.8±1.8
I/R+MMF	-7.1±2.3	-9.2±1.3	-5.4±2.4
HCO₃⁻ [mmol/L]			
Control	19.1±2.9	19.2±2.4	19.3±1.5
I/R	19.3±1.9	16.8±2.5	18.7±1.6
I/R+MMF	19.2±2.6	17.2±0.7	20.3±0.8
Na⁺ [mmol/L]			
Control	149±9.1	150±7	151±3
I/R	142±3	143±3	143±5
I/R+MMF	142±4	144±1	144±3
K⁺ [mmol/L]			
Control	3.5±0.4	3.5±0.5	3.3±0.4
I/R	4.2±0.5	4.1±0.6	4.3±0.6*
I/R+MMF	4±0.5	4.2±0.5	4.2±0.4*

Values are presented as Mean ± SD, *p < 0.05 vs. Control group.

Abbreviations: BL; baseline, R15; reperfusion at 15 min, R120; reperfusion at 120 min, I/R; ischemia/reperfusion, MMF; mycophenolate mofetil.

Effect of MMF on renal function after 120 min of reperfusion

The results of the measured renal creatinine clearances ($\text{Clear}_{\text{crea}}$) and tubular sodium reabsorption (TNa^+) are presented in Figure 1A and B, respectively. The $\text{Clear}_{\text{crea}}$ and TNa^+ were significantly decreased after 120 min of reperfusion ($p < 0.01$, $p < 0.001$, respectively) compared to the control group. Fractional excretion of sodium (EFNa^+) was only increased in I/R group at R15 ($p < 0.05$) and R120 ($p < 0.05$) compared to the control and it was significantly improved by the treatment of MMF at R120 ($p < 0.05$) compared to I/R group (Figure 1C). No change was found in VO_2/TNa^+ ratio between the groups (Figure 1D).

MMF treatment reduces I/R-induced renal injury

The markers of renal oxidative stress and tissue injury at 120 min reperfusion are presented in Figure 2. The extent of intrarenal oxidative stress, or at least in terms of the oxidative breakdown of polyunsaturated lipids to MDA, did not differ between the groups

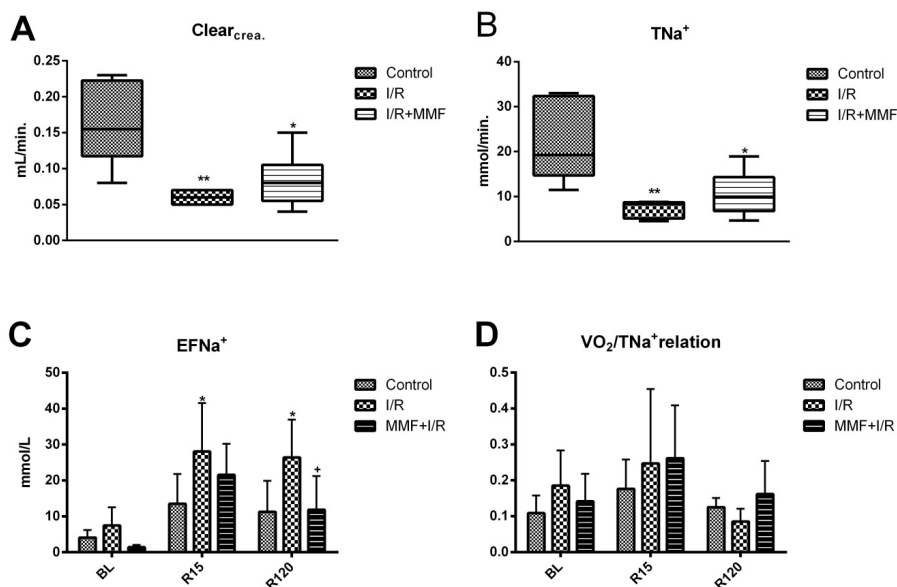


Figure 1. Levels of creatinine clearance (A) and tubular sodium reabsorption between groups Control, I/R and I/R+MMF after 120 min. reperfusion. I/R; ischemia/reperfusion, MMF; mycophenolate mofetil, $Clear_{crea}$; creatinine clearances, TNa^+ ; tubular sodium reabsorption, $EFNa^+$; fractional excretion of sodium. Values are presented as Mean \pm SD, * $p < 0.05$, ** $p < 0.01$ and *** $p < 0.001$ vs. Control group.

(Figure 2A). In contrast, extensive hypoxia as reflected by plasma lactate levels was observed in the I/R group ($p < 0.01$) compared to the control values at R120 (Figure 2B). Similarly, NGAL (Figure 2C) and L-FABP (Figure 2D), which are well-established biomarkers of kidney injury, were increased in the I/R group ($p < 0.001$ vs. control) and reduced to pre-ischemia levels by MMF ($p < 0.001$ vs. I/R).

MMF abrogates pro-inflammatory signaling in ischemia-subjected kidneys

In the renal cortex, iNOS staining was increased in the I/R group compared to control ($p < 0.001$). MMF exerted a reductive effect on iNOS expression in the I/R-subjected renal cortex ($p < 0.001$) (Figure 3A). With respect to inflammation, IL-6 staining was elevated in I/R group compared to the control group ($p < 0.001$). The pro-inflammatory signaling was completely abrogated by MMF at 120 min reperfusion ($p < 0.001$) (Figure 3B). In the I/R group, histological expression of MPO concurred with increased influx of neutrophils in the glomerular (Figure 3C) and the peritubular regions (Figure 3D), as evidenced by the increased MPO staining intensity ($p < 0.001$). MMF reduced post-ischemic neutrophil chemotaxis to the glomeruli and completely abolished neutrophil accumulation in the peritubular region.

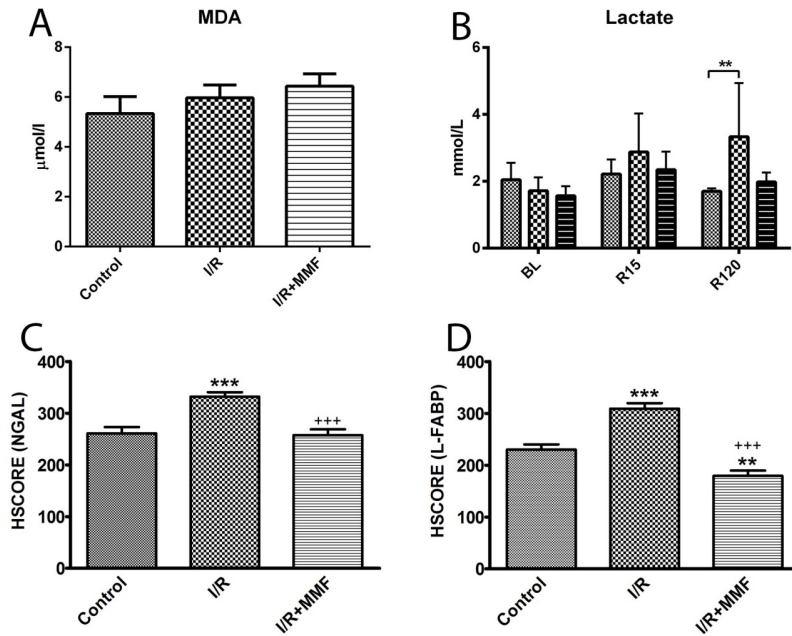


Figure 2. Tissue MDA levels (A), plasma lactate levels (B), tissue NGAL expression (C), and tissue L-FABP expression (D) between the Control, I/R, and I/R + MMF groups after 120 min. reperfusion. I/R; ischemia/reperfusion, MMF; mycophenolate mofetil, MDA; malondialdehyde, NGAL; neutrophil gelatinase-associated lipocalin, L-FABP; liver fatty acid binding protein. Values are presented as Mean \pm SD, * p < 0.05, ** p < 0.01 and *** p < 0.001 vs. Control group; *** p < 0.001 vs. I/R group. Bsln = baseline, i.e., before I/R.

DISCUSSION AND CONCLUSION

This study confirmed that supra-aortic occlusion mediated I/R caused acute and progressive impairment of kidney microcirculatory cortical and medullar oxygenation as well as loss of kidney function and renal injury. These microcirculatory alterations were associated with decreased renal oxygen supply, increased renal vascular resistance, as well as oxidative stress, inflammation, and tissue injury despite sustained arterial pressure. Our study showed that administration of MMF effectively preserved renal microcirculatory oxygenation, renal oxygen delivery and renal hemodynamics in lower body I/R-induced AKI. Results suggest that the underlying mechanisms for this effect may involve the inhibition of immune cell-mediated inflammatory activation and ROS production.

Although systemic blood pressure did not change in our I/R model, the RVR was considerably elevated during reperfusion as a result of reduced RBF, most likely due to I/R-induced perfusion defects. In addition to reduction of renal oxygen supply, increased

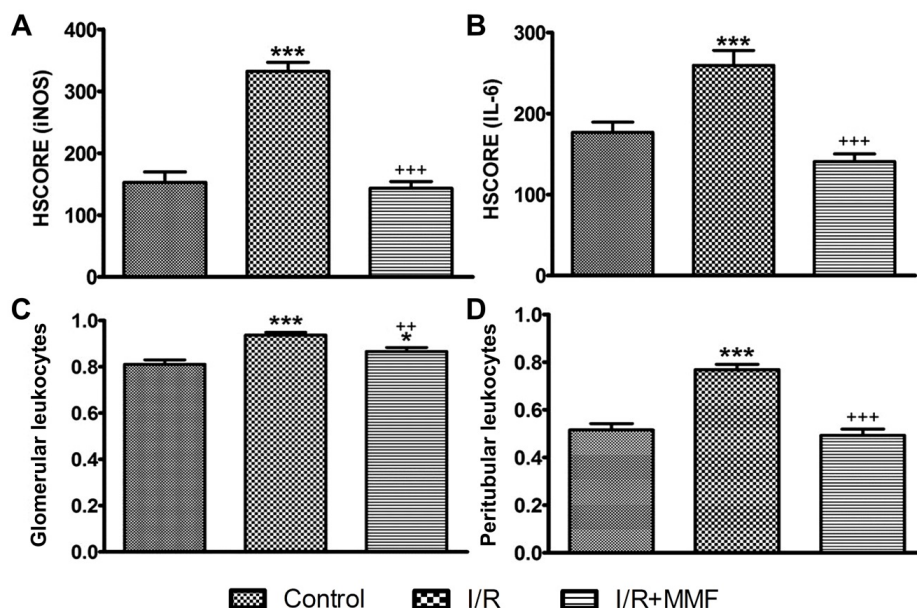


Figure 3. Immunostaining intensity (HSCORE) of renal cortical iNOS (A), IL-6 (B), MPO of glomerular leukocytes (C), and MPO of peritubular leukocytes (D) between the Control, I/R, and I/R + MMF groups after 120 min. reperfusion. I/R; ischemia/reperfusion, MMF; mycophenolate mofetil, iNOS; inducible nitric oxide, IL-6; interleukin 6. Values are presented as Mean \pm SD, * p < 0.05 and *** p < 0.001 vs. Control group; ** p < 0.01 and *** p < 0.001 vs. I/R group.

plasma lactate levels suggesting the presence of the remote organ hypoxia following I/R due to aortic clamping. This is a major contributing factor that causes a further impairment of renal microcirculation and oxygenation because of the release of large amount of inflammatory and oxidative substances following reperfusion. These might be translated to a decrease in renal oxygen supply, corollary decrease in cortical and medullar μPO_2 , and increase in the fractional excretion of sodium. In line with these findings, Legrand *et al.* showed that hypoxia prevails during the first hours of post-ischemic kidney reperfusion in both the renal cortex and medulla.³ The hypoxia concurred with a reduction in the $\text{DO}_{2\text{ren}}$ and $\text{VO}_{2\text{ren}}$ associated with iNOS upregulation and downregulated expression of eNOS (33,34). Our data suggest that the alterations in renal oxygenation may emanate from microvascular dysfunction and reduced renal oxygen supply in the kidney. The consequent decrease in microvascular oxygenation, oxygen delivery, and oxygen utilization followed by reperfusion promotes hypoxia-related inflammation and oxidative injury leading ultimately to AKI associated with a reduction in creatinine clearances and tubular sodium reabsorption shown in the present study. Ventura *et al.* showed that pretreatment of MMF can prevent in an decreasing of renal blood flow after 2 days of bilateral renal

arteries occlusion for 60 min (21), however we showed that administration of MMF improved renal blood flow, renal oxygen delivery (not only at late reperfusion but also at BL), renal vascular resistance, renal cortical oxygenation and fractional excretion of sodium in short term of reperfusion by protecting the microcirculation and preventing vascular constriction of peripheral and renal vessels with its anti-inflammatory action. However, all these improvements associated by MMF administration relatively normalized the renal function despite EFNa^+ was substantially ameliorated that because of reperfusion period of this study was too short to decide whether the renal function was completely recovered or not. At the same time, no study testing the effects of MMF on renal oxygenation, function and inflammation after supra-aortic occlusion. In this line, Kelly and Dominguez showed that besides MMF provided in amelioration of progressive renal dysfunction following 14 weeks post-bilateral renal ischemia, MMF also caused a reduction of leukocytes infiltration and adherence, reduce in pro inflammatory ICAM-1 and Lectin-like oxidized low-density lipoprotein (LDL) receptor-1 (LOX-1) expression. They had also demonstrated that MMF prevented an elevation of microvascular permeability and renal damage on obese-diabetic rats treated with MMF starting 2 days prior to 25 min. renal ischemia and continued for 2 weeks (35). However, Sabbatini et al. suggests that the administration of MMF corrected nor impairment of renal function or renal damage commonly observed after I/R induced acute kidney injury with a follow up of both 24 hours and 5 months despite suppression of ICAM-1 expression and monocytes recruitment after 24 hours of ischemia (36). Ysebaert *et al.* showed that MMF in combination with severe I/R did not influence initial morphologic damage and dysfunction. However, MMF led to decrease especially to number of CD4 T cells, monocytes/macrophage (ED-1) and cytotoxic T cell in the outer stripe of the medulla after 60 min. renal arterial cross clamping. This correlated with a decrease of tubular cell proliferation and hence tubular regeneration (37). Therefore, the effect of the MMF on the renal function between these studies is seemed to relate with the methodological discrepancy such as occlusion methods, doses and treatment periods of this drug but its anti-inflammatory effects is to seem quite persistent along with several mechanism.

It is well known that globally produced pro-inflammatory cytokines (e.g., IL-6) (38) and ROS (14) fuel the progression of AKI during lower body ischemia/reperfusion. Similarly to our result, Xu *et al.* showed that plasma IL-6 levels become elevated after 45 min. bilateral renal pedicle occlusion following 24 hours reperfusion and contribute to a pro-inflammatory state that is partly responsible for induction of cell death by activation of the c-Jun N-terminal kinase (JNK) pathway (38). Moreover, Youssef *et al.* also showed that renal I/R resulted in an elevation of tumor necrosis factor-alpha ($\text{TNF-}\alpha$), NF-kB, and caspase-3 in both kidney and heart tissue (39). In terms of inflammation, MMF reduced pro-inflammatory signaling and neutrophil chemotaxis to the affected kidneys,

as evidenced by a considerable reduced IL-6 and MPO HSCORE in both the glomerular and peritubular region. Other authors also demonstrated that administration of MMF led to reduced TNF- α plasma levels and MPO activity as well as inhibition of BAX expression (a pro-apoptotic protein) in a rat model of myocardial I/R injury through inhibition of the TLR4/NF- κ B signaling pathway (40), which was associated with reduced inflammation and cell death.

The pro-inflammatory signaling during the reperfusion phase is connected to the hemodynamic perturbations through the NO signaling axis. Excessive activation of iNOS, which is strongly linked to NF- κ B activation (41), may contribute to microcirculatory derangement by activation of leukocytes and enhancement of peroxynitrite formation (42), which causes vasoconstriction and cell damage (43). NO is of prime importance because of its central regulatory role in intrarenal microcirculation and VO_{2ren} regulation (44-46). Moreover, iNOS expression was shown to be upregulated in vascular smooth muscle cells, renal tubular cells, and in monocytes, macrophages, and neutrophils following renal I/R (44), which is in agreement with our results. Thus, inhibition of the immune cell activation by MMF resulted in reduced iNOS production and therefore decreased peroxynitrite formation. In addition to its anti-inflammatory and cell protective effects, it is possible that MMF may improve renal cortical microvascular oxygenation, DO_{2ren} , and RVR through its peroxynitrite-reducing effects and thereby limited the extent of renal vasoconstriction.

The most critical question that arises from these data is how MMF reduces the renal injury as the result of NGAL and L-FABP reduction, without affecting lipid peroxidation (no change in MDA), particularly in light of the putative contention that I/R-induced lipid peroxidation is detrimental to organ viability (47,48). Based on our findings, it is likely that the renoprotective properties of MMF are related to its renal anti-vasoconstrictive properties in combination with its global anti-inflammatory effects because of lower body ischemia/reperfusion not only influence in the kidney but also throughout body. Therefore, it should be also considered that all the renal progression and improvements revealed by MMF on the kidney is to associates with its global effects.

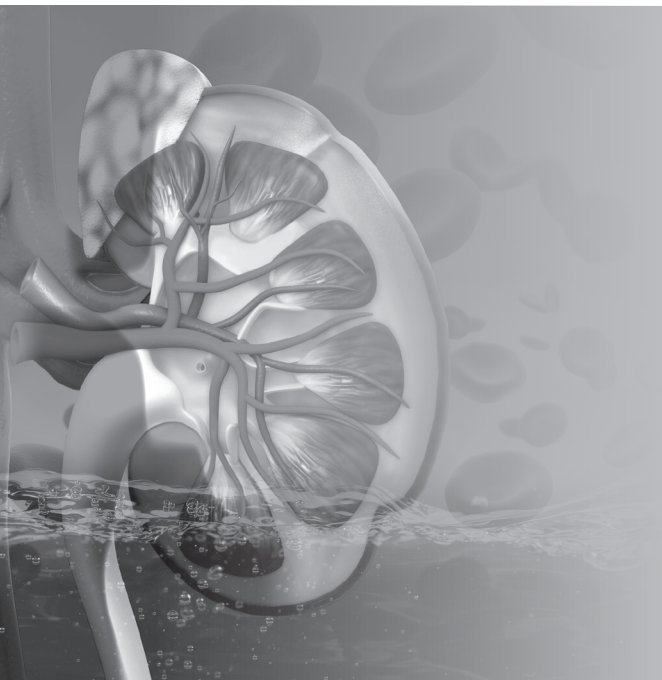
In conclusion, renal I/R induced by supra-aortic clamping causes acute and progressive impairment of kidney cortical and medullar oxygenation with immune cell-mediated sterile/hypoxic inflammation, oxidative stress, and renal injury. Treatment with MMF was not only effective in preserving renal hemodynamic parameters and renal oxygenation, but also reduced the degree of inflammation and injury. Pre-treatment with MMF may potentially have a prophylactic role in settings where I/R are induced in a controlled manner such as aortic surgery or kidney transplantation. Further studies are needed to explain the underlying mechanisms of MMF in affecting tissue oxygenation.

REFERENCES

1. Bonventre JV, Yang L. Cellular pathophysiology of ischemic acute kidney injury. *J. Clin. Invest.* 121:4210–21, 2011.
2. Tuuminen R, Nykänen AI, Saharinen P, *et al.* Donor simvastatin treatment prevents ischemia-reperfusion and acute kidney injury by preserving microvascular barrier function. *Am. J. Transplant.* 13:2019–34, 2013.
3. Naito M, Zager RA, Bomsztyk K. BRG1 increases transcription of proinflammatory genes in renal ischemia. *J. Am. Soc. Nephrol.* 20:1787–96, 2009.
4. van Golen RF, van Gulik TM, Heger M. Mechanistic overview of reactive species-induced degradation of the endothelial glycocalyx during hepatic ischemia/reperfusion injury. *Free Radic. Biol. Med.* 52:1382–402, 2012.
5. van Golen RF, Reiniers MJ, Vrisekoop N, *et al.* The mechanisms and physiological relevance of glycocalyx degradation in hepatic ischemia/reperfusion injury. *Antioxid. Redox Signal.* 21:1098–118, 2014.
6. Andersson M, Nilsson U, Hjalmarsson C, *et al.* Mild renal ischemia-reperfusion reduces charge and size selectivity of the glomerular barrier. *Am. J. Physiol. Renal Physiol.* 292:F1802–1809, 2007.
7. Snoeijis MG, Vink H, Voesten N, *et al.* Acute ischemic injury to the renal microvasculature in human kidney transplantation. *Am. J. Physiol. Renal Physiol.* 299:F1134–1140, 2010.
8. Wu H, Chen G, Wyburn KR, *et al.* TLR4 activation mediates kidney ischemia/reperfusion injury. *J. Clin. Invest.* 117:2847–59, 2007.
9. Celie JWAM, Rutjes NWP, Keuning ED, *et al.* Subendothelial heparan sulfate proteoglycans become major L-selectin and monocyte chemoattractant protein-1 ligands upon renal ischemia/reperfusion. *Am. J. Pathol.* 170:1865–78, 2007.
10. Wu H, Ma J, Wang P, *et al.* HMGB1 contributes to kidney ischemia reperfusion injury. *J. Am. Soc. Nephrol.* 21:1878–90, 2010.
11. van Golen RF, van Gulik TM, Heger M. The sterile immune response during hepatic ischemia/reperfusion. *Cytokine Growth Factor Rev.* 23:69–84, 2012.
12. Schmitz V, Schaser K-D, Olschewski P, *et al.* In vivo visualization of early microcirculatory changes following ischemia/reperfusion injury in human kidney transplantation. *Eur. Surg. Res.* 40:19–25, 2008.
13. Brady HR. Leukocyte adhesion molecules: potential targets for therapeutic intervention in kidney diseases. *Curr. Opin. Nephrol. Hypertens.* 2:171–82, 1993.
14. Kloek JJ, Maréchal X, Roelofsen J, *et al.* Cholestasis is associated with hepatic microvascular dysfunction and aberrant energy metabolism before and during ischemia-reperfusion. *Antioxid. Redox Signal.* 17:1109–23, 2012.
15. Singbartl K, Green SA, Ley K. Blocking P-selectin protects from ischemia/reperfusion-induced acute renal failure. *FASEB J.* 14:48–54, 2000.
16. Dragun D, Tullius SG, Park JK, *et al.* ICAM-1 antisense oligodeoxynucleotides prevent reperfusion injury and enhance immediate graft function in renal transplantation. *Kidney Int.* 54:590–602, 1998.
17. Mele TS, Halloran PF. The use of mycophenolate mofetil in transplant recipients. *Immunopharmacology* 47:215–45, 2000.
18. Jayne D. Non-transplant uses of mycophenolate mofetil. *Curr. Opin. Nephrol. Hypertens.* 8:563–7, 1999.
19. Allison AC, Eugui EM. Mycophenolate mofetil and its mechanisms of action. *Immunopharmacology* 47:85–118, 2000.
20. Allison AC, Eugui EM. Purine metabolism and immunosuppressive effects of mycophenolate mofetil (MMF). *Clin. Transplant.* 10:77–84, 1996.
21. Ventura CG, Coimbra TM, de Campos SB, *et al.* Mycophenolate mofetil attenuates renal ischemia/reperfusion injury. *J. Am. Soc. Nephrol.* 13:2524–33, 2002.
22. Kelly KJ, Williams WW, Colvin RB, *et al.* Antibody to intercellular adhesion molecule 1 protects the kidney against ischemic injury. *Proc. Natl. Acad. Sci. U.S.A.* 91:812–6, 1994.

23. Kelly KJ, Williams WW, Colvin RB, *et al.* Intercellular adhesion molecule-1-deficient mice are protected against ischemic renal injury. *J. Clin. Invest.* 97:1056–63, 1996.
24. Jones EA, Shoskes DA. The effect of mycophenolate mofetil and polyphenolic bioflavonoids on renal ischemia reperfusion injury and repair. *J. Urol.* 163:999–1004, 2000.
25. Jiang S, Tang Q, Rong R, *et al.* Mycophenolate mofetil inhibits macrophage infiltration and kidney fibrosis in long-term ischemia-reperfusion injury. *Eur. J. Pharmacol.* 688:56–61, 2012.
26. Ergin B, Bezemer R, Kandil A, *et al.* TEMPOL has limited protective effects on renal oxygenation and hemodynamics but reduces kidney damage and inflammation in a rat model of renal ischemia/reperfusion by aortic clamping. *J. Clin. Transl. Res.* 116–28, 2015.
27. Johannes T, Mik EG, Ince C. Dual-wavelength phosphorimetry for determination of cortical and subcortical microvascular oxygenation in rat kidney. *J. Appl. Physiol.* 100:1301–10, 2006.
28. Dunphy I, Vinogradov SA, Wilson DF. Oxyphor R2 and G2: phosphors for measuring oxygen by oxygen-dependent quenching of phosphorescence. *Anal. Biochem.* 310:191–8, 2002.
29. Mik EG, Johannes T, Zuurbier CJ, *et al.* In vivo mitochondrial oxygen tension measured by a delayed fluorescence lifetime technique. *Biophys. J.* 95:3977–90, 2008.
30. Forman HJ, Augusto O, Brigelius-Flohe R, *et al.* Even free radicals should follow some rules: a guide to free radical research terminology and methodology. *Free Radic. Biol. Med.* 78:233–5, 2015.
31. Demirci C, Gargili A, Kandil A, *et al.* Inhibition of inducible nitric oxide synthase in murine visceral larva migrans: effects on lung and liver damage. *Chin. J. Physiol.* 49:326–34, 2006.
32. Senturk LM, Seli E, Gutierrez LS, *et al.* Monocyte chemotactic protein-1 expression in human corpus luteum. *Mol. Hum. Reprod.* 5:697–702, 1999.
33. Legrand M, Almac E, Mik EG, *et al.* L-NIL prevents renal microvascular hypoxia and increase of renal oxygen consumption after ischemia-reperfusion in rats. *Am. J. Physiol. Renal Physiol.* 296:F1109–1117, 2009.
34. Legrand M, Kandil A, Payen D, *et al.* Effects of sepiapterin infusion on renal oxygenation and early acute renal injury after suprarenal aortic clamping in rats. *J. Cardiovasc. Pharmacol.* 58:192–8, 2011.
35. Kelly KJ, Dominguez JH. Treatment of the post-ischaemic inflammatory syndrome of diabetic nephropathy. *Nephrol. Dial. Transplant.* 25:3204–12, 2010.
36. Sabbatini M, Uccello F, Serio V, *et al.* Effects of mycophenolate mofetil on acute ischaemia-reperfusion injury in rats and its consequences in the long term. *Nephrol. Dial. Transplant.* 25:1443–50, 2010.
37. Ysebaert DK, De Greef KE, Vercauteren SR, *et al.* Effect of immunosuppression on damage, leukocyte infiltration, and regeneration after severe warm ischemia/reperfusion renal injury. *Kidney Int.* 64:864–73, 2003.
38. Xu Y, Liu M, Peng B, *et al.* Protective effects of SP600125 on renal ischemia-reperfusion injury in rats. *J. Surg. Res.* 169:e77–84, 2011.
39. Youssef MI, Mahmoud AAA, Abdelghany RH. A new combination of sitagliptin and furosemide protects against remote myocardial injury induced by renal ischemia/reperfusion in rats. *Biochem. Pharmacol.* 96:20–9, 2015.
40. Li T, Yu J, Chen R, *et al.* Mycophenolate mofetil attenuates myocardial ischemia-reperfusion injury via regulation of the TLR4/NF- κ B signaling pathway. *Pharmazie* 69:850–5, 2014.
41. Chatterjee PK, Brown PA, Cuzzocrea S, *et al.* Calpain inhibitor-1 reduces renal ischemia/reperfusion injury in the rat. *Kidney Int.* 59:2073–83, 2001.
42. Chatterjee PK, Patel NSA, Kvale EO, *et al.* Inhibition of inducible nitric oxide synthase reduces renal ischemia/reperfusion injury. *Kidney Int.* 61:862–71, 2002.
43. Ajayi AAL, Hercule HC, Pamugo J, *et al.* Interactions of the renin-angiotensin system and alpha-1 adrenoceptors on renal hemodynamics in healthy and acute renal failure rats: the role of nitric oxide. *Blood Press.* 10:238–46, 2001.
44. Cowley AW, Mori T, Mattson D, *et al.* Role of renal NO production in the regulation of medullary blood flow. *Am. J. Physiol. Regul. Integr. Comp. Physiol.* 284:R1355–1369, 2003.
45. Adler S, Huang H, Loke KE, *et al.* Endothelial nitric oxide synthase plays an essential role in regulation of renal oxygen consumption by NO. *Am. J. Physiol. Renal Physiol.* 280:F838–843, 2001.

46. Laycock SK, Vogel T, Forfia PR, *et al.* Role of nitric oxide in the control of renal oxygen consumption and the regulation of chemical work in the kidney. *Circ. Res.* 82:1263–71, 1998.
47. Joannidis M, Bonn G, Pfaller W. Lipid peroxidation--an initial event in experimental acute renal failure. *Ren. Physiol. Biochem.* 12:47–55, 1989.
48. Fuller BJ, Gower J, Cotterill L, *et al.* Reperfusion injury and renal metabolism: the temporal relationship between oxidative stress and functional change. *Adv. Exp. Med. Biol.* 264:389–92, 1990.



CHAPTER 6

Divergent effects of hypertonic fluid resuscitation on renal pathophysiological and structural parameters in a rat model of lower body ischemia/reperfusion-induced sterile inflammation

Adapted from *Shock* 2017 Dec 27.doi:10.1097/SHK

Bulent Ergin¹, Coert J Zuurbier², Aysegul Kapucu³, Can Ince¹

¹ Department of Translational Physiology, Academic Medical Center, University of Amsterdam, Amsterdam, The Netherlands

² Laboratory of Experimental Anesthesiology and Intensive Care, Department of Anesthesiology, Academic Medical Center, University of Amsterdam, The Netherlands

³ Department of Zoology, Faculty of Science, University of Istanbul, Istanbul, Turkey

⁴ Department of Intensive Care, Erasmus MC, University Medical Center, Rotterdam, The Netherlands

ABSTRACT

The pathogenesis of AKI is characterized by the deterioration of tissue perfusion and oxygenation and enhanced inflammation. The purpose of this study was to investigate 1) whether or not the hemodynamic and inflammatory effects of HSal protects the kidney by promoting renal microcirculatory oxygenation and 2) possible deleterious effects of HSal due to its high sodium content on renal functional and structural injury following ischemia/reperfusion. Mechanically ventilated and anesthetized rats were randomly divided into 4 groups ($n = 6/\text{group}$): (1) a sham-operated control group; (2) a group subjected to renal ischemia for 45 min by supra-aortic occlusion followed by 2 h of reperfusion (I/R); and (3-4) I/R group treated with a continuous i.v. infusion (5 ml/kg/h) of either % 0.9 NaCl (IR+NS) or %10 NaCl (I/R+HSal) after releasing the clamp. Systemic and renal hemodynamic, renal cortical ($C_{\mu}\text{PO}_2$) and medullar microcirculatory $p\text{O}_2$ ($M_{\mu}\text{PO}_2$) measured by the oxygen-dependent quenching of phosphorescence lifetime technique. Renal functional, inflammatory and tissues damage parameters were also assessed. HSal, but not NS, treatment restored I/R-induced reduced mean arterial pressure, $C_{\mu}\text{PO}_2$, renal oxygen delivery ($\text{DO}_{2\text{ren}}$) and consumption ($\text{VO}_{2\text{ren}}$). HSal caused a decrease in tubular sodium reabsorption (TNa^+) that correlated with an elevation of fractional sodium excretion (EFNa^+) and urine output. HSal had anti-inflammatory effect by reducing the levels $\text{TNF-}\alpha$, IL-6 and hyaluronic acid in the renal tissue samples as compared to the I/R and I/R+NS group ($p < 0.05$). HSal treatment was also associated with mild acidosis and an increased renal tubular damage. Despite HSal resuscitation improves the systemic hemodynamics, microcirculatory oxygenation and renal oxygen consumption as well as inflammation, it should be limited or strictly controlled for long term used because of provoking widespread renal structural damage.

Keywords: acute kidney injury, reperfusion injury, microvascular oxygenation, hypertonic saline.

INTRODUCTION

Acute kidney injury (AKI) is a common pathophysiological condition that is associated with extreme early and late mortality, resulting in high financial cost (1). The kidney is vulnerable to ischemia and reperfusion injury in many clinical scenarios where there is a need to clamp the abdominal aorta such as in renal transplantation, surgery of suprarenal aneurysms (2), renal artery reconstructions and contrast agent-induced nephropathy (3). Under steady state condition, the kidney possesses a unique autoregulatory system composed of metabolic, myogenic and tubuloglomerular feedback mechanisms which maintain a balance between oxygen delivery (DO_2) and oxygen demand by adaptation of the renal blood flow (RBF) (4). Renal oxygen demands is directly related to renal metabolic requirements due to a linear relationship between tubular transport of filtered sodium (TNa^+) and oxygen consumption (VO_2) (5). It has been shown that inhibition of Na^+ transport in the thick ascending limb (TAL) and proximal tubules by specific diuretics increases pO_2 in the medulla and cortex respectively (6). Hence, tubular sodium transport, renal metabolic needs and delivery of oxygen are thought to be the principal determinants of intrarenal oxygenation. The pathogenesis of AKI involve deterioration of the tissue perfusion, oxygenation and the renal microcirculation (7) resulting in an increased inflammation, oxidative stress, endothelial and tubular injury.

Hypertonic solutions have been investigated as alternative resuscitation strategies in critically injured patients (8,9). Hypertonic saline (HSal) solution increases serum osmolarity that results in a redistribution of fluid from the interstitial and intracellular spaces to the intravascular space causing an improved hemodynamic status (10). Gazitua *et al.* demonstrated that hyperosmotic NaCl solutions induces vasodilation when selectively infused in the renal, coronary, and limb circulations (11). Experimental studies suggest that small volume resuscitation with HS may be more effective than conventional crystalloid solutions in improving organ perfusion to re-establish cardiac output and systemic arterial pressure in shock (12,13). Recently, new findings have suggested that HS can also modulates local and systemic inflammatory response (14). The mechanisms of action of hypertonic saline are increasingly well understood, and include inhibition of tumor necrosis factor-alpha ($\text{TNF-}\alpha$) and interleukin-1 (IL-1) production (15). However, the effects of hypertonic saline on renal I/R pathology with emphasis on the renal microcirculatory oxygenation are not yet investigated.

In this study, we aimed to investigate whether the potential benefit effects of hypertonic saline on systemic hemodynamic and inflammatory variables may protect the renal microcirculation in terms of promoting renal oxygenation, oxygen utilisation, renal

function, tubular transport and morphological integrity following supra-aortic occlusion induced sterile inflammation or not.

MATERIALS AND METHODS

Animals

All experiments in this study were approved by the institutional Animal Experimentation Committee of the Academic Medical Center of the University of Amsterdam (DFL 83). Care and handling of the animals were in accordance with the guidelines for Institutional and Animal Care and Use Committees. The study has been carried out in accordance with the Declaration of Helsinki. Experiments were performed on 24 male *Wistar albino* rats (Harlan Netherlands BV, Horst, The Netherlands) with a mean \pm SD body weight of 331 ± 25 g.

Surgical Preparation

All animals were anesthetized with an intraperitoneal injection of a mixture of 90 mg/kg ketamine (Nimatek[®], Eurovet, Bladel, The Netherlands), 0.5 mg/kg dexmedetomidine (Dexdomitor, Pfizer Animal Health BV, Capelle aan den IJssel, The Netherlands), and 0.05 mg/kg atropine-sulfate (Centrafarm Pharmaceuticals BV, Etten-Leur, The Netherlands) (16). After preparing a tracheotomy the animals were mechanically ventilated with a FiO_2 of 0.4. Body temperature was maintained at 37 ± 0.5 °C during the entire experiment by an external thermal heating pad. Ventilator settings were adjusted to maintain end-tidal pCO_2 between 30 and 35 mmHg and arterial pCO_2 between 35 and 40 mmHg.

For drug and fluid administration and hemodynamic monitoring, vessels were cannulated with polyethylene catheters with an outer diameter of 0.9 mm (Braun, Melsungen, Germany). A catheter in the right carotid artery was connected to a pressure transducer to monitor mean arterial blood pressure (MAP) and heart rate (HR). The right jugular vein was cannulated for continuous infusion of Ringer's Lactate (Baxter, Utrecht, The Netherlands) at a rate of 15 mL/kg/hour against fluid loss and 50 mg/kg/h ketamine dissolved in 5 ml ringer's lactate for maintenance of anesthesia. The right femoral artery was cannulated for drawing blood samples and the right femoral vein for drug administration.

The left kidney was exposed, decapsulated, and immobilized in a Lucite kidney cup (K. Effenberger, Pfaffingen, Germany) via ~4 cm incision in the left flank in each animal. Renal vessels were carefully separated under preservation of nerves and the adrenal gland. A perivascular ultrasonic transient time flow probe was placed around the left renal artery (type 0.7 RB Transonic Systems Inc., Ithaca, NY, USA) and connected to a flow meter (T206, Transonic Systems Inc., Ithaca, NY, USA) to continuously measure renal blood

flow (RBF). The left ureter was isolated, ligated, and cannulated with a polyethylene catheter for urine collection.

After the surgical preparation an optical fiber was placed 1 mm above the decapsulated kidney and another optical fiber was placed 1 mm above the renal vein to measure renal microvascular and venous oxygen pressures using phosphorimetry, respectively (explained in more detail below). A small piece of aluminum foil was placed on the dorsal side of the renal vein to prevent contribution of the underlying tissues to the phosphorescence signal in the venous pO_2 measurements. Oxyphor G2, a two-layer glutamate dendrimer of tetra-(4-carboxy-phenyl) benzoporphyrin (Oxygen Enterprises Ltd., Philadelphia, PA, USA) was subsequently infused (i.e. 6 mg/kg IV over 5 min), followed by 30 min of stabilization time. The surgical field was covered with a humidified gauze compress throughout the entire experiment to prevent drying of the exposed tissues.

Experimental Protocol

The rats were divided into 4 groups ($n = 6$ per group determined by the power analysis (nQuery advisor)): (1) a sham-operated time control group; (2) a group subjected to renal ischemia for 45 min by supra-aortic occlusion with a custom-made vascular occluder placed in between left renal artery and superior mesenteric artery followed by 2 h of reperfusion (I/R) starting just after releasing the clamp; and (3-4) a group subjected to I/R and treated with continuous i.v. infusion of either 5 ml/kg/h of Normal Saline (I/R+NS) (%0.9 NaCl) or of Hypertonic Saline (%10 NaCl) (I/R+HSal). The saline infusion was started just after the removal of occluder and blindly randomized by using the sealed envelope randomization service.

Blood and plasma variables

Arterial blood samples (0.25 ml) were taken from the femoral artery at three time points: 1) before aortic occlusion, (baseline, BL); 2) 15 min after reperfusion (initial reperfusion phase, T_1); and 3) 120 min after reperfusion (late reperfusion phase, T_2). The blood samples were replaced by the same volume of HES130/0.4 (Volumen, 6% HES 130/0.4; Fresenius Kabi Schelle, Belgium). The samples were used for determination of blood gas values, as well as for determination of the hemoglobin concentration, hemoglobin oxygen saturation, and sodium and potassium concentrations (ABL80 Flex blood gas analyzer; Radiometer, Copenhagen, Denmark). The plasma samples were used for evaluation of plasma creatinine levels (modular P800 automatic analyzer, Roche Diagnostics, Basel, Switzerland).

Renal microvascular and venous oxygenation

Microvascular oxygen tension in the renal cortex ($C_{\mu}PO_2$), outer medulla ($M_{\mu}PO_2$), and renal venous oxygen tension ($P_{rv}O_2$) were measured by oxygen-dependent

quenching of phosphorescence lifetimes of the systemically infused albumin-targeted (and therefore circulation-confined) phosphorescent dye Oxyphor G2 (17). Oxygen measurements based on phosphorescence lifetime techniques rely on the principle that phosphorescence can be quenched by energy transfer to oxygen resulting in shortening of the phosphorescence lifetime. A linear relationship between reciprocal phosphorescence lifetime and oxygen tension (i.e., the Stern-Volmer relation) allows quantitative measurement of PO_2 (18).

Calculation of derivative oxygenation parameters and renal vascular resistance

Arterial oxygen content (AOC) was calculated by following equation; $(1.31 \times \text{hemoglobin} \times S_aO_2) + (0.003 \times P_aO_2)$, where S_aO_2 is arterial oxygen saturation and P_aO_2 is arterial partial pressure of oxygen. Renal venous oxygen content (RVOC) was calculated as $(1.31 \times \text{hemoglobin} \times S_{rv}O_2) + (0.003 \times P_{rv}O_2)$, where $S_{rv}O_2$ is venous oxygen saturation and $P_{rv}O_2$ is renal vein partial pressure of oxygen (measured using phosphorimetry). The $S_{rv}O_{2ren}$ was calculated using the Hill equation with $P50 = 37$ Torr (4.9 kPa) and Hill coefficient = 2.7. Renal oxygen delivery was calculated as $DO_{2ren} \text{ (mL/min)} = RBF \times AOC$. Renal oxygen consumption was calculated as $VO_{2ren} \text{ (mL/min)} = RBF \times (AOC - RVOC)$. An estimation of the renal vascular resistance (RVR) was made as: $RVR \text{ (dynes.sec.cm}^{-5}) = (MAP/RBF) \times 100$.

Assessment of kidney function

The high plasma creatinine level was accepted as short term AKI definition based on the KDIGO criteria (19). Creatinine clearance ($Clear_{crea} \text{ (mL/min)}$) was measured as an index of the glomerular filtration rate and calculated with the following formula: $Clear_{crea} = (U_{crea} \times V) / P_{crea}$, where U_{crea} was the concentration of creatinine in urine, V is the urine volume per unit time and P_{crea} was the concentration of creatinine in plasma. Additionally, excretion fraction of Na^+ [$EFNa^+ \text{ (%)}$] was calculated and used as a marker of tubular function in the following formula: $EFNa^+ = (U_{Na} \times P_{crea}) / (P_{Na} \times U_{crea}) \times 100$, where U_{Na} was Na^+ concentration in urine and P_{Na} was the Na^+ concentration in plasma. The renal oxygen extraction ratio was calculated as $ERO_{2ren} \text{ (%) } = VO_{2ren} / DO_{2ren} \times 100$. $Clear_{crea}$ and $EFNa^+$ were determined at all time points. Furthermore, the renal energy efficiency for sodium transport (VO_{2ren} / TNa^+) was assessed using a ratio portrayed by total amount of VO_{2ren} over the total amount of sodium reabsorbed (TNa^+ , mmol/min) that was calculated according to: $(Clear_{crea} \times P_{Na}) - U_{Na} \times V$.

Determination of lipid peroxidation

Snap frozen kidney samples were homogenized in ice-cold 5 mM sodium phosphate buffer. The homogenates were centrifuged at 12,000 $\times g$ for 15 min at 4 °C and supernatants were used for malondialdehyde (MDA) and cytokines determination.

MDA was quantified using a Quattro Premier XE tandem mass spectrometer (MS/MS, Waters, Milford, MA) with an Acquity sample manager and an Acquity binary solvent manager in accordance with (20). The level of MDA was expressed as per gram of protein (Bradford assay).

Nitric oxide (NO) metabolism

Tissue NO undergoes a series of reactions with several molecules present in biological fluids leading to the accumulation of the final products, nitrite and nitrate. Thus, the index of total NO production was the sum of both nitrite and nitrate accumulated in the tissue samples. The reducing agent used for the analysis was a saturated solution of vanadium (III) chloride (VCl_3) in 1 mol/L HCl. At a temperature of 90 °C, VCl_3 reagent quantitatively converts nitrite, nitrate, and S-nitroso compounds to NO in a glass reaction vessel. NO then was flushed out of the reaction vessel by a flow of helium gas which was then measured by the Sievers NO analyzer as the amount of light from the ozone-NO reaction in the apparatus NO measurement chamber. NO levels were determined in frozen kidney tissues. A ratio of tissue NO to tissue protein content was used to for standardization of NO release per gr protein.

Measurement of inflammatory cytokines and glyocalyx component

Inflammatory cytokines TNF- α , IL-6 and hyaluronan (HA) (Rat TNF- α ELISA kit, DY510; Rat IL-6 ELISA kit, DY506 and Rat Hyaluronan DuoSet ELISA kit, DY3614, R&D System Inc. Minneapolis, USA) were determined by ELISA from renal tissue samples. The level of cytokines and hyaluronan was expressed as per gram of protein (Bradford assay).

Kidney immunohistochemistry

Immunohistochemical methods is detailed in elsewhere (21). Briefly, kidney tissues were blindly fixed in 4% formalin according to unique generated code determined for each samples and embedded in paraffin. Kidney sections were incubated for overnight at 4°C with rabbit polyclonal endothelial nitric oxide synthase (eNOS) (1:100) and inducible nitric oxide synthase (iNOS) (1:100) antibodies (eNOS NeoMarkers; Ab iNOS Ab-1, Rabbit PAB, RB-1605-P, NeoMarkers Fremont, CA. Antibodies were diluted in a large volume of UltrAb Diluent (Thermo Scientific, TA-125-UD). The sections were washed in PBS three times for 5 min each time and then incubated for 30 min at room temperature with biotinylated goat anti-rabbit antibodies (LabVision, TP-125-BN). After slides were washed in PBS, the streptavidin peroxidase label reagent (LabVision, TS-125-HR) was applied for 30 min at room temperature in a humid chamber. The colored product was developed by incubation with AEC. The slides were counterstained with Mayer's hematoxylin (LabVision, TA-125-MH) and mounted in vision mount (LabVision, TA-060-UG) after being washed in distilled water. Both the intensity and the distribution of

specific iNOS, and eNOS staining were scored. For each sample, a histological score (HSCORE) value was derived by summing the percentages of cells that stained at each intensity multiplied by the weighted intensity of the staining [$HSCORE = \sum P_i (i+1)$], where i is the intensity score and P_i is the corresponding percentage of the cells] (21).

Histological Analysis

The kidney sections were stained with periodic acid-schiff reagent (PAS) + Hematoxyline. Histologic changes in the cortex were assessed by quantitative measurements of tissue damage. Tubular damage was defined as loss of brush border, vacuolar degeneration and cast formation. The degree of kidney damage was estimated at 400x magnification using 10 randomly selected fields for each animal by the following criteria: 0, normal; 1, areas of damage <10% of tubules; 2, damage involving 10% to 25% of tubules; 3, damage involving 25% to 50% of tubules; 4, damage involving 50% to 75% of tubules; 5, damage more than 75% of tubules.

Statistical Analysis

Data analysis and presentation were performed using GraphPad Prism 6 (GraphPad Software, San Diego, CA, USA). Values are reported as the mean \pm SD. Two-way ANOVA for repeated measurements with a Bonferroni post hoc test were used for comparative analysis between different time points of the groups. The repeated-measures analysis of variance (one-way ANOVA with Bonferroni post hoc test) was used for comparative analysis between groups. Statistical analysis of immunohistochemical and histological results (Values are reported mean \pm SE) was performed by one-way analysis of variance with Tukey's Multiple Comparison Test. p -value of <0.05 was considered statistically significant.

RESULTS

Systemic and renal hemodynamic

The systemic and renal hemodynamic variables are shown in Table 1. MAP values were reduced in IR group at T2 (63.1 ± 5.2 , $p < 0.05$), but significantly elevated by treatment of HSal at T2 (83.4 ± 6.9 , $p < 0.05$) with respect to the IR group. Whereas RBF decreased in the IR group at T2 (2.1 ± 0.5 , $p < 0.05$) with respect to the control (5.2 ± 1.4), it was improved by treatment of HSal at T2 (4 ± 1.2 , $p < 0.05$) compared to I/R group. MAP and RBF were not improved in the NS group. RVR was a stable in all groups at T2.

Results of renal oxygenation parameters

The C_{uPO_2} , M_{uPO_2} , DO_{2ren} and VO_{2ren} variables are shown in Figure 1. During the course of experiments, C_{uPO_2} levels were reduced by ~14.4% in the control group, and ~33%

Table 1. Results of systemic and renal hemodynamics variables.

	BL			T1			T2		
MAP (mmHg)									
Control	85.98	±	4.85	103.17	±	7.88	78.83	±	7.63
IR	91.33	±	7.63	94.67	±	15.02	63.17	±	5.27*
IR+NS	85.74	±	3.73	109.17	±	19.70	70.33	±	11.78
IR+HSal	88.17	±	7.83	108.17	±	13.93	83.42	±	6.94*
RBF (ml/min.)									
Control	5.23	±	0.48	4.12	±	1.07	5.25	±	1.46
IR	5.83	±	1.21	2.76	±	1.13	2.13	±	0.54*
IR+NS	4.50	±	1.07	2.20	±	0.99*	2.53	±	1.50*
IR+HSal	5.23	±	0.95	3.30	±	0.75	4.07	±	1.21*
RVR (dyn.s.cm⁻⁵)									
Control	1656.3	±	193.9	2707.6	±	1016.0	1616.8	±	537.8
IR	1646.8	±	488.7	4423.1	±	3195.5	3126.8	±	868.1
IR+NS	2008.6	±	532.4	5747.2	±	2242.3*	3929.1	±	2676.3
IR+HSal	1744.0	±	424.6	3438.7	±	904.0	2235.2	±	757.1

Values are presented as Mean ± SD, *p < 0.05 vs. Control group; *p < 0.05 vs. I/R group.

Abbreviations: BL; baseline, T1; reperfusion at 15 min, T2; reperfusion at 120 min, MAP; mean arterial pressure, RBF; renal blood flow, RVR; renal vascular resistance, I/R; ischemia/reperfusion, HSa; hypertonic saline, NS; normal saline.

after the I/R (p<0.05 vs. Control). Whereas NS did not attenuate the I/R induced decrease in $C_{\mu}PO_2$ (~25.1%, p<0.05 vs. Control), HSa was able to improve this variable (~22%, p<0.05 vs. IR) (Figure 1A). $M_{\mu}PO_2$ levels only reduced significantly in IR group (~27.5%) compared to the Control (~15.1%) (p<0.05) (Fig.1B). I/R resulted in a ~69.5% reduction of DO_{2ren} that was significantly improved by HSa (p<0.05) but not by treatment with NS (Figure 1C). The percentage change of VO_{2ren} in the IR groups was significantly lower than the Control group (p<0.05), and NS and HSa equally improved this relative reduction in VO_{2ren} (Figure 1D).

Renal functional parameters

The TNa^+ , ERO_{2ren} , $EFNa^+$, $Clear_{crea}$ and urine output variables are shown in Figure 2. TNa^+ decreased in all I/R groups at T1 (4.2 ± 2.7 mmol/min., p<0.05) and T2 (7.9 ± 3.5 mmol/min., p<0.05) compared to control at T1 and T2 (17.5 ± 0.6 mmol/min., 19.9 ± 1.3 respectively). At T2, TNa^+ values in the IR+HSa group (-2.9 ± 6.3 mmol/min.) was further lowered, and lower than the IR+NS group (9 ± 2.5 mmol/min.) (p<0.05) (Figure 2A). $EFNa^+$ value increased in IR group treated with both NS (39.2 ± 22.5 % Na^+ at T1, 23.5 ± 13.8 % Na^+ at T2) and HSa (70.6 ± 40.6 % Na^+ at T1, 118.2 ± 45 % Na^+ at T2) compared to the Control group at T1 (7.5 ± 3.2 % Na^+) (p<0.05) and T2 (3.3 ± 1.3 % Na^+) (p<0.05), and the values of the IR+HSa group was also significantly higher than that of the NS group at T1 and T2 (p<0.05) (Figure 2B). Creatinine clearances decreased in

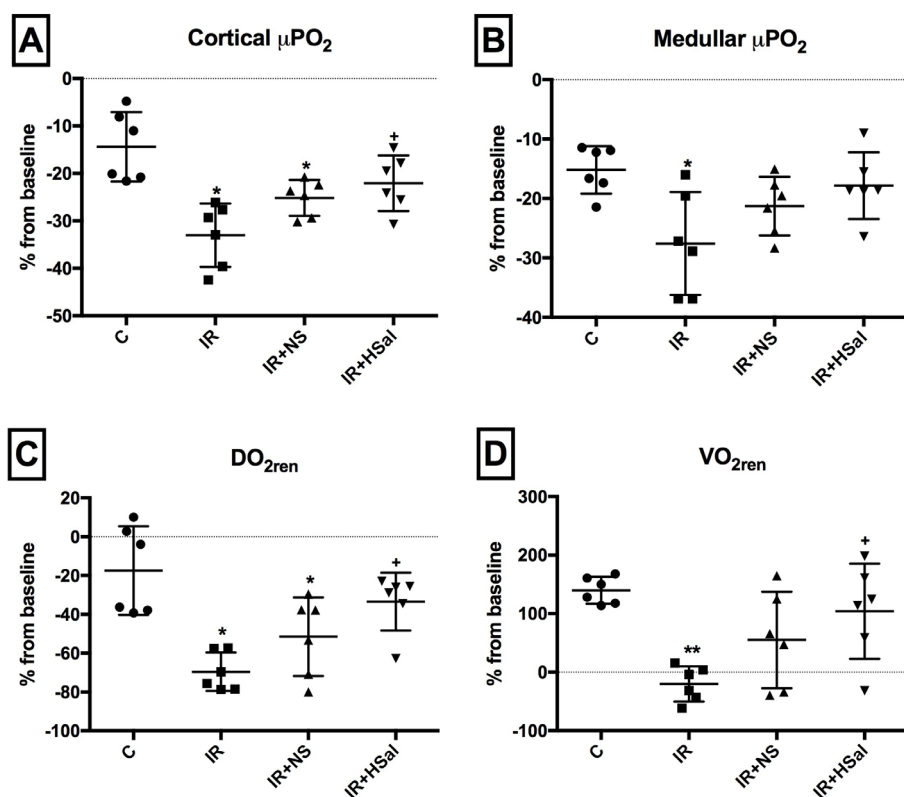


Figure 1. Percentage changes of the renal $\text{C}\mu\text{PO}_2$ (Panel A), $\text{M}\mu\text{PO}_2$ (Panel B), $\text{DO}_{2\text{ren}}$ (Panel C) and $\text{VO}_{2\text{ren}}$ (Panel D) values from BL to T2 between the Control, I/R, I/R+NS and I/R+HSal groups. I/R; ischemia/reperfusion, NS; normal saline, HSa; hypertonic saline. Values are presented as Mean \pm SD, * $p < 0.05$ vs. Control group; + $p < 0.05$ vs. I/R group.

all I/R groups at T1 ($p < 0.05$) but it was equally improved by both NS (0.1 ± 0.04) and HSa (0.11 ± 0.06) at T2 compared to the control at T2 (0.14 ± 0.02) ($p < 0.05$) (Figure 2C). No difference was found in $\text{ERO}_{2\text{ren}}$ levels between the groups (Figure 2D). Urine output was reduced in I/R (0.26 ± 0.1) and I/R+NS (0.35 ± 0.3) group at T1 compared to the control (0.95 ± 0.2) ($p < 0.05$) and it was elevated as a result of HSa treatment at T1 (0.62 ± 0.2 , $p < 0.05$) and T2 (0.95 ± 0.2 , $p < 0.05$) compared to I/R, and at T2 (0.61 ± 0.3 , $p < 0.05$) compared to IR+NS group (Figure 2E).

Biochemical results

No changes were observed in levels of plasma anion gap and the Hct between groups. While HSa was associated with mild acidosis in the blood probably due to the excess Cl in the HSa and in contrast to NS, HSa did not correct to plasma creatinine level

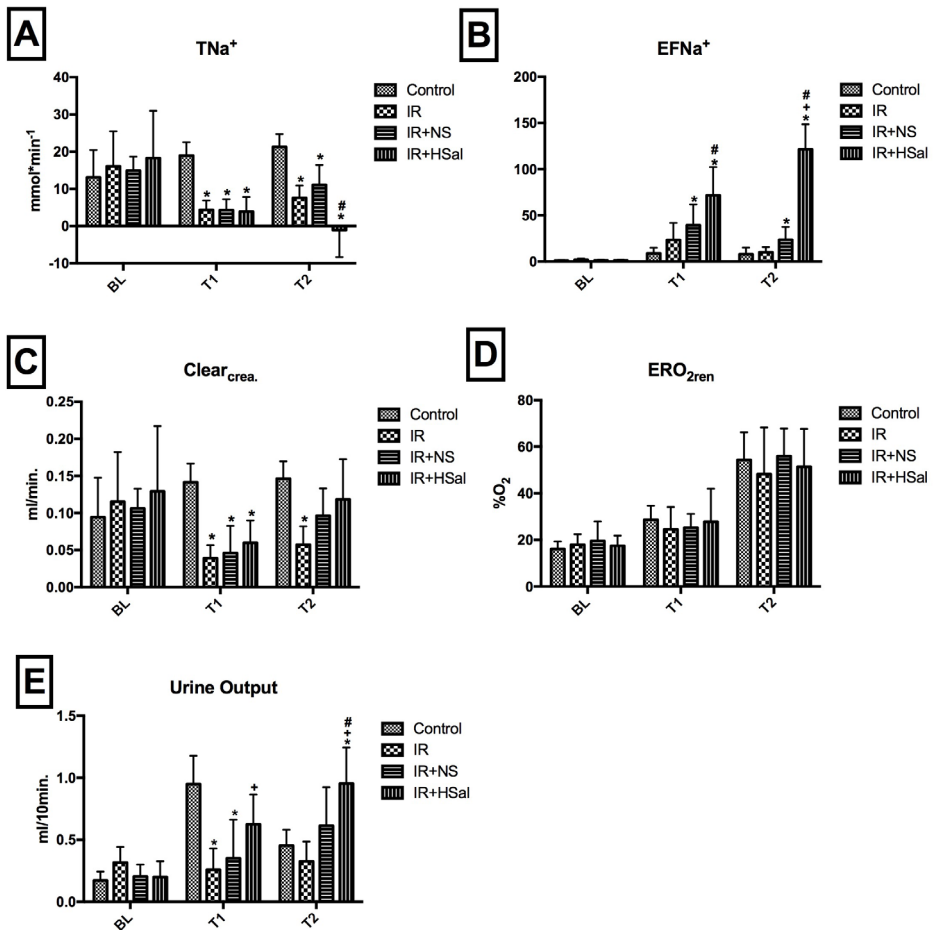


Figure 2. The renal TNa⁺ (Panel A), EFNa⁺ (Panel B), Cre_{cl} (Panel C), ER % O₂ (Panel D) and urine output (Panel E) between the Control, I/R, I/R+NS and I/R+HS at BL, T1 and T2. I/R; ischemia/reperfusion, NS; normal saline, HSal; hypertonic saline. Values are presented as Mean \pm SD, *p < 0.05 vs. Control group; #p < 0.05 vs. I/R group; *p < 0.05 vs. I/R+NS group.

indicating persistent AKI (Stage I according to KDIGO criteria) compared to the control group (p < 0.05) (Table 2). TNF- α and IL-6 levels showed a non-significant increase after ischemia/reperfusion as compared to control. Only the HSal treatment significantly lowered TNF- α and IL-6 as compared to the non-treated I/R group (p < 0.05) (Figure 3A-B). Hyaluronic acid levels increased in IR (p < 0.05) and IR+NS (p < 0.05) groups compared to the Control group but was lowered by treatment of the HSal with respect to the IR (p < 0.05) and IR+NS (p < 0.05) group (Figure 3D).

Table 2. Plasma creatinine, anion gap, pH and Hct level between groups.

	BL	T1	T2
Hct (%RBC)			
Control	50.1 ± 1.9	47.5 ± 2.2	41.3 ± 3.8
IR	50.1 ± 3	46 ± 3.5	40 ± 3.5
IR+NS	45.8 ± 5.3	47.3 ± 1.8	41.8 ± 1.7
IR+HSal	46.6 ± 2.5	44.8 ± 1.7	39.8 ± 3
Plasma Creatinine (μmol/L)			
Control	29.1 ± 3.4	28.5 ± 4.5	27.6 ± 3.7
IR	26.5 ± 13.5	29.1 ± 2.5	37 ± 2.7*
IR+NS	27 ± 2.9	30.6 ± 3.4	33.6 ± 2.4*+
IR+HSal	26.3 ± 3.8	37.1 ± 4.4*	34.5 ± 4.8*
pH			
Control	7.41 ± 0.03	7.4 ± 0.01	7.42 ± 0.03
IR	7.42 ± 0.01	7.39 ± 0.03	7.42 ± 0.01
IR+NS	7.42 ± 0.06	7.37 ± 0.04	7.40 ± 0.05
IR+HSal	7.41 ± 0.04	7.37 ± 0.04	7.36 ± 0.04*+
Anion gap (mmol/L)			
Control	13.8 ± 1.4	15.9 ± 1.42	16.8 ± 3.2
IR	15.8 ± 1.6	16 ± 2	16 ± 1.4
IR+NS	15.6 ± 1.9	16 ± 1.4	15.1 ± 1.3
IR+HS	15.5 ± 1.3	16.6 ± 2.5	16.4 ± 1.2

Values are presented as Mean ± SD, *p < 0.05 vs. Control group; *p < 0.05 vs. I/R group.

Abbreviations: BL; baseline, T1; reperfusion at 15 min, T2; reperfusion at 120 min, I/R; ischemia/reperfusion, HSal; hypertonic saline, NS; normal saline.

Immunohistochemistry

There was no difference in the distributions of eNOS immunostaining intensity (H-Score) between the groups (Figure 4A). iNOS reactivity increased in kidney cortex of both IR+NS and IR+HSal group compared to the control ($p < 0.01$, $P < 0.05$ respectively) and IR ($p < 0.001$, $p < 0.01$ respectively) groups (Figure 4B).

Renal Histology

Tubular vacuolization increased in I/R, I/R+NS and I/R+HSal compared to the control group ($p < 0.0001$, $p < 0.5$ and $p < 0.0001$ respectively). However, NS treatment caused a decrease in vacuolization in comparison to the IR ($p < 0.05$) and I/R+HSal ($p < 0.05$) groups (Figure 5B).

Tubular brush border loss and luminal cast formation in the peritubular cortex of kidney were increased in all IR groups ($p < 0.0001$). The reperfusion with NS reduced both tubular brush border loss and tubular cast formation with respect to the I/R+HSal group ($p < 0.01$ and $p < 0.0001$ respectively). Reperfusion with HSal increased tubular cast formation relative to the I/R only ($p < 0.001$ vs. I/R) (Figure 5C-D).

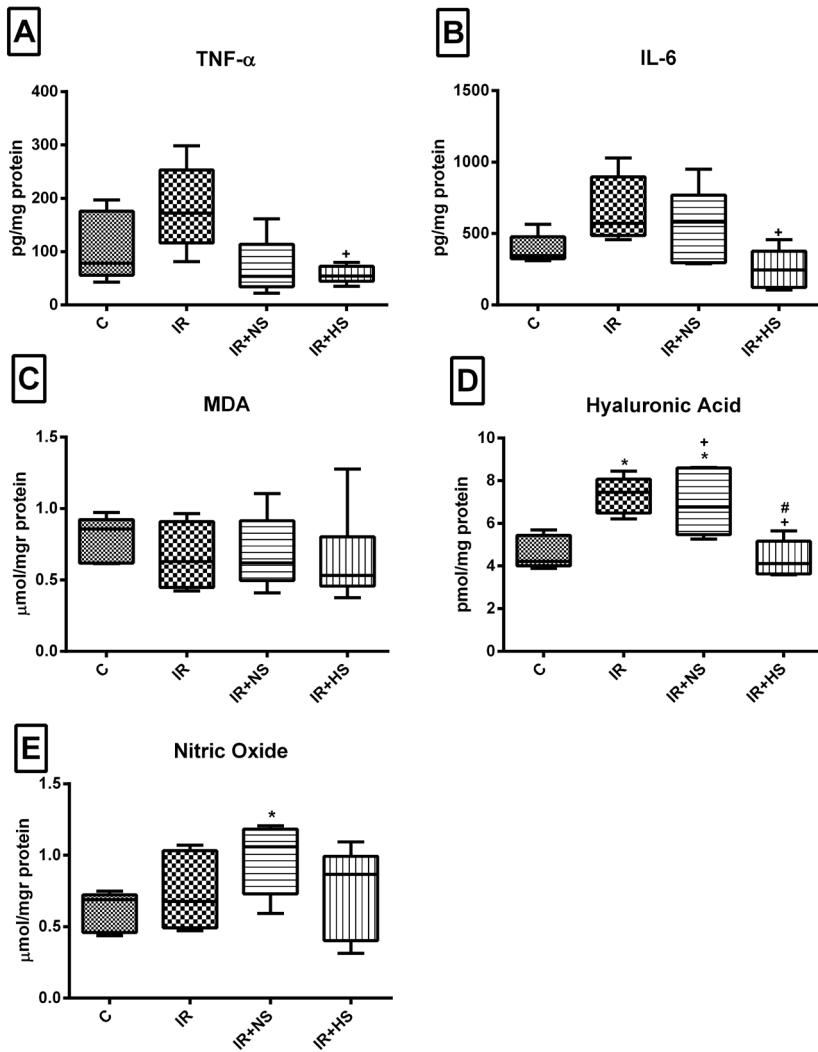


Figure 3. Renal tissue TNF- α (panel A), IL-6 (panel B), MDA (Panel C), hyaluronic acid (Panel D) and NO (Panel E) between the Control, I/R, and I/R + NH, I/R+HSal groups after 120 min. reperfusion. I/R; ischemia/reperfusion, NS; normal saline, HS; hypertonic saline. Values are presented as Mean \pm SD, * $p < 0.05$ vs. Control group; # $p < 0.05$ vs. I/R group; * $p < 0.05$ vs. I/R+NS group.

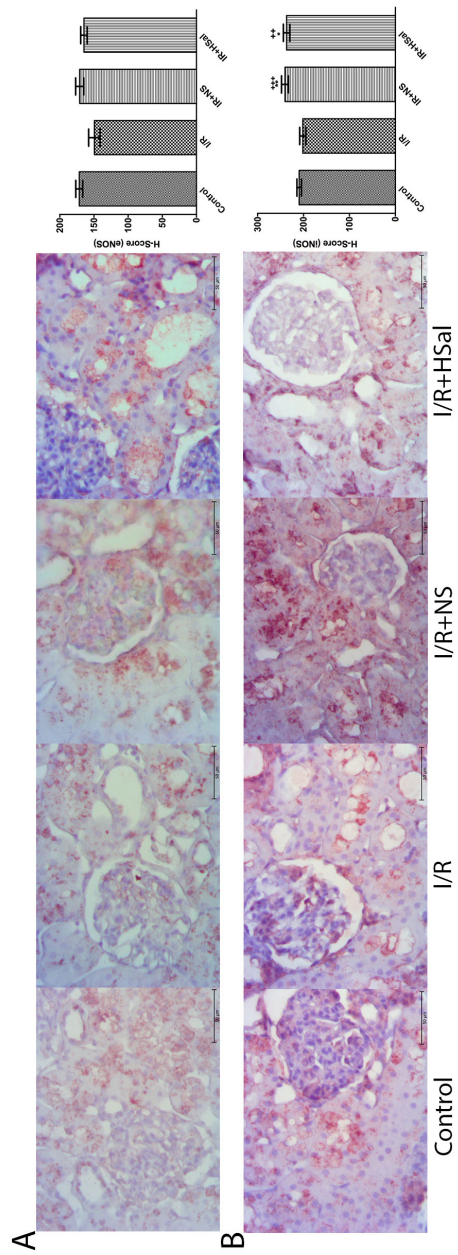


Figure 4. The representative images (Bar=50mm) and distributions of eNOS and iNOS immunostaining intensity (H-Score) in kidney cortex of all groups (Panel A and B). Values are presented as Mean ± SD, * $p < 0.05$ and ** $p < 0.01$ vs. Control group; *** $p < 0.001$ vs. I/R group.

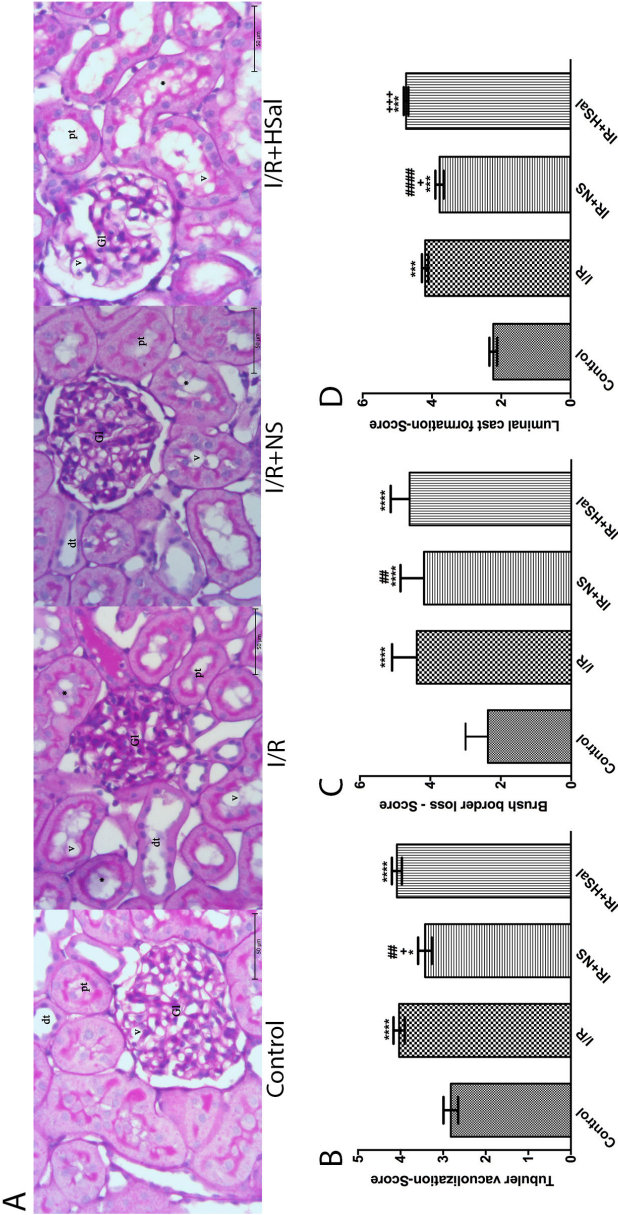


Figure 5. The histological images (Bar=50_m) of renal cortex in all groups (Panel A). Histological damage score of tubular vacuolization, brush border loss and cast formation in peritubular cortex between the groups (Panel B-D). GL; glomerulus, v; vacuole, pt; proximal tubul, dt; distal tubul, *; cast formation. Values are presented as Mean \pm SD, * $p<0.05$, ** $p<0.01$ and *** $p<0.0001$ vs. Control group; * $p<0.05$ and *** $p<0.001$ vs. I/R group; ** $p<0.01$ and *** $p<0.0001$ vs. I/R+Hsal group.

DISCUSSION AND CONCLUSION

In the present study, we firstly examined whether resuscitation by HSSal solution would be able to improve the IR-induced AKI in terms of systemic and renal hemodynamic, renal oxygenation, renal function, oxidative stress, inflammation and structural damage. We demonstrated that despite sustained RBF and renal oxygen delivery, 45 min. ischemia followed by 2 hours of reperfusion resulted in a significant decrease in the MAP, renal microcirculatory oxygenation, oxygen consumption and an increased in inflammation, and that all these parameters could be considerably improved by HSal administration. In addition to its positive effects on systemic hemodynamic, inflammation and renal function, HS also improved renal oxygenation, probably as a result of reduced tubular Na reabsorption and increased excretion fraction of Na^+ due to high Na^+ load in renal tubules. Despite these positive effects, our results also showed that HS might have an overwhelming effect to provoke to distinct renal epithelial and tubular damage following ischemia/reperfusion.

Many regulatory factors contribute to the homeostasis of oxygen supply and consumption of the kidney including the systemic and renal hemodynamics, and renal microvascular circumstance as well as metabolic needs. Brezis *et al.* have shown that moderate hypotension after hemorrhage was associated with a decrease in C_μPO_2 and an increase in M_μPO_2 in healthy rats (22). However, in the present study we showed that lower body I/R induced systemic hypotension was associated with a decrease in both cortical and medullar PO_2 levels. Despite relatively sustained renal blood flow and RVR, we found that $\text{DO}_{2\text{ren}}$ and $\text{VO}_{2\text{ren}}$ were decreased after ischemia/reperfusion in this study. Legrand *et al.* found that 30 min. of suprarenal aortic occlusion resulted in a decrease in RBF, $\text{DO}_{2\text{ren}}$, $\text{VO}_{2\text{ren}}$ and renal oxygenation, and in an increase in $\text{ERO}_{2\text{ren}}$ % levels in the kidneys of their I/R renal group despite a stable MAP (23). Although they did not find any differences in TNa^+ , we found that TNa^+ levels were significantly reduced in the I/R group, probably due to ATP depletion after the hypoxic episode leading to less Na^+ reabsorption as a result of an inactivation of the Na-K ATPase. Even though a reduced TNa^+ levels and microvascular pO_2 were found, $\text{ERO}_{2\text{ren}}$ % levels was stable in the I/R group. This result may indicates that renal oxygen utilization does not directly correlate with Na^+ reabsorption, even though reduction of $\text{VO}_{2\text{ren}}$ was also confirmed by low creatinine clearances and urine output after I/R. The major determinants of kidney microcirculatory oxygen pressures includes the amount of oxygen in the arterial blood, intrarenal distribution of the oxygen, oxygen consumed by the cells and renal arterial-to-venous oxygen shunting which occurs as a result of diffusion of oxygen from preglomerular arteries to post-glomerular veins without being available to the cells for consumption. It has been hypothesized that renal arterial-to-

venous O₂ shunting is an adaptation to prevent hyperoxia due to high renal perfusion needed to sustain glomerular filtration (GFR) (24).

In this study, we showed that administration of % 10 HSal improved systemic and renal hemodynamic parameters by an increase in cardiac performance without any alteration on the Hct or intravascular volume and was associated with high urine output following ischemia. Frithiof *et al.* had also shown that HSal improves hemodynamic parameter such as MAP, cardiac output and heart rate by stimulating cardiac sympatic nerves activity (CSNA) but not renal sympatic activity (RSNA) (25). Cox *et al.* showed that a high serum level of arginine vasopressin following 7.5 % hypertonic saline resuscitation contributing to diuresis (26) as an explanation of high urine output in present study. Like vasopressin, adenosine is another potential endogenous agent that may affect the intrarenal vascular tonicity and oxygenation in the case of high plasma sodium content or hypertonicity. Deray *et al.* had shown that intrarenal infusion of HSal enhances the endogenous production of adenosine and that the ability of adenosine reduce renal blood flow dependent on the presence of angiotensin II (AngII) (27). Osswald *et al.* also reported that a rapid increase in renal transport work leads to a fall in ATP and an increase of adenosine tissue content, following infusion of HSal into the thoracic aorta (28) or into the vein (29). To contrast, our renal hemodynamic findings indicate an improvement in both both renal blood flow and vascular resistance following HSal administration. In first time, we showed that administration of 10 % HSal led to an increase in $CuPO_2$, DO_{2ren} and VO_{2ren} levels. This improved renal microvascular oxygenation profile was associated with a low TNa^+ and high $EFNa^+$ level leading to loss of sodium and water from the plasma. Additionally, in parallel to the diuretic effect of HSal, we also found that the renal transport work (TNa^+) was considerably reduced by HSal administration following the ischemic insult. These results may confirm that hypertonicity does not provoke to renal transport or adenosine release or in far a high energy demand of kidney. Indeed, we clearly demonstrated the renal Na^+ transport as a result of high renal sodium excretion and low tubular reabsorption was reduced after HSal administration indicating that oxygen utilization driven by Na-ATPase in the kidney was also depleted that might be a reason of enhanced renal oxygenation. In comparison to HSal, we also found that using normal saline as a resuscitation fluid in this model led to less renal functional impairment and correlated with higher TNa^+ and lesser $EFNa^+$ levels. However, in a different model, Legrand *et al.* demonstrated that no superior effect of HS resuscitation on the systemic hemodynamics and renal oxygenation parameters with regard to NS in hemorrhagic shock (30).

Similar to our renal oxygenation findings, Ni *et al.*, recently demonstrated that early administration of 7,5 % HSal improves both hemodynamics and peripheral oxygenation

in a pig model of acute pancreatitis (31). Except for adenosine, endothelin, vasopressin, ATP or AngII, the activity of eNOS as a potent vasodilator has been shown to be essential in the regulation of renal oxygenation, preventing platelet aggregation and leukocyte adhesion at the microcirculatory level (32). In this study, we did not find any differences in total NO levels. Although chemiluminescence method only allowed to measurement of total NO values, in immunohistochemistry measurements, we clearly showed an enhanced iNOS levels as a contributor to renal oxygenation and inflammation following NS or HSal resuscitation despite an unaltered eNOS reactivity of renal cortex.

In this study, we also found that renal tissue TNF- α and IL-6 levels were partially increased in I/R group, and attenuated after 10 % HSal administration but not after NS. Chimabucuro *et al.* Reported that 4ml/kg 7.5 % hypertonic saline and normal saline administration resulted a decrease in MDA level, proinflammatory cytokines (IL-6) myeloperoxidase activity and increase anti-inflammatory marker (IL-10) in lung, liver and gut after 45 min. superior mesenteric arterial occlusion in rat (33). In the present study, we found that hyaluronic acid levels as a glycocalyx shedding marker was also improved by the treatment of hypertonic saline. However, in our histological findings revealed that resuscitation with the HSal, but not NS, was also associated with an increase in renal damage such as cast formation occurring after lower body I/R, probably due to an impairment of the tubular cell hemostasis provoked by high intracellular and renal tubular Na⁺. This discrepancy between the high renal damage and low glycocalyx shedding may be explained by anti-inflammatory effect of HSal. Nevertheless, Nieuwdorp *et al.* showed that inhibition of TNF- α resulted an improvement of glycocalyx thickness and hyaluronan loss (34). As parallel to our results, Bahrami *et al.* demonstrated that despite the anti inflammatory effect of hypertonic saline resuscitation in hemorrhagic shock, on 7 days after shock, survival rate of HS group was lower than the NS group (35). This also support that there is a divergent reaction of pathophysiological and structural damage parameters to HS treatment, and argues that both types of parameters should be evaluated when examining fluid resuscitation strategies in AKI.

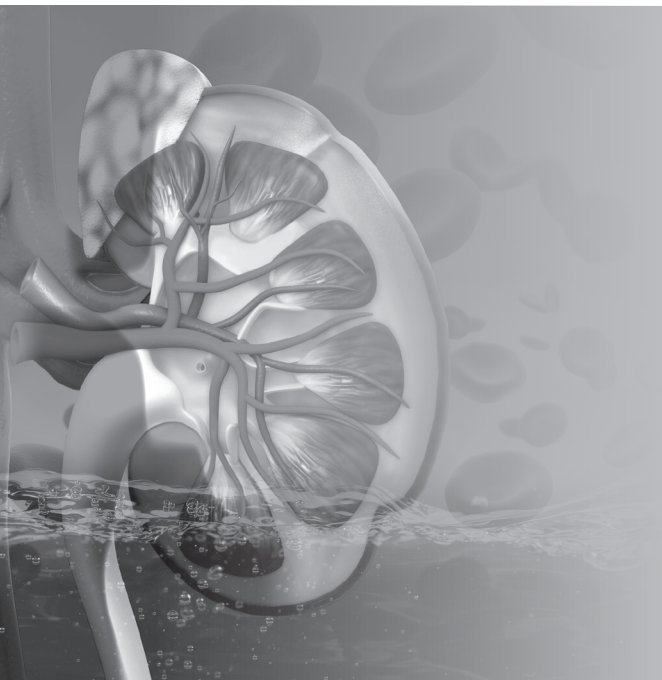
In conclusion, our study demonstrated that I/R induced AKI was correlated with the deterioration of the microcirculatory oxygenation, oxygen supply and utilization including hemodynamic instability. The high energy demand of kidney and impairment of the oxygen utilization following ischemia may be a major contributor factors leading to microcirculatory disturbance and oxygen shunting. In addition to its hemodynamics, anti-inflammatory and glycocalyx protective effects, our study also showed that administration of 10 % hypertonic saline as a resuscitation strategy might improve the renal microvascular oxygenation probably due to a diminished renal transport load, energy demand and Na-K ATPase function. Moreover, we also found that resuscitation

with HSal may result in renal tubular damage due to high sodium load accompanied with an impaired tubular cell hemostasis. These findings suggest that hypertonic saline should be avoided or strictly controlled for long-term used in conditions of sterile inflammation because of these deleterious effects on the kidney despite the finding that the functional properties of the kidney seem to be sustained.

REFERENCES

1. Bagshaw SM. The long-term outcome after acute renal failure. *Curr. Opin. Crit. Care.* 12(6):561–566, 2006.
2. Ellenberger C, Schweizer A, Diaper J, *et al.* Incidence, risk factors and prognosis of changes in serum creatinine early after aortic abdominal surgery. *Intensive Care Med.* 32(11):1808–1816, 2006.
3. Wong GTC, Irwin MG. Contrast-induced nephropathy. *Br. J. Anaesth.* 99(4):474–483, 2007.
4. Cupples WA, Braam B. Assessment of renal autoregulation. *Am. J. Physiol. Renal Physiol.* 292(4):F1105–F1123, 2007.
5. Blantz RC, Deng A, Miracle CM, *et al.* Regulation of kidney function and metabolism: a question of supply and demand. *Trans. Am. Clin. Climatol. Assoc.* 118:23–43, 2007.
6. Brezis M, Agmon Y, Epstein FH. Determinants of intrarenal oxygenation. I. Effects of diuretics. *Am. J. Physiol.* 267(6 Pt 2):F1059–F1062, 1994.
7. Legrand M, Almac E, Mik EG, *et al.* L-NIL prevents renal microvascular hypoxia and increase of renal oxygen consumption after ischemia-reperfusion in rats. *Am. J. Physiol. Renal Physiol.* 296(5):F1109–F1117, 2009.
8. Cooper DJ, Myles PS, McDermott FT, *et al.* Prehospital hypertonic saline resuscitation of patients with hypotension and severe traumatic brain injury: a randomized controlled trial. *JAMA* 291(11):1350–1357, 2004.
9. Younes RN, Aun F, Accioly CQ, *et al.* Hypertonic solutions in the treatment of hypovolemic shock: a prospective, randomized study in patients admitted to the emergency room. *Surgery* 111(4):380–385, 1992.
10. Strandvik GF. Hypertonic saline in critical care: a review of the literature and guidelines for use in hypotensive states and raised intracranial pressure. *Anaesthesia* 64(9):990–1003, 2009.
11. Gazitúa S, Scott JB, Chou CC, *et al.* Effect of osmolarity on canine renal vascular resistance. *Am. J. Physiol.* 217(4):1216–1223, 1969.
12. de Felipe J, Timoner J, Velasco IT, *et al.* Treatment of refractory hypovolaemic shock by 7.5% sodium chloride injections. *Lancet* 2(8202):1002–1004, 1980.
13. Velasco IT, Pontieri V, Rocha e Silva M, *et al.* Hyperosmotic NaCl and severe hemorrhagic shock. *Am. J. Physiol.* 239(5):H664–673, 1980.
14. Rocha-e-Silva M, Poli de Figueiredo LF. Small volume hypertonic resuscitation of circulatory shock. *Clinics (Sao Paulo)* 60(2):159–172, 2005.
15. Shields CJ, Winter DC, Manning BJ, *et al.* Hypertonic saline infusion for pulmonary injury due to ischemia-reperfusion. *Arch. Surg.* 138(1):9–14, 2003.
16. Zuurbier CJ, Emons VM, Ince C. Hemodynamics of anesthetized ventilated mouse models: aspects of anesthetics, fluid support, and strain. *Am. J. Physiol. Heart Circ. Physiol.* 282(6):H2099–H2105, 2002.
17. Johannes T, Mik EG, Ince C. Dual-wavelength phosphorimetry for determination of cortical and subcortical microvascular oxygenation in rat kidney. *J. Appl. Physiol.* 100(4):1301–1310, 2006.
18. Vanderkooi JM, Maniara G, Green TJ, *et al.* An optical method for measurement of dioxygen concentration based upon quenching of phosphorescence. *J. Biol. Chem.* 262(12):5476–5482, 1987.
19. KDIGO Board Members. *Kidney Int. Suppl.* (2011) 2(1):3, 2012.
20. Ergin B, Bezemer R, Kandil A, *et al.* TEMPOL has limited protective effects on renal oxygenation and hemodynamics but reduces kidney damage and inflammation in a rat model of renal ischemia/reperfusion by aortic clamping. *J. Clin. Transl. Res.* (1):116–128, 2015.
21. Birman H, Dar KA, Kapucu A, *et al.* Effects of Luteolin on Liver, Kidney and Brain in Pentylenetetrazol-Induced Seizures: Involvement of Metalloproteinases and NOS Activities. *Balkan Med. J.* 29(2):188–196, 2012.
22. Brezis M, Heyman SN, Epstein FH. Determinants of intrarenal oxygenation. II. Hemodynamic effects. *Am. J. Physiol.* 267(6 Pt 2):F1063–F1068, 1994.
23. Legrand M, Kandil A, Payen D, *et al.* Effects of sepiapterin infusion on renal oxygenation and early acute renal injury after suprarenal aortic clamping in rats. *J. Cardiovasc. Pharmacol.* 58(2):192–198, 2011.

24. Evans RG, Gardiner BS, Smith DW, *et al.* Intrarenal oxygenation: unique challenges and the biophysical basis of homeostasis. *Am. J. Physiol. Renal Physiol.* 295(5):F1259-1270, 2008.
25. Frithiof R, Ramchandra R, Hood SG, *et al.* Hypertonic sodium resuscitation after hemorrhage improves hemodynamic function by stimulating cardiac, but not renal, sympathetic nerve activity. *Am. J. Physiol. Heart. Circ. Physiol.* 300(2):H685-692, 2011.
26. Cox AT, Ho HS, Gunther RA. High level of arginine vasopressin and 7.5% NaCl/6% dextran-70 solution: cardiovascular and renal effects. *Shock* 1(5):372-376, 1994.
27. Deray G, Sabra R, Herzer WA, *et al.* Interaction between angiotensin II and adenosine in mediating the vasoconstrictor response to intrarenal hypertonic saline infusions in the dog. *J. Pharmacol. Exp. Ther.* 252(2):631-635, 1990.
28. Osswald H, Nabakowski G, Hermes H. Adenosine as a possible mediator of metabolic control of glomerular filtration rate. *Int. J. Biochem.* 12(1-2):263-267, 1980.
29. Osswald H, Mühlbauer B, Schenk F. Adenosine mediates tubuloglomerular feedback response: an element of metabolic control of kidney function. *Kidney Int. Suppl.* 32:S128-131, 1991.
30. Legrand M, Mik EG, Balestra GM, *et al.* Fluid resuscitation does not improve renal oxygenation during hemorrhagic shock in rats. *Anesthesiology* 112(1):119-127, 2010.
31. Ni H-B, Ke L, Sun J-K, *et al.* Beneficial effect of hypertonic saline resuscitation in a porcine model of severe acute pancreatitis. *Pancreas* 41(2):310-316, 2012.
32. Bertuglia S, Giusti A. Role of nitric oxide in capillary perfusion and oxygen delivery regulation during systemic hypoxia. *Am. J. Physiol. Heart Circ. Physiol.* 288(2):H525-531, 2005.
33. Chimabucuro WK, da Silva Junior BA, Moretti AIS, *et al.* The impact of hypertonic and normal saline in gut reperfusion after ischemia in rats. *Rev. Bras. Ter. Intensiva* 26(3):277-286, 2014.
34. Nieuwdorp M, Meuwese MC, Mooij HL, *et al.* Tumor necrosis factor- α inhibition protects against endotoxin-induced endothelial glycocalyx perturbation. *Atherosclerosis* 202(1):296-303, 2009.
35. Bahrami S, Zimmermann K, Szelényi Z, *et al.* Small-volume fluid resuscitation with hypertonic saline prevents inflammation but not mortality in a rat model of hemorrhagic shock. *Shock* 25(3):283-289, 2006.



CHAPTER 7

Fully balanced fluids do not improve microvascular oxygenation, acidosis and renal function in a rat model of endotoxemia

Adapted from *Shock* 2016 Jul;46(1):83-91

Bulent Ergin¹, Lara Zafrani¹, Asli Kandil², Silke Baasner³, Corinna Lupp³, Cihan Demirci²
Martin Westphal^{3,4} and Can Ince^{1,5}

¹ Department of Translational Physiology, Academic Medical Center, Amsterdam, The Netherlands

² Department of Biology and Zoology Division, University of Istanbul, Istanbul, Turkey

³ Fresenius Kabi Deutschland GmbH, Bad Homburg, Germany

⁴ Department of Anesthesiology, Pain Medicine and Intensive Care, University Hospital of Muenster, Muenster, Germany

⁵ Department of Intensive Care Medicine, Erasmus MC, University Medical Center Rotterdam, Rotterdam, The Netherlands

ABSTRACT

The expectation of fluid therapy in patients with septic shock is that it corrects hypovolemia, with the aim of restoring tissue perfusion and oxygenation and organ function. This study investigated whether different types of resuscitation fluids were effective in improving renal microcirculatory oxygenation, acidosis, oxidative stress, and renal function in a rat model of endotoxemic shock. 5 groups of rats were used: a sham group, a lipopolysaccharide (LPS) group and 3 LPS groups that received 30 ml/kg/h of 0.9% sodium chloride (0.9% NaCl), a new bicarbonate buffered crystalloid solution closely resembling the composition of plasma (FB-Cxt) or a hydroxyethyl starch-ringer acetate (HES-RA) solution. Systemic hemodynamic variables, renal blood flow, microvascular oxygenation, oxidative/nitrosative stress and renal function were measured. LPS-induced shock was only partially resolved by fluid administration. Animals became arterially hypotensive despite adequate venous pressures. HES-RA was more effective at improving arterial pressures and RBF than 0.9%NaCl or FB-Cxt. Fluids had marginal effects on pH and HCO_3^- levels irrespective of the buffer, or on renal μPO_2 and dysfunction. Colloids increased the markers of renal oxidative stress ($p<0.001$), whereas unbalanced crystalloids increased the markers of nitrosative stress during sepsis ($p<0.01$). Endotoxemia-induced acidosis and decreases in renal μPO_2 or renal injury were not corrected solely by fluid resuscitation, irrespective of the buffer of the fluid. Our study supported the idea that fluids must be supplemented by other compounds that specifically correct renal inflammation and oxygenation to be effective in resolving septic shock-induced renal failure.

Keywords: acute kidney injury, microcirculation, sepsis, renal oxygenation, fluid resuscitation

INTRODUCTION

In the early stage of sepsis, impairment of the renal microcirculation is a key complication that can lead to renal failure through hypoxia-induced tubular epithelial cell injury and acute tubular necrosis (1-3). Fluid resuscitation following shock is considered crucial for the preservation of an adequate intravascular volume to achieve the microvascular perfusion and tissue oxygenation needed for organ function (4). Experimental studies have demonstrated the persistence of hypoxic microvascular areas in the renal cortex in cases of untreated endotoxemic shock (5). Because renal dysfunction is a major complication in intensive care units, there has been continuing concern regarding the efficacy of fluid resuscitation. Expectations for the correction of states of hypovolemia in sepsis have often focused solely on the composition of fluids, and as such, the type of fluids best suited for the resolution of sepsis remains a source of uncertainty and debate (6). This debate concerns the use of crystalloid versus colloid solutions and the use of balanced versus unbalanced colloid or crystalloid solutions, with the ability of fluids to correct or even induce acidosis being a central issue overshadowing other important outcome parameters of renal function, such as tissue oxygenation and inflammatory mediators (7).

Because most solutions differ from the composition of plasma, liberal fluid resuscitation regimens can result in non-physiologically high ion concentrations, affecting homeostasis. Such conditions can occur with the abundant use of 0.9% NaCl, which in itself can cause acidosis unrelated to the metabolic condition of the host and can result in altered inflammatory and coagulation homeostasis, in turn resulting in deteriorating organ function (8,9). The (ab)use of 0.9% NaCl is central to the debate surrounding the efficacy of fluids and their composition in resuscitation medicine (10,11). Both molecular weight and molar substitution can influence the rheological, microvascular, pharmacokinetic and inflammatory effects of fluid solutions (12). This physiological insight has led to the development of various preparations based on balanced, plasma-adapted solutions and to the development of the concept of totally balanced fluid resuscitation (13). However, whether these new, balanced fluids are able to improve renal oxygenation, oxidative stress, and renal function under septic shock conditions remains to be elucidated.

Recently a new, bicarbonate based, fully balanced crystalloid solution (FB-Cxt) was introduced, which as closely as possible mimics the composition of plasma. The effectiveness of such fluids, with greater physiological buffering capacity and composition, in correcting sepsis-induced microcirculation dysfunction, hypoxia, and acid-base disturbances remains to be determined. The aim of this study was to compare both the beneficial and detrimental effects of three different types and compositions of resuscitation

solutions, i.e., a new, fully balanced crystalloid solution (FB-Cxt), a balanced, acetate-based colloid solution (HES-RA) and 0.9% sodium chloride as an unbalanced solution, on sepsis-induced microcirculatory alterations and tissue hypoxia. Specifically, we investigated the effects of these solutions on renal hemodynamics, the relationship between oxygenation and acidosis, inflammatory and oxidative stress, and renal function in a rat model of LPS-induced severe endotoxemic shock.

MATERIALS AND METHODS

Animals

All of the experiments in this study were approved by the institutional Animal Experimentation Committee of the Academic Medical Center of the University of Amsterdam (DFL 102538). The care and handling of the animals were performed in accordance with the guidelines of the Institutional and Animal Care and Use Committees. Experiments were performed on 35 male *Wistar albino* rats (Harlan, Netherlands) with a mean \pm SD body weight of 350 ± 20 g. An additional 9 animals were used for venous pressure measurements to establish that the amount of fluids administered was sufficient to correct filling pressures.

Surgical preparation

The rats were anesthetized with an intraperitoneal injection of a mixture of 100 mg/kg ketamine (Nimatek[®]; Eurovet, Bladel, Netherlands), 0.5 mg/kg medetomidine (Domitor; Pfizer, New York, NY, USA), and 0.05 mg/kg atropine sulfate (Centrafarm, Etten-Leur, The Netherlands). After tracheotomy, the animals were mechanically ventilated with a fraction of inspired oxygen (FiO_2) of 0.4. The body temperature was maintained at $37 \pm 0.5^\circ\text{C}$ throughout the experiment by external warming. The ventilator settings were adjusted to maintain an end-tidal partial pressure of carbon dioxide (PCO_2) between 30 and 35 mm Hg and an arterial PCO_2 between 35 and 40 mm Hg.

Vessels were cannulated with polyethylene catheters (outer diameter = 0.9 mm; Braun, Melsungen, Germany) for drug and fluid administration and for hemodynamic monitoring. A catheter in the right carotid artery was connected to a pressure transducer to monitor the mean arterial blood pressure (MAP) and heart rate. The right jugular vein was cannulated for continuous infusion of Ringer Lactate (Baxter, Utrecht, Netherlands) at a rate of $15 \text{ ml kg}^{-1} \text{ h}^{-1}$, and $50 \text{ mg kg}^{-1} \text{ h}^{-1}$ of ketamine was added for the maintenance of anesthesia. Separate experiments were performed, in which central venous pressures were measured to demonstrate that the provided colloid and crystalloid volumes resulted in adequate filling pressures compared with control values. To this end, the right jugular vein was used for central vein catheterization to measure central venous pressure (CVP),

using a pressure transducer. These experiments were performed on 9 rats, and the results are included in the supplementary data. The left femoral vein was cannulated for fluid administration of either 30 ml/kg/h HES-RA or 0.9% NaCl in these groups, and a third control group was investigated, which received endotoxin but was not administered fluids. The right femoral artery was cannulated for blood sampling, and the right femoral vein was cannulated for fluid resuscitation. The left kidney was exposed, decapsulated, and immobilized in a Lucite kidney cup (K. Effenberger, Pfaffingen, Germany) via a 4-cm incision in the left flank. The renal vessels were carefully separated with preservation of the nerves and adrenal gland. A perivascular ultrasonic transient time flow probe was placed around the left renal artery (type 0.7 RB; Transonic Systems Inc., Ithaca, NY, USA) and was connected to a flow meter (T206; Transonic Systems Inc.) to measure the renal blood flow (RBF) continuously. An estimation of the renal vascular resistance (RVR) was calculated as $RVR \text{ (dynes.sec.cm}^{-5}\text{)} = (MAP/RBF) \times 100$. The left ureter was isolated, ligated and cannulated with a polyethylene catheter for urine collection. The surgical field was covered with a humidified gauze compress throughout the entire experiment to prevent drying of the exposed tissue. After the surgical protocol (approximately 60 minutes), one optical fiber was placed 1 mm above the decapsulated kidney, and another optical fiber was placed 1 mm above the renal vein to measure microcirculatory oxygen pressures using the oxygen-dependent quenching of phosphorescence lifetime technique. A small piece of aluminum foil was placed on the dorsal site of the renal vein to prevent the contribution of the underlying tissue to the phosphorescence signal in the venous partial pressure of oxygen (PO_2) measurements. For the quenching of phosphorescence measurements, Oxyphor G2 (a two-layer glutamate dendrimer of tetra-(4-carboxy-phenyl) benzoporphyrin; Oxygen Enterprises Ltd, Philadelphia, PA, USA) was subsequently infused (6 mg/kg IV over 5 min), followed by a 30-minute stabilization period. A short description of the phosphorescence quenching method is provided below, and a more detailed description of the technology has been published previously (14,15).

Experimental protocol

The rats were randomized into 5 groups ($n = 7$ per group) after the surgical procedure. Severe endotoxemic shock was induced by an intravenous dose of 10 mg/kg LPS (LPS group; *Escherichia coli* A127:B8, Sigma, Paris, France; $n = 7$), or vehicle (time-control group, $n = 7$) was administered for a period of 30 min, followed by a waiting period of 240 min without fluid resuscitation until a MAP of 40 mm Hg was attained. Following this condition of severe septic shock associated with severe hypotension, the different LPS groups were randomized to receive no fluid resuscitation, a volume replacement regimen consisting of a balanced 6% HES 130/0.4 dissolved in a balanced preparation (HES-RA) (Volulyte® 6%; Fresenius Kabi; 30 ml $\text{kg}^{-1}\text{h}^{-1}$) (LPS + HES-RA) (16), a new experimental, fully balanced crystalloid (FB-Cxt) (AQIX®RS; 30 ml $\text{kg}^{-1}\text{h}^{-1}$) (LPS + FB-

Cxt) dissolved in 900 ml of Aqua bidest® Fresenius with 100 ml AQIX®RS and 2.10 g of NaHCO_3 , or isotonic saline resuscitation ($30 \text{ ml kg}^{-1}\text{h}^{-1}$) (LPS + 0.9% NaCl) ($n = 7$) (for composition of the fluids see Table S1) (17) over 2 hours.

Renal microvascular and venous oxygenation

The microvascular oxygen tension in the renal cortex ($C_{\mu}\text{PO}_2$) and outer medulla ($M_{\mu}\text{PO}_2$) and the renal venous oxygen tension ($P_{rv}\text{O}_2$) were determined by measurement of the oxygen-dependent quenching of the phosphorescence lifetimes of the systemically infused albumin-bound (and thus circulation-confined) phosphorescent dye Oxyphor G2 (a two-layer glutamate dendrimer of tetra-(4-carboxy-phenyl) benzoporphyrin), which has two excitation peaks ($\lambda_{\text{excitation1}} = 440 \text{ nm}$, $\lambda_{\text{excitation2}} = 632 \text{ nm}$) and one emission peak ($\lambda_{\text{emission}} = 800 \text{ nm}$). These optical properties allow for (near) simultaneous lifetime measurements in the microcirculation of the kidney cortex and the outer medulla because of the different optical penetration depths of the excitation light. For the measurement of the renal venous PO_2 ($P_{rv}\text{O}_2$), a mono-wavelength phosphorimeter was used. Oxygen measurements based on the phosphorescence lifetime techniques rely on the principle that phosphorescence could be quenched by energy transfer to oxygen, resulting in shortening of the phosphorescence lifetime. The linear relationship between the reciprocal phosphorescence lifetime and oxygen tension (given by the Stern-Volmer relation) allows for quantitative measurements of the PO_2 . Details regarding this technique have been published previously (15,18).

Renal oxygen delivery and consumption

The arterial oxygen content (AOC) was calculated by the formula ($1.31 \times \text{hemoglobin} \times S_a\text{O}_2$) + ($0.003 \times P_a\text{O}_2$), where $S_a\text{O}_2$ is the arterial oxygen saturation, and $P_a\text{O}_2$ is the arterial partial pressure of oxygen. The renal venous oxygen (RVOC) content was calculated as ($1.31 \times \text{hemoglobin} \times S_{rv}\text{O}_2$) + ($0.003 \times P_{rv}\text{O}_2$), where $S_{rv}\text{O}_2$ is venous oxygen saturation, and $P_{rv}\text{O}_2$ is the renal vein partial pressure of oxygen. The renal oxygen delivery was calculated as $\text{DO}_{2\text{ren}} (\text{ml/min}) = \text{RBF} \times \text{AOC}$. The renal oxygen consumption was calculated as $\text{VO}_{2\text{ren}} (\text{ml/min}) = \text{RBF} \times (\text{AOC} - \text{RVOC})$. The renal oxygen extraction ratio was calculated as $\text{ERO}_{2\text{ren}} (\%) = \text{VO}_2 / \text{DO}_2 \times 100$.

Blood gas parameters, total hemoglobin (tHb), HCO_3^- , lactate and creatinine

Arterial blood samples (0.5 ml) were obtained from the femoral artery at the following time points: (1) baseline ($t = 0 \text{ min}$), (2) after LPS infusion ($t = 240 \text{ min}$), (3) 30 min after the start of resuscitation ($t = 270 \text{ min}$) and (4) at the end of the protocol ($t = 360 \text{ min}$). The blood samples were replaced by the same volume of test solution. The samples were used to determine the blood gas parameters, pH, HCO_3^- , arterial hemoglobin concentration, and hemoglobin oxygen saturation (ABL80 Flex blood gas analyzer; Radiometer, Copenhagen, Denmark).

Table S1. Composition of the resuscitation fluids and human serum

Components	AQIX [®] RS FB-Cxt	Volulyte [®] 6% HES-RA	Saline	Human serum
Na ⁺	135	137	154	131-148
K ⁺	5.00	4.00		3.4-5.2
Ca ⁺	1.25			1.12-1.46
Mg ⁺⁺	0.45	1.50		0.38-0.72
Cl ⁻	119	110	154	101-111
HCO ₃	25.0			21-29
D-glucose	10.0			3.6-6.1
Glycerol	0.11			0.131
Glutamate	300			20-110
Glutamine	400			140-570
Aspartate	20 µmol/l			1-11 µmol/l
Carnitine	50 µmol/l			35-85 µmol/l
Choline	10 µmol/l			18-70 µmol/l
Thiamine Phosphate	40.0 nmol/l			6-135 nmol/l
Human insulin	28.0 mIU/l			6-35 mIU/l
BES taurine-based Good's buffer	5.00			
Acetate (CH ₃ COO ⁻)		34.0		
Hydroxyethyl starch (130/0.4)		6%		
pH	7.30-7.46	5.7-6.5	4.5-7.0	7.32-7.45
Osmolality (mOsm/L)	265-286	287	290	264-290

Values represent the concentration in mmol/l unless otherwise stated.

The plasma lactate and creatinine levels were analyzed at baseline and at the end of the experiments by an enzymatic colorimetric method using the Roche Modular P800 automatic analyzer (Roche Diagnostics).

Nitric oxide metabolism

Kidney tissue samples were homogenized in cold 5 mM sodium phosphate buffer. The homogenates were centrifuged at 12,000 g for 15 min at 4°C, and the supernatants were used for the NO and MDA determinations. As an index of the total nitric oxide (NO) bioavailability, the sum of the nitrite and nitrate accumulated in the renal tissue samples was determined. The samples were treated with vanadium (III) chloride (VCl₃) in 1 mol/l HCl at 90°C to reduce the nitrite, nitrate, and S-nitroso compounds to NO. During the experiments, the tested samples were maintained in a closed system, and the gas flow leaving the samples was guided to an NO chemiluminescence signal analyzer (Sievers 280i analyzer, GE Analytical Instruments), allowing for the direct detection of NO (13).

Within the reaction vessel, NO reacted with ozone to generate oxygen and excited-state NO species, the decay of which is associated with the emission of weak near-infrared chemiluminescence. This signal was detected by a sensitive photodetector and was converted to millivolts (mV). The area under the curve of the detected chemiluminescence (mV·s) represents the amount of NO-ozone reactions in time and, therefore, the amount of bioavailable NO in the tested samples. The tissue NO measurements were normalized to the tissue protein content.

Measurement of oxidative stress

The tissue malondialdehyde (MDA) levels were used to quantify oxidative stress by assessing lipid peroxidation. The amount of MDA was quantified using a Quattro Premier XE tandem mass spectrometer (MS/MS) from Waters (Milford, MA, USA), with an Acquity sample manager and an Acquity binary solvent manager, in accordance with Foreman *et al.* (19). MDA and MDA-d2 were separated on a Supelco LC-18DB column (250-mm length x 4.-mm diameter, with 5- μ m particles) using an isocratic run from 50% acetonitrile, 50% water and 0.2% acetic acid; the flow rate was 1 ml/min, with a total run time of 10 min. Both compounds were detected and quantified by MRM acquisition in the positive electrospray ionization mode, using the transitions m/z 235 > 159 for MDA and 237 > 161 for MDA-d2. The levels of lipid peroxides were expressed as micromoles of MDA per milligram of protein (Bradford assay).

Statistical analysis

The data plotting and analysis were performed using GraphPad Prism software version 5.0 (GraphPad Software, San Diego, CA, USA). All of the values are reported as the mean \pm SD. The comparative analysis of data sets obtained in different groups and at different time points was performed using two-way ANOVA with Bonferroni's post-hoc corrections. Repeated-measures analysis of variance (one-way ANOVA with Tukey's post-test) was used to compare responses in the control rats with the responses in the rats that received LPS. For all of the analyses, p-values <0.05 were considered statistically significant.

RESULTS

Effects of different resuscitation fluids on systemic and renal hemodynamic parameters

Mean arterial pressure (MAP), renal blood flow (RBF) and renal vascular resistance (RVR) are shown in Table 1. The infusion of LPS induced an early decrease in MAP to 45% of the baseline during the initial phase of endotoxic shock and to 30% of the baseline at the end of the protocol in the LPS group without fluid resuscitation. RBF decreased rapidly, and RVR increased rapidly after LPS administration. Of the fluids tested, HES-

Table 1. Systemic and renal hemodynamic parameters.

	T0 (baseline)		T1 (shock)		T2 (30 min)		T3 (120 min)	
MAP [mmHg]								
Control	106	± 11	72	± 8	71	± 9	64	± 7
LPS	94	± 8	41	± 2 ^{***}	43	± 2 ^{***}	28	± 3 ^{***}
0.9 % NaCl	101	± 7	40	± 0 ^{***}	47	± 6 ^{***}	40	± 2 ^{***+}
HES-RA	92	± 7	40	± 0 ^{***}	56	± 8 ^{***+}	36	± 11 ^{***}
FB-Cxt	92	± 10	40	± 1 ^{***}	46	± 4 ^{***}	39	± 9 ^{***+}
RBF [mL/min]								
Control	5.2	± 0.8	5.3	± 2.5	6.0	± 1.9	4.4	± 1.4
LPS	5.7	± 1.2	1.3	± 0.5 ^{***}	1.5	± 0.8 ^{***}	0.9	± 0.3 ^{***}
0.9 % NaCl	4.9	± 0.8	1.1	± 0.6 ^{***}	2.2	± 0.8 ^{***}	0.9	± 0.6 ^{***}
HES-RA	6.9	± 1.5	1.5	± 1.1 ^{***}	5.0	± 1.9 ^{***+}	3.3	± 1.2 ⁺⁺
FB-Cxt	5.6	± 1.3	1.2	± 0.8 ^{***}	2.6	± 1.0 ^{***}	1.9	± 0.5 ^{**}
RV R [dyn.s.sec⁻⁵]								
Control	2094	± 424	1578	± 601	1263	± 344	1537	± 396
LPS	1739	± 493	3455	± 1119	3618	± 2161	3657	± 1837
0.9 % NaCl	2108	± 273	4846	± 2551 ^{**}	2306	± 645	6011	± 4012 ^{***}
HES-RA	1423	± 483	3470	± 1796	1296	± 620	1158	± 332
FB-Cxt	1688	± 290	5550	± 4452 ^{***}	2057	± 988	2176	± 336

Values are represented as Mean ± SD, *p<0.01, ***p<0.001 vs. Control group; +p<0.05, ++p<0.01 and ***p<0.001 vs. LPS group. Abbreviations: MAP; mean arterial pressure, RBF; renal blood flow; RVR renal vascular resistance, LPS; lipopolysaccharide, NaCl; sodium chloride, HES-RA; Hydroxy-ethyl-starches-ringer acetate, FB-Cxt; fully balanced crystalloid.

RA was the most effective in improving MAP and RBF during early resuscitation (T2, p<0.01 and p<0.001, respectively) and RBF during late resuscitation (T3, p<0.01) compared with the LPS group without fluid resuscitation. Crystalloid solutions showed significant improvement in MAP at T3 (p<0.05), but not in RBF, with regard to the LPS group. Of the 3 fluid resuscitation fluids tested, 0.9% NaCl caused the greatest increase in RVR (T3, p<0.001). The administered volumes of colloid and crystalloid solution were adequate in increasing the filling pressures to acceptable levels (e.g., higher than control levels, which were between 4 and 5 mm Hg), as shown in experiments in separate groups of animals, in which the responses of central venous pressure (CVP) to the given volume of 0.9% NaCl and HES-RA amounted to 7.2 and 7.8 mm Hg at T2 and to 7.1 and 10.6 mm Hg at T3, respectively. These values were significantly different from the baseline values (between 4 and 5 mm Hg) and T3 values with LPS alone. (Table S2).

Table S2. CVP, MAP and RBF values between the additional groups (n=3).

	T0 (Baseline)	T1 (Shock)	T2 (Resc. 30min.)	T3 (Resc. 120min.)
CVP [mmHg]				
LPS	4.2±0.1	5.8±1.4*	5.7±1.1*	6.1±1.4*
LPS+HES-RA	4.9±1.8	5.5±1.2	7.8±1.9*	10.6±2.5****
LPS+NaCl	4.8±0.2	5.6±0.8	7.2±0.9**	7.1±1.1**
MAP [mmHg]				
LPS	84±7	34.5±9.1***	34±11.3***	30.5±10.6***
LPS+HES-RA	82.3±2.5	40.6±0.5***	57±6.5***	41.6±10.6***
LPS+NaCl	80±1	40.3±2**	46±12.1*	38±8**
RBF [ml/min.]				
LPS	6.4±2.6	0.15±0.07***	0.1±0***	0***
LPS+HES-RA	5.9±0.6	0.3±0.2***	3.3±0.9**	2.4±1.2**
LPS+NaCl	5.6±2.1	0.3±0.2**	1.4±1.5*	0.5±0.4**

Values are presented as Mean ± SD, *p<0.05, **p<0.01 vs. LPS group; *p<0.05, **p<0.01, ***p<0.001 vs. T0 time point. Abbreviations: CVP; central venous pressure, MAP; mean arterial pressure, RBF; renal blood flow, LPS; lipopolysaccharide, NaCl; sodium chloride, HES-RA; hydroxy-ethyl-starches-ringer acetate.

Effects of the different resuscitation fluids on renal microvascular oxygenation

DO_{2ren} , VO_{2ren} , ERO_{2ren} %, $CuPO_2$ and $MuPO_2$ are shown in Table 2 and Figure 1. Compared with the controls, LPS infusion induced a significant decrease in the VO_{2ren} and an increase in renal oxygen extraction ratio at T1, T2 and T3. LPS infusion induced a significant decrease in DO_{2ren} , $CuPO_2$ and $MuPO_2$ at all time points. Percentage changes in VO_{2ren} , DO_{2ren} , $CuPO_2$ and $MuPO_2$ from baseline to T3 are shown in Figure 1. Compared with the LPS group and the fluid resuscitation groups with 0.9% NaCl and FB-Cxt, HES-RA most significantly improved the DO_{2ren} and the VO_{2ren} at T2 (p<0.01), but the percentage changes in DO_{2ren} and VO_{2ren} did not show any improved effects on HES-RA administration from baseline to T3 (Figure 1c and 1d). Despite increases in % ERO_{2ren} in the LPS group at T1 (p<0.001) and T2 (p<0.01), the LPS+HES-RA group at T1 (p<0.05) and T3 (p<0.05) and the LPS+%NaCl group at T1 (p<0.001) and T2 (p<0.01), this parameter was stable in the LPS group that received FB-Cxt at T1, T2 and T3 with regard to the control group (Table 2). Administration of HES-RA, 0.9% NaCl and FB-Cxt did not result in any significant improvements in cortical and medullar microvascular renal oxygenation (Table 2) (Figure 1a and 1b).

Effects of the different fluid resuscitation solutions on renal function

Urine output and creatinine levels during endotoxemic shock are shown in Table 3. Although all of the rats in the LPS group suffered from acute kidney injury (AKI), as reflected by anuria and increased plasma creatinine levels, none of the fluid types used could prevent AKI. The plasma creatinine levels did not differ between the LPS group and the different fluid resuscitation groups; however, the levels were significantly higher than the levels in the control group (p<0.0001).

Table 2. Renal microvascular oxygenation variables during shock and resuscitation periods.

	T0 (baseline)	T1 (shock)	T2 (30 min)	T3 (120 min)
DO_{2ren} [ml O₂/min]				
Control	4.0 ± 0.8	3.6 ± 1.7	4.0 ± 1.4	2.9 ± 0.8
LPS	4.8 ± 1.3	1.0 ± 0.5^{***}	1.1 ± 0.6^{***}	0.6 ± 0.2^{***}
0.9 % NaCl	3.9 ± 0.7	0.6 ± 0.4^{***}	1.2 ± 0.5^{***}	0.5 ± 0.3^{***}
HES-RA	5.5 ± 1.1[*]	1.0 ± 0.6^{***}	3.0 ± 1.3⁺⁺	1.6 ± 0.6[*]
FB-Cxt	4.6 ± 4.6	0.8 ± 0.5^{***}	1.8 ± 0.7^{***}	1.0 ± 0.3^{**}
VO_{2ren} [ml O₂/min]				
Control	1.82 ± 0.53	2.13 ± 1.18	2.74 ± 1.18	2.33 ± 0.71
LPS	2.35 ± 0.77	0.81 ± 0.40^{**}	0.98 ± 0.58^{***}	0.56 ± 0.20^{***}
0.9 % NaCl	2.02 ± 0.43	0.50 ± 0.25^{***}	1.03 ± 0.29^{***}	0.48 ± 0.32^{***}
HES-RA	2.68 ± 0.69	0.68 ± 0.43^{***}	2.34 ± 1.09⁺⁺	1.49 ± 0.57
FB-Cxt	2.23 ± 0.69	0.59 ± 0.43^{***}	1.45 ± 0.68^{**}	0.86 ± 0.22^{***}
ERO_{2ren} %				
Control	45.01 ± 5.03	57.82 ± 10.07	67.30 ± 15.59	80.11 ± 15.82
LPS	48.83 ± 5.72	85.19 ± 10.46^{***}	85.82 ± 10.74^{**}	93.88 ± 3.81
0.9 % NaCl	52.13 ± 6.09	80.25 ± 10.93^{***}	85.18 ± 10.05^{**}	94.05 ± 6.01
HES-RA	48.61 ± 5.87	72.86 ± 14.43[*]	79.21 ± 11.61	94.55 ± 2.20[*]
FB-Cxt	47.99 ± 3.55	71.91 ± 10.83	77.48 ± 9.94	86.02 ± 6.67
CuPO₂ [mmHg]				
Control	84 ± 6	77 ± 9	74 ± 10	72 ± 14
LPS	85 ± 5	46 ± 14^{***}	42 ± 13^{***}	28 ± 9^{***}
0.9 % NaCl	86 ± 6	52 ± 17^{***}	51 ± 15^{**}	41 ± 10^{***}
HES-RA	86 ± 9	52 ± 16^{**}	56 ± 9[*]	37 ± 16^{***}
FB-Cxt	89 ± 4	50 ± 8^{***}	46 ± 10^{***}	42 ± 4^{***}
MuPO₂ [mmHg]				
Control	63 ± 7	58 ± 7	57 ± 9	55 ± 11
LPS	70 ± 4	37 ± 14^{**}	36 ± 13^{**}	24 ± 9^{***}
0.9 % NaCl	70 ± 6	42 ± 14[*]	43 ± 13	37 ± 10^{**}
HES-RA	71 ± 9	44 ± 12	49 ± 8	31 ± 15 ^{***}
FB-Cxt	75 ± 4	37 ± 10^{**}	37 ± 7^{**}	31 ± 11^{***}

Values are presented as Mean ± SD, *p<0.05, **p<0.01, ***p<0.001 vs. Control group; ++p<0.01 vs. LPS group. Abbreviations: DO_{2ren}; renal oxygen delivery, VO_{2ren}; renal oxygen consumption, ERO_{2ren}%; renal oxygen extraction ratio, CuPO₂; renal cortical oxygen pressure, MuPO₂; renal medullary oxygen pressure, LPS; lipopolysaccharide, NaCl; sodium chloride, HES-RA; Hydroxy-ethyl-starches-ringer acetate, FB-Cxt; fully balanced crystalloid.

Effects of different fluid resuscitation on tHb, plasma lactate, pH and HCO₃⁻ levels

Total Hb (tHb) levels became considerably lower in the septic group receiving HES-RA (p<0.001) compared with the control and LPS groups, but not in the crystalloid groups, indicating the volume expansive effect of the use of a colloid solution (Figure 2a). The plasma lactate levels during endotoxemic shock, with or without fluid resuscitation, are shown in Table 3 and Figure 2b. LPS infusion induced an increase in plasma lactate levels

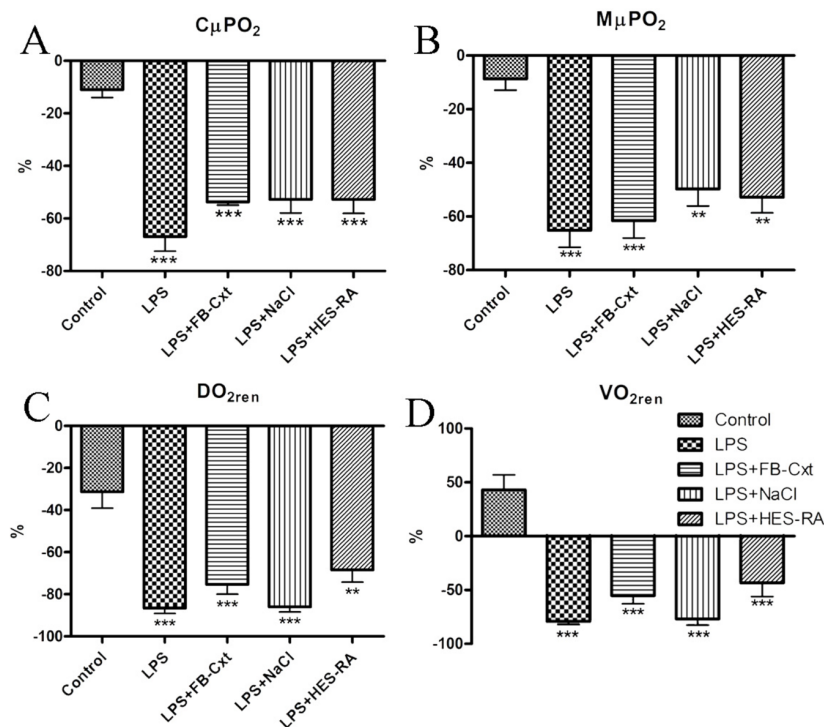


Figure 1. Changing values of renal $C_{\mu}PO_2$ (Panel A), $M_{\mu}PO_2$ (Panel B), DO_{2ren} (Panel C) and VO_{2ren} (Panel D) from baseline to T3 in all groups. LPS; lipopolysaccharide, NaCl; sodium chloride, HES-RA; Hydroxy-ethyl-starches-ringer acetate, FB-Cxt; fully balanced crystalloid. Values are presented as percentage differences from baseline to T3. ** $p < 0.01$ and *** $p < 0.001$ vs. Control group.

from T1 to T3 ($p < 0.001$). Compared with the LPS group, plasma lactate levels increased after colloid administration at T3 ($p < 0.05$) and decreased after crystalloid administration at T3 ($p < 0.01$) in the 0.9% NaCl group and ($p < 0.05$) the FB-Cxt group, without any significant differences between fluid resuscitation with 0.9% NaCl and with FB-Cxt. The percentage differences in plasma lactate levels from baseline to T3 are shown in Figure 2b. None of the fluid resuscitation regimes significantly improved plasma lactate levels after LPS induction, but the decrease in plasma lactate levels was greater with crystalloid resuscitation than with colloid resuscitation ($p < 0.01$) (Figure 2b).

Endotoxemia induced significant acidosis ($p < 0.001$) and bicarbonate depletion ($p < 0.001$) (Figure 2c and 2d). The administration of fluid therapy, irrespective of the fluid composition or buffer type, was not successful in correcting this sepsis-induced acidosis or bicarbonate depletion after LPS induction, although there was a slight benefit in favor of the balanced crystalloid and colloid solutions over 0.9% NaCl (Figure 2c and 2d).

Table 3. Levels of plasma lactate, creatinine and urine volume among all of the groups.

	T0 (baseline)			T1 (shock)			T2 (30 min)			T3 (120 min)		
Lactate [mmol/L]												
Control	2.38	±	0.54	1.26	±	0.3	1.18	±	0.19	1.62	±	0.41
LPS	1.85	±	0.50	4.72	±	0.74***	5.15	±	0.92***	7.17	±	0.78***
0.9 % NaCl	2.02	±	0.30	3.62	±	0.90*	3.52	±	0.57*	4.64	±	0.95***++
HES-RA	2.15	±	0.73	4.13	±	1.42***	4.53	±	1.44***	9.23	±	3.55***+
FB-Cxt	1.92	±	0.31	4.80	±	1.29***	4.74	±	1.43***	5.02	±	1.27***+
Creatinine[μmol/L]												
Control	32	±	3.81	33.2	±	7.4	33.4	±	6.27	45.8	±	9.42
LPS	24	±	2.76	74.5	±	10.3***	82.67	±	14.49***	103.6	±	18.33***
0.9 % NaCl	29.2	±	9.31	79.2	±	10.3***	79.8	±	11.26***	97.2	±	8.7***
HES-RA	30	±	5.37	76.1	±	12.92***	80.5	±	13.58***	109.3	±	24.25***
FB-Cxt	28.4	±	5.22	81.8	±	5.63***	78.4	±	9.37***	89.8	±	5.12***
Urine volume[mL/min]												
Control	34	±	11	16	±	4	15	±	2	11	±	0.04
LPS	21	±	9	3	±	3	1	±	1	0	±	0
0.9 % NaCl	38	±	16	7	±	11	7	±	9	2	±	0
HES-RA	30	±	34	2	±	3	24	±	13	3	±	3
FB-Cxt	18	±	9	1	±	2	2	±	4	2	±	3

Values are presented as a Mean ± SD, *p<0.05, ***p<0.001 vs. Control group; +p<0.05, ++p<0.01 vs. LPS group. Abbreviations: LPS; lipopolysaccharide, NaCl; sodium chloride, HES-RA; Hydroxy-ethyl-starches-ringer acetate, FB-Cxt; fully balanced crystalloid.

Effects of different fluid resuscitation on oxidative and nitrosative stress

Tissue malondialdehyde (MDA) levels were used to quantify oxidative stress by assessing lipid peroxidation. The tissue NO level measurements were used to quantify nitrosative stress. The results of the MDA levels and NO levels are shown in Figure 3a and 3b, respectively. Compared with the controls, MDA levels were increased in the LPS group (p<0.05) and the LPS group treated with 0.9% NaCl (p<0.05) and HES-RA (p<0.001), although they were not increased in the FB-Cxt group. During endotoxemic shock, oxidative stress levels were increased by resuscitation with HES-RA (p<0.01). Compared with the LPS group receiving HES-RA, MDA levels were decreased by the administration of 0.9% NaCl (p<0.01) and FB-Cxt (p<0.001) (Figure 3a). Although nitrosative stress was not significantly different among the controls, the LPS and LPS groups receiving HES-RA and FB-Cxt, 0.9% NaCl induced a significant increase in NO levels in the kidneys compared with the controls (p<0.05) (Figure 3b).

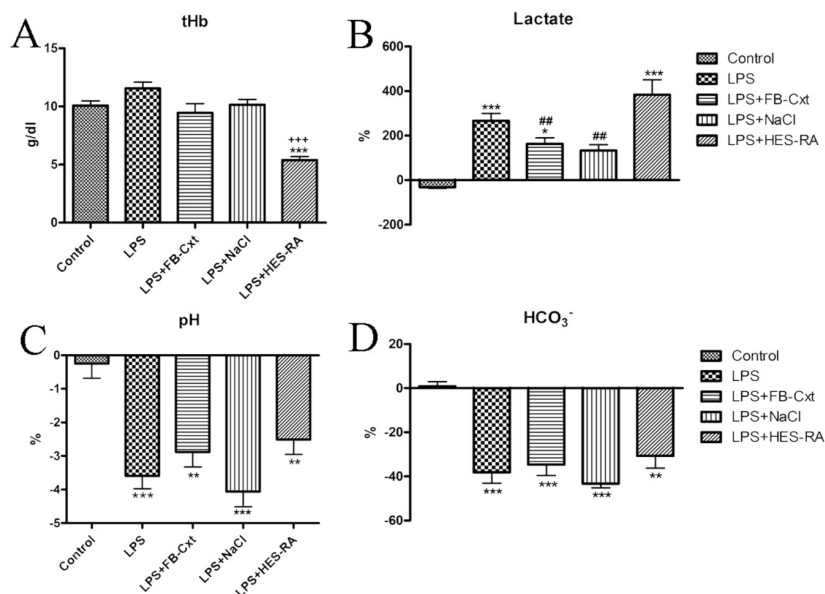


Figure 2. Total Hb levels at the end of experiment (Panel A) and changing values of plasma lactate (Panel B), pH (Panel C) and HCO₃⁻ (Panel D) from baseline to T3 in all of the groups. LPS; lipopolysaccharide, NaCl; sodium chloride, HES-RA; Hydroxy-ethyl-starches-ringer acetate, FB-Cxt; fully balanced crystalloid. Values are presented as percentage differences from baseline to T3. **p*<0.05, ***p*<0.01 and ****p*<0.001 vs. Control group; ****p*<0.001 vs. LPS group; #*p*<0.01 vs. LPS+HES-RA group.

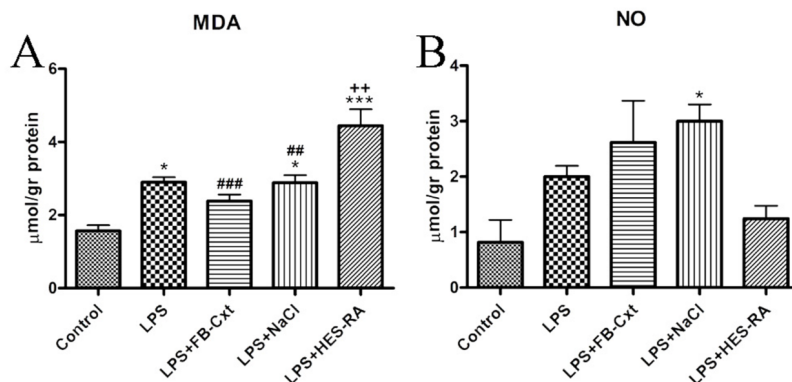


Figure 3. Tissue MDA (Panel A) and NO (Panel B) levels. LPS; lipopolysaccharide, NaCl; sodium chloride, HES-RA; Hydroxy-ethyl-starches-ringer acetate, FB-Cxt; fully balanced crystalloid. Values are presented as the Mean \pm SD, **p*<0.05 and ****p*<0.001 vs. Control group; +*p*<0.01 vs. LPS group; #*p*<0.01, ###*p*<0.001 vs. LPS+HES-RA group.

DISCUSSION AND CONCLUSION

The purpose of this study was to investigate whether the composition of fluids had a beneficial effect on the known pathogenic factors involved in sepsis-induced acute kidney injury. To this end, we tested the effects of a balanced crystalloid solution (0.9% NaCl), a fully balanced crystalloid solution (a bicarbonate-based crystalloid solution called Aqix, mimicking the composition of plasma) and a balanced, starch-based colloid solution (HES-Ringers Acetate) in an endotoxemic shock model in rats. Our study showed that despite improving venous pressures, resulting in an initial improvement in some hemodynamic variables, none of the fluids tested were able to improve the altered renal microcirculatory oxygenation, inflammation or acid-base alterations known to be associated with sepsis-induced acute kidney failure (e.g., 20). In this study, we found that in the early stage of fluid resuscitation, the use of a colloid solution was more effective than the use of crystalloid solutions in reversing sepsis-induced macrocirculatory dysfunction, including MAP and RBF. However, in the later stages of shock, fluid therapy was unable to sustain hemodynamic variables. Severe hypotension prevailed, associated with the progression of endotoxemia-related capillary leakage. Our study showed that the composition of the fluids, in terms of being either balanced or unbalanced or a colloid or crystalloid, despite the administration of adequate volumes, was in itself ineffective in supporting renal function during endotoxic shock. The findings suggest that for fluids to be effective in resolving renal failure under such conditions, additional compounds are needed that are more effective in the control of inflammation and the promotion of oxygen transport to the parenchymal cells.-

HES-RA was the most effective in improving MAP and RBF during early resuscitation and RBF during late resuscitation as well as central venous pressure. In the late resuscitation stage, with the exception of venous pressures, systemic and regional hemodynamic variables could not be normalized with fluid resuscitation alone. We choose in our model to administer fixed equal volumes (30 ml/kg/hr) of crystalloids and colloids, which were equal to or greater than the fluid volumes used in the literature (e.g., 21-24) and were sufficient to restore filling pressures, as indicated by our measurement of CVP. It could be argued that fluids should have been administered targeting the correction of a specific hemodynamic variable. However, almost without exception, experimental studies in rats, investigating the effects of different fluid compositions in models of endotoxemia, have used fixed fluid volume resuscitation, instead of targeting a hemodynamic variable (e.g., 21-26). The total amounts of fluids administered in our study amounted to more than twice the circulating volume in the rat, so it is unlikely that the administration of more fluids would have changed the hemodynamic responses to the fluid regimes that we administered. In experimental rat hemorrhagic shock models, in contrast, administering

fluids targeting the correction of a systemic hemodynamic variable is more successful in correcting systemic arterial hemodynamics, such as the return of MAP to baseline (e.g., 15,17), presumably because of the absence of capillary leakage, thus allowing the fluids to remain more effectively in the vasculature. Our study demonstrated that the volumes administered provided adequate venous pressures, with, as expected, the colloid group achieving higher venous pressures than the crystalloid groups.

Recently, Aksu *et al.* found that administration of balanced colloid solution (HES-RA) at 15 ml/kg/h resulted in the improvement of both macrohemodynamic and renal cortical microvascular perfusion during endotoxemia in rats (26). However, they did not assess renal oxygenation under endotoxin challenge. In our study, we found that none of the studied fluids were able to correct adequately the decrease in renal microvascular oxygenation during endotoxemia despite achieving adequate filling pressures. Although the colloid solution, compared with the balanced and unbalanced crystalloids, increased the delivery of oxygen by increasing RBF, this change did not translate into improved renal medullary or cortical oxygenation compared with the other fluid types. In contrast, the colloid solution significantly decreased arterial Hb levels, as would be expected from its increased intravascular expansive properties compared with crystalloids, leading to a reduction in the oxygen-carrying capacity of the blood associated with this hemodilution. This finding may explain the higher levels of plasma lactate in the septic groups receiving colloids compared with those receiving crystalloids. These results indicated that the improvement in macrovascular perfusion by a non-oxygen-carrying resuscitation fluid does not automatically translate into improvement in microcirculatory oxygenation in severe septic conditions. Legrand *et al.* previously showed that endotoxemia-induced renal microcirculatory dysfunction could exist, although systemic hemodynamic, as well renal arterial perfusion, was maintained (16). Leong *et al.* suggested that arterial-to-venous shunting may be a contributing factor in the regulation of renal tissue oxygenation and the bioavailability of the microcirculation (27). Indeed, Johannes *et al.* showed that renal cortical microcirculatory PO_2 decreased during normovolemic hemodilution more than the PO_2 of renal venous blood. The authors suggested that the increased “gap” between the tissue and the venous PO_2 during hemodilution indicated increased arterial-to-venous oxygen shunting (28). Thus, increased renal arterial shunting may also explain the lack of efficacy of fluids to support renal microcirculatory oxygenation found in our study. Indeed, our study showed transient improvements in renal DO_2 , VO_2 and ERO_2 following colloid resuscitation in the early stage of resuscitation, although this effect was not sustained in the later stages of fluid resuscitation.

The literature on fluid resuscitation overwhelmingly compromises papers in which one composition of fluids is found to be superior to another in terms of resuscitation

endpoints and organ failure, a discussion referred to as the Great Fluid debate (7,29). This issue has specifically focused on the use of chloride-containing solutions (0.9% saline), which are thought to cause hyperchloremic (or dilutional) acidosis (9,10). In a rat model of hemorrhagic shock, we previously observed that balanced solutions were better at correcting hemorrhagic shock-induced acidosis than unbalanced crystalloid solutions (17). Moreover, Zhou *et al.* in an experimental model of sepsis by cecal ligation and puncture, determined that volume resuscitation with Plasma-Lyte, a balanced electrolyte solution, resulted in less acidosis and less kidney injury than 0.9% saline (30). However, the SPLIT trial compared these solutions in a randomized, controlled trial setting and could not find any differences between balanced crystalloids and 0.9% NaCl resuscitation regarding renal outcomes (31). Our present study also did not show specific benefit in favor of balanced solutions over unbalanced solutions concerning their effects on renal outcomes or even on acid-base alterations. The solutions were also equally ineffective in correcting sepsis-induced acidosis. The discrepancies between our study and the study by Zhou *et al.* (30) may be explained in part by the more severe presence of metabolic acidosis and renal failure in our model. Moreover, the compositions of the fluids that we used were different than the fluids used in the Zhou *et al.* study. In our study design, we used three different solutions, each of which had a different anion component that was expected to have a variable effect on acid-base status, in addition to simply providing volume; the solutions were bicarbonate in FB-Cxt, acetate in HES-RA and chloride in saline.

Our findings could be of special interest in light of the ongoing discussions about the impact of different fluid compositions on shock-induced acidosis. Even a bicarbonate-based solution, such as FB-Cxt, was ineffective in normalizing endotoxin-induced acidosis and bicarbonate depletion in our model. Choosing a resuscitation endpoint based on optimizing microcirculatory oxygen transport variables may be a more effective approach to correcting acidosis because it would directly target the origin of metabolic acidosis (32). However, such an approach would require other drugs than fluids alone. These findings emphasize the importance of resolving hypoxia to correct acidosis instead of focusing on a particular type of buffer.

In our study, HES-RA induced an increase in renal MDA levels, but not NO production, compared with LPS without fluid resuscitation. Based on this observation, it could be hypothesized that the beneficial effect of HES-RA may be counterbalanced by the increase in oxidative stress. Compared with the unbalanced crystalloids, the balanced crystalloid caused less oxidative stress (as assessed by the decrease in MDA levels). However, the unbalanced crystalloids increased nitrosative stress (as assessed by the increase in renal NO levels). In septic cells, Kahn *et al.* observed an increase in neutrophil superoxide

production induced by resuscitation fluids, including Ringers Lactate, albumin, dextrans and starches (33). The deleterious effects of oxidative and nitrosative stress on endothelial cell function, leading to disturbed microvascular function and consequent tissue hypoxia resulting in renal failure, have been documented previously (34-36). Recently, Wang *et al.* using a murine cecal ligation and puncture model, demonstrated that sepsis-induced AKI was associated with hypoxia and oxidant generation in the peritubular microenvironment, associated with a decrease in renal capillary perfusion. These authors were able to break the cycle of injury by targeting oxidant generation by the administration of a superoxide dismutase mimetic/peroxynitrite scavenger (37). Our study suggested that nitrosative stress and oxidative stress are also dependent on the both the dose and the type of fluid administered for resuscitation.

Our study had several limitations. First, it could be argued that our model was under-resuscitated due to the persistence of hypotension despite adequate volume administration. In our study, we wanted to focus solely on the role of fluids and their compositions, and we did not intend to involve the confounding effects of other supportive medication. From this point of view, it was a mechanistic study that did not mimic a clinical scenario. Indeed, our study showed that despite providing more than adequate fluid volume and achieving more than adequate filling pressures, these fluids, irrespective of their composition, were ineffective in correcting microcirculatory oxygenation, acid-base alterations, inflammation and oxidative stress. This effect was more pronounced in the later stages of resuscitation. It could be argued that we should have corrected arterial hypotension with the administration of vasopressors. However, there has been controversy about the importance of correcting blood pressure variables, as opposed to correcting flow-derived hemodynamic variables (38). In addition, we had shown in rat models of hemorrhage and sepsis that correcting blood pressure levels was also ineffective in restoring renal variables of resuscitation (15,16). Nevertheless, the administration of vasopressors and increasing arterial pressures could be an interesting next phase of our study to investigate whether there are differences related to the composition of the various fluids when such procedures are applied. Our study results could have clinical relevance, because they suggested that in the design of clinical trials investigating the efficacy of fluid composition as well fluid resuscitation targets the total resuscitation procedure needs to be taken into account since they can be equally important in determining the success of resuscitation in terms of correcting parameters essential for organ function.

A second limitation of our study may have been our choice of a starch product for use as a colloid solution in light of the adverse views regarding the use of starches in sepsis. Although there has been evidence of the adverse effects of starches on renal function, it must be acknowledged that this evidence likely holds true for all colloids, as shown by

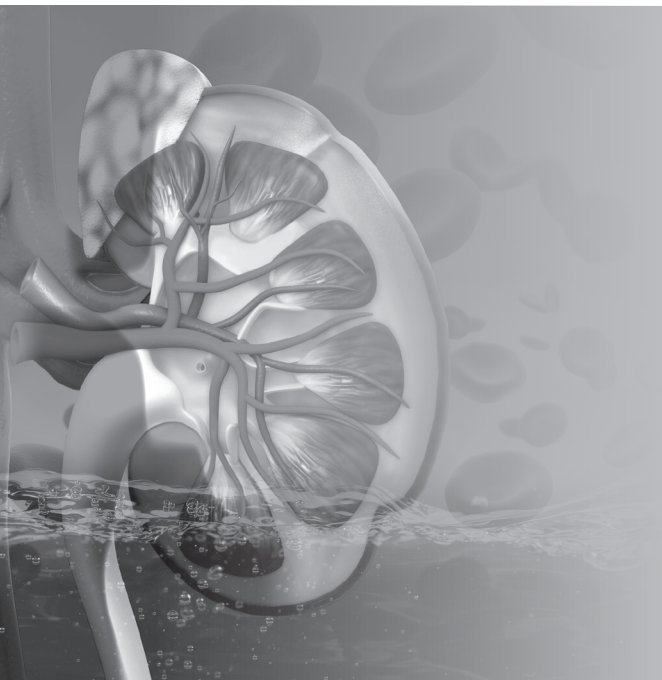
experimental and clinical studies of gelatins and albumin (e.g., 39-41). Indeed, it was not the purpose of our study to compare different types of colloids regarding renal outcomes but, rather, to focus on the mechanistic effects on hemodynamics and renal oxygenation relative to acid-base balance and the use of balanced and unbalanced solutions and crystalloid and colloid solutions. A further consideration for the use of a starch solution as a colloid is that it is by far the most studied type of colloid in the type of model we investigated, allowing us to better compare our findings with those reported in the literature.

In summary, our study demonstrated that fluid therapy alone, irrespective of its composition, was only marginally effective in correcting physiological parameters that are essential for correcting renal function in an LPS-induced endotoxemic shock model in the rats. Fluid therapy, irrespective of the buffer used, was ineffective in correcting sepsis-induced acidosis or sepsis-induced reductions in renal microcirculatory oxygen values. These findings supported the view that the correction of acidosis in this setting was more closely related to the correction of tissue oxygenation than to the choice of a specific type of buffer because of its origin as a metabolic defect related to oxygen delivery to the tissues. Our results directly identified tissue hypoxia as a major determinant of sepsis-induced acidosis. We believe that a therapeutic strategy using fluids with enhanced oxygen-carrying capacity and anti-inflammatory properties could hold promise for future fluids needed for resuscitation in sepsis.

REFERENCES

1. Gomez H, Ince C, De Backer D, *et al.* A unified theory of sepsis-induced acute kidney injury: inflammation, microcirculatory dysfunction, bioenergetics, and the tubular cell adaptation to injury. *Shock* 41(1):3-11, 2014.
2. Bonventre JV, Yang L. Cellular pathophysiology of ischemic acute kidney injury. *J. Clin. Invest.* 121(11):4210-21, 2011.
3. Prowle JR, Bellomo R. Sepsis-associated acute kidney injury: macrohemodynamic and microhemodynamic alterations in the renal circulation. *Semin. Nephrol.* 35(1):64-74, 2015.
4. Vincent JL, De Backer D. Circulatory shock. *N. Engl. J. Med.* 369(18):1726-34, 2013.
5. Johannes T, Mik EG, Ince C. Nonresuscitated endotoxemia induces microcirculatory hypoxic areas in the renal cortex in the rat. *Shock* 31:97-103, 2009.
6. Marx G. Fluid therapy in sepsis with capillary leakage. *Eur. J. Anaesthesiol.* 20:429-42, 2003.
7. Ince C. The great fluid debate: when will physiology prevail? *Anesthesiol.* 119:248-249, 2013.
8. Morgan TJ. The meaning of acid-base abnormalities in the intensive care unit: part III- effects of fluid administration. *Crit. Care* 9:204-11, 2005.
9. Kellum JA, Song M, Almasri E. Hyperchloremic acidosis increases circulating inflammatory molecules in experimental sepsis. *Chest* 130(4):962-7, 2006.
10. Lobo DN, Awad S. Should chloride-rich crystalloids remain the mainstay of fluid resuscitation to prevent 'pre-renal' acute kidney injury?: con. *Kidney Int.* 86(6):1096-105, 2014.
11. Ince C, Groenveld ABJ. The case for 0.9%Na Cl: Is the indefensible, defensible? *Kidney Int.* 86(6):1087-95, 2014.
12. Treib J, Haass A, Pindur G, *et al.* All medium starches are not the same: influence of the degree of hydroxyethyl substitution of hydroxyethyl starch on plasma volume, hemorrheologic conditions, and coagulation. *Transfusion* 36:450-5, 1996.
13. Morgan TJ. The ideal crystalloid – what is 'balanced'? *Curr. Opin. Crit. Care* 19:299-307, 2013.
14. Johannes T, Mik EG, Nohe B, *et al.* Influence of fluid resuscitation on renal microvascular PO₂ in a normotensive rat model of endotoxemia. *Crit. Care* 10:R88, 2006.
15. Legrand M, Mik EG, Balestra GM, *et al.* Fluid resuscitation does not improve renal oxygenation during hemorrhagic shock in rats. *Anesthesiology* 112:119-27, 2010.
16. Legrand M, Bezemer R, Kandil A, *et al.* The role of renal hypoperfusion in development of renal microcirculatory dysfunction in endotoxemic rats. *Intensive Care Med.* 37(9):1534-42, 2011.
17. Aksu U, Bezemer R, Yavuz B, *et al.* Balanced vs unbalanced crystalloid resuscitation in a near-fatal model of hemorrhagic shock and the effects on renal oxygenation, oxidative stress, and inflammation. *Resuscitation* 83(6):767-73, 2012.
18. Johannes T, Mik EG, Ince C. Dual-wavelength phosphorimetry for determination of cortical and subcortical microvascular oxygenation in rat kidney. *J. Appl. Physiol.* 100:1301-10, 2006.
19. Forman HJ, Augusto O, Brigelius-Flohe R, *et al.* Even free radicals should follow some rules: a guide to free radical research terminology and methodology. *Free Radic. Biol. Med.* 78:233-235, 2015.
20. Ergin B, A Kapucu, C Demirci, *et al.* The renal microcirculation in sepsis. *Nephrol. Dial. Transp.* 30(2):169-77, 2015.
21. Hogue B, Chagnon F, Lesur O. Resuscitation fluids and endotoxin-induced myocardial dysfunction: is selection a load-independent differential issue? *Shock* 38(3):307-13, 2012.
22. Petroni RC, Biselli PJ, Lima TM, *et al.* Impact of time on fluid resuscitation with hypertonic saline (NaCl 7.5%) in rats with LPS-Induced acute lung injury. *Shock* 44(6):609-15, 2015.
23. Schick MA, Isbary TJ, Schlegel N, *et al.* The impact of crystalloid and colloid infusion on the kidney in rodent sepsis. *Intensive Care Med.* 36:541-548, 2010.
24. Wafa K, Herrmann A, Kuhnert T, *et al.* Short time impact of different hydroxyethyl starch solutions on the mesenteric microcirculation in experimental sepsis in rats. *Microvasc. Res.* 95:88-93, 2014.
25. Sherer K, Li Y, Cui X, Li X, *et al.* Fluid support worsens outcome and negates the benefit of protective antigen-directed monoclonal antibody in a lethal toxin-infused rat *Bacillus anthracis* shock model. *Crit. Care Med.* 35:1560-1567, 2007.

26. Aksu U, Bezemer R, Demirci C, *et al.* Acute effects of balanced versus unbalanced colloid resuscitation on renal macrocirculatory and microcirculatory perfusion during endotoxemic shock. *Shock* 37:205-9, 2012.
27. Leong CL, Anderson WP, O'Connor PM, *et al.* Evidence that renal arterial-venous oxygen shunting contributes to dynamic regulation of renal oxygenation. *Am. J. Physiol. Renal Physiol.* 292: F1726-33, 2007.
28. Johannes T, Mik EG, Nohe B, *et al.* Acute decrease in renal microvascular PO₂ during acute normovolemic hemodilution. *Am. J. Physiol. Renal Physiol.* 292:F796-803, 2007.
29. Myburgh JA, Mythen MG. Resuscitation fluids. *N. Engl. J. Med.* 26;369(13):1243-51, 2013.
30. Zhou F, Peng ZY, Bishop JV, *et al.*: Effects of fluid resuscitation with 0.9% saline versus a balanced electrolyte solution on acute kidney injury in a rat model of sepsis. *Crit. Care Med.* 42:270-8, 2014.
31. Young P, Bailey M, Beasley R, *et al.* SPLIT Investigators; ANZICS CTG. Effect of a Buffered Crystalloid Solution vs Saline on Acute Kidney Injury Among Patients in the Intensive Care Unit: The SPLIT Randomized Clinical Trial. *JAMA* 27; 314(16):1701-10, 2015.
32. Ince C. The rationale for microcirculatory guided fluid therapy. *Curr. Opin. Crit. Care* 20: 301-8, 2014.
33. Khan R, Kirschenbaum LA, Larow C, *et al.* The effect of resuscitation fluids on neutrophil-endothelial cell interactions in septic shock. *Shock* 36:440-4, 2011.
34. Lum H, Roebuck KA. Oxidant stress and endothelial cell dysfunction. *Am. J. Physiol. Cell Physiol.* 280: C719-41, 2001.
35. Ince C, Mayeux PR, Nguyen T, *et al.* The endothelium in sepsis. *Shock* 45(3):259-70, 2016.
36. Legrand M, Mik EG, Johannes T, *et al.* Renal hypoxia and dysoxia after reperfusion of the ischemic kidney. *Mol. Med.* 14:502-16, 2008.
37. Wang Z, Holthoff JH, Seely KA, *et al.* Development of oxidative stress in the peritubular capillary microenvironment mediates sepsis-induced renal microcirculatory failure and acute kidney injury. *Am. J. Pathol.* 180:505-16, 2012.
38. Dünser MW, Takala J, Brunauer A, *et al.* Re-thinking resuscitation: leaving blood pressure cosmetics behind and moving forward to permissive hypotension and a tissue perfusion-based approach. *Critical Care* 17:326, 2013.
39. Schick MA, Isbary JT, Stueber T, *et al.* Effects of crystalloids and colloids on liver and intestine microcirculation and function in cecal ligation and puncture induced septic rodents. *BMC Gastroenterol.* 17;12:179, 2012.
40. Zhang H, Voglis S, Kim C, *et al.* Effects of albumin and Ringer's lactate on production of lung cytokines and hydrogen peroxide after resuscitated hemorrhage and endotoxemia in rats. *Crit. Care Med.* 31:1515-1522, 2003.
41. Frenette AJ, Bouchard J, Bernier P, *et al.* Albumin administration is associated with acute kidney injury in cardiac surgery: a propensity score analysis. *Crit. Care* 18(6):602, 2014.



CHAPTER 8

Activity of a human recombinant alkaline phosphatase on renal hemodynamics, oxygenation and inflammation in rat models of ischemia/reperfusion- and endotoxemia-induced acute kidney injury

Adapted from *Toxicol. Appl. Pharmacol.* 2016 Dec 15;313:88-96

Esther Peters^{1,2}, Bulent Ergin³, Asli Kandil⁴, Ebru Gurel-Gurevin⁴, Andrea van Elsas⁵, Rosalinde Masereeuw⁶, Peter Pickkers¹, Can Ince³

¹ Department of Intensive Care Medicine, Radboud University Medical Center, Nijmegen, The Netherlands

² Department of Pharmacology and Toxicology, Radboud University Medical Center, Nijmegen, The Netherlands

³ Department of Translational Physiology, Academic Medical Center, University of Amsterdam, The Netherlands

⁴ Department of Biology, Faculty of Science, Istanbul University, Istanbul, Turkey

⁵ AM-Pharma, Bunnik, The Netherlands

⁶ Division of Pharmacology, Utrecht Institute for Pharmaceutical Sciences, Faculty of Science, The Netherlands

E. Peters and B. Ergin contributed equally to this study

ABSTRACT

Two small clinical trials indicated that administration of bovine intestinal alkaline phosphatase (AP) improves renal function in critically ill patients with sepsis-associated acute kidney injury (AKI), for which the mechanism of action is not completely understood. Here, we investigated the effects of a newly developed human recombinant AP (recAP) on renal oxygenation and hemodynamics and prevention of kidney damage and inflammation in two in vivo AKI models. To induce AKI, male Wistar rats (n=18) were subjected to renal ischemia (30 min) and reperfusion (I/R), or sham-operated. In a second model, rats (n=18) received a 30 min infusion of lipopolysaccharide (LPS; 2.5 mg/kg), or saline, and fluid resuscitation. In both models, recAP (1000 U/kg) was administered intravenously (15 min before reperfusion, or 90 min after LPS). Following recAP treatment, I/R-induced changes in renal blood flow, renal vascular resistance and oxygen delivery at early, and cortical microvascular oxygen tension at late reperfusion were no longer significantly affected. RecAP did not influence I/R-induced effects on mean arterial pressure. During endotoxemia, recAP treatment did not modulate the LPS-induced changes in systemic hemodynamics and renal oxygenation. In both models, recAP did exert a clear renal protective anti-inflammatory effect, demonstrated by attenuated immunostaining of inflammatory, tubular injury and pro-apoptosis markers. Whether this renal protective effect is sufficient to improve outcome of patients suffering from sepsis-associated AKI is being investigated in a large clinical trial.

Keywords: alkaline phosphatase, acute kidney injury, therapy, inflammation, ischemia-reperfusion, lipopolysaccharide

INTRODUCTION

Sepsis-associated acute kidney injury (AKI) is a serious complication in critically ill patients and is accompanied by high morbidity and mortality rates (1). Treatment is limited to supportive care, as up to now pharmacological interventions are not available. The current lack of treatment options appears primarily due to the multifactorial pathogenesis of AKI, in which inflammation, hemodynamic instability, renal microcirculatory dysfunction and unbalanced renal bioenergetics play pivotal roles (2). Sepsis is accompanied by the systemic release of pro-inflammatory mediators, activation of complement and coagulation pathways, and endothelial leukocyte adhesion and extravasation, thereby promoting inflammation (3). Within the kidney, the vascular endothelium is directly exposed to pathogens and danger-associated molecular patterns that induce a local inflammatory response. The release of harmful mediators like cytokines, reactive oxygen (ROS) and nitrogen species (RNS) characterize this response which, together with endothelial swelling and arteriolar vasoconstriction, leads to a compromised renal microcirculation and renal hypoxia (4). However, the role of renal vasoconstriction and a reduced renal blood flow (RBF) is still under debate since animal and human data suggest that during sepsis, AKI can develop in the setting of sustained or even increased renal blood flow (RBF) (5, 6). This is in contrast to renal ischemia/reperfusion (I/R) injury, during which hemodynamic instability, hypoperfusion and a dysbalance of renal oxygen delivery and oxygen consumption may play key roles (7, 8). Considering its complex pathogenesis, a new treatment option for AKI should be able to modulate the various processes involved in disease development. One of a limited number of candidate drugs that might facilitate such a multimodal approach is the enzyme alkaline phosphatase (AP). According to two patient studies, treatment with bovine intestinal AP increased endogenous creatinine clearance, reduced the need for and duration of renal replacement therapy and decreased the urinary excretion of renal injury markers during sepsis-associated AKI (9, 10). Following these promising results, a human recombinant AP (recAP) was developed, which is both highly stable and biologically active (11).

The possible mechanism of action that accounts for the renal protective effects of AP is still not completely understood and requires further investigation. Recently, using human renal proximal tubule cells it was demonstrated that recAP exerts protective effects through dephosphorylation of endotoxin (LPS, lipopolysaccharide), part of the outer membrane of gram-negative bacteria involved in sepsis pathogenesis, as well as by dephosphorylation of detrimental purines adenosine triphosphate (ATP) and adenosine diphosphate (ADP), released during inflammation (12). These results offer a plausible explanation of the anti-inflammatory effects of recAP locally in the kidney. Considering

the various processes involved in the development of sepsis-associated AKI, we now investigated whether recAP can modulate renal microcirculatory dysfunction and hemodynamic changes following I/R- or endotoxin-induced AKI.

MATERIAL AND METHODS

Animals

All experiments in this study were approved and reviewed by the Animal Research Committee of the Academic Medical Center at the University of Amsterdam (DFL 102669). Care and handling of the animals were in accordance with the guidelines for Institutional and Animal Care and Use Committees (NIH Publication 85-23, 1985). Experiments were performed with 36 male *Wistar albino* rats (Harlan, Horst, The Netherlands) with a mean \pm SD body weight of 402 ± 74 g.

Anesthesia and surgical preparation

Rats were anesthetized and instrumented as described previously (13-15). Rats received an intraperitoneal injection of 90 mg/kg b.w. ketamine (Nimatek[®]; Eurovet, Bladel, The Netherlands), 0.5 mg/kg b.w. dexmedetomidine (Domitor[®]; Pfizer, New York, NY) and 0.05 mg/kg b.w. atropine sulfate (Centrafarm, Etten-Leur, The Netherlands). After tracheotomy, rats were mechanically ventilated with a fraction of inspired O₂ (FiO₂) of 0.4. Body temperature was maintained at 37 ± 0.5 °C during the entire experiment using a heating pad. The ventilator settings were adjusted to maintain an end-tidal partial pressure of carbon dioxide (PCO₂) between 30 and 35 mmHg and an arterial PCO₂ between 35 and 40 mmHg. Blood vessels were cannulated with polyethylene catheters (outer diameter 0.9 mm; Braun, Melsungen, Germany). A catheter in the right carotid artery was connected to a pressure transducer to monitor mean arterial pressure (MAP). The right jugular vein was cannulated for continuous infusion of Ringer's lactate (Baxter, Utrecht, The Netherlands) at a rate of 15 mL/kg/h and maintenance anesthesia (50 mg/kg ketamine dissolved in Ringer's lactate, 5 mL/kg/h). The right femoral artery was cannulated for blood sampling, and the right femoral vein was cannulated to enable fluid resuscitation, oxyphor G2, recAP and Lipopolysaccharide (LPS) administration. The left kidney was exposed, decapsulated, and immobilized in a Lucite kidney cup (K. Effenberger, Pfaffingen, Germany) via a ~4 cm incision of the left flank. Renal vessels were carefully separated under preservation of nerves and adrenal gland. A perivascular ultrasonic transient time flow probe (type 0.7 RB; Transonic Systems Inc., Ithaca, NY) was placed around the left renal artery and connected to a flow meter (T206; Transonic Systems Inc.) to allow continuous measurement of renal blood flow (RBF).

After the surgical protocol (approximately 60 min) one optical fiber was placed 1 mm above the decapsulated kidney and another optical fiber 1 mm above the renal vein to

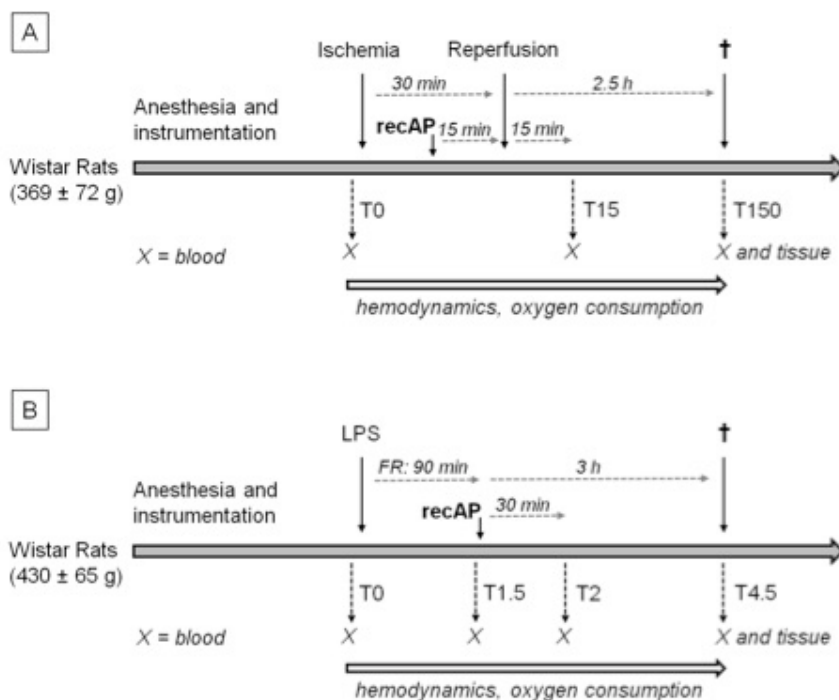
measure oxygenation using the phosphorescence decay time technique (as described below). A small piece of aluminum foil was placed on the dorsal site of the renal vein to prevent contribution of underlying tissue to the phosphorescence signal in the venous partial pressure of oxygen (PO_2) measurements. The operation field was covered with a humidified gauze compress throughout the entire experiment to prevent desiccation of the tissue exposed. At the end of the experiments, animals were sacrificed by systemic administration of 1 mL/kg 20% pentobarbital sodium (Euthasol; AST Farma, Oudewater, The Netherlands) through the femoral vein. Kidneys were harvested, weighed, and sectioned into two parts. One part was fixed in 10% buffered formalin for immunohistochemical analysis and the other part of the kidney was snap frozen in liquid nitrogen and stored at -80 °C before homogenization.

Ischemia/reperfusion protocol

Instrumented rats (369 ± 72 g) were randomized and divided into two groups: I/R ($n = 12$) or sham control ($n = 6$). Rats were subjected to renal ischemia for 30 min by supra-renal aortic occlusion with a custom-made vascular occluder, followed by 2.5 h reperfusion as described previously (13). The vascular occluder was placed on the aorta above the renal arteries, and beneath the mesenteric artery. The sham control group was instrumented and surgically prepared without subsequent cross-clamping of the aorta. Subsequently, ischemic rats were randomized to receive an intravenous bolus injection in the femoral vein with 1000 U/kg b.w. recAP ($n=6$) or saline ($n = 6$) 15 min after initiation of ischemia (Supplemental Fig. 1A). The sham control group received saline. Arterial blood samples (0.5 mL) were taken at 1) before aortic occlusion (T0), 2) 15 min after reperfusion (T15), and 3) 150 min after reperfusion (T150) (Suppl. Fig 1A). Blood samples were replaced by the same volume of 6% HES130/0.4 (Volumen; Fresenius Kabi Nederland B.V., Schelle, Belgium).

Endotoxemia protocol

Endotoxemia was induced on fully instrumented rats (430 ± 65 g) as described previously (15). Rats were randomized at baseline (T0) to receive an intravenous 30 min infusion of 2.5 mg/kg b.w. LPS (*E. coli* 0127:B8; Sigma-Aldrich, Paris, France; $n = 12$), or placebo (saline; $n = 6$). Fluid resuscitation was performed with 20 mL/kg/h 6% HES130/0.4 and continued after cessation of the LPS infusion for a period of 1 h. After this period, LPS-treated groups were randomized to receive either an intravenous infusion of recAP (1000 U/kg b.w.) or saline ($n = 6$ per group) over 30 min. Control groups received saline. Arterial blood (0.5 mL) was sampled at 1) baseline (T0), 2) 90 min after start of LPS administration (T1.5), 3) 120 min post LPS (T2; 30 min after start of recAP treatment), and 4) 4.5 h post-LPS (T4.5; 3 h after recAP infusion) (Suppl. Fig. 1B). Each blood sample drawn was replaced by the same volume of 6% HES130/0.4.



Supplemental Figure 1. Schematic set-up of rat models of I/R-induced AKI (A) or endotoxemia-induced AKI (B). FR, fluid resuscitation; I/R, ischemia/reperfusion; RecAP, human recombinant alkaline phosphatase.

Phosphorimetric measurement of renal microvascular and venous PO_2

The oxygen-quenched phosphorescent decay time of a systemically infused albumin-targeted phosphorescent dye (Oxyphor G2; Oxygen Enterprises, Ltd. Philadelphia, PA) was used for measuring the microvascular oxygen tension in the renal cortex (Cortical μPO_2), outer medulla (Medullar μPO_2) and renal venous oxygen tension ($\text{P}_{\text{rv}}\text{O}_2$). Oxyphor G2 was infused (6 mg/kg b.w.) intravenously for 15 min followed by 30 min stabilization time. Oxyphor G2 has two excitation peaks (440 and 632 nm) and one emission peak (800 nm), which allowed simultaneous decay time measurements in the kidney cortex and the outer medulla due to different optical penetration depths of the light excited by dual-wavelength phosphorimetry (16). For the measurement of $\text{P}_{\text{rv}}\text{O}_2$, a mono-wavelength frequency-domain phosphorimeter was used (17). Phosphorescence was quenched by energy transfer to oxygen, resulting in shortening of the phosphorescence decay time. PO_2 was calculated by determining the correlation between reciprocal phosphorescence decay time and oxygen tension (Stern-Volmer relation) (18). Decay curves of phosphorescent intensity were analyzed using software programmed in Labview 6.1 (National Instruments, Austin, TX).

Renal vascular resistance and derivative oxygen parameters

Blood samples were used to determine blood gas values (ABL505 blood gas analyzer; Radiometer, Copenhagen, Denmark) as well as hemoglobin concentration and hemoglobin oxygen saturation. Renal vascular resistance (RVR) was estimated by the formula $\text{MAP/RBF} \times 100$. Renal oxygen delivery ($\text{DO}_{2\text{ren}}$) was determined by the formula $\text{RBF} \times \text{arterial oxygen content}$ ($\text{C}_a\text{O}_2 = \text{hemoglobin} \times 1.31 \times \text{S}_a\text{O}_2 + 0.003 \times \text{P}_a\text{O}_2$), where S_aO_2 is the arterial oxygen saturation and P_aO_2 the arterial partial oxygen pressure. Renal oxygen consumption ($\text{VO}_{2\text{ren}}$) was determined by the formula $\text{RBF} \times (\text{C}_a\text{O}_2 - \text{C}_v\text{O}_2)$, where renal venous oxygen content (C_vO_2) was calculated as $\text{hemoglobin} \times 1.31 \times \text{S}_{rv}\text{O}_2 + 0.003 \times \text{P}_{rv}\text{O}_2$. The S_{rv}O_2 (renal venous O_2 saturation) was estimated with the Hill equation, with $\text{P50} = 37$ Torr (4.9 kPa) and Hill coefficient = 2.7. The renal oxygen extraction ratio (ER) was estimated as $\text{VO}_2/\text{DO}_2 \times 100$.

NO metabolism

Kidney tissue samples were homogenized in ice-cold 5 mM sodium phosphate buffer using the Heidolph homogenizer DIAx 900 (Sigma-Aldrich, St. Louis, MO). Homogenates were centrifuged at 12,000 g for 15 min at 4 °C, and supernatant was used for NO determination. The index of total NO production is the sum of NO and its reaction products nitrite, nitrate and nitrosothiols accumulated in tissue samples. The reducing agent used for total NO analysis was a saturated solution of vanadium (III) chloride (VCL_3) in 1 M HCL. At a temperature of 90 °C, VCL_3 reagent quantitatively converts all reaction products into NO in a glass vial vessel. NO is flushed out of the reaction vessel by flow of helium gas, which is then measured by the NO chemiluminescence signal analyzer (Sievers 280i, GE Analytical Instruments, Manchester, United Kingdom) as the amount of light from the ozone-NO reaction in the NO measurement chamber. NO tissue protein content was expressed as NO release per g protein, determined by the Bradford assay (ThermoFisher Scientific, Chicago, IL).

Oxidative stress, inflammatory cytokines and AP

Supernatant of kidney homogenates were obtained as described above. Supernatant was used to measure tissue malondialdehyde (MDA) levels to quantify oxidative stress by assessing lipid peroxidation by tandem mass spectrometry as described previously (13). Lipid peroxide content was expressed as MDA content per g protein, determined by the Bradford assay. TNF- α and IL-6 were determined by ELISA (DY510, DY506; R&D Systems, Minneapolis, MN).

Immunohistochemical analysis

After fixation in 10% formalin, tissue was processed and embedded in paraffin. Kidney sections (5 μm) were deparaffinized, antigen retrieval was accomplished using citrate

buffer (pH 6.0) and endogenous peroxidase activity was blocked using 3% H₂O₂. Sections were incubated o/n at 4 °C with antibody rabbit anti-rat inducible nitric oxide synthase (iNOS) (RB-1605-P; NeoMarkers Fremont, CA) or rabbit-anti-human IL-6 (ab6672; Cambridge, UK; cross-reactive to rat), or incubated for 1 h at RT with antibody rabbit anti-rat myeloperoxidase (MPO) (RB-373-A; NeoMarkers), rabbit anti-human Lipocalin-2 (NGAL, neutrophil gelatinase-associated lipocalin) (ab41105; Abcam; cross-reactive to rat), rabbit-anti-rat liver-type fatty acid binding protein (L-FABP) (HP8010; Hycult Biotect, Uden, The Netherlands), or rabbit-anti-rat Bcl-2-associated X protein (Bax) (4 µm; sc-493; Santa Cruz, Heidelberg, Germany). Antibodies were used at a 1:100 dilution in UltraAb Diluent (TA-125-UD; LabVision, Thermo Scientific, Chicago, Illinois), or 1:50 in case of Bax. Subsequently, sections were stained with secondary biotinylated goat-anti-rabbit antibody (1:100; TR-125-BN; LabVision) for 30 min at RT. Immunostaining was visualized with AEC substrate (TA-007-HAC; LabVision), followed by hematoxylin counterstain. Both intensity and distribution were scored in a semiquantitative fashion. Positively stained cells were counted and graded according to staining intensity: 0 (no staining), 1+ (weak but detectable above control), 2+ (distinct), 3+ (intensive). A histological score (HSCORE) value was derived by summing the percentages of cells that stained at each intensity multiplied by the weighted intensity of the staining ($HSCORE = \sum S_i \cdot P_i$), where i is the intensity score and P_i is the corresponding percentage of the cells (19). MPO was scored in 240 selected glomeruli and peritubular areas in each group using a binary scoring system; 1 if leukocytes were observed, 0 if not. Scoring was performed by investigators blinded to the treatment-protocol.

Statistical analysis

Normal distribution of the data could not be assumed due to the sample size. Therefore, data is expressed as median (25th percentile, 75th percentile). Significant differences within groups were estimated using Friedman test with Dunn's post-test, differences between groups were estimated using two-way repeated measures ANOVA with Bonferonni's post-test on log-transformed data. Chi-square test was used to analyze binary outcomes. A two-sided p-value less than 0.05 was considered statistically significant. All tests were performed with Graphpad Prism 5.00 for Windows (Graphpad Software Inc., Ja Lolla, CA).

RESULTS

RecAP prevents I/R-induced alterations of renal hemodynamics immediately following reperfusion

The renal protective effect of recAP was investigated during I/R-induced AKI in rats, performed by 30 min suprarenal aortic clamping followed by a 2.5 h reperfusion period (Suppl. Fig. 1A). MAP was reduced at the end of reperfusion period in all groups

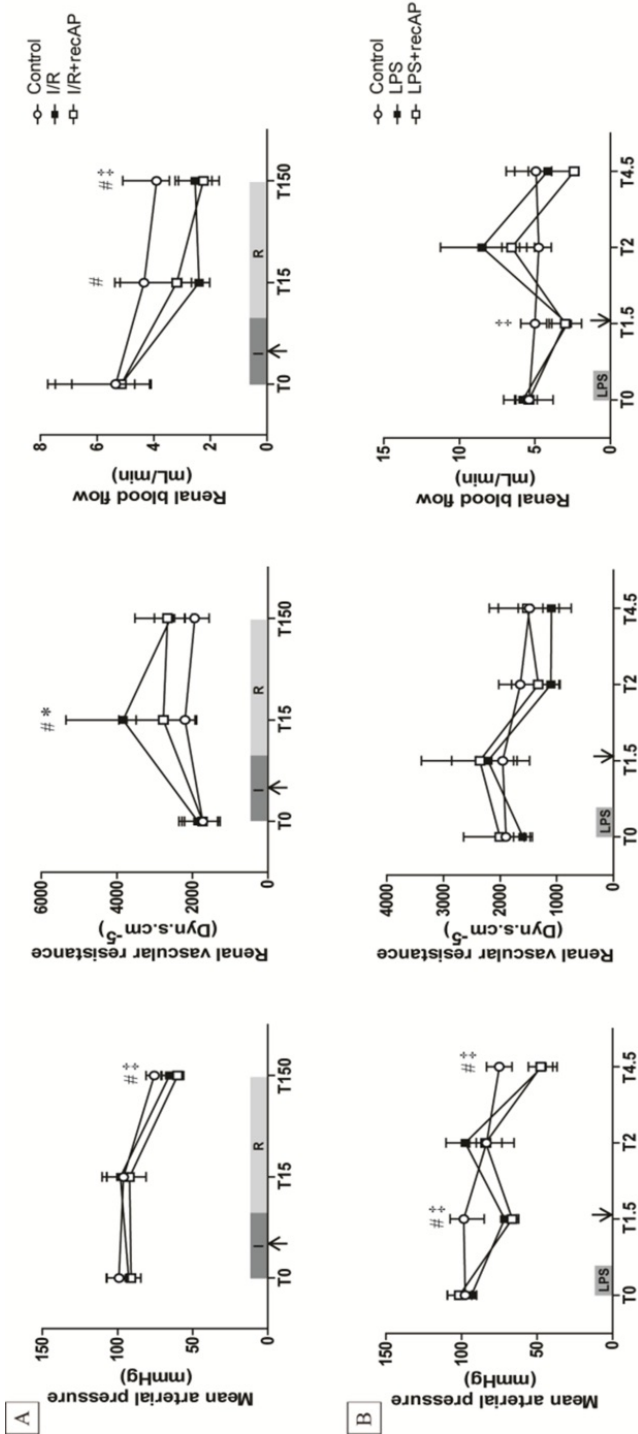


Figure 1. Hemodynamic parameters during I/R-induced AKI (A) or LPS-induced AKI (B). A) Parameters were determined at baseline (T0) and after 15 min (T15) and 150 min (T150) reperfusion. RecAP was administered 15 min preceding reperfusion. B) Parameters were determined at baseline (T0) and 1.5 (T1.5), 2 (T2) and 4.5 h (T4.5) after start of LPS infusion, which was followed by fluid resuscitation until T1.5. RecAP was administered directly after T1.5. Data is expressed as median (25th percentile, 75th percentile). Significant differences estimated using two-way repeated measures ANOVA with Bonferroni's post-test on log-transformed data (n=6 per group). * p<0.05 Control vs. I/R or Control vs. LPS, † p<0.05 I/R vs. I/R+recAP, ‡ p<0.05 Control vs. I/R+recAP or Control vs. LPS+recAP. I/R: ischemia/reperfusion, LPS: lipopolysaccharide, RecAP: human recombinant alkaline phosphatase.

compared to baseline ($p<0.05$), which was more pronounced in the I/R group, and not affected by recAP treatment (Figure 1A), administered 15 min preceding reperfusion. RecAP prevented the detrimental effect of I/R on RVR and RBF immediately following reperfusion (T15). At 2.5 h post-reperfusion (T150), RBF was impaired in all three groups compared to baseline (Figure 1A) and to a more severe extent in the I/R groups. Regarding renal oxygenation (Table 1), both renal oxygen delivery (DO_{2ren}) and oxygen consumption (VO_{2ren}) were significantly reduced post-reperfusion compared to baseline (T0), which was prevented by recAP immediately following reperfusion. The oxygen extraction ratio (ERO_{2ren} %) increased in all three groups at the end of reperfusion, with no differences between groups. While cortical microvascular oxygen tension (μPO_2) was impaired in both I/R groups at the end of reperfusion, recAP treatment significantly improved this parameter compared to the I/R group. Medullar μPO_2 was decreased in all groups after the 2.5 h reperfusion period compared to baseline, and remained unaffected by recAP administration.

Table 1. Renal oxygenation during I/R-induced AKI.

		T0	T15	T150
Cortical μPO_2 (mmHg)	Control	79 (62-89)	76 (69-87)	68 (64-77)
	I/R	80 (75-87)	70 (64-75)	54 (46-60)‡[#]
	I/R+recAP	85 (80-86)	79 (67-89)	67 (56-79)‡[#]*
Medullar μPO_2 (mmHg)	Control	60 (55-66)	56 (50-62)	49 (46-53)‡
	I/R	63 (58-64)	53 (51-58)	44 (39-48)‡
	I/R+recAP	65 (62-68)	54 (51-57)	44 (39-53)‡
DO_{2ren} (mL O₂ min⁻¹)	Control	4.2 (3.9-6.4)	3.4 (2.6-4.5)	3.0 (2.5-3.7)‡
	I/R	4.4 (3.9-5.4)	2.1 (1.7-2.5)‡[#]	1.9 (1.6-2.4)‡[#]
	I/R+recAP	4.3 (3.5-6.1)	2.7 (2.1-4.0)	1.6 (1.2-2.2)‡[#]
VO_{2ren} (mL O₂ min⁻¹)	Control	2.3 (2.0-3.4)	1.9 (1.5-2.1)	1.8 (1.5-2.3)
	I/R	2.4 (2.3-2.7)	1.2 (1.0-1.6)‡	1.2 (1.2-1.7)‡
	I/R+recAP	2.4 (1.7-3.2)	1.6 (1.0-2.2)	0.9 (0.7-1.4)‡[#]
ERO_{2ren} %	Control	52 (46-57)	56 (50-60)	61 (55-63)‡
	I/R	53 (50-62)	60 (56-68)	67 (62-76)‡
	I/R+recAP	52 (49-58)	54 (50-58)	65 (51-71)‡

Parameters were determined at baseline (T0) and after 15 min (T15) and 150 min (T150) reperfusion, which followed a 30 min period of ischemia. RecAP was administered 15 min preceding reperfusion. Data is expressed as median (25th percentile, 75th percentile). Significant differences within groups were estimated using Friedman test with Dunn's post-test, differences between groups were estimated using two-way repeated measures ANOVA with Bonferonni's post-test on log-transformed data ($n=6$ per group). ‡ $p<0.05$ compared to baseline within a group, * $p<0.05$ compared to Control, † $p<0.05$ compared to I/R. DO_{2ren} : renal oxygen delivery, ERO_{2ren} : renal oxygen extraction ratio, I/R; ischemia-reperfusion, recap; human recombinant alkaline phosphatase, μPO_2 : microvascular oxygen tension, VO_{2ren} : renal oxygen consumption.

Table 2. Renal tissue levels of inflammatory and oxidative stress during AKI.

	IR protocol		Sepsis protocol	
	Placebo	IR	IR+recAP	Placebo
MDA (μmol/g)	4.3 (3.4-4.6)	5.5 (4.6-6.0)	4.7 (4.4-5.0)	1.5 (1.1-1.7)
NO (μmol/g)	2.4 (1.4-2.9)	3.8 (2.9-4.5)	3.3 (1.9-4.9)	0.9 (0.6-1.1)
TNF-α (pg/μg)	1.5 (1.3-2.2)	6.9 (6.4-7.9)[#]	5.8 (2.9-6.6)	0.9 (0.8-1.2)
IL-6 (pg/μg)	5.3 (4.2-6.8)	22.8 (16.9-26.2)[#]	18.6 (10.1-21.1)	7.6 (5.7-9.4)

Data is expressed as median (25th percentile, 75th percentile). Significant differences estimated using Kruskal-Wallis test with Dunns post-test (n=6 per group). [#] p<0.05 compared to Control. IL-6; interleukin-6, IR; ischemia-reperfusion, MDA; malondialdehyde, NO; nitric oxide, RecAP; human recombinant alkaline phosphatase, TNF-α; tumor necrosis factor-α.

RecAP treatment prevents I/R injury-induced renal inflammation

Renal MDA and NO levels, markers of oxidative and nitrosative stress respectively, were not affected by I/R itself or by I/R+recAP treatment (Table 2). However, immunohistochemistry demonstrated that recAP treatment attenuated iNOS staining, representing nitrosative stress, which was not significantly increased by I/R injury alone (Figure 2). The renal content of pro-inflammatory mediators TNF- α and IL-6 was significantly increased by I/R injury, which was prevented by recAP treatment (Table 2).

Immunohistochemistry data showed that IL-6 tended to be increased by I/R and was significantly reduced in recAP treated kidneys (Figure 2). As biomarkers of renal injury, staining of L-FABP and proapoptotic protein Bax was not affected by I/R compared to control animals, but was significantly reduced in the recAP-treated kidneys (Figure 2). NGAL expression was not increased by I/R injury nor influenced by recAP treatment (data not shown). As another marker of acute inflammation, MPO-stained leukocyte influx (20) was assessed in the glomerulus and in the peritubular areas. MPO staining was similar in the glomeruli of the control group compared to the I/R group (positive areas: 80 vs. 75%; $p=NS$), while it was decreased in the I/R+recap group compared to control (68%; $p=0.01$). In the peritubular areas, I/R injury decreased leukocyte influx compared to control (83 vs. 65%; $P<0.0001$), which was further attenuated by recAP treatment (52%; $p<0.0001$ compared to control; $p<0.05$ compared to I/R)

LPS-induced systemic hemodynamic instability and impaired renal oxygenation is not improved by recAP

In a second rat AKI model, the renal protective effect of recAP was assessed following shock induced by LPS infusion in rats (Supplemental Figure 1B). LPS administration decreased MAP ($p<0.01$) compared to placebo, and this decrease in MAP was not affected by recAP administration (Figure 1B). RVR was not different between the groups (Figure 1B), but was reduced in the LPS+recAP group 2 h post-LPS (T2, 30 min after recAP administration) compared to baseline ($p<0.05$). RBF remained stable over time in all groups compared to baseline. Endotoxemia did not affect DO_2 or VO_2 significantly, but DO_2 was significantly lower in the LPS+recap group at T1.5 and T4.5 compared to control (Table 3). The oxygen extraction ratio was increased in all groups at T4.5 compared to baseline, and was higher in the LPS and the LPS+recAP group compared to control (Table 3). Similar results were observed for cortical and medullar μPO_2 , which were impaired during endotoxemia at T4.5, with no effect of recAP administration (Table 3).

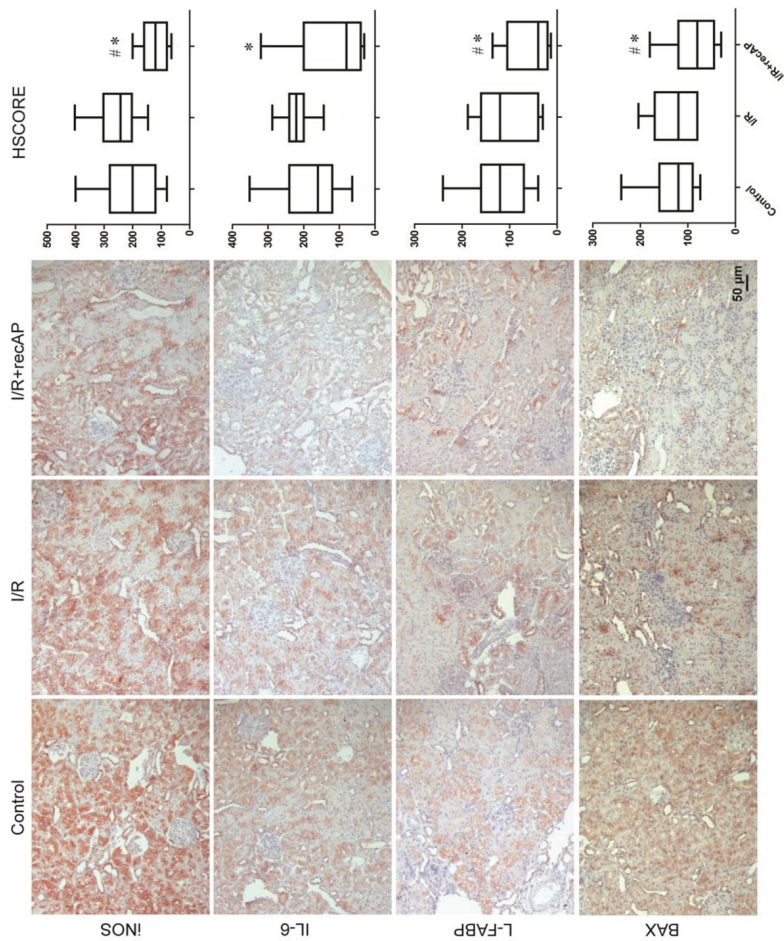


Figure 2. Immunohistochemical results during I/R-induced AKI. Kidneys were harvested after the 2.5 h reperfusion period. A histological score (HSCORE) value was derived by summing the percentages of cells that stained at each intensity multiplied by the weighted intensity of the staining. Data is expressed as box and whiskers plots with 10-90 percentile. Significant differences estimated using Kruskal-Wallis test with Dunn's post-test (n=6 per group). * p<0.05 Control vs. I/R+recAP, # p<0.05 I/R vs. I/R+recAP. Bax; bcl-2-associated X protein, IL-6; interleukin-6, iNOS; inducible nitric oxide synthase, L-FABP; liver-type fatty acid binding protein, RecAP; human recombinant alkaline phosphatase.

Table 3. Kidney oxygenation during LPS-induced AKI.

	Baseline (T0)	Endotoxemia (T1)	Early Resuscitation (T2)	Late Resuscitation (T3)
Cortical μPO_2 (mmHg)				
Control	84 (78-95)	74 (68-83)	69 (66-77)‡	65 (60-72)‡
LPS	88 (82-92)	79 (73-84)	78 (76-80)	56 (53-59)‡#
LPS+recap	88 (84-93)	81 (74-84)	70 (66-75)‡	50 (46-55)‡#
Medullar μPO_2 (mmHg)				
Control	66 (61-71)	56 (52-62)	54 (49-57)‡	50 (44-55)‡
LPS	68 (64-70)	62 (55-64)	61 (57-62)	42 (39-47)‡#
LPS+recap	65 (64-72)	61 (58-65)	55 (52-56)‡	41 (35-44)‡#
$\text{DO}_{2\text{ren}}$ ($\text{mL O}_2 \text{ min}^{-1}$)				
Control	4.1 (3.5-5.0)	3.7 (3.0-4.2)	3.1 (2.8-4.5)	3.2 (2.4-4.4)
LPS	4.6 (4.3-4.8)	2.1 (2.0-3.0)	6.0 (3.8-8.2)	2.3 (1.3-3.7)
LPS+recap	4.0 (3.2-5.5)	2.0 (1.4-2.9)‡#	4.2 (3.4-5.0)	1.2 (1.0-3.1)‡#
$\text{VO}_{2\text{ren}}$ ($\text{mL O}_2 \text{ min}^{-1} \text{ g}^{-1}$)				
Control	1.9 (1.5-2.3)	1.9 (1.5-2.3)	1.8 (1.5-2.7)	2.3 (1.4-3.4)
LPS	2.0 (1.9-2.3)	1.3 (1.2-1.4)	3.6 (2.5-4.8)	2.0 (1.1-3.3)
LPS+recap	1.9 (1.3-2.5)	1.0 (0.6-1.9)	2.9 (1.8-3.2)	1.0 (0.9-2.8)
$\text{ERO}_{2\text{ren}} \%$				
Control	44 (43-46)	49 (49-53)	56 (51-62)‡	72 (55-79)‡
LPS	45 (41-51)	59 (51-61)	67 (57-69)‡	87 (84-91)‡#
LPS+recap	43 (41-48)	52 (44-58)	65 (53-74)	88 (84-93)‡#

Parameters were determined at baseline (T0) and 1.5 (T1), 2 (T2) and 4.5 h (T3) after start of LPS infusion. RecAP was administered directly after T1. Data is expressed as median (25th percentile, 75th percentile). Significant differences within groups were estimated using Friedman's test with Dunn's post-test, differences between groups were estimated using two-way repeated measures ANOVA with Bonferonni's post-test on log-transformed data (n=6 per group). ‡ p<0.05 compared to baseline within a group, # p<0.05 compared to Control group. $\text{DO}_{2\text{ren}}$; renal oxygen delivery, $\text{ERO}_{2\text{ren}}$; renal oxygen extraction ratio, IR; ischemia-reperfusion, recAP; human recombinant alkaline phosphatase, μPO_2 ; microvascular oxygen tension, $\text{VO}_{2\text{ren}}$; renal oxygen consumption.

RecAP inhibits markers of renal inflammation and damage during endotoxin-induced shock

Tissue NO and MDA levels were significantly increased by LPS treatment, irrespective of recAP coadministration (Table 1). However, recAP treatment attenuated LPS-induced iNOS reactivity (Figure 3). While LPS had no effect on tissue levels of TNF- α and IL-6, immunohistochemistry data demonstrated a significant increase in expression of IL-6, L-FABP and Bax, which was ameliorated by recAP treatment (Figure 3). Similar results were shown for NGAL immunoreactivity (HSCORE Control: 90 [60-200], LPS: 200 [135-310], LPS+recAP:100 [60-160]; p<0.0001), and for leukocyte infiltration. LPS administration induced leukocyte influx in both the glomerulus (positive areas: 93 vs. 75% in the control group; p<0.0001) and the peritubular areas (77 vs. 65%; p<0.01).

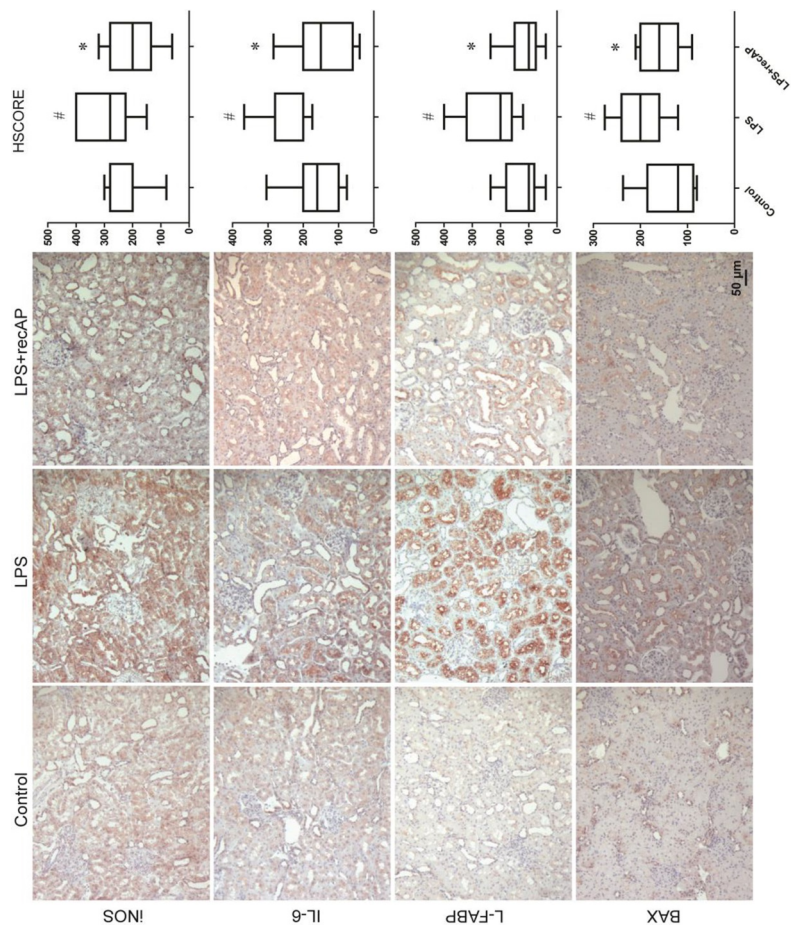


Figure 3. Immunohistochemical results during LPS-induced AKI. Kidneys were harvested 4.5 h after initiations of LPS treatment. A histological score (HSCORE) value was derived by summing the percentages of cells that stained at each intensity multiplied by the weighted intensity of the staining. Data is expressed as box and whiskers plots with 10-90 percentile. Significant differences estimated using Kruskal-Wallis test with Dunn's post-test (n=6 per group). * p<0.05 Control vs. LPS, # p<0.05 LPS vs. LPS+recAP. Bax; bcl-2-associated X protein, IL-6; interleukin-6, iNOS; inducible nitric oxide synthase, L-FABP; liver-type fatty acid binding protein, LPS; lipopolysaccharide, RecAP; human recombinant alkaline phosphatase.

RecAP treatment did not reduce the influx in the glomerulus (87%; $p=NS$ compared to the LPS group), but did prevent the peritubular influx (66%, $p<0.05$).

DISCUSSION AND CONCLUSION

Sepsis-associated AKI is a multifactorial syndrome in which several processes, including inflammation, hemodynamic instability, renal microcirculatory dysfunction and unbalanced renal bioenergetics play a crucial role (2). RecAP represents a potential therapy targeting these multiple processes, which was previously shown to exert anti-inflammatory effects on cultured tubular cells (12). The effects of recAP on hemodynamics and renal oxygenation were not assessed previously. Here, we demonstrate mild modulatory effects of recAP on these parameters during I/R-induced AKI, while hemodynamics and renal oxygenation are not affected by recAP during endotoxemia-induced AKI. However, in both models, recAP attenuated renal injury and inflammation, confirming the protective effects observed previously during LPS-induced renal inflammation *in vivo* (12).

The kidney is highly susceptible to hypoxic injury as the organ is borderline ischemic and has to meet high energy demands (21). As such, tissue oxygenation within the kidney is strictly regulated. Under normal conditions, there is a delicate balance between oxygen delivery, mainly determined by RBF, local tissue perfusion and blood oxygen content; and oxygen consumption, influenced by GFR, sodium reabsorption, mitochondrial function and tubular integrity (22). I/R-induced injury disturbs this balance by reducing RBF and causing hypoperfusion in the ischemic phase, followed by a decreased renal oxygen delivery and oxygen consumption and increased intrarenal oxygen shunting during the reperfusion phase (23). However, in daily clinical practice, AKI may also occur without clear signs of hypoperfusion (24). Animal and human data suggest that during sepsis, AKI can develop in the setting of sustained or even increased RBF (5, 6). Due to this discrepancy in kidney perfusion, the effects of recAP were investigated in two distinct models of AKI.

In the I/R model, RBF was impaired during the post-reperfusion period. After recAP treatment, RBF was not longer significantly affected immediately following reperfusion and neither were renal oxygen delivery and consumption at this time-point. Although these microcirculatory improvements were modest and were not maintained until the end of reperfusion, the anti-inflammatory effect of recAP may have reduced arterial to venous shunting, resulting in an improved cortical microvascular oxygen pressure during the 2.5 h reperfusion period.

In contrast, recAP was found not to improve renal oxygenation during endotoxemia. Apart from the timing of the intervention (recAP was administered 15 min following ischemia and 60 min following LPS administration), the nature of the inflammatory response may account for this observed discrepancy. I/R-induced hypoxia triggers renal inflammation via several mechanisms, including structural alterations of proteins and cell surfaces, active synthesis of pro-inflammatory mediators and downregulation of anti-inflammatory molecules (7). In addition, ischemic stress induces the release of cellular factors such as high mobility group 1 protein (25) and heat shock proteins (26). Toll-like receptor (TLR)-2 and TLR4, pattern recognition receptors (PRR) localized on proximal tubule epithelial cells, are triggered by these endogenous ligands, thereby further exacerbating renal injury together with complement system activation, oxidative and nitrosative stress and mitochondrial dysfunction (27,28). This is in contrast to endotoxemia-induced AKI, during which renal inflammation is not only triggered by endogenous PRR ligands, but mainly by the bacterial ligand LPS which induces a profound inflammatory insult upon binding to TLR4 on multiple cells including proximal tubular epithelial cells (29). In addition, binding of LPS to TLR4 on immune cells elicits systemic release of inflammatory mediators (30), to which both vascular endothelium and renal tubular cells respond. In concert with a prolonged leukocyte transit time in dysfunctional capillaries (31,32), this may further amplify renal inflammation.

RecAP affected the inflammatory response induced by IR, as protein levels of IL-6 and TNF- α were not longer significantly increased and the expression of renal injury parameters was lower, although these were not significantly increased by I/R-injury itself. Possibly, renal injury partially recovered after the 2.5 h reperfusion period in this relatively mild model (13,33,34). Also during endotoxemia, administration of recAP attenuated renal inflammation, as was shown by a less pronounced peritubular influx of leukocytes and IL-6 expression. Moreover, recAP inhibited proximal tubule injury and markers of apoptosis, reflected by L-FABP and BAX immunostaining. Likely, these protective effects may be attributed to dephosphorylation of LPS and the endogenous proinflammatory molecules ATP and ADP, released by proximal tubule cells during inflammation (12). Of note, and in contrast to the I/R-model, we did not find an increase in renal cytokine protein levels, but did detect a high level of oxidative and nitrosative stress.

Despite its anti-inflammatory effects following LPS-induced shock, recAP treatment did not result in improved renal oxygenation in this model. This might be explained by the finding that in a rat model of severe shock recAP cannot restore the imbalance between NO, a major regulator of the microvascular oxygen supply, ROS and oxygen, which is key for an adequate physiological control of renal function (22).

Several limitations have to be acknowledged. First, although recAP modulated renal hemodynamics and oxygenation during I/R-induced AKI, these effects were modest and the clinical relevance of these findings might be limited. Second, following endotoxin administration, RBF remained stable over time, thereby limiting the possibility to demonstrate effects of recAP on renal hemodynamics. Although one may argue that the LPS dose administered is not high enough to severely affect renal hemodynamics, we aimed to investigate the effects of recAP in a clinically relevant model. As recently demonstrated in an intensive care-supported model of *E. coli*-induced septic shock in sheep, early AKI is not associated with changes in renal blood flow, oxygen delivery or histological changes, suggesting other mechanisms contributing to septic AKI (35). These findings corroborate previous studies (5,6). As our model presents with signs of impaired systemic hemodynamics, renal oxygenation, as well as clear signs of renal injury, we believe that this is a representative model of endotoxemia-induced AKI in which we were able to confirm the renal protective effect of recAP. Third, the fact that recAP is administered not preventively but therapeutically, namely following initiation of the ischemic or endotoxic insult, may have hampered the potential of recAP to modulate renal microcirculatory dysfunction and hemodynamic changes.

However, this protocol is more clinically relevant as it is in line with the ongoing phase II trial, in which recAP is administered to patients with confirmed sepsis-associated AKI. Moreover, previous findings demonstrate that recAP provides renal protection when administered two hours after administration of LPS (12), indicating that recAP can still exert protective effects when LPS-induced inflammation is fully developed (36, 37). Also, the renal protective anti-inflammatory effects were primarily determined by immunostaining, a non-quantitative method. Although these results could have been corroborated by employing quantitative assays (e.g. assessing renal gene expression levels), the primary aim of this study was to investigate the effect of recAP on renal hemodynamics and oxygenation as the renal protective effect of recAP has already been demonstrated *in vivo* previously (12). Finally, as sepsis-associated AKI is a complex syndrome, the potential activity of recAP on other inflammatory components, such as the complement and coagulation pathways, eicosanoids, PRR ligands, and platelet activation factors, would be relevant to assess, but was beyond the scope of the current study. Of interest, the protective potential of AP has been confirmed in several other inflammatory models. AP administration reduced fever after *Escherichia coli*-induced inflammation in mice (38), improved gas exchange (PaO₂:FiO₂ ratio) during septic shock induced in sheep (39), prevented liver and lung damage in mice after cecal ligation and puncture (40) and increased thrombocyte counts in piglets following LPS administration (38). Also, AP attenuated circulating cytokine levels in mice (40) and sheep (39), which was confirmed in a phase 2 clinical study in which bovine intestinal

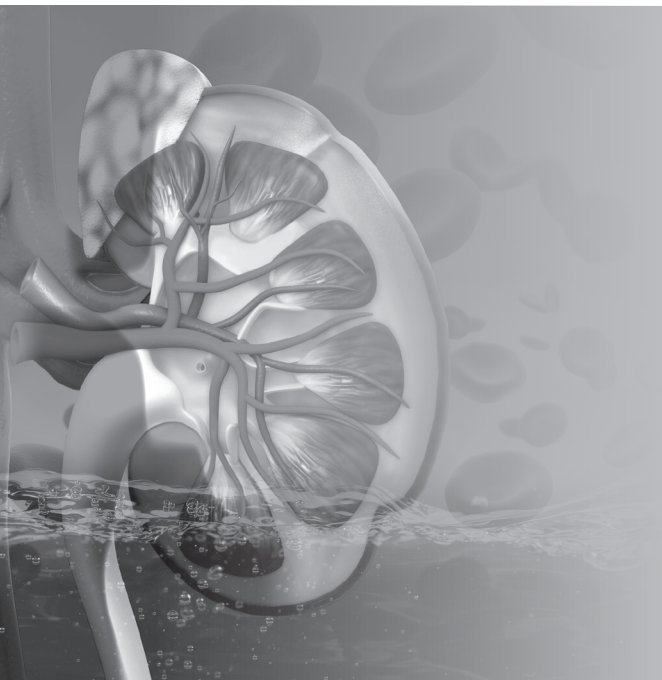
AP more swiftly reduced several systemic inflammatory parameters in patients with sepsis-associated AKI (10).

In conclusion, recAP can modulate renal oxygenation and hemodynamics immediately following I/R-induced AKI, but did not influence these during endotoxemia-induced AKI. RecAP did exert a clear renal protective anti-inflammatory effect in both models. Whether this renal protective effect is sufficient to improve outcome of patients suffering from sepsis-associated AKI is currently being investigated in a large phase II a/b clinical trial (NTC02182440).

REFERENCES

1. Bagshaw SM, George C, Bellomo R, Committee ADM. Early acute kidney injury and sepsis: a multicentre evaluation. *Crit. Care* 12(2):R47, 2008.
2. Peters E, Heemskerk S, Masereeuw R, *et al.* Alkaline phosphatase: a possible treatment for sepsis-associated acute kidney injury in critically ill patients. *Am. J Kid. Dis* : the official journal of the National Kidney Foundation. 63(6):1038-48, 2014.
3. Gustot T. Multiple organ failure in sepsis: prognosis and role of systemic inflammatory response. *Curr. Opin. Crit. Care*.17(2):153-9, 2011.
4. Ince C. The microcirculation is the motor of sepsis. *Crit. Care* 9 Suppl 4:S13-9, 2005.
5. Langenberg C, Bellomo R, May C, *et al.* Renal blood flow in sepsis. *Crit. Care* 9(4):R363-74, 2005.
6. Langenberg C, Wan L, Egi M, *et al.* Renal blood flow in experimental septic acute renal failure. *Kidney Int.* 69(11):1996-2002, 2006.
7. Thurman JM. Triggers of inflammation after renal ischemia/reperfusion. *Clinical Immunology* 123(1):7-13, 2007.
8. Legrand M, Mik EG, Johannes T, *et al.* Renal hypoxia and dysoxia after reperfusion of the ischemic kidney. *Mol. Med.* 14(7-8):502-16, 2008.
9. Heemskerk S, Masereeuw R, Moesker O, *et al.* Alkaline phosphatase treatment improves renal function in severe sepsis or septic shock patients. *Crit. Care Med.* 37(2):417-23, 2009.
10. Pickkers P, Heemskerk S, Schouten J, *et al.* Alkaline phosphatase for treatment of sepsis-induced acute kidney injury: a prospective randomized double-blind placebo-controlled trial. *Crit. Care* 16(1):R14, 2012.
11. Kiffer-Moreira T, Sheen CR, Gasque KC, *et al.* Catalytic signature of a heat-stable, chimeric human alkaline phosphatase with therapeutic potential. *PLoS One* 9(2):e89374, 2014.
12. Peters E, Geraci S, Heemskerk S, *et al.* Alkaline phosphatase protects against renal inflammation through dephosphorylation of lipopolysaccharide and adenosine triphosphate. *B. J. Pharmacol.* 172(20):4932-45, 2015.
13. Ergin B, Bezemer R, Kandil A, *et al.* TEMPOL has limited protective effects on renal oxygenation and hemodynamics but reduces kidney damage and inflammation in a rat model of renal ischemia/reperfusion by aortic clamping. *J. Clin. Transl. Res.* 1(2), 2015.
14. Aksu U, Ergin B, Bezemer R, *et al.* Scavenging reactive oxygen species using tempol in the acute phase of renal ischemia/reperfusion and its effects on kidney oxygenation and nitric oxide levels. *Intensive Care Med. Exp.* 3(1):57, 2015.
15. Legrand M, Bezemer R, Kandil A, *et al.* The role of renal hypoperfusion in development of renal microcirculatory dysfunction in endotoxemic rats. *Intensive Care Med.* 37(9):1534-42, 2011.
16. Johannes T, Mik EG, Ince C. Dual-wavelength phosphorimetry for determination of cortical and subcortical microvascular oxygenation in rat kidney. *J. Appl. Physiol.* 100(4):1301-10, 2006.
17. Mik EG, Johannes T, Ince C. Monitoring of renal venous PO₂ and kidney oxygen consumption in rats by a near-infrared phosphorescence lifetime technique. *Am. J. Physiol. Renal Physiol.* 294(3):F676-81, 2008.
18. Bezemer R, Faber DJ, Almac E, *et al.* Evaluation of multi-exponential curve fitting analysis of oxygen-quenched phosphorescence decay traces for recovering microvascular oxygen tension histograms. *Medical & Biological Engineering & Computing* 48(12):1233-42, 2010.
19. Senturk LM, Seli E, Gutierrez LS, *et al.* Monocyte chemotactic protein-1 expression in human corpus luteum. *Mol. Hum. Reproduction* 5(8):697-702, 1999.
20. Ysebaert DK, De Greef KE, Vercauteren SR, *et al.* Identification and kinetics of leukocytes after severe ischaemia/reperfusion renal injury. *Nephrol. Dial. Transplant.* 15(10):1562-74, 2000.
21. Ergin B, Kapucu A, Demirci-Tansel C, *et al.* The renal microcirculation in sepsis. *Nephrol. Dial. Transplant.* 30(2):169-77, 2015.
22. Evans RG, Ince C, Joles JA, *et al.* Haemodynamic influences on kidney oxygenation: clinical implications of integrative physiology. *Clin. Exp. Pharma. Physiol.* 40(2):106-22, 2013.
23. Legrand M, Almac E, Mik EG, *et al.* L-NIL prevents renal microvascular hypoxia and increase of renal oxygen consumption after ischemia-reperfusion in rats. *Am. J. Physiol. Renal Physiol.* 296(5):F1109-17, 2009.

24. Murugan R, Karajala-Subramanyam V, Lee M, *et al.* Acute kidney injury in non-severe pneumonia is associated with an increased immune response and lower survival. *Kidney Int.* 77(6):527-35, 2010.
25. Kruger B, Krick S, Dhillon N, *et al.* Donor Toll-like receptor 4 contributes to ischemia and reperfusion injury following human kidney transplantation. *Proceedings of the National Academy of Sciences of the United States of America* 106(9):3390-5, 2009.
26. Smoyer WE, Ransom R, Harris RC, *et al.* Ischemic acute renal failure induces differential expression of small heat shock proteins. *JASN* 11(2):211-21, 2000.
27. Wu H, Ma J, Wang P, *et al.* HMGB1 contributes to kidney ischemia reperfusion injury. *JASN* 21(11):1878-90, 2010.
28. Quintana FJ, Cohen IR. Heat shock proteins as endogenous adjuvants in sterile and septic inflammation. *Journal of Immunology* 175(5):2777-82, 2005.
29. Kalakeche R, Hato T, Rhodes G, *et al.* Endotoxin uptake by S1 proximal tubular segment causes oxidative stress in the downstream S2 segment. *JASN* 22(8):1505-16, 2011.
30. Cohen J. The immunopathogenesis of sepsis. *Nature* 420(6917):885-91, 2002.
31. Holthoff JH, Wang Z, Seely KA, *et al.* Resveratrol improves renal microcirculation, protects the tubular epithelium, and prolongs survival in a mouse model of sepsis-induced acute kidney injury. *Kidney Int.* 81(4):370-8, 2012.
32. Goddard CM, Allard MF, Hogg JC, *et al.* Prolonged leukocyte transit time in coronary microcirculation of endotoxemic pigs. *Am. J. Physiol.* 269(4 Pt 2):H1389-97, 1995.
33. Szeto HH, Liu S, Soong Y, *et al.* Mitochondria-targeted peptide accelerates ATP recovery and reduces ischemic kidney injury. *JASN* 22(6):1041-52, 2011.
34. Weight SC, Furness PN, Nicholson ML. New model of renal warm ischaemia-reperfusion injury for comparative functional, morphological and pathophysiological studies. *B. J. Surg.* 85(12):1669-73, 1998.
35. Maiden MJ, Otto S, Brealey JK, *et al.* Structure and Function of the Kidney in Septic Shock. A Prospective Controlled Experimental Study. *Am. J. Resp. Crit. Care Med.* 94(6):692-700, 2016.
36. Pickkers P, Dorresteyn MJ, Bouw MP, *et al.* In vivo evidence for nitric oxide-mediated calcium-activated potassium-channel activation during human endotoxemia. *Circulation* 114(5):414-21, 2006.
37. Sadeghi S, Wallace FA, Calder PC. Dietary lipids modify the cytokine response to bacterial lipopolysaccharide in mice. *Immunology* 96(3):404-10, 1999.
38. Beumer C, Wulferink M, Raaben W, *et al.* Calf intestinal alkaline phosphatase, a novel therapeutic drug for lipopolysaccharide (LPS)-mediated diseases, attenuates LPS toxicity in mice and piglets. *J. Pharmacol. Exp. Therap.* 307(2):737-44, 2003.
39. Su F, Brands R, Wang Z, *et al.* Beneficial effects of alkaline phosphatase in septic shock. *Crit. Care Med.* 34(8):2182-7, 2006.
40. van Veen SQ, van Vliet AK, Wulferink M, *et al.* Bovine intestinal alkaline phosphatase attenuates the inflammatory response in secondary peritonitis in mice. *Infection and immunity* 73(7):4309-14, 2005.



CHAPTER 9

Effects of supplementing resuscitation fluids with N-acetylcysteine (NAC) on renal microcirculatory oxygenation, inflammation, and function in a rat model of septic shock

Adapted from *Intensive Care Med. Exp.* 2016 Dec;4(1):29

Bulent Ergin¹, Philippe Guerci^{1,2}, Lara Zafrani¹, Frank Nocken³, Asli Kandil⁴, Ebru Gurel⁴, Cihan Demirci-Tansel⁴, and Can Ince¹

¹ Department of Translational Physiology, Academic Medical Center, Amsterdam, The Netherlands

² University of Lorraine, Vandoeuvre-lès-Nancy, France

³ Divisional Medical & Clinical Affairs Generics & Standard Solutions, Volume Therapy, Fresenius Kabi Deutschland GmbH

⁴ Department of Biology, Faculty of Science, University of Istanbul, Istanbul, Turkey

ABSTRACT

Modulation of inflammation and oxidative stress appears to limit sepsis-induced damage in experimental models. The kidney is one of the most sensitive organs to injury during septic shock. In this study, we evaluated the effect of N-acetylcysteine (NAC) administration in conjunction with fluid resuscitation on renal oxygenation and function. We hypothesized that reducing inflammation would improve the microcirculatory oxygenation in the kidney and limit the onset of acute kidney injury (AKI). Rats were randomized into five groups ($n = 8/\text{group}$): (1) control group, (2) control + NAC, (3) endotoxemic shock with lipopolysaccharide (LPS) without fluids, (4) LPS + fluid resuscitation, and (5) LPS + fluid resuscitation + NAC (150 mg/kg/h). Fluid resuscitation was initiated at 120 min and maintained at fixed volume for 2 h with hydroxyethyl starch (HES 130/0.4) dissolved in acetate-balanced Ringer's solution (Volulyte) with or without supplementation with NAC (150 mg/kg/h). Oxygen tension in the renal cortex ($C_{\mu PO_2}$), outer medulla ($M_{\mu PO_2}$), and renal vein was measured using phosphorimetry. Biomarkers of renal injury, inflammation, and oxidative stress were assessed in kidney tissues. Fluid resuscitation significantly improved the systemic and renal macrohemodynamic parameters after LPS. However, the addition of NAC further improved cortical renal oxygenation, oxygen delivery, and oxygen consumption ($p < 0.05$). NAC supplementation dampened the accumulation of NGAL or L-FABP, hyaluronic acid, and nitric oxide in kidney tissue ($p < 0.01$). Conclusion: The addition of NAC to fluid resuscitation may improve renal oxygenation and attenuate microvascular dysfunction and AKI. Decreases in renal NO and hyaluronic acid levels may be involved in this beneficial effect. A therapeutic strategy combining initial fluid resuscitation with antioxidant therapies may prevent sepsis-induced AKI.

Keywords: acute kidney injury, sepsis, N-acetyl cysteine, kidney oxygenation, inflammation

INTRODUCTION

Inflammation is a key process in the pathophysiology of septic shock (1). The whole activation of leukocytes, the cascade of inflammation, the associated cytokine storm, and the endothelial cell dysfunction will concur to alterations of the microcirculation (2,3). Subsequently, tissue hypoxia and dysoxia due to the heterogeneity of the microcirculation will occur (4). Fluid resuscitation may help resolving some of these issues, but it may also lead to the activation of oxidative pathways in itself, resulting in a heterogeneous distribution of blood flow and tissue oxygenation, especially in the renal cortex (5,6). Because reactive oxygen species (ROS) participate in the pathophysiology of endotoxic shock, it is suggested that moderating the oxidative stress and inflammation reaction would translate into improvement in microcirculation and a better oxygenation of the tissues. Previous studies have demonstrated an interest in the use of antioxidants for preventing the sepsis-induced damage in these organs (7-9). Indeed, the experimental literature abounds in drugs targeting and effective at dampening inflammation and oxidative stress. Several trials have experienced several anti-inflammatory or antioxidant drugs with discordant effects on major outcomes (10,11). As a matter of fact, antioxidant therapies might be of interest for specific organs. Acute kidney injury (AKI) and acute lung injury are particularly common complications of sepsis and the development of either increases mortality, probably because these organs are more sensitive to inflammation and oxidative stress insults. Thus, the kidney could benefit from antioxidant drugs.

A common approach for the inhibition of oxidant-mediated injury is the use of glutathione-modulating agents like sulfhydryl or thiol compounds. Among all the drugs used to interact with this pathway, N-acetylcysteine (NAC) is the most studied, for its lung and renal protective effects (12-16). NAC is a thiol compound with antioxidant and vasodilatory properties (12). NAC is then regarded as an important antioxidant as it is a source of sulfhydryl and glutathione groups in cells and, due to its interaction with ROS, a scavenger of free radicals. In septic patients, the endogenous antioxidant glutathione is depleted (17). Decreased levels of glutathione may lead to decreased protection of cell membranes against oxygen radicals. NAC serves as a precursor of glutathione and, thus, can replenish the intracellular glutathione stores (12). Moreover, NAC targets kidney microcirculatory blood flow (18,19). NAC has also been widely studied for its nephroprotective effects in various settings.

Hypoxia and inflammation share interdependent relationship. Several molecular pathways of cross-talk between hypoxia and inflammation in the kidney have been identified (20-22). From a physiological perspective, although hypoxia may lead to inflammation and

vice versa, it is not clear if correcting or modulating either of these states would translate into better tissue oxygenation and improve outcome. NAC would be interesting for testing if the modulation of inflammation would correct tissue hypoxia during sepsis.

To date, no study focused on tissue oxygenation in specific organs such as the kidney but rather demonstrated that pretreatment or post-treatment with NAC decreased the markers of organ injury. In this study, we assessed kidney tissue oxygenation in an endotoxemic shock model resuscitated with hydroxyethyl starch – ringer's acetate with and without supplementation with NAC. We sought to promote blood flow and oxygenation to the organs by the means of reducing inflammation and oxidative stress.

MATERIAL AND METHODS

Animals

All experiments in this study were approved by the institutional Animal Experimentation Committee of the Academic Medical Center of the University of Amsterdam (DFL102538). Care and handling of the animals were in accordance with the guidelines for Institutional and Animal Care and Use Committees. The study has been carried out in accordance with the Declaration of Helsinki. Experiments were performed on *Wistar albino* rats (Harlan Netherlands BV, Horst, The Netherlands) with a mean \pm SD body weight of 325 ± 6 g.

Surgical Preparation

All animals were anesthetized with an intraperitoneal injection of a mixture of 90 mg/kg ketamine (Nimatek®, Eurovet, Bladel, The Netherlands), 0.5 mg/kg dexmedetomidine (Dexdomitor, Pfizer Animal Health BV, Capelle aan den IJssel, The Netherlands), and 0.05 mg/kg atropine-sulfate (Centrafarm Pharmaceuticals BV, Etten-Leur, The Netherlands). After performing a tracheotomy, the animals were mechanically ventilated with a fraction of inspired oxygen (FiO_2) of 0.4. Body temperature was maintained at 37 ± 0.5 °C during the entire experiment by an external thermal heating pad. Ventilator settings were adjusted to maintain arterial partial pressure of carbon dioxide (PaCO_2) between 35 and 40 mmHg. For drug, fluid administration and hemodynamic monitoring, vessels were cannulated with polyethylene catheters with an outer diameter of 0.9 mm (Braun, Melsungen, Germany). A catheter in the right carotid artery was connected to a pressure transducer to monitor mean arterial blood pressure (MAP) and heart rate. The right jugular vein was cannulated for continuous infusion of Ringer's Lactate (Baxter, Utrecht, The Netherlands) at a rate of 15 mL/kg/hour and maintenance of anesthesia. The right femoral artery was cannulated for drawing blood samples and the right femoral vein for drug administration. The left kidney was exposed, decapsulated, and immobilized

in a Lucite kidney cup (K. Effenberger, Pfaffingen, Germany) via ~4 cm incision in the left flank in each animal. Renal vessels were carefully separated under preservation of nerves and the adrenal gland. A perivascular ultrasonic transient time flow probe was placed around the left renal artery (type 0.7 RB Transonic Systems Inc., Ithaca, NY, USA) and connected to a flow meter (T206, Transonic Systems Inc., Ithaca, NY, USA) to continuously measure renal blood flow (RBF). The left ureter was isolated, ligated, and cannulated with a polyethylene catheter for urine collection. After the surgical preparation one optical fiber was placed 1 mm above the decapsulated kidney and another optical fiber was placed 1 mm above the renal vein to measure renal microvascular and venous oxygenation using phosphorimetry. A small piece of aluminum foil was placed on the dorsal side of the renal vein to prevent contribution of the underlying tissues to the phosphorescence signal in the venous pO_2 measurements. The surgical field was covered with a humidified gauze compress throughout the entire experiment to prevent drying of the exposed tissues.

Experimental protocol

After a 30-min stabilization, the rats were randomized into the five following groups at baseline: (1) control group, (2) control +NAC, (3) endotoxemic shock with lipopolysaccharide (LPS) without fluid resuscitation, (4) LPS + fluid resuscitation, and (5) LPS + fluid resuscitation + NAC (150 mg/kg/h). The groups received either an intravenous bolus of 5 mg/kg LPS (LPS group; *Escherichia coli* 0127:B8, Sigma, Paris, France; three groups of eight rats each) or vehicle (control group, two groups of eight rats each). Animals were observed or kept in shock for over 120 min. Fluid resuscitation (15 ml/kg/h) was then started and maintained for 180 min in the LPS groups with 6 % hydroxyethyl starch (HES130/0.4) dissolved in Ringer's acetate (HES-RA; Volulyte® 6 %, Fresenius Kabi Deutschland GmbH, Germany) as a balanced colloid solution. NAC was administered to the appropriate groups at a rate of 150 mg/kg/h as previously reported (15). An LPS group was not resuscitated to serve as a shock control. Time points for the measurements were baseline (T_0), during shock 120 min after administration of LPS (T_1), 30 min after initiating fluid resuscitation (early reperfusion phase) (T_2), and 120 min after starting fluid resuscitation (late reperfusion phase) (T_3), which was the final endpoint of the experiment (Fig. 1).

Blood gas measurements and biochemistry

Arterial blood samples of 0.5 ml were taken from the femoral artery at T_0 , T_1 , T_2 , and T_3 . The blood samples were replaced by the same volume of balanced colloid solution. The samples were used to determine blood gas parameters (Radiometer ABL 505 Blood Gas Analyzer, Copenhagen, Denmark). The hematocrit and the levels of potassium, bicarbonate and the anion gap were given by the analyzer.

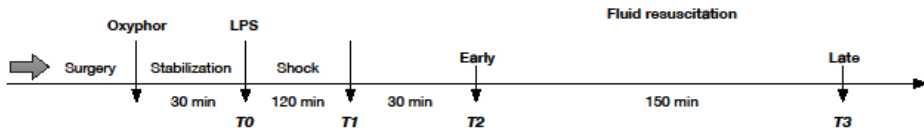


Figure 1. Timeline of the experimental protocol

Measurement of renal microvascular oxygenation and venous PO₂

Renal microvascular partial pressure of oxygen (μPO_2) and renal venous PO₂ (rvPO_2) were measured by oxygen-dependent quenching of phosphorescence lifetimes of phosphorescent dye Oxyphor G2 (Oxygen Enterprises Ltd., Philadelphia, PA, USA) as described elsewhere (23, 24). A total of 6 mg/kg IV over 5 min was administered followed by 30 min of stabilization time before baseline measurements.

Calculation of derivatives of oxygenation parameters and renal vascular resistance

Renal oxygen delivery was calculated as: $\text{DO}_{2\text{ren}} (\text{ml/min}) = \text{RBF} \times \text{arterial oxygen content} (1.31 \times \text{hemoglobin} \times \text{SaO}_2) + (0.003 \times \text{PaO}_2)$, where SaO_2 was arterial oxygen saturation and PaO_2 was arterial partial pressure of oxygen. Renal oxygen consumption was calculated as: $\text{VO}_{2\text{ren}} (\text{ml/min/g}) = \text{RBF} \times (\text{CaO}_2 - \text{CvO}_2)$, where renal venous oxygen content (CvO_2) was calculated as $(1.31 \times \text{hemoglobin} \times \text{SrvO}_2) + (0.003 \times \text{rvPO}_2)$. The $\text{SrvO}_{2\text{ren}}$ was calculated using the Hill equation with $P_{50} = 37 \text{ mmHg}$ and Hill coefficient = 2.7. An estimation of the renal vascular resistance (RVR) was made as: $\text{RVR} (\text{dynes. sec.cm}^{-5}) = (\text{MAP/RBF}) \times 100$.

Assessment of kidney function

Creatinine clearance ($\text{Cl}_{\text{crea}} (\text{ml/min})$) was assessed as an index of the glomerular filtration rate. Clearance was calculated using the following formula: $\text{Cl}_{\text{crea}} = (\text{U}_{\text{crea}} \times \text{V}) / \text{P}_{\text{crea}}$, where U_{crea} was the concentration of creatinine in urine, V was the urine volume per unit time, and P_{crea} was the concentration of creatinine in plasma. Additionally, excretion fraction of Na^+ [$\text{EF}_{\text{Na}} (\%)$] was calculated and used as a marker of tubular function in the following formula: $\text{EF}_{\text{Na}} = (\text{U}_{\text{Na}} \times \text{P}_{\text{crea}}) / (\text{P}_{\text{Na}} \times \text{U}_{\text{crea}}) \times 100$, where U_{Na} was Na^+ concentration in urine and P_{Na} was the Na^+ concentration in plasma. The renal energy efficiency for sodium transport ($\text{VO}_{2\text{ren}} / \text{TNa}^+$) was assessed using a ratio calculated from the total amount of $\text{VO}_{2\text{ren}}$ over the total amount of sodium reabsorbed (TNa^+ , mmol/min) according to: $(\text{Clearcrea} \times \text{P}_{\text{Na}}) - \text{U}_{\text{Na}} \times \text{V}$.

NO metabolism

Index of total nitric oxide (NO) production is the sum of both nitrite and nitrate accumulated in the tissue samples. To determine this, a reducing agent, a saturated

solution of vanadium (III) chloride (VCl₃) in 1 mol/l HCl, was used. At a temperature of 90°C, the VCl₃ reagent quantitatively converts nitrite, nitrate, and S-nitroso compounds to NO in a glass reaction vessel. NO was then flushed out of the reaction vessel by a flow of helium gas, which was then measured by the Sievers NO analyzer (General Electric Company, GE Water & Process Technologies Analytical Instruments) by chemiluminescence, as the amount of light from the ozone-NO reaction in the measurement chamber of the analyzer. NO levels were determined in homogenized frozen kidney tissues. A ratio of tissue NO to tissue protein content was used for standardization of NO release per gram of protein.

Glycocalyx component assessments

Hyaluronan is the main component of endothelial glycocalyx, and alterations in its concentration are attributed to glycocalyx volume loss. Tumor necrosis factor- α inhibition protects against endotoxin-induced endothelial glycocalyx perturbation. Plasma hyaluronan concentrations were determined using the Corgenix hyaluronic acid test kit (Corgenix Inc., Westminster, CO, USA) based on an enzyme-linked hyaluronic acid-binding protein assay.

Measurement of oxidative stress and inflammatory cytokines

All kidneys were homogenized in cold 5 mM sodium phosphate buffer. The homogenates were centrifuged at 12,000 g for 15 min at 4°C and the supernatants were used for determination of TNF- α , IL-6, hyaluronic acid, malondialdehyde (MDA) and protein carbonyl. The levels of these markers were expressed as per gram of protein (Bradford assay). For determination of oxidative stress and inflammatory cytokines levels was used in enzyme-linked immunosorbent assay (ELISA) kits. Tumor Necrosis Factor- α (TNF- α) (DY510, R&D system, Inc. Minneapolis, USA) and Interleukin-6 (IL-6) (DY506, R&D system, Inc. Minneapolis, USA), tissue MDA and protein carbonyl were determined in homogenized tissue samples.

Immunohistochemical analysis

Kidney tissues were fixed in 4% formalin and embedded in paraffin. After preparation, kidney sections were incubated with neutrophil gelatinase-associated lipocalin (NGAL) antibody (NGAL antibody 41105, Abcam, Cambridge, UK), and a polyclonal antibody to rat liver-type fatty acid protein (L-FABP) (HP8010, Hycult Biotect, Uden Holland). Antibodies were diluted in a large volume of UltrAb Diluent (TA-125-UD, Thermo Fischer Scientific, Breda, Holland). The slides were counterstained with Mayer's hematoxylin (LabVision TA-125-MH Thermo Fischer Scientific, Breda, Holland) and mounted in vision mount (LabVision, TA-060-UG, Thermo Fischer Scientific, Breda, Holland) after being washed in distilled water. Both the intensity and the distribution of L-FABP and NGAL staining were scored. For each sample, a histological score (HSCORE)

value was derived by summing the percentages of cells that stained at each intensity multiplied by the weighted intensity of the staining: $HSCORE = \sum P_i (i+1)$, where i was the intensity score and P_i was the corresponding percentage of the cells.

Statistical Analyses

The results were expressed as mean \pm SD. Statistical significance was calculated by one-way and two-way analysis of variance (ANOVA), followed by Tukey's or Bonferroni multiple comparison tests using GraphPad Prism (GraphPad Prism, Version 5, Software Program, San Diego, CA, USA). A $p < 0.05$ was considered to be statistically significant.

RESULTS

Systemic and renal hemodynamic parameters

The evolution of systemic and renal hemodynamics is presented in Table 1. Infusion of LPS induced an early drop in MAP, 76.8 ± 9.3 mmHg vs 45.8 ± 7.9 mmHg ($p < 0.001$) and RBF 4.5 ± 1.5 ml/min vs 0.7 ± 0.6 ml/min in the control group and in the LPS group at T_3 , respectively ($p < 0.001$). Fluid resuscitation with HES-RA with and without NAC, significantly improved RBF compared to LPS group ($p < 0.05$). Both HES-RA and HES-RA+NAC significantly decreased the RVR compared to LPS alone ($p < 0.001$). After LPS, addition of NAC to the fluid did not result in better hemodynamic parameters compared to fluid resuscitation alone. The infusion of NAC led to a decrease in MAP in the absence of LPS (57.3 ± 5.6 mmHg versus 76.8 ± 9.3 in the control group, $p < 0.001$).

Renal microvascular oxygenation

The percentage variation in $C_{\mu PO_2}$, $M_{\mu PO_2}$, DO_{2ren} , and VO_{2ren} between baseline (T_0) and the end of experiment (T_3) are shown in Figure 2. Compared to controls, LPS infusion induced a significant decrease of $C_{\mu PO_2}$ (40.6 ± 8.8 mmHg vs. 68.2 ± 4.1 mmHg in the control group at T_3 , $p < 0.001$) and $M_{\mu PO_2}$ (32.2 ± 7.9 mmHg vs. 51.6 ± 3.2 mmHg in the control group, $p < 0.001$). Fluid resuscitation with HES-RA alone did not improve $C_{\mu PO_2}$ nor $M_{\mu PO_2}$. HES-RA combined with NAC significantly improved $C_{\mu PO_2}$ during sepsis ($p < 0.01$). LPS induced a significant decrease of DO_{2ren} and VO_{2ren} (respectively 8.3 ± 6.1 ml O_2 /min in the LPS group versus 67.2 ± 23.2 ml O_2 /min in the control group at T_3 and 7.8 ± 6.5 ml O_2 /min in the LPS group versus 32.9 ± 10 ml O_2 /min in the control group at T_3 , $p < 0.05$). Fluid resuscitation with or without NAC significantly improved VO_{2ren} compared to LPS group ($p < 0.05$). Of note, the addition of NAC to the control group also increased VO_{2ren} compared to the control group alone ($p < 0.05$). Hematocrit values are reported in Table 3. A significant decrease in hematocrit occurred after fluid resuscitation in both groups compared to control and LPS groups ($p < 0.001$). The magnitude of hemodilution in both groups was in the same range.

Table 1. Evolution of systemic and renal hemodynamics parameters during the experiment.

	T ₀ (baseline)		T ₁ (shock)		T ₂ (30 min)		T ₃ (120 min)	
MAP (mmHg)								
Time control	102	± 9.0	86.3	± 13.4	80.1	± 8.8	76.8	± 9.3
Control+NAC	87.7	± 7.6	75.3	± 10.5	70.5	± 8.0	57.3	± 5.6 ^{***}
LPS	101	± 11.1	56.8	± 10.5 ^{***}	53.7	± 9.4 ^{***}	45.8	± 7.9 ^{***}
LPS+HES-RA	92.1	± 8.7	55.6	± 9.5 ^{***}	65.5	± 4.9 ⁺	51.6	± 3.7 ^{***}
LPS+HES-RA+NAC	98.8	± 8.7	49.8	± 8.5 ^{***}	64.1	± 4.7 ^{***}	52.6	± 6.1 ^{***}
RBF (mL/min)								
Time control	5.4	± 0.6	4.8	± 0.8	5.3	± 0.9	4.5	± 1.5
Control+NAC	5.7	± 0.7	4.3	± 0.9	4.8	± 1.5	4	± 1.1
LPS	5.7	± 1.4	1.3	± 0.7 ^{***}	1.4	± 0.5 ^{***}	0.7	± 0.6 ^{***}
LPS+HES-RA	6.6	± 0.3	1.9	± 1.5 ^{***}	5.6	± 1.8 ^{***}	5.0	± 0.4 ^{***}
LPS+HES-RA+NAC	5.5	± 0.4	1	± 0.4 ^{***}	3.5	± 0.9 ⁺⁺	4.8	± 2.2 ^{***}
RVR (dyn.s.sec ⁻⁵)								
Time control	1910.2	± 260.5	1793.7	± 227.4	1524.3	± 188.2	1861.3	± 751.2
Control+NAC	1548.6	± 249.2	1782.6	± 368.6	1606.7	± 583.2	1521.9	± 511.1
LPS	1774.8	± 302.4	5911.5	± 3333.4 ^{***}	4182.9	± 829.7 ^{***}	10372	± 5182.2 ^{***}
LPS+HES-RA	1410	± 152.2	3293.2	± 1978.9 ⁺	1130.2	± 348.1 ⁺⁺	1004.3	± 48.3 ^{***}
LPS+HES-RA+NAC	1787.2	± 236	5795.8	± 2517.4 ^{***}	1909.8	± 375.7	1199.1	± 318.3 ^{***}

Values are presented as Mean ± SD, *p<0.05, **p<0.01 and ***p<0.001 vs. Control group; +p<0.05, ++p<0.01 and +++p<0.001 vs. LPS group.

Abbreviations: MAP; mean arterial pressure, RBF; renal blood flow; RVR; renal vascular resistance, LPS; lipopolysaccharide, HES-RA; Hydroxyethyl starch-ringer acetate; NAC; N-acetyl cysteine.

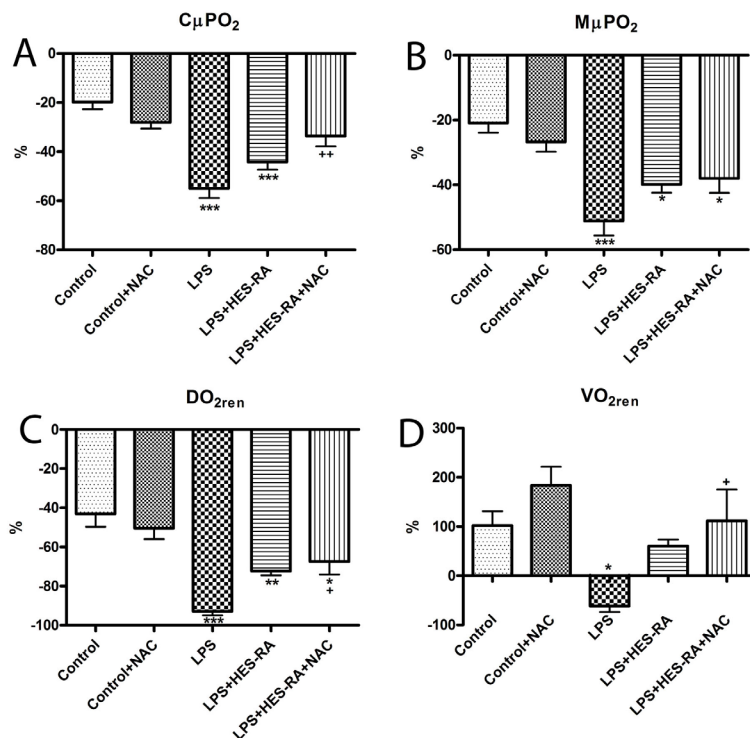


Figure 2. Percentage change of renal microvascular oxygen tension, oxygen delivery and consumption from baseline to T_3 in the renal cortex ($C_{\mu}PO_2$) (Panel A), in the medulla ($M_{\mu}PO_2$) (Panel B), renal oxygen delivery (DO_{2ren}) (Panel C), and renal oxygen consumption (VO_{2ren}) (Panel D). Values are presented as Mean \pm SD, * $p < 0.05$, ** $p < 0.01$, *** $p < 0.001$ vs. Control group; + $p < 0.05$ LPS vs. LPS group.

Kidney function and biomarkers of kidney injury

The evolution of TNa^+ , VO_{2ren}/TNa^+ , Cl_{Creat} and $EFNa^+$ at different time points are presented in Table 2. TNa^+ level was lower in LPS, LPS+HES-RA and LPS+HES+RA+NAC ($p < 0.001$) than the control at T_1 , T_2 , and T_3 . Fluid resuscitation did not restore these values. The addition of NAC decreased also the TNa^+ in the control+NAC group compared to control ($p < 0.01$). VO_{2ren}/TNa^+ increased in LPS groups receiving HES-RA and HES+RA+NAC at T_3 compared to the Control ($p < 0.05$ and $p < 0.001$, respectively) and LPS ($p < 0.05$ and $p < 0.001$ respectively). Compared to the Control and LPS, $EFNa^+$ values were increased in LPS group treated with the HES-RA with and without NAC at T_2 and T_3 . NAC administration in the control group tended to decrease TNa^+ and $EFNa^+$ values without reaching a significant level. Fluid resuscitation improved urine output irrespective of the addition of NAC compared to the LPS group ($p < 0.001$). No effect of NAC was noted on urine output in the control+NAC group compared to control, but a significant decrease in Cl_{creat} was observed ($p < 0.001$).

Table 2. Parameters of renal function and excretion at different time points of the experiment.

	T0 (baseline)		T1 (shock)		T2 (30 min)		T3 (120 min)	
TNa⁺ (mmol/min⁻¹)								
Time control	15.3	± 9.6	14.1	± 7.0	18.8	± 6.8	19.7	± 4.7
Control+NAC	15.0	± 6.4	13.2	± 6.5	15.9	± 6.5	9.5	± 4.3 ^{**}
LPS	12.3	± 5.5	0.00	± 0.00 ^{***}	0.00	± 0.00 ^{***}	0.00	± 0.00 ^{***}
LPS+HES-RA	12.0	± 8.3	0.00	± 0.00 ^{***}	5.0	± 1.12 ^{***}	2.2	± 1.3 ^{***}
LPS+HES-RA+NAC	11.9	± 5.7	0.00	± 0.00 ^{***}	2.8	± 2.8 ^{***}	2.2	± 1.8 ^{***}
VO_{2ren}/TNa⁺								
Time control	1.77	± 1.6	2.19	± 1.3	1.59	± 0.6	1.79	± 0.7
Control+NAC	1.36	± 0.4	2.19	± 0.9	1.95	± 1.18	6.32	± 3.9
LPS	2.5	± 1.2	0.00	± 0.00	0.00	± 0.00	0.00	± 0.00
LPS+HES-RA	2.24	± 1.1	0.00	± 0.00	6.06	± 1.7	17.17	± 7.1 ⁺
LPS+HES-RA+NAC	1.97	± 1.3	0.00	± 0.0 [*]	23.36	± 22.2	28.53	± 28 ^{***++}
Cl_{creat} (mL/min.)								
Time control	0.11	± 0.6	0.10	± 0.04	0.14	± 0.04	0.14	± 0.03
Control+NAC	0.11	± 0.04	0.09	± 0.04	0.11	± 0.04	0.06	± 0.03 ^{***}
LPS	0.09	± 0.04	0.00	± 0.00 ^{***}	0.00	± 0.00 ^{***}	0.00	± 0.00 ^{***}
LPS+HES-RA	0.09	± 0.06	0.00	± 0.00 ^{***}	0.05	± 0.01 ^{***}	0.02	± 0.01 ^{***}
LPS+HES-RA+NAC	0.09	± 0.04	0.00	± 0.00 ^{***}	0.04	± 0.01 ^{***}	0.02	± 0.01 ^{***}
EFNa⁺								
Time control	4.8	± 4.7	13.2	± 5.7	11.9	± 4.9	10.4	± 2.4
Control+NAC	2.3	± 0.8	3.22	± 1.7	2.9	± 1.7	6.9	± 6.6
LPS	3.7	± 1.4	0.00	± 0.00	0.00	± 0.00	0.00	± 0.00
LPS+HES-RA	3.5	± 2.8	0.00	± 0.00	35.3	± 7.3 ^{***++}	17.1	± 8.1
LPS+HES-RA+NAC	4.4	± 3.9	0.00	± 0.00	45.8	± 36.7 ^{***++}	31.4	± 28.4 ^{***++}
Urine volume (mL)								
Time control	0.39	± 0.14	0.53	± 0.13	0.45	± 0.13	0.19	± 0.03
Control+NAC	0.25	± 0.09	0.34	± 0.17	0.2	± 0.04	0.16	± 0.06
LPS	0.31	± 0.13	0.06	± 0.09 ^{***}	0.04	± 0.05 ^{***}	0.02	± 0.05 ^{***}
LPS+HES-RA	0.37	± 0.3	0.12	± 0.19 ^{**}	0.6	± 0.23 ^{***}	0.16	± 0.08 ^{***}
LPS+HES-RA+NAC	0.33	± 0.26	0.04	± 0.09 ^{***}	0.65	± 0.47 ^{***}	0.2	± 0.13 ^{***}

Values are presented as Mean ± SD, *p<0.05, **p<0.01 and ***p<0.001 vs. Control group; +p<0.05 and +++p<0.001 vs. LPS group. Abbreviations: TNa⁺; tubular sodium reabsorption, EFNa⁺; excretion fraction of Na⁺, Cl_{creat}; clearance of creatinine, VO_{2ren}/TNa⁺; renal energy efficiency for sodium transport, LPS; lipopolysaccharide, HES-RA; Hydroxyethyl starch-ringer acetate, NAC; N-acetyl cysteine.

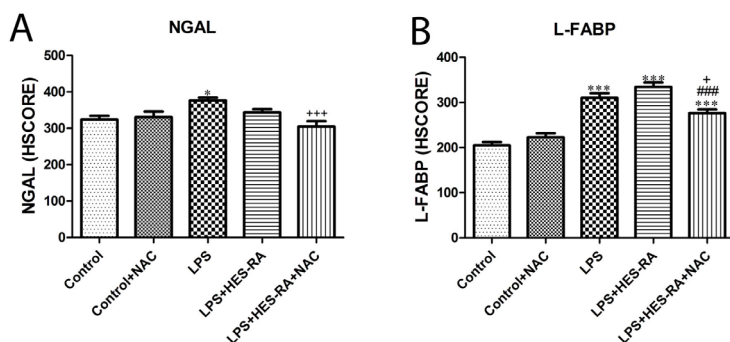


Figure 3. Immunostaining intensity (HSCORE) of NGAL (Panel A) and L-FABP (Panel B) in kidney cortex of all groups. Values are presented as Mean \pm SD, * p <0.05, *** p <0.001 vs. Control group; + p <0.05, *** p <0.001 vs. LPS group, *** p <0.001 vs. LPS+HES-RA group.

Biomarkers of AKI (NGAL and L-FABP) increased significantly in the kidney after LPS infusion (respectively p <0.05 and p <0.001 versus control group) (Figure 3). The resuscitation fluid combined with NAC significantly decreased these biomarkers compared to LPS group (p <0.001 and <0.05 respectively). Moreover, L-FABP was lower in the group of septic rats resuscitated with HES-RA+NAC than with HES-RA alone (p <0.001).

Plasma electrolytes and acid-base status

Bicarbonate and plasma lactate levels, pH, base excess and anion gap with K^+ are shown in Table 3. LPS infusion significantly increased the plasma lactate level and anion gap and could not be corrected by administration of either HES-RA with or without NAC (p <0.001) compared to control group. Base excess, pH, bicarbonate levels similarly decreased after LPS infusion and were partially corrected by fluid resuscitation. NAC infusion alone in the control group resulted in a significant decrease in pH, base excess and bicarbonate levels compared to control group (p <0.01). NAC administration worsened the acid-base status in LPS resuscitated and control groups. The level of bicarbonate and base excess was significantly lower in rats resuscitated with fluid plus NAC than fluid alone (p <0.01).

Oxidative stress and inflammatory cytokines

The levels of biomarkers of oxidative stress, pro-inflammatory cytokines and products of degradation of glycocalyx are represented in Figure 4. Levels of TNF- α (3A) and IL-6 (3B) in kidney homogenates were significantly increased, 528.1 ± 143.9 pg/mg protein in LPS group versus 291.8 ± 99.1 pg/mg protein in control group (p <0.05), and 1246 ± 441 pg/mg protein in LPS group versus 753.8 ± 122 pg/mg protein in control group, (p <0.05).

Table 3. Time-course of acid-base status, lactate levels and hematocrit resuscitated with and without the addition of NAC.

	T0 (baseline)	T1 (shock)	T2 (30 min)	T3 (120 min)
pH				
Time control	7.37 ± 0.03	7.39 ± 0.06	7.42 ± 0.03	7.42 ± 0.04
Control+NAC	7.48 ± 0.12	7.42 ± 0.03	7.38 ± 0.02	7.32 ± 0.05[*]
LPS	7.36 ± 0.03	7.27 ± 0.06^{**}	7.26 ± 0.07^{***}	7.2 ± 0.07^{***}
LPS+HES-RA	7.36 ± 0.03	7.26 ± 0.07^{***}	7.31 ± 0.07[*]	7.27 ± 0.05^{***}
LPS+HES-RA+NAC	7.37 ± 0.04	7.26 ± 0.09^{***}	7.27 ± 0.08^{***}	7.20 ± 0.03^{***}
HCO₃⁻ (mmol/L)				
Time control	20.6 ± 0.9	21 ± 0.6	21.2 ± 1.3	21.6 ± 1.3
Control+NAC	18.8 ± 0.6	18.4 ± 1.5[*]	19.3 ± 1.2	14.2 ± 3.8^{***}
LPS	20.2 ± 0.7	15 ± 0.9^{***}	15.3 ± 1.2^{***}	12.8 ± 0.5^{***}
LPS+HES-RA	21.6 ± 0.7	14.8 ± 1.5^{***}	18.1 ± 0.9^{***+}	16.7 ± 1.6^{***++}
LPS+HES-RA+NAC	20.7 ± 0.8	14.7 ± 2.5^{***}	16.6 ± 1.6^{***}	14 ± 1.7^{***##}
Base excess (mmol/L)				
Time control	-3.5 ± 1.2	-2.7 ± 1.6	-1.7 ± 1.3	-1.8 ± 1.5
Control+NAC	-3.5 ± 0.5	-4.4 ± 1.7	-4.5 ± 1.3	-8.9 ± 2.4^{***}
LPS	-4 ± 1.3	-10.8 ± 1.9^{***}	-10.5 ± 1.7^{***}	-14.1 ± 1.3^{***}
LPS+HES-RA	-2.9 ± 1.1	-11.3 ± 2.7^{***}	-7 ± 2^{***+}	-8.9 ± 1.9^{***++}
LPS+HES-RA+NAC	-3.4 ± 1.5	-11.2 ± 4.1^{***}	-9.1 ± 2.8^{***}	-12.5 ± 1.7^{***##}
Anion Gap K⁺ (mmol/L)				
Time control	17.7 ± 0.8	18.0 ± 0.7	16.4 ± 0.5	16.8 ± 1.3
Control+NAC	18.9 ± 2.0	18.5 ± 2.0	17.0 ± 1.2	18.9 ± 4.8
LPS	18.9 ± 2.3	21.8 ± 1.1	21.6 ± 1.8	23.2 ± 1.6^{***}
LPS+HES-RA	17.5 ± 1.3	22.7 ± 1.3	19.2 ± 1.0	20.9 ± 2.5^{***}
LPS+HES-RA+NAC	18.4 ± 1.0	22.5 ± 2.5^{**}	20.6 ± 2.3[*]	23.1 ± 1.9^{***}
Lactate (mmol/L)				
Time control	2.32 ± 0.52	2.22 ± 0.34	2.08 ± 0.31	1.73 ± 0.27
Control+NAC	3.10 ± 0.64	2.92 ± 0.76	2.17 ± 0.36	2.10 ± 0.33
LPS	2.42 ± 0.32	3.08 ± 0.28	3.08 ± 0.5	4.32 ± 0.6^{***}
LPS+HES-RA	1.92 ± 0.2	3.32 ± 0.55	2.75 ± 0.48	5.08 ± 1.83^{***}
LPS+HES-RA+NAC	2.70 ± 0.21	3.83 ± 1.36^{**}	3.30 ± 1.17[*]	4.98 ± 1.21^{***}
Hct (%)				
Time control	49.6 ± 1.3	41.6 ± 1.9	39 ± 2.9	33.3 ± 3
Control+NAC	48.8 ± 2.6	42.8 ± 4.4	41.1 ± 4.2	33.8 ± 2.6
LPS	49.3 ± 4.0	39.6 ± 3.0	35.1 ± 2.9	34.0 ± 3.5
LPS+HES-RA	49.3 ± 1.7	43.3 ± 2.5	30.1 ± 4.5^{***+}	17.5 ± 3^{***++}
LPS+HES-RA+NAC	48.6 ± 0.8	44.1 ± 3.2⁺	33.0 ± 2.6^{**}	18.0 ± 2.0^{***++}

Values are presented as Mean ± SD, *p<0.05, **p<0.01 and ***p<0.001 vs. Control group; ** p<0.05, ***p<0.001 vs. LPS group; ##p<0.01 vs. LPS+HES-RA group. Abbreviations: LPS; lipopolysaccharide, HES-RA; Hydroxyethyl starch-ringer acetate, NAC; N-acetyl cysteine, HCO₃⁻; bicarbonate, Hct; hematocrit.

respectively. Same results were observed regarding hyaluronic acid (HA) (3C), nitric oxide (3D) and MDA (3E) after LPS infusion ($p < 0.05$). The addition of NAC to HES-RA during fluid resuscitation resulted in a significant lower level of HA and nitric oxide only compared to LPS group ($p < 0.01$). Infusion of HES-RA alone decreased the level of MDA compared to LPS ($p < 0.01$) (3E). Protein carbonyl levels were not altered (3E).

DISCUSSION AND CONCLUSION

In the present study, we found that fluid supplemented with NAC improved cortical renal oxygenation, oxygen delivery, and oxygen consumption compared to the LPS group. Fluid resuscitation alone was partially effective in correcting kidney hypoxia but did not reach a significant level compared to the LPS group. The addition of NAC to the resuscitation fluid did not further improve systemic or renal hemodynamics compared to HES-RA alone. It has been suggested that a specific effect of NAC on microvascular oxygenation exists independent of renal macrovascular perfusion. In an experimental study, Heyman *et al.* showed that NAC induced vasodilation in a precontracted renal microvasculature rat model (18). The vasculature may be similarly constricted after LPS infusion leading to microcirculation heterogeneity (25). Although creatinine levels did not differ between septic rats receiving fluids either with or without NAC, the fluid resuscitation combined with NAC decreased the levels of renal NO, hyaluronic acid, and early markers of acute kidney injury such as NGAL or L-FABP. Previous studies demonstrated a significant decrease in inflammatory biomarkers in specific organs such as the lungs and kidneys in models of sepsis (14–16, 26–29). However, none of these studies reported the beneficial effects of NAC on tissue oxygenation during sepsis by decreasing oxidative stress and inflammation.

Several studies using microcirculatory techniques have now questioned the significance of arterial RBF and have focused on the renal microcirculation as the hemodynamic culprit in the pathophysiology of septic AKI (6,25,30). Microcirculatory dysfunction may contribute to renal hypoxia even in the absence of overt renal hypoperfusion. The microcirculation of the renal cortex has been shown to be severely injured in animal models of sepsis. After LPS infusion in rats, Legrand *et al.* showed that fluid resuscitation could not fully restore renal microcirculatory dysfunction (6). In dogs, endotoxemia was found to be associated with renal hypoperfusion and hypoxia in the renal cortex but was concomitant with increased renal venous PO_2 , supporting the concept that convective shunting of oxygen may contribute to the development of tissue hypoxia (31). In our study, the LPS-induced renal microvascular heterogeneity and hypoxia appeared to be corrected with the NAC-supplemented fluid.

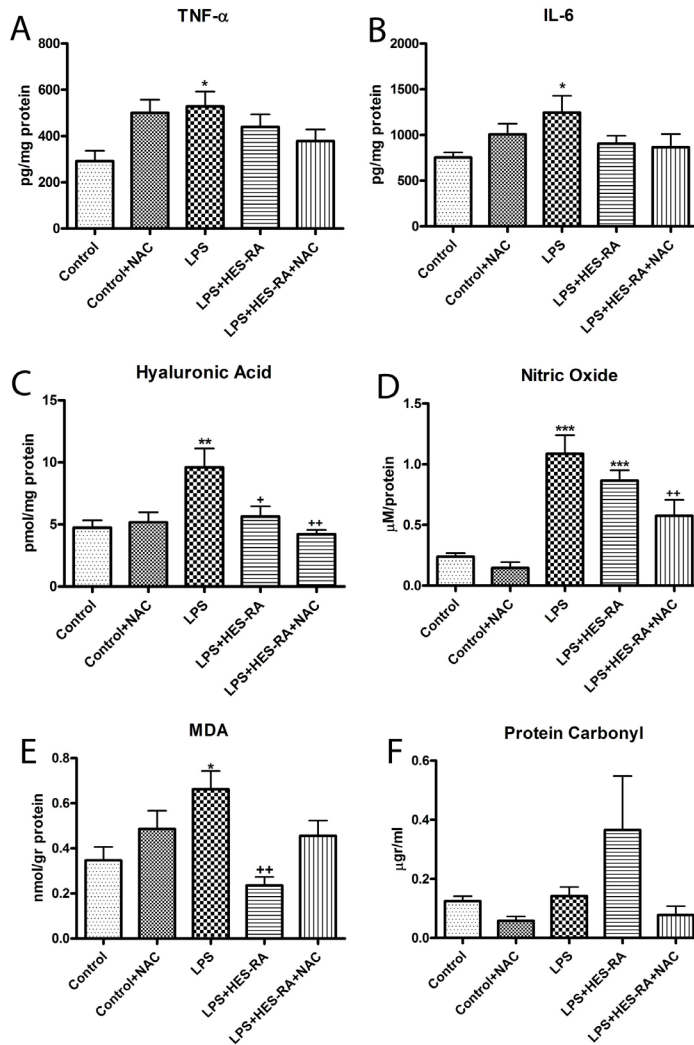


Figure 4. Levels of biomarkers of oxidative stress and pro-inflammatory cytokines in renal tissue. Renal tissue TNF- α (Panel A), IL-6 (Panel B), hyaluronic acid (Panel C), nitric oxide (Panel D), MDA (Panel E) and protein carbonyl (Panel F). Values are presented as Mean \pm SD, * $p < 0.05$, ** $p < 0.01$, *** $p < 0.001$ vs. Control group; + $p < 0.05$, ** $p < 0.01$ vs. LPS group

We also observed negative effects of NAC infusion. Delayed hypotension occurred in the control + NAC group, highlighting the vasodilatory effects of this compound as previously described (12,32). The mechanism involved in this lowering effect might be mediated by the interaction of sulfhydryl groups with enzymes such as the guanylate cyclase, which is the primary receptor for NO (32). This drop in the MAP may contribute to tissue

hypoperfusion and hypoxia as well as the lower pH observed in the control + NAC group compared to the control group. However, no significant change was observed in renal blood flow measured in the renal artery. Conflicting data exist between experimental and human clinical studies regarding the effects of NAC on regional blood flow and cardiac output (19,33–37). First, NAC administration was shown to improve survival in experimental models of peritonitis-induced sepsis (38,39). In mongrel dogs subjected to endotoxemia, Zhang *et al.* demonstrated the myocardial protective effects of NAC pretreatment (150 mg/kg) with enhanced oxygen delivery but lower systemic and pulmonary pressures (37). In contrast, in a study involving 20 patients with septic shock, NAC infusion (150 mg/kg for 15 min followed by continuous infusion) that was initiated within 24 h after the onset of septic shock resulted in a decrease in left ventricular stroke work revealing myocardial depression without a significant impact on MAP at 48 h after treatment initiation (33). In a similar population, Rank *et al.* demonstrated the exact opposite effect with an improvement in liver blood flow, oxygen delivery, and oxygen consumption related to an increase in cardiac index (34). However, the infusion of NAC lasted less than 2 h in this latter study. Agusti *et al.* reported an increase in the cardiac index associated with vasodilatation but without improvements in splanchnic microcirculation after NAC infusion in patients presenting with septic shock and multiple organ failure (35). Clinical studies yielded controversial results with the use of NAC in sepsis (11). NAC treatment during the first hours of sepsis or septic shock may decrease peroxidative stress (40), improve hepatic function (34), and enhance tissue oxygenation and cardiac function (41), whereas delayed administration adversely affected the outcomes of critically ill patients with multiple organ failure (33,42).

Most published studies have examined the effects of NAC when given as a pretreatment, e.g., before the insult. Here, we evaluated the ability of NAC when administered during the resuscitation process to correct tissue hypoxia and inflammation already present. It seems that the beneficial effects on tissue oxygenation, if any, are not similar if NAC is administered before or after the insult. The effects also depend on the time elapsed since the insult. We showed that NAC-supplemented fluid did not provide additional benefits on the acid status and renal function compared to fluid alone. Only kidney oxygenation was significantly higher in the group receiving fluid supplemented with NAC compared to the LPS alone group, whereas fluid alone did not reach a level of significance. Pretreatment with NAC appeared to be more efficient than post-injury treatment in protecting tissues against oxidative stress and inflammation in models of sepsis and ischemia/reperfusion injury. Due to the mechanisms of action of NAC, it is conceivable that it would be easier to prevent certain pathways from being activated rather than to modulate already highly activated signals with redundant or alternative pathways.

The effects of NAC on renal oxygenation could be mediated by different mechanisms. First, tissue NO levels were significantly increased after LPS infusion. By decreasing NO levels in the cortex, NAC combined with fluid administration may improve microvascular dysfunction, microvascular delivery of oxygen, and cortical oxygenation. Similarly, our group previously demonstrated that the prostaglandin analog iloprost restored kidney function in a rat model of endotoxemia and prevented the occurrence of hypoxic regions (43). The improvement of renal microvascular oxygenation was mediated in part by the inhibition of inducible nitric oxide synthase expression in the kidney. Another major player involved in endothelial dysfunction in sepsis-induced AKI is the widespread damage to the endothelial glycocalyx, which may contribute to microvascular dysfunction via impaired flow-dependent vasodilatation. Hyaluronic acid levels reflect the disruption of the glycocalyx (44). In the present study, hyaluronic acid levels were significantly increased after LPS infusion. Fluid resuscitation either with or without the addition of NAC significantly dampened these levels. However, the decrease was more prevalent with NAC treatments, but all of the significant benefits were due to the fluids as opposed to NAC. NAC may still further improve microvascular oxygenation by decreasing endothelial glycocalyx damage in addition to fluid resuscitation. In contrast, a clinical study monitored volume loading with HES during elective surgery (20 ml/kg) and observed increased serum glycocalyx biomarkers with HES alone (45). In our study, fluid resuscitation with HES seemed to be beneficial with regard to these biomarkers levels. One of the main pathways of glycocalyx disruption is thought to be the formation of ROS such as peroxynitrite. As NAC is a well-known scavenger of ROS, we measured the tissue levels of malondialdehyde as a marker of lipid peroxidation. We did not observe a significant decrease when using NAC-supplemented fluid compared to fluid alone. This result can be explained because of the high dose of NAC in our study. Some authors have previously suggested that high doses of NAC may increase MDA levels, whereas lower doses may decrease MDA levels (46). Additionally, a lack of effect of NAC on lipid peroxidation in cases of established endotoxemia has been shown (47).

Limitations

In the light of the ongoing debate about the deleterious effects of HES on the kidney, a possible limitation of our study is our use of HES as a resuscitation fluid. However, the present study is a mechanistic study wherein we investigated whether we could ameliorate the inflammatory effects of fluid administration in a sepsis model. In our experience, all fluids cause inflammation (48), and it is the fluid volume that determined the extent of injury. It could be argued that we should have chosen a balanced crystalloid solution instead of a colloid-based solution. However, crystalloid solutions have issues as well. For example, Ringer's lactate causes even more inflammation than HES (49,50), and we would also have had to administer a larger volume to maintain blood pressure causing

more hemodilution. We chose a colloid solution to keep the amount of fluid required to correct blood pressure to a minimum. We could have used albumin, but even albumin can promote renal failure, as has been shown in a recent study in cardiac surgery (51). In conclusion, arguably, all fluids have deleterious effects on the kidney to a greater or lesser extent. However, in this proof of concept study, we hope to have introduced the idea that controlling the inflammatory component imposed by fluids such as HES can be implemented by co-administration of an anti-inflammatory drug such as NAC. Our results suggest that such an approach could be used for other fluids, but this approach would require testing in subsequent studies.

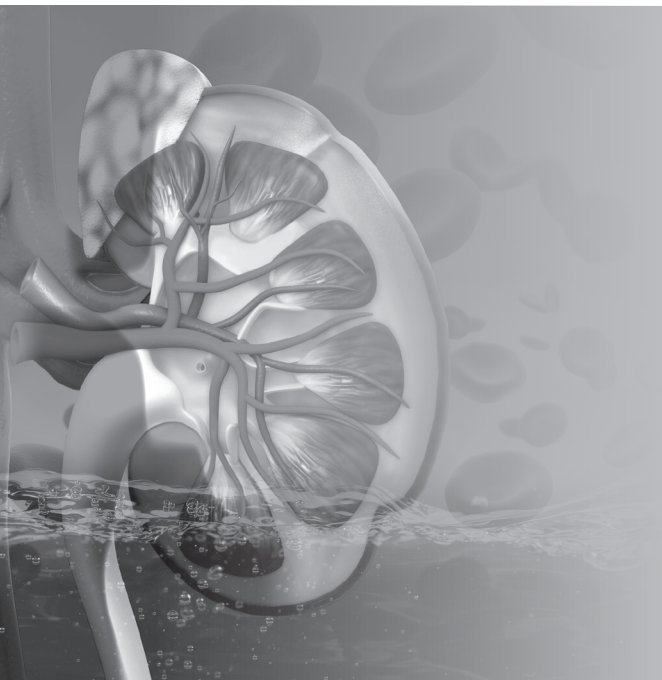
In conclusion, the addition of NAC to fluid resuscitation may improve renal oxygenation and attenuate microvascular dysfunction and AKI. Decreases of renal NO levels and hyaluronic acid levels may be involved in this beneficial effect. A therapeutic strategy combining the macrovascular effects of fluids and the microvascular effects of NAC may be critical to preventing sepsis-induced AKI. This study sets forth a new concept for changing the procedure of fluid resuscitation by the addition of antioxidant therapy during the initial phase of resuscitation.

REFERENCES

1. Angus DC, van der Poll T. Severe sepsis and septic shock. *N. Engl. J. Med.* 369:840–851, 2013.
2. Ait-Oufella H, Maury E, Lehoux S, *et al.* The endothelium: physiological functions and role in microcirculatory failure during severe sepsis. *Intensive Care Med.* 36:1286–1298, 2010.
3. Ince C, Mayeux PR, Nguyen T, *et al.* The endothelium in sepsis. *Shock* 45:259–270, 2016.
4. Ince C. The microcirculation is the motor of sepsis. *Crit. Care* 9(Suppl 4):S13–9, 2005.
5. Legrand M, Mik EG, Johannes T *et al.* Renal hypoxia and dysoxia after reperfusion of the ischemic kidney. *Mol. Med.* 14:502–516, 2008.
6. Legrand M, Bezemer R, Kandil A, *et al.* The role of renal hypoperfusion in development of renal microcirculatory dysfunction in endotoxemic rats. *Intensive Care Med.* 37:1534–1542, 2011.
7. Oudemans-van Straaten HM, Spoelstra-de Man AM, de Waard MC. Vitamin C revisited. *Crit. Care* 18:460, 2014.
8. Galley HF, DiMatteo MA, Webster NR. Immunomodulation by anaesthetic, sedative and analgesic agents: does it matter? *Intensive Care Med.* 26:267–274, 2000.
9. Berger MM, Chioléro RL. Antioxidant supplementation in sepsis and systemic inflammatory response syndrome. *Crit. Care Med.* 35:S584–90, 2007.
10. Angstwurm MWA, Engelmann L, Zimmermann T, *et al.* Selenium in intensive care (SIC): results of a prospective randomized, placebo-controlled, multiple-center study in patients with severe systemic inflammatory response syndrome, sepsis, and septic shock. *Crit. Care Med.* 35:118–126, 2007.
11. Szakmany T, Hauser B, Radermacher P. N-acetylcysteine for sepsis and systemic inflammatory response in adults. *Cochrane Database Syst. Rev.* 9:CD006616, 2012.
12. Zafarullah M, Li WQ, Sylvester J, *et al.* Molecular mechanisms of N-acetylcysteine actions. *Cell Mol Life Sci.* 60:6–20, 2003.
13. Sehirli AO, Sener G, Satioglu H, *et al.* Protective effect of N-acetylcysteine on renal ischemia/reperfusion injury in the rat. *J. Nephrol.* 16:75–80, 2003.
14. Ozdulger A, Cinel I, Koksel O, *et al.* The protective effect of N-acetylcysteine on apoptotic lung injury in cecal ligation and puncture-induced sepsis model. *Shock* 19:366–372, 2003.
15. Hsu B-G, Lee R-P, Yang F-L, *et al.* Post-treatment with N-acetylcysteine ameliorates endotoxin shock-induced organ damage in conscious rats. *Life Sci.* 79:2010–2016, 2006.
16. Carbonell LF, Díaz J, Hernández I, *et al.* N-acetylcysteine exerts protective effects and prevents lung redox imbalance and peroxynitrite generation in endotoxemic rats. *Med. Chem.* 3:29–34, 2007.
17. Huet O, Cherreau C, Nicco C, *et al.* Pivotal role of glutathione depletion in plasma-induced endothelial oxidative stress during sepsis. *Crit. Care Med.* 36:2328–2334, 2008.
18. Heyman SN, Goldfarb M, Shina A, *et al.* N-acetylcysteine ameliorates renal microcirculation: studies in rats. *Kidney Int.* 63:634–641, 2003.
19. Schaller G, Pleiner J, Mittermayer F, *et al.* Effects of N-acetylcysteine against systemic and renal hemodynamic effects of endotoxin in healthy humans. *Crit. Care Med.* 35:1869–1875, 2007.
20. Eltzschig HK, Carmeliet P. (2011) Hypoxia and inflammation. *N. Engl. J. Med.* 364:656–665, 2011.
21. Bartels K, Grenz A, Eltzschig HK. Hypoxia and inflammation are two sides of the same coin. *Proc. Natl. Acad. Sci. U S A* 110:18351–18352, 2013.
22. Haase VH. (2015) Inflammation and hypoxia in the kidney: friends or foes? *Kidney Int.* 88:213–215, 2015.
23. Johannes T, Mik EG, Ince C. Dual-wavelength phosphorimetry for determination of cortical and subcortical microvascular oxygenation in rat kidney. *J. Appl. Physiol.* 100:1301–1310, 2006.
24. Mik EG, Johannes T, Ince C. Monitoring of renal venous PO₂ and kidney oxygen consumption in rats by a nearinfrared phosphorescence lifetime technique. *Am. J. Physiol. Renal Physiol.* 294:F676–81, 2008.
25. Ergin B, Kapucu A, Demirci-Tansel C, *et al.* The renal microcirculation in sepsis. *Nephrol. Dial. Transplant.* 30: 169–177, 2015.

26. Hsu B-G, Yang F-L, Lee R-P, *et al.* N-acetylcysteine ameliorates lipopolysaccharide-induced organ damage in conscious rats. *J. Biomed. Sci.* 11:152–162, 2004.
27. Andrades M, Ritter C, de Oliveira MR, *et al.* Antioxidant treatment reverses organ failure in rat model of sepsis: role of antioxidant enzymes imbalance, neutrophil infiltration, and oxidative stress. *J. Surg. Res.* 167:e307–13, 2011.
28. Campos R, Shimizu MHM, Volpini RA, *et al.* N-acetylcysteine prevents pulmonary edema and acute kidney injury in rats with sepsis submitted to mechanical ventilation. *Am. J. Physiol. Lung Cell Mol. Physiol.* 302:L640–50, 2012.
29. Lee JH, Jo YH, Kim K, *et al.* Effect of N-acetylcysteine (NAC) on acute lung injury and acute kidney injury in hemorrhagic shock. *Resuscitation* 84:121–127, 2013.
30. Zafrani L, Payen D, Azoulay E, *et al.* The microcirculation of the septic kidney. *Semin. Nephrol.* 35:75–84, 2015.
31. Gullichsen E, Nelimarkka O, Halkola L, *et al.* Renal oxygenation in endotoxin shock in dogs. *Crit. Care Med.* 17:547–550, 1989.
32. Girouard H, Chulak C, Wu L, *et al.* N-acetylcysteine improves nitric oxide and alphaadrenergic pathways in mesenteric beds of spontaneously hypertensive rats. *Am. J. Hypertens.* 16:577–584, 2003.
33. Peake SL, Moran JL, Leppard PI. N-acetyl-L-cysteine depresses cardiac performance in patients with septic shock. *Crit. Care Med.* 24:1302–1310, 1996.
34. Rank N, Michel C, Haertel C, *et al.* N-acetylcysteine increases liver blood flow and improves liver function in septic shock patients: results of a prospective, randomized, double-blind study. *Crit. Care Med.* 28:3799–3807, 2000.
35. Agustí AGN, Togores B, Ibañez J, *et al.* Effects of N-acetylcysteine on tissue oxygenation in patients with multiple organ failure and evidence of tissue hypoxia. *Eur. Respir. J.* 10:1962–1966, 1997.
36. Zhang H, Spapen H, Nguyen DN, *et al.* Effects of N-acetyl-L-cysteine on regional blood flow during endotoxic shock. *Eur. Surg. Res.* 27:292–300, 1995.
37. Zhang H, Spapen H, Nguyen DN, *et al.* Protective effects of N-acetyl-L-cysteine in endotoxemia. *Am. J. Physiol.* 266:H1746–54, 1994.
38. Ritter C, Andrades ME, Reinke A, *et al.* Treatment with N-acetylcysteine plus deferoxamine protects rats against oxidative stress and improves survival in sepsis. *Crit. Care Med.* 32:342–349, 2004.
39. de Mello RO, Lunardelli A, Caberlon E, *et al.* Effect of N-acetylcysteine and fructose-1,6-bisphosphate in the treatment of experimental sepsis. *Inflammation* 34:539–550, 2011.
40. Ortolani O, Conti A, De Gaudio AR, *et al.* The effect of glutathione and Nacetylcysteine on lipoperoxidative damage in patients with early septic shock. *Am. J. Respir. Crit. Care Med.* 161:1907–1911, 2000.
41. Spies CD, Reinhart K, Witt I, *et al.* Influence of N-acetylcysteine on indirect indicators of tissue oxygenation in septic shock patients: results from a prospective, randomized, double-blind study. *Crit. Care Med.* 22:1738–1746, 1994.
42. Molnár Z, Shearer E, Lowe D. N-Acetylcysteine treatment to prevent the progression of multisystem organ failure: a prospective, randomized, placebo-controlled study. *Crit. Care Med.* 27:1100–1104, 1999.
43. Johannes T, Ince C, Klingel K, *et al.* Iloprost preserves renal oxygenation and restores kidney function in endotoxemia-related acute renal failure in the rat. *Crit. Care Med.* 37:1423–1432, 2009.
44. Dane MJC, van den Berg BM, Lee DH, *et al.* A microscopic view on the renal endothelial glycocalyx. *Am. J. Physiol. Renal Physiol.* 308: F956–66, 2015.
45. Chappell D, Bruegger D, Potzel J, *et al.* Hypervolemia increases release of atrial natriuretic peptide and shedding of the endothelial glycocalyx. *Crit. Care* 18:538, 2014.
46. Fitri LE, Sardjono TW, Simamora D, *et al.* High dose of N-acetylcysteine increase H2O2 and MDA levels and decrease GSH level of HUVECs exposed with malaria serum. *Trop. Biomed.* 28:7–15, 2011.
47. Caglikulekci M, Dirlik M, Pata C, *et al.* Effect of N-acetylcysteine on blood and tissue lipid peroxidation in lipopolysaccharide-induced obstructive jaundice. *J. Invest. Surg.* 19:175–184, 2006.

48. Aksu U, Bezemer R, Yavuz B, *et al.* Balanced vs unbalanced crystalloid resuscitation in a near-fatal model of hemorrhagic shock and the effects on renal oxygenation, oxidative stress, and inflammation. *Resuscitation* 83:767–773, 2012.
49. Hussmann B, Lendemans S, de Groot H, *et al.* Volume replacement with Ringer-lactate is detrimental in severe hemorrhagic shock but protective in moderate hemorrhagic shock: studies in a rat model. *Crit. Care* 18:R5, 2014.
50. Rohrig R, Rönn T, Lendemans S, *et al.* Adverse effects of resuscitation with lactated ringer compared with ringer solution after severe hemorrhagic shock in rats. *Shock* 38:137– 145, 2012.
51. Frenette AJ, Bouchard J, Bernier P, *et al.* Albumin administration is associated with acute kidney injury in cardiac surgery: a propensity score analysis. *Crit. Care* 18:602, 2014.



CHAPTER 10

Blood transfusion improves renal oxygenation and renal outcome in sepsis induced acute kidney injury in rats

Adapted from *Crit. Care.* 2016 Dec 20;20(1):406

Lara Zafrani¹, Bulent Ergin¹, Aysegul Kapucu² and Can Ince¹

¹ Department of Translational Physiology, Academic Medical Center, Amsterdam, The Netherlands

² Department of Biology and Zoology Division, Faculty of Science, University of Istanbul, Istanbul, Turkey.

L. Zafrani and B. Ergin contributed equally to this study

ABSTRACT

The effects of blood transfusion on renal microcirculation during sepsis are unknown. This study aimed to investigate the effect of blood transfusion on renal microvascular oxygenation and renal function during sepsis-induced acute kidney injury. Twenty-seven *Wistar albino* rats were randomized into four groups: a sham group ($n = 6$), a lipopolysaccharide (LPS) group ($n = 7$), a LPS group that received fluid resuscitation ($n = 7$), and a LPS group that received blood transfusion ($n = 7$). The mean arterial blood pressure, renal blood flow, and renal microvascular oxygenation within the kidney cortex were recorded. Acute kidney injury was assessed using the serum creatinine levels, metabolic cost, and histopathological lesions. Nitrosative stress (expression of endothelial (eNOS) and inducible nitric oxide synthase (iNOS)) within the kidney was assessed by immunohistochemistry. Hemoglobin levels, pH, serum lactate levels, and liver enzymes were measured. Fluid resuscitation and blood transfusion both significantly improved the mean arterial pressure and renal blood flow after LPS infusion. Renal microvascular oxygenation, serum creatinine levels, and tubular damage significantly improved in the LPS group that received blood transfusion compared to the group that received fluids. Moreover, the renal expression of eNOS was markedly suppressed under endotoxin challenge. Blood transfusion, but not fluid resuscitation, was able to restore the renal expression of eNOS. However, there were no significant differences in lactic acidosis or liver function between the two groups. Blood transfusion significantly improved renal function in endotoxemic rats. The specific beneficial effect of blood transfusion on the kidney could have been mediated in part by the improvements in renal microvascular oxygenation and sepsis-induced endothelial dysfunction via the restoration of eNOS expression within the kidney.

Keywords: acute kidney injury, sepsis, microcirculation, blood transfusion, renal oxygenation, endothelial dysfunction

INTRODUCTION

Acute kidney injury (AKI) is a serious complication of sepsis in the intensive care setting that is associated with increases in the likelihood of death, prolonged hospital stays, and increased costs of care (1,2). The balance between renal microcirculatory oxygen delivery and cellular oxygen consumption is significantly disturbed during sepsis. Indeed, renal microvascular oxygenation is highly sensitive to endotoxemia, and renal hypoxia plays a crucial role in the pathogenesis of sepsis-induced AKI (3). Moreover, the negative effects of anemia in critically ill patients with AKI have been previously described, and a hemoglobin concentration below 9 g/dl upon intensive care unit admission has been found to be an independent risk factor for mortality (4). Previous studies that have measured renal microcirculatory oxygen pressure in experimental models of shock have consistently demonstrated that while fluid resuscitation (FR) is able to correct systemic hemodynamic variables it is unable to correct renal microcirculatory dysfunction (5,6). Based on this inability of fluids to improve oxygen delivery to the renal microcirculation, we hypothesized that the transfusion of oxygen-carrying red blood cells would improve sepsis-induced hypoxia. Two clinical studies have examined the ability of blood transfusion (BT) to correct the perfusion and oxygenation of the microcirculation in septic shock patients (7,8). These studies demonstrated that the microcirculation is globally unaltered by BT in septic patients; however, patients with altered capillary perfusion at baseline improve after BT (7). To date, no study has focused on the effect of BT on sepsis-induced AKI. The purpose of this study was to investigate the effect of BT on renal microvascular oxygenation and renal outcome (e.g., renal function and structural changes) during sepsis-induced AKI. We used an endotoxemic model to examine the questions: (1) whether BT can correct sepsis-induced renal microcirculatory hypoxemia; (2) whether BT is superior to FR in terms of restoring renal hypoxemia during sepsis; and (3) whether an improvement in renal hypoxemia translates into a better renal outcome. We compared the effects of FR involving a crystalloid solution and BT on renal hemodynamic parameters, renal oxygenation, renal function, renal damage, and nitrosative stress to investigate the extent to which improvements could be achieved by the administration of an oxygen-carrying resuscitation fluid.

MATERIAL AND METHODS

Animals

All experiments in this study were approved by the institutional Animal Experimentation Committee of the Academic Medical Center of the University of Amsterdam (DFL 103073). The experiments were performed on *Wistar albino* rats (Harlan Netherlands BV, Horst, The Netherlands) with a mean body weight of 325 ± 19 g.

Experimental protocol

All animals were anesthetized with an intraperitoneal injection of a mixture of 90 mg/kg ketamine (Nimatek[®], Eurovet, Bladel, The Netherlands), 0.5 mg/kg dexmedetomidine (Dexdomitor, Pfizer Animal Health BV, Capelle aan den IJssel, The Netherlands), and 0.05 mg/kg atropine-sulfate (Centrafarm Pharmaceuticals BV, Etten-Leur, The Netherlands). After performing a tracheotomy, the animals were mechanically ventilated with a fraction of inspired oxygen (FiO_2) of 0.4. Body temperature was maintained at 37 ± 0.5 °C during the entire experiment by an external thermal heating pad. Ventilator settings were adjusted to maintain arterial partial pressure of carbon dioxide (pCO_2) between 35 and 40 mmHg. For drug, fluid administration and hemodynamic monitoring, vessels were cannulated with polyethylene catheters with an outer diameter of 0.9 mm (Braun, Melsungen, Germany). A catheter in the right carotid artery was connected to a pressure transducer to monitor mean arterial blood pressure (MAP) and heart rate. The right jugular vein was cannulated for continuous infusion of 50mg/kg/h Ketamine dissolved in saline at a rate of 15 mL/kg/hour for maintenance of intravascular volume and anesthesia. The right femoral artery was cannulated for drawing blood samples and the right femoral vein for drug administration. The left kidney was exposed, decapsulated, and immobilized in a Lucite kidney cup (K. Effenberger, Pfaffingen, Germany) via ~4 cm incision in the left flank in each animal. Renal vessels were carefully separated under preservation of nerves and the adrenal gland. A perivascular ultrasonic transient time flow probe was placed around the left renal artery (type 0.7 RB Transonic Systems Inc., Ithaca, NY, USA) and connected to a flow meter (T206, Transonic Systems Inc., Ithaca, NY, USA) to continuously measure renal blood flow (RBF). The left ureter was isolated, ligated, and cannulated with a polyethylene catheter for urine collection. After the surgical preparation one optical fiber was placed 1 mm above the decapsulated kidney to measure renal microvascular and oxygenation using phosphorimetry. The surgical field was covered with a humidified gauze compress throughout the entire experiment to prevent drying of the exposed tissues. Changes in oxygen-dependent quenching of Palladium-porphyrin (Pd-porphyrin) phosphorescence (7) in the renal cortex were measured with an optical fiber and positioned a few millimeters above the kidney and were converted to local microvascular PO₂ values as previously described (8-9).

The rats were randomized into 4 groups: (1) a sham operation group (Control) ($n = 6$), (2) a LPS group ($n = 7$), (3) a LPS group with fluid resuscitation and a targeted MAP at 80-90mmHg (LPS+FR) ($n = 7$), (4) a LPS group with blood transfusion and a targeted MAP at 80-90mmHg (LPS+BT) ($n = 7$). In the septic groups, a 30-minute infusion of LPS (LPS, 10 mg/kg; serotype 0127:B8, Sigma, The Netherlands) was given to induce septic shock. Fluid resuscitation was performed with crystalloid solution (Ringer's lactate (Baxter)). Fluid resuscitation and blood transfusion were started 120 min after the end of LPS infusion and ended 15 min later. The experiment was ended 180 min after the end of LPS infusion or a corresponding time point for the control group (Figure 1).

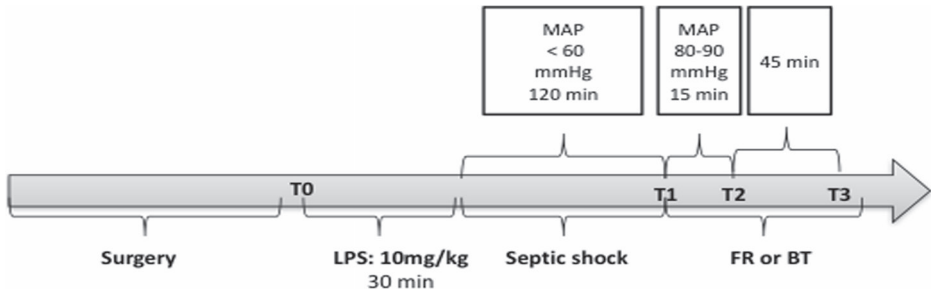


Figure 1. Experimental protocol. BT; blood transfusion, FR; fluid resuscitation, LPS; lipopolysaccharide, MAP; mean arterial pressure

Blood transfusion

Blood samples were obtained from donor, inbred *Wistar albino* rats. Donor rats were anesthetized, and mechanically ventilated. The right femoral artery was cannulated for drawing blood samples. Blood samples were mixed with a standard citrate-phosphate-dextrose-adenosine anticoagulant solution at 4: 1 volume ratio. An allogeneic BT from these donor rats was given to the study group through the right jugular vein with a targeted MAP between 80 and 90 mmHg.

Blood gas measurements

After infusion of the palladium-porphyrin (Pd-porphyrin) solution and 45 min of stabilization, a baseline blood sample (0.3ml) was taken from the femoral artery (T0), followed by blood samples 120 min after LPS infusion (T1), 15 min after resuscitation (early resuscitation phase, T2), and 180 min after resuscitation (late resuscitation phase, T3). The blood samples were replaced by the same volume of balanced colloid solution. The venous blood was obtained from the renal vein at the end of experiment. The samples were used to determine blood gas parameters (Radiometer ABL 505 Blood Gas Analyzer, Copenhagen, Denmark).

Measurement of Renal Microvascular Oxygenation

The renal microvascular partial pressure of oxygen ($C_{\mu}PO_2$) within the kidney cortex was measured by oxygen-dependent quenching of palladium-porphyrin phosphorescence using a phosphorimeter with a gated photomultiplier as previously described (10,11). Briefly, intravenously infused palladium-porphyrin binds to albumin. If excited by a flash of light (wavelength 530 nm), the palladium-porphyrin albumin complex emits phosphorescence (wavelength >700 nm). Depending on the oxygen concentration, the phosphorescence intensity decreases, and the relationship between the measured decay time and the partial pressure of oxygen (PO_2) can be estimated using the Stern-Volmer relation (11).

Calculation of derivatives of oxygenation parameters and renal vascular resistance

Renal oxygen delivery was calculated as follows: DO_{2ren} (ml/min) = renal blood flow \times arterial oxygen content ($1.31 \times \text{hemoglobin} \times \text{arterial oxygen saturation}$) + ($0.003 \times \text{arterial pressure of oxygen}$). Renal oxygen consumption was calculated as follows: VO_{2ren} (ml/min/g) = renal blood flow \times ($CaO_2 - CvO_2$), where renal venous oxygen content (CvO_2) is calculated as ($1.31 \times \text{hemoglobin} \times \text{renal venous oxygen saturation}$) + ($0.003 \times \text{renal venous partial pressure of oxygen (rvPO}_2)$) (12). An estimation of the renal vascular resistance was made as follows: renal vascular resistance ($\text{dynes}\cdot\text{sec}\cdot\text{cm}^{-5}$) = $(\text{MAP/RBF}) \times 100$ (13).

Creatinine clearance

Creatinine clearance (ml/min) was assessed as an index of the glomerular filtration rate. Clearance was calculated using the following formula: Creatinine clearance = $(U_{crea} \times V) / P_{crea}$, where U_{crea} was the concentration of creatinine in urine, V was the urine volume per unit time, and P_{crea} was the concentration of creatinine in plasma.

Renal energy efficiency for sodium transport: metabolic cost

The renal energy efficiency for sodium transport (VO_{2ren} / TNa^+) was assessed using a ratio that was calculated from the total amount of VO_{2ren} over the total amount of sodium reabsorbed (TNa^+ , mmol/min) according to the follow equation: $((U_{crea} \times V) / P_{crea} \times P_{Na}) - U_{Na} \times V$, where U_{crea} is the concentration of creatinine in the urine, V the urine volume per unit time, P_{crea} is the concentration of creatinine in the plasma, P_{Na} is the concentration of sodium in plasma, and U_{Na} is the concentration of sodium in the urine (14).

Histological analysis

The 4% formalin-fixed, paraffin-embedded renal tissue sections ($4 \mu\text{m}$) were stained with periodic acid-Schiff + Hematoxyline-Eosin reagent. Histological changes in the cortex were assessed by quantitative measurements of tissue damage. Histological criteria for renal damage were tubular epithelial swelling, brush border loss, vacuolar degeneration, necrotic tubules, luminal cast formation, and invagination. The degree of kidney damage was estimated at 400x magnification using 10 randomly selected fields for each animal by the following criteria: 0, normal; 1, areas of damage <10% of tubules; 2, damage involving 10% to 25% of tubules; 3, damage involving 25% to 50% of tubules; 4, damage more than 50% of tubules.

Immunohistochemical analysis

Kidney sections ($4 \mu\text{m}$) were deparaffinized with xylene and rehydrated with decreasing percentages of ethanol and finally with water. Antigen retrieval was accomplished by

microwaving the slides in citrate buffer (pH 6.0, Thermo Scientific, AP-9003-500) for 10 min. The slides were left to cool for 20 min at room temperature and then rinsed with distilled water. The endogenous peroxidase activity was blocked with 3% H₂O₂ for 10 min at room temperature, and the slides were later rinsed with distilled water and phosphate-buffered saline (PBS). Blocking reagent (Lab Vision, TA-125-UB) was applied to each slide followed by 10 min of incubation at room temperature in a humid chamber. Kidney sections were incubated overnight at 4 °C with rabbit polyclonal endothelial nitric oxide synthase (eNOS, 1:100) and inducible nitric oxide synthase (iNOS, 1:100) antibodies (eNOS NeoMarkers; Ab iNOS Ab-1, Rabbit PAb, RB-1605-P, NeoMarkers Fremont, CA, USA), anti-tumor necrosis factor (TNF)- α (1:200) (rabbit polyclonal, Abcam ab66579, Abcam Cambridge, UK), and anti-interleukin (IL)-6 (1:200) antibodies (rabbit polyclonal, Abcam 6672, Abcam Cambridge, UK) and incubated for 1 h at room temperature with anti-myeloperoxidase (MPO) antibody (MPO rabbit RB-373-A, NeoMarkers Fremont, CA, USA) and antilipocalin-2 (NGAL) antibody (Abcam 41105, Abcam Cambridge, UK). The sections were washed in PBS three times for 5 min each time and then incubated for 30 min at room temperature with biotinylated goat anti-rabbit antibodies (LabVision, TP-125-BN). After the slides were washed in PBS, the streptavidin peroxidase label reagent (LabVision, TS-125-HR) was applied for 30 min at room temperature in a humid chamber. The colored product was developed by incubation with AEC. The slides were counterstained with Mayer's hematoxylin (LabVision, TA-125-MH) and mounted in vision mount (LabVision, TA-060-UG) after being washed in distilled water. Both the intensities and distributions of iNOS and eNOS staining were scored. For each sample, a histological score (HSCORE) was derived by summing the percentage of cells that were stained at each intensity multiplied by the weighted intensity of the staining—HSCORE = $\sum I_i \times P_i$, where I_i is the intensity score, and P_i is the corresponding percentage of cells. The kidney sections were photographed using a Leica Qwin microscope.

As the measurement of cortical oxygenation and hemodynamic parameters were performed during the experiment, investigators were not blinded. However, creatinine levels, lactate and liver enzymes, and histological analysis were performed blinded.

Statistical Analyses

The results are expressed as the mean \pm SEM. A normality test (D'Agostino test) was performed and, if data did not follow a gaussian distribution, a nonparametric test was used (Kruskal-Wallis test with a Dunn's post hoc test). If data follow a gaussian distribution, statistical significance was calculated by one and two-way analyses of variance (ANOVA) followed by Bonferroni post-tests using GraphPad Prism (GraphPad Prism, Version 5, Software Program, San Diego, CA, USA). A p value <0.05 was considered statistically significant.

RESULTS

Effects of fluid resuscitation and blood transfusion on systemic and renal hemodynamic parameters during sepsis.

The MAP, renal blood flow and renal vascular resistance are provided in Table 1. Infusion of LPS induced early and persistent decreases in MAP and renal blood flow. FR significantly improved the MAP at T2 and T3 and the renal blood flow at T2. Similarly, BT significantly improved the MAP at T2 and T3 and the renal blood flow at T2. At the end of the experiment, there were no significant differences in terms of the systemic or renal hemodynamic parameters between the groups that received FR or BT after LPS infusion.

Table 1. Hemodynamic parameters at four time points T0 (Baseline), T1, T2, T3 of the 4 groups.

	Baseline (T0)	T1	T2	T3
Mean arterial pressure (mmHg)				
Control	91.5±11.2	93±10.8	94±12.7	76.1±6
LPS	88.7±3.5	49±13.6####	54.9±16.3####	42.2±11.7####
LPS+FR	90.8±3.5	53.5±8.4####	82.7±5.7****	56.6±5.7**
LPS+BT	89.5±5.9	54.1±4.5####	86.8±4.5****	61.1±8.5**
Heart rate per minute				
Control	232.9±22.6	247.7±20.3	248±16.9	249.9±35.4
LPS	236.3±31.6	225.6±13.8	226.9±15.7	221±22.5
LPS+FR	227.9±23	219±13.5	259±20.6	258±14.1
LPS+BT	255.3±20.3	252.1±14.9	258±14.1	254.6±17.2
Renal blood flow (ml/min)				
Control	7.5±2.2	5.1±0.6	5.2±0.9	4.3±0.5
LPS	7.1±1.3	0.8±0.8####	0.9±0.9	0.6±0.8
LPS+FR	6.3±0.6	0.4±0.2####	5.4±2.4****	1.6±0.9#
LPS+BT	6.6±1.9	0.8±0.7####	3.2±0.9*†	1.8±0.7#
Renal vascular resistances (dynes s cm⁻⁵)				
Control	1291.9±339.2	1823.2±233.4	1844.4±412.7	1784.3±255.1
LPS	1275.2±205.4	17820±20195.9	18631.9±30147.9	20237.7±21005.3
LPS+FR	1449.9±153.6	18860.5±17881.2	1853.3±889.5	4390.5±2434.9
LPS+BT	1431.3±328.3	12133.9 ±9243.2	2919.9±1028.6	4860.7±4836.8

Data expressed in Mean ± SD, ##p<0.01, ####p< 0.0001 vs. Control group; *p <0.05, ** p<0.01, **** p<0.0001 vs. LPS group; † p <0.05 vs. LPS+FR group.

Abbreviations: LPS; lipopolysaccharide, BT; blood transfusion, FR; fluid resuscitation.

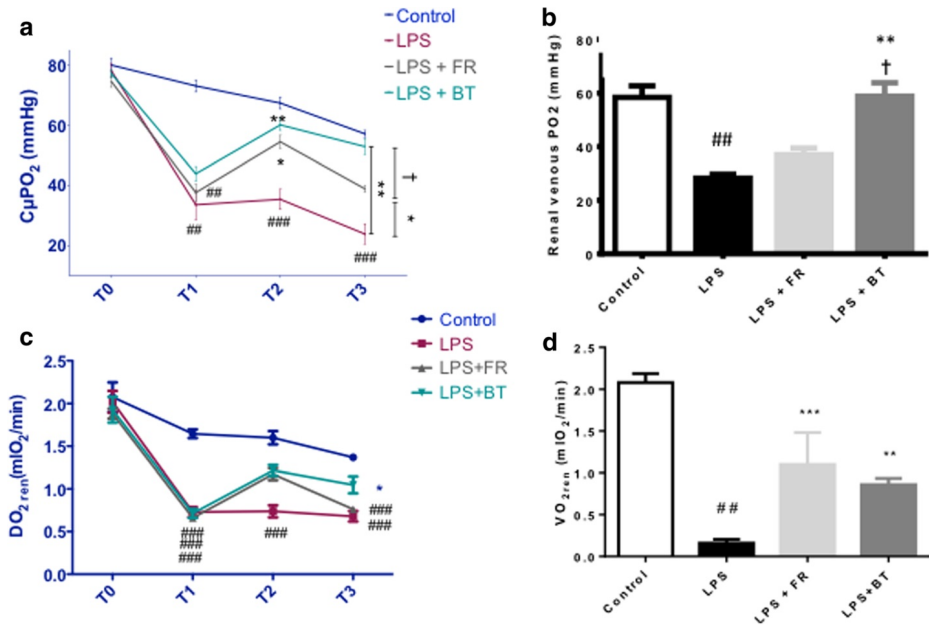


Figure 2. Renal oxygenation parameters. **a** Evolution of microvascular oxygen tension in the renal cortex ($C_{\mu}PO_2$) in the four groups at baseline (T0), T1, T2, and T3. **b** Renal venous partial pressure of oxygen (PO_2) at T3 in the four groups. **c** Evolution of renal oxygen delivery (DO_{2ren}) in the four groups at T0, T1, T2, and T3. **d** Renal oxygen consumption (VO_{2ren}) at T3 in the four groups. ## $p < 0.01$, ### $p < 0.001$ vs. Control group; * $p < 0.05$, ** $p < 0.01$, *** $p < 0.001$ vs. LPS group; † $p < 0.05$ vs. LPS + FR group. The values are shown as Mean \pm SEM. See Figure 1 for definitions of the time points. BT; blood transfusion, FR; fluid resuscitation, LPS; lipopolysaccharide.

Effect of fluid resuscitation and blood transfusion on renal microvascular oxygenation during sepsis.

The $C_{\mu}PO_2$, $rvPO_2$, DO_{2ren} , and VO_{2ren} values are illustrated in Figure 2. LPS induced significant decreases in $C_{\mu}PO_2$ and $rvPO_2$ from baseline to T3 (23.9 ± 8.9 mmHg in the LPS group versus 57.2 ± 2.9 mmHg in the control group at T3, $p < 0.001$, and 28.3 ± 3.9 mmHg in the LPS group versus 58.4 ± 9.7 mmHg in the control group at T3, respectively, $p < 0.01$). FR significantly improved the $C_{\mu}PO_2$ at T2 (54.5 ± 5.8 mmHg versus 35.4 ± 8.8 mmHg in the LPS group, $p < 0.05$), but this value began to decrease from T2 to T3 (38.9 ± 2.8 mmHg in the FR group at T3). BT significantly improved the $C_{\mu}PO_2$ at T2 (60.15 ± 4.9 mmHg, $p < 0.01$ versus the LPS group) and T3 (52.9 ± 6.9 mmHg versus 23.9 ± 8.9 mmHg in the LPS group, $p < 0.01$). There was a significant difference in the $C_{\mu}PO_2$ values at T3 between the LPS + FR group and the LPS + BT group ($p < 0.05$; Figure 2a). BT improved the $rvPO_2$ (58.9 ± 13.3 mmHg versus 28.3 ± 3.9 mmHg in the LPS group, $p < 0.01$). The increase in $rvPO_2$ induced by BT was significantly greater than the increase in $rvPO_2$ that was induced by FR ($p < 0.05$; Figure 2b). The DO_{2ren} was significantly

decreased after LPS and was partially restored at T3 in the BT group ($p < 0.05$ at T3 versus LPS). Differences between $\text{DO}_{2\text{ren}}$ in the BT group and the FR group at T3 did not reach statistical significance (Figure 2c). There was a significant drop in $\text{VO}_{2\text{ren}}$ in the LPS group compared to the controls ($p < 0.01$). FR and BT both restored the $\text{VO}_{2\text{ren}}$ at T3 ($p < 0.001$ and $p < 0.01$, respectively, at T3).

Effect of fluid resuscitation and blood transfusion on hemoglobin, pH, serum lactate and liver function.

The hemoglobin levels, pH, serum lactate levels, and liver enzymes are illustrated in Figure 3. As expected, FR induced significant decreases in hemoglobin values due to hemodilution (Figure 3a). LPS infusion induced a significant drop in pH at T3 ($p < 0.01$ versus the control group) that was partially restored by FR and BT without any significant difference between the two groups (Figure 3b). The serum lactate levels increased during sepsis ($p < 0.01$ at T2 and $p < 0.05$ at T3 in the LPS group versus the control group), but neither FR nor BT completely restored these values (Figure 3c). Moreover, neither FR nor BT improved the LPS-induced increase in aspartate aminotransferase (AST), which is a surrogate marker for liver damage (Figure 3d).

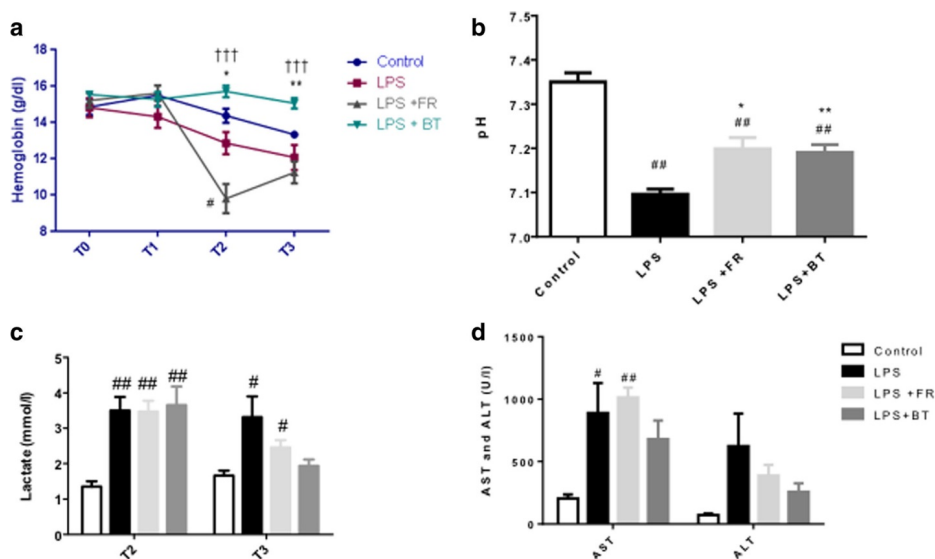


Figure 3. Hemoglobin, pH, serum lactate, and liver function during septic shock and resuscitation. **a** Hemoglobin concentrations at T0, T1, T2, and T3 in the four groups. **b** pH at T3 in the four groups. **c** Serum lactate levels at T2 and T3 in the four groups. **d** Aspartate aminotransferase (AST) and alanine aminotransferase (ALT) levels at T3 in the four groups. * $p < 0.05$, ** $p < 0.01$ vs. Control group; * $p < 0.05$, ** $p < 0.01$ vs. LPS group; *** $p < 0.001$ vs. LPS + FR group. The values are shown as Mean \pm SEM. See Figure 1 for definitions of the time points. BT; blood transfusion, FR; fluid resuscitation, LPS; lipopolysaccharide.

Effect of fluid resuscitation and blood transfusion on renal function , metabolic cost and tubular lesions during sepsis.

The creatinine levels are illustrated in Figure 4a. At T1, all of the LPS-treated animals were anuric. This condition did not improve in the non-resuscitation group. All rats that received LPS suffered from AKI as reflected by increased plasmatic creatinine levels, and FR was not able to prevent AKI. The plasma creatinine levels did not differ significantly between the LPS group and the LPS + FR group. However, BT significantly decreased the plasma creatinine levels ($39.6 \pm 7.4 \mu\text{mol/l}$ in the LPS + BT group versus $77.7 \pm 8.9 \mu\text{mol/l}$ in the LPS group at T3, $p < 0.01$, and $64 \pm 7.2 \mu\text{mol/l}$ in the LPS + FR group, $p < 0.05$). Similarly, creatinine clearance significantly improved at T3 in the LPS + BT group ($p < 0.05$ versus LPS + FR group) (Figure 4b).

The metabolic cost of sodium reabsorption as assessed with the VO_2/TNa^+ could not be calculated in the LPS group due to the absence of urine output after LPS administration without resuscitation. However, whereas LPS + FR induced an increase in VO_2/TNa^+ ($p < 0.05$ compared to the controls), the VO_2/TNa^+ ratio was not different after LPS + BT compared with the controls ($p < 0.05$ versus the FR group; Figure 4c).

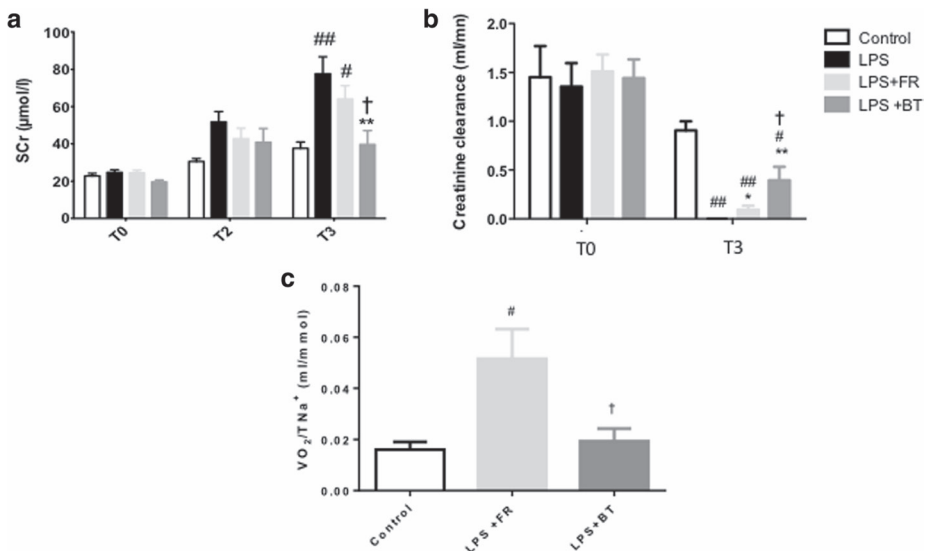


Figure 4. Kidney function and metabolic cost during septic shock and resuscitation. **a** Serum creatinine (Scr; $\mu\text{mol/l}$) at T0 and T3 in the four groups. **b** Creatinine clearance (ml/min) at T0 and T3 in the four groups. **c** VO_2/TNa^+ (oxygen consumption per sodium reabsorbed (metabolic cost)) at T3 in the control group, LPS + FR group and LPS + BT group. * $p < 0.05$, ** $p < 0.01$ vs. Control group; † $p < 0.05$, †† $p < 0.01$ vs. LPS group; ‡ $p < 0.05$ vs. LPS + FR group. The values are shown as Mean \pm SEM. See Figure 1 for definitions of the time points. BT; blood transfusion, FR; fluid resuscitation, LPS; lipopolysaccharide.

LPS induced tubular damage, including tubular vacuolization, tubular invagination, brush border loss, and luminal cast formation. BT, but not FR, significantly improved the tubular damage (mean histological score of 3 ± 0.06 in the LPS + BT group versus 3.4 ± 0.06 in the LPS group, $p < 0.01$, and 3.3 ± 0.06 in the LPS + FR group, $p < 0.05$; Figure 5a and b).

Effects of fluid resuscitation and blood transfusion on renal iNOS, eNOS expression, and tissue inflammatory markers.

The renal expression of eNOS was markedly suppressed under endotoxin challenge ($p < 0.001$; Figure 5c). BT significantly increased eNOS expression after LPS (mean Hscore of 243 ± 4 in the LPS + BT group versus 192.3 ± 1.5 in the LPS group, $p < 0.001$). The renal expression of eNOS did not increase after FR (mean H-score of 190.4 ± 2.6). In contrast, the renal expression of iNOS was markedly increased under endotoxin challenge ($p < 0.01$; Figure 5d). Whereas FR decreased iNOS expression after LPS ($p < 0.01$ in the LPS + FR group compared to the LPS group), BT did not change iNOS expression after LPS.

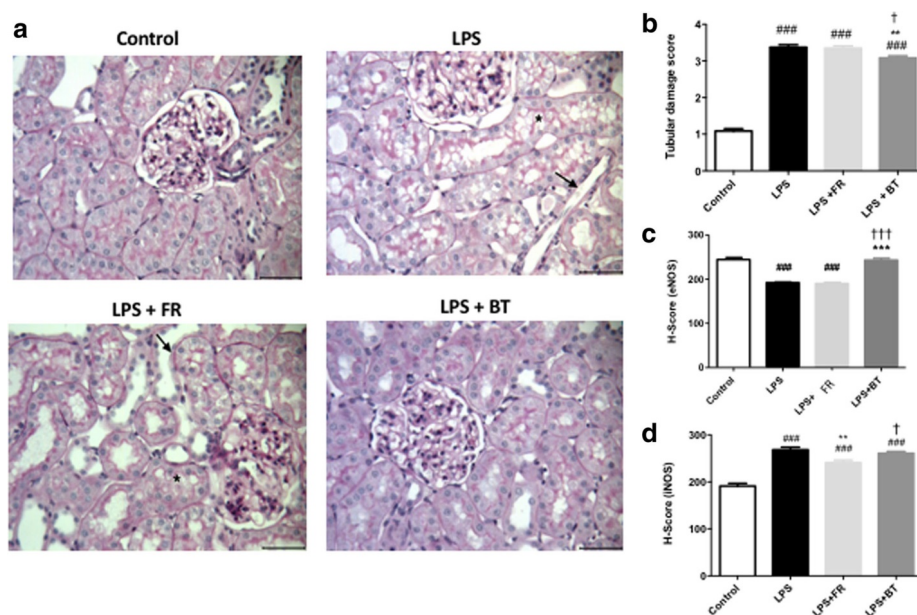
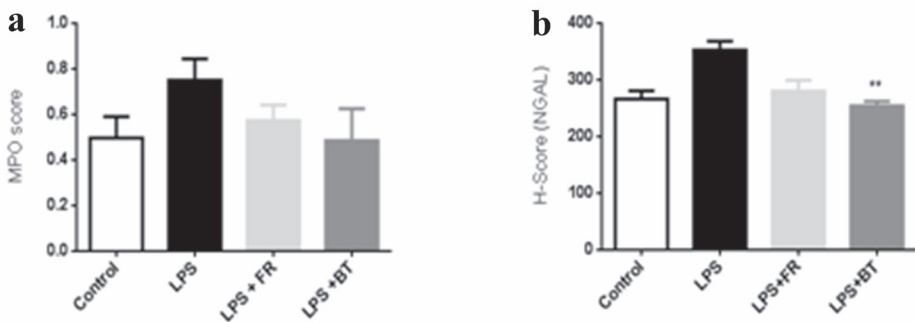
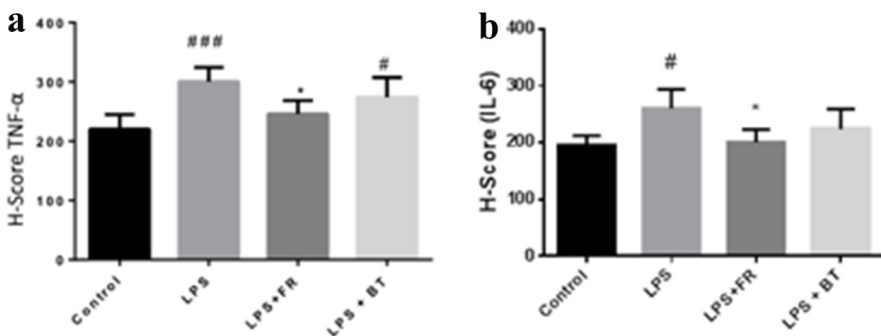


Figure 5. Renal histological changes and renal expressions of eNOS and iNOS during septic shock and resuscitation. **a** Representative periodic acid Schiff staining in the kidneys of the control, LPS, LPS + FR, and LPS + BT rats (original magnification $\times 400$) and tubular injury scores in the four groups. Tubular vacuolization images of the LPS and LPS + FR groups further demonstrate the considerable tubular vacuolization (asterisks) as well as the loss of the brush border in the renal tubule (closed arrows). **b** Quantification of the tubular injury scores in the kidney sections. **c** Quantification of endothelial nitric oxide synthase (eNOS) staining intensities (H-score) in the kidney sections. **d** Quantification of inducible nitric oxide synthase (iNOS) staining intensities (H-score) in the kidney sections. The values are shown as Mean \pm SEM. $^{###}p < 0.001$ vs. Control group; $^{*}p < 0.01$ vs. LPS group; $^{†}p < 0.05$, $^{†††}p < 0.001$ vs. LPS + FR group. BT; blood transfusion, FR; fluid resuscitation, LPS; lipopolysaccharide.

Neutrophil gelatinase-associated lipocalin (NGAL), a marker of AKI and kidney inflammation, significantly improved after BT compared to the LPS group ($p < 0.05$). However, the immunostaining intensity of NGAL was not statistically different between the LPS + FR and LPS + BT groups (Additional file 1: Figure S1). Sepsis induced an increase in pro-inflammatory cytokines (TNF- α and IL-6) into the kidney, but there was no statistical difference between the LPS + FR and LPS + BT groups (Additional file 1: Figure S2). Similarly, MPO activity within the kidney, a marker of oxidative stress, was not different between the two groups (Additional file 1: Figure S1).



S1. a Myeloperoxidase immunostaining and **b** Neutrophil Gelatinase Associated Lipocalin (NGAL) immunostaining in kidney sections in the four groups. The values are shown as Mean \pm SEM, ** $p < 0.01$ vs. Control group.



S2. a Immunostaining of Tumor Necrosis Factor- α (TNF- α) and **b** Interleukin-6 (IL-6) in kidney sections in the four groups. The values are shown as Mean \pm SEM, # $p < 0.05$, ### $p < 0.001$ vs. Control group; * $p < 0.05$ vs. LPS group.

DISCUSSION AND CONCLUSION

In the present study, we demonstrated that BT restored renal microcirculatory oxygenation and, by extension, kidney function in a rat model of endotoxemia. BT had beneficial effects on kidney microvascular oxygenation, metabolic costs, and AKI. Sepsis-induced eNOS deficiency and renal damage were corrected by BT but not by FR.

Johannes *et al.* previously demonstrated the appearance of cortical microcirculatory hypoxic areas in endotoxin-induced renal failure in the rat (3). In the present study, we confirmed the drop in renal cortical oxygenation induced by LPS. A part of this anoxia was due to the drop of the renal blood flow during septic shock. Indeed, FR was only able to temporarily improve cortical oxygenation by improving the renal blood flow. However, BT had stronger and longer-lasting effects on renal microvascular oxygenation despite similar renal blood flows. Microcirculatory dysfunction may contribute to renal hypoxia even in the absence of frank renal hypoperfusion. Several studies using microcirculatory techniques have now questioned the significance of arterial renal blood flow (15) and have suggested that the renal microcirculation is the hemodynamic culprit in the pathophysiology of septic AKI (16). The microcirculation of the renal cortex has been demonstrated to be severely injured in animal models of sepsis (3, 5). Legrand *et al.* demonstrated that the prevention of renal macrovascular hypoperfusion by FR cannot fully prevent renal microcirculatory oxygenation and perfusion dysfunction after LPS infusion in rats, despite a normalized renal blood flow (5). Severe sepsis is characterized by a reduction in functional capillary density and an increase in blood flow heterogeneity. Indeed, the ischemic component is not found in global renal arterial blood flow but rather in a defect in the distribution of renal cortex microcirculation involving patchy areas of micro-ischemia (5). Our study was not designed to demonstrate the distribution of red blood cells inside the kidneys after BT, and we cannot rule out the possibility that some areas inside the kidneys did not receive the oxygen delivered by the erythrocytes. However, the global effect of BT was an improvement in microvascular oxygenation that was independent of renal macrovascular perfusion. Moreover, the $\text{VO}_{2\text{ren}}/\text{TNa}^+$, which is a functional index of the efficiency of oxygen utilization for TNa^+ and a functional parameter that reflects tubular injury (17), demonstrated more efficiency in oxygen utilization for tubular transport following BT than following FR. This improvement in kidney oxygenation participated in the improvement in kidney function. Indeed, renal tissue hypoxia is an important common feature of AKI (18) and is a major driver of the cascade of events that leads to cellular injury and vascular and tubular dysfunction (19). In our study, improvements in kidney oxygenation translated into better renal outcomes as assessed by the serum creatinine levels and tubular damage.

These effects could be mediated in part by a restoration of eNOS activity after BT. Indeed, in accordance with previous studies we found a significant decrease in eNOS expression in the kidney under endotoxin challenge. In a murine model of cecal ligation and puncture-induced septic shock, Coletta *et al.* Demonstrated that the lack of eNOS production alone may be sufficient to markedly exacerbate the severity of septic shock (20). Nitric oxide (NO) is an important mediator of microvascular patency and blood flow, and strategies that aim to enhance endothelial eNOS activity have been found to decrease sepsis-induced neutrophil-endothelial cell interactions and may play a role in maintaining microvascular patency in septic shock (21). Notably, Souza *et al.* reported similar findings that increasing hemoglobin levels using erythropoietin in septic rats preserves renal eNOS expression and thereby prevents sepsis-induced AKI (22). Thus, we hypothesize that the specific effect of BT on eNOS expression in the kidney may have improved the endothelial dysfunction and renal microcirculation in our model.

However, there are contradictory results from clinical studies in which BT was administered during sepsis. BT has been associated with increased mortality in subgroups of critically ill patients in both cohort studies and randomized trials (23, 24), but there have also been cohort studies in which transfusion was associated with improved survival, including in patients with sepsis (25,26). In a recent randomized controlled study, Holst *et al.* found that mortality rates were similar in patients who received BT at a higher hemoglobin threshold and those who received BT at a lower threshold during septic shock (27). Our study did not investigate long-term survival or outcomes. We measured serum lactate as a global perfusion biomarker and liver enzymes as markers of liver function. In accordance with the study of Holst *et al.* we did not find any benefit of BT on liver function or lactic acidosis when compared with FR. How then can we explain the specific protective effect of BT on renal function? First, some data suggest a direct influence of hemodilution on microvascular flow and renal oxygen supply. The critical hematocrit associated with a decrease in microvascular PO₂ has already been found to be much higher for the kidney than for the intestines and the heart (28). The benefit of increasing the hematocrit level with BT may therefore be greater for the kidney than for other organs. Second, there is accumulating evidence that endothelial cell phenotypes vary between different organs and exhibit remarkable heterogeneity in structure and function (29,30). Under similar conditions, eNOS activity is also highly variable between organs (30,31). eNOS is highly expressed in glomerular endothelial cells and the endothelium of cortical vessels in control and diseased kidneys (32). Thus, we hypothesize that, depending on the level of eNOS activity and the interaction between BT and endothelial cells, the influence of BT may vary greatly from one organ to another.

When studying the effect of BT during sepsis, another important issue needs to be accounted for: the failure to identify significant improvements in outcomes in clinical studies may pertain to the potentially deleterious effect of blood storage. In our study, we transfused fresh blood to the septic rats. During storage, erythrocytes are exposed to and produce substances that impair their function when they are returned to the circulation (33). In this situation, BT may, rather than improving oxygenation, worsen oxygen balance and AKI. The use of fresh blood in our study may therefore, in part, explain the beneficial effects we observed in terms of renal oxygenation and AKI. However, a recent randomized trial comparing transfusion of fresh red cells to standard-issue red cells did not find any difference in terms of mortality in a large population of critically ill patients (34).

In conclusion, BT might be useful as a renal protective strategy to preserve renal oxygenation and kidney function during sepsis. However, additional studies are warranted to evaluate the true clinical value of BT in this setting and its prolonged beneficial effects on kidney function.

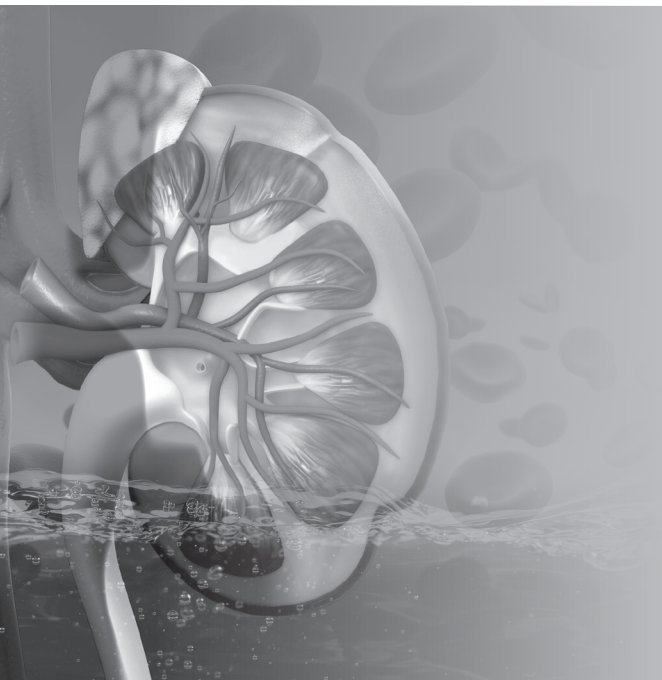
Limitations

Our study has several limitations. First, the acute and lethal model of endotoxic shock (in a limited sample size of animals) used herein is clearly not fully representative of human septic shock. LPS causes much earlier and higher peak levels of cytokine expression compared with levels observed in human sepsis. However, endotoxemic challenge with LPS remains a useful tool for interrogating a simpler subset of the complex trajectory of sepsis. Second, our rats were resuscitated with fluids but not norepinephrine. The use of norepinephrine has been shown to be associated with better tissue oxygenation when compared with fluid resuscitation alone (35, 36). Finally, the modalities, timing, and threshold of hemoglobin that need to be targeted have to be defined before conducting a clinical trial focusing on sepsis-induced AKI.

REFERENCES

1. Chertow GM, Burdick E, Honour M, *et al.* Acute kidney injury, mortality, length of stay, and costs in hospitalized patients. *J. Am. Soc. Nephrol.* 16:3365–70, 2005.
2. Uchino S, Kellum JA, Bellomo R, *et al.* Acute renal failure in critically ill patients: a multinational, multicenter study. *JAMA* 294:813–8, 2005.
3. Johannes T, Mik EG, Ince C. Nonresuscitated endotoxemia induces microcirculatory hypoxic areas in the renal cortex in the rat. *Shock* 31: 97–103, 2009.
4. du Cheyron D, Parienti JJ, Fekih-Hassen M, *et al.* Impact of anemia on outcome in critically ill patients with severe acute renal failure. *Intensive Care Med.* 31:1529–36, 2005.
5. Legrand M, Bezemer R, Kandil A, *et al.* The role of renal hypoperfusion in development of renal microcirculatory dysfunction in endotoxemic rats. *Intensive Care Med.* 37:1534–42, 2011.
6. Legrand M, Mik EG, Balestra GM, *et al.* Fluid resuscitation does not improve renal oxygenation during hemorrhagic shock in rats. *Anesthesiology* 112:119–27, 2010.
7. Sakr Y, Chierego M, Piagnerelli M, *et al.* Microvascular response to red blood cell transfusion in patients with severe sepsis. *Crit. Care Med.* 35:1639–44, 2007.
8. Creteur J, Neves AP, Vincent JL. Near-infrared spectroscopy technique to evaluate the effects of red blood cell transfusion on tissue oxygenation. *Crit. Care* 13 Suppl 5:S11, 2009.
9. Lee HB, Blafox MD. Blood volume in the rat. *J. Nucl. Med. Off. Publ. Soc. Nucl. Med.* 26:72–6, 1985.
10. Vanderkooi JM, Maniara G, Green TJ, Wilson DF. An optical method for measurement of dioxygen concentration based upon quenching of phosphorescence. *J. Biol. Chem.* 262:5476–82, 1987.
11. Sinaasappel M, Ince C. Calibration of Pd-porphyrin phosphorescence for oxygen concentration measurements in vivo. *J. Appl. Physiol.* 81: 2297–303, 1985.
12. Mik EG, Johannes T, Ince C. Monitoring of renal venous PO₂ and kidney oxygen consumption in rats by a near-infrared phosphorescence lifetime technique. *Am. J. Physiol. Ren. Physiol.* 294:F676–81, 2008.
13. Inoue RY, Gontijo JA, Franchini KG. Hemodilution mediates hemodynamic changes during acute expansion in unanesthetized rats. *Am. J. Physiol. Regul. Integr. Comp. Physiol.* 279:R2243–51, 2000.
14. Johannes T, Ince C, Klingel K, *et al.* Iloprost preserves renal oxygenation and restores kidney function in endotoxemia-related acute renal failure in the rat. *Crit. Care Med.* 37:1423–32, 2009.
15. Matejovic M, Radermacher P, Joannidis M. Acute kidney injury in sepsis: is renal blood flow more than just an innocent bystander? *Intensive Care Med.* 33:1498–500, 2007.
16. Chvojka J, Sykora R, Krouzecky A, *et al.* Renal haemodynamic, microcirculatory, metabolic and histopathological responses to peritonitis-induced septic shock in pigs. *Crit. Care* 12:R164, 2008.
17. Evans RG, Harrop GK, Ngo JP, *et al.* Basal renal O₂ consumption and the efficiency of O₂ utilization for Na⁺ reabsorption. *Am. J. Physiol. Ren. Physiol.* 306:F551–60, 2014.
18. Rosenberger C, Rosen S, Heyman SN. Renal parenchymal oxygenation and hypoxia adaptation in acute kidney injury. *Clin. Exp. Pharmacol. Physiol.* 33:980–8, 2006.
19. Bonventre JV, Weinberg JM. Recent advances in the pathophysiology of ischemic acute renal failure. *J. Am. Soc. Nephrol.* 14:2199–210, 2003.
20. Coletta C, Modis K, Olah G, *et al.* Endothelial dysfunction is a potential contributor to multiple organ failure and mortality in aged mice subjected to septic shock: preclinical studies in a murine model of cecal ligation and puncture. *Crit. Care* 18:511, 2014.
21. Khan R, Kirschenbaum LA, LaRow C, *et al.* Augmentation of platelet and endothelial cell eNOS activity decreases sepsis-related neutrophilendothelial cell interactions. *Shock* 33:242–6, 2010.
22. Souza AC, Volpini RA, Shimizu MH, *et al.* Erythropoietin prevents sepsis-related acute kidney injury in rats by inhibiting NF- κ B and upregulating endothelial nitric oxide synthase. *Am. J. Physiol. Ren. Physiol.* 302:F1045–54, 2012.
23. Hebert PC, Wells G, Blajchman MA, *et al.* A multicenter, randomized, controlled clinical trial of transfusion requirements in critical care. Transfusion Requirements in Critical Care Investigators, Canadian Critical Care Trials Group. *N. Engl. J. Med.* 340:409–17, 1999.

24. Marik PE, Corwin HL. Efficacy of red blood cell transfusion in the critically ill: a systematic review of the literature. *Crit. Care Med.* 36:2667–74, 2008.
25. Vincent J-L, Sakr Y, Sprung C, *et al.* Are blood transfusions associated with greater mortality rates? Results of the Sepsis Occurrence in Acutely Ill Patients study. *Anesthesiology* 108:31–9, 2008.
26. Park DW, Chun BC, Kwon SS, *et al.* Red blood cell transfusions are associated with lower mortality in patients with severe sepsis and septic shock: a propensity-matched analysis. *Crit. Care Med.* 40:3140–5, 2012.
27. Holst LB, Haase N, Wetterslev J, *et al.* Lower versus higher hemoglobin threshold for transfusion in septic shock. *N. Engl. J. Med.* 371:1381–91, 2014.
28. van Bommel J, Siegemund M, Henny CP, Ince C. Heart, kidney, and intestine have different tolerances for anemia. *Transl. Res. J. Lab. Clin. Med.* 151: 110–7, 2008.
29. Aird WC. Endothelial cell heterogeneity. *Cold Spring Harb. Perspect. Med.* 2:a006429, 2012.
30. Yano K, Liaw PC, Mullington JM, *et al.* Vascular endothelial growth factor is an important determinant of sepsis morbidity and mortality. *J. Exp. Med.* 203:1447–58, 2006.
31. Aird WC. Phenotypic heterogeneity of the endothelium: I. Structure, function, and mechanisms. *Circ. Res.* 100:158–73, 2007.
32. Furusu A, Miyazaki M, Abe K, *et al.* Expression of endothelial and inducible nitric oxide synthase in human glomerulonephritis. *Kidney Int.* 53: 1760–8, 1998.
33. Tsai AG, Cabrales P, Intaglietta M. Microvascular perfusion upon exchange transfusion with stored red blood cells in normovolemic anemic conditions. *Transfusion (Paris)*. 44:1626–34, 2004.
34. Lacroix J, Hébert PC, Fergusson DA, *et al.* Age of transfused blood in critically ill adults. *N. Engl. J. Med.* 372:1410–8, 2015..
35. Sennoun N, Montemont C, Gibot S, *et al.* Comparative effects of early versus delayed use of norepinephrine in resuscitated endotoxic shock. *Crit. Care Med.* 35:1736–40, 2007.
36. Maiden MJ, Otto S, Brealey JK, *et al.* Structure and function of the kidney in septic shock. A prospective controlled experimental study. *Am. J. Respir. Crit. Care Med.* 194:692–700, 2016.



CHAPTER 11

The role of bicarbonate precursors in balanced fluids during hemorrhagic shock with and without compromised liver function

Adapted from *Br. J. Anaesth.* 2016 Oct;117(4):521-528

Bulent Ergin ¹, Aysegul Kapucu ², Philippe Guerci ^{1,3,5}, Can Ince ^{1,4}

¹ Department of Translational Physiology, Academic Medical Centre, Amsterdam, The Netherlands

² Department of Biology, Science Faculty, University of Istanbul, Istanbul, Turkey

³ INSERM U1116, University of Lorraine, Vandoeuvre-les-Nancy, France

⁴ Department of Intensive Care Medicine, Erasmus MC, University Medical Centre, Rotterdam, Rotterdam, The Netherlands.

⁵ Departement of Anaesthesiology and Critical Care Medicine, University Hospital of Nancy, France

ABSTRACT

Lactate, acetate and gluconate are anions used in balanced resuscitation fluids of which lactate and acetate are considered bicarbonate precursors. This study investigated the role of the liver in the efficacy of balanced and unbalanced solutions to correct acid-base alterations and renal hemodynamics and microvascular oxygenation in a rat model of resuscitated hemorrhagic shock (HS). Ringer's Lactate (RL), Ringer's Acetate (RA), Plasma-Lyte (RA-Glu/Mg) or normal saline (NS) were administered following HS in the presence or absence of a 70% partial liver resection (PLR). Renal hemodynamics and microvascular oxygenation (by oxygen-dependent quenching of phosphorescence) were measured as well as concentrations of lactate, gluconate and acetate in plasma and urine. Kidney wet and dry weighing was also assessed. PLR resulted in increased liver enzymes compared in control and HS groups ($p < 0.01$). HS decreased systemic and renal perfusions and reduced microvascular kidney oxygenation with lactic acidosis ($p < 0.01$). Resuscitation with balanced fluids did not fully restore renal oxygenation ($p < 0.01$). RA and RA-Glu/Mg increased bicarbonate contents and restored pH better than RL or NS in the PLR experiment ($p < 0.01$). PLR caused an increase in plasma gluconate after RA-Glu/Mg resuscitation ($p < 0.05$). To conclude, acetate buffered balanced fluids show superior buffering effects than RL and NS. Gluconate is partially metabolized by the liver although it does not contribute to acid-base control because of large excretion in urine. Acetate is metabolized regardless of liver function and may be the most efficient bicarbonate precursor. Lactate infusion tends to overwhelm the metabolism capacities of the residual liver.

Keywords: microcirculation, hemorrhagic shock, buffered solution, plasma-lyte, gluconate

INTRODUCTION

Current evidence suggests that the type of fluid used for resuscitation, particularly colloids, may lead to unfavourable outcomes or have no effect compared to normal saline (1-5). Several studies have demonstrated that balanced fluids are commonly used for volume expansion of critically ill patients (6-8). This has led to increased attention on the role of crystalloids and the effects of their different compositions (9,10). Fluid preparation may be based on a simple, non-buffered salt solution, such as normal saline or, be balanced with anion substitutes, such as maleate, gluconate, lactate or acetate of which the two latter are considered bicarbonate precursors. Plasma-Lyte (Baxter Healthcare, Illinois, US) is a crystalloid fluid encompassing two weak anions, acetate and gluconate and is engineered to closely mimic the plasma electrolyte content while not altering its osmolality (11). However, the role of gluconate in terms of acid-base control is unknown.

There is a growing body of evidence indicating that balanced fluids improve the acid-base status and preserve strong ion difference (12). The purpose of using these solutions is based on two principles: (i) reducing the chloride content and its detrimental effects (13), with providing a plasma-like ionic content, and (ii) increasing bicarbonate content and pH by metabolism of bicarbonate precursors (14). It is commonly accepted that these precursors are mainly metabolized in the liver (15,16). To our knowledge there is little information on the role of liver function in acid-base control during fluid balanced resuscitation for hemorrhagic shock. What is unclear and not well described is the metabolic fate of such components during shock states associated with compromised liver function and the degree to which other organ beds are effective in metabolizing these precursors to produce bicarbonate and correct acid-base alterations (9). Whereas it is generally assumed that lactate is primarily metabolized in the liver in case of shock, the acetate is metabolized in other organs (17). We hypothesized that acetate-based resuscitation fluids would have superior buffering effect than non-acetate based fluids in case of liver dysfunction.

To this end we assessed the buffering effect of three commonly used balanced fluids, Ringer's Lactate (RL), Ringer's Acetate (RA) and Plasma-Lyte (RA-Glu/Mg) (Supplementary Table 1) in a relevant model of fixed-pressure hemorrhagic shock. In the first part of the study, we aimed to determine the role of the liver in the metabolism of these buffers. To accomplish this, a ~70% partial liver resection (PLR) was performed to reduce the capacity of the liver to metabolize these precursors. In addition, we studied the fate of gluconate in these models. Secondly, we investigated the extent to which each type of fluid is effective in improving acid-base status, and tissue oxygenation, which can

be considered the primary goals fluid resuscitation in states of shock. We focused on the kidney because it is considered to be the organ most at risk during states of shock and fluid overuse.

MATERIAL AND METHODS

Animals

All experiments in this study were approved by the Animal Research Committee of the Academic Medical Centre of the University of Amsterdam (DFL 102919). Care and handling of the animals were in accordance with the guidelines from the Institutional and Animal Care and Use Committees. A total of 75 rats were needed in these experiments ($n = 6/\text{group}$), including 3 animals for setting up the model of PLR. Experiments were performed on male *Sprague-Dawley* rats (Harlan, The Netherlands), aged 10 ± 2 weeks with a mean \pm SD body weight of 330 ± 20 g.

Surgical preparation

The rats were anesthetized with an intraperitoneal injection of a mixture of 100 mg kg^{-1} ketamine (Nimatek[®]; Eurovet, Bladel, The Netherlands), 0.5 mg kg^{-1} medetomidine (Domitor; Pfizer, New York, NY) and 0.05 mg kg^{-1} atropine-sulfate (Centrafarm, Etten-Leur, The Netherlands) and maintained with 50 mg kg^{-1} ketamine at a dose of $5 \text{ ml kg}^{-1} \text{ h}^{-1}$. After tracheotomy, the animals were mechanically ventilated with 0.4 FiO_2 . A heating pad under the animal allowed the body temperature to be controlled and maintained at $37 \pm 0.5^\circ\text{C}$. The end-tidal PCO_2 was maintained between 4 and 4.7 kPa .

The right carotid (pressure) and femoral (for blood shedding and samples) arteries and jugular anaesthesia) and femoral (fluid resuscitation) veins were cannulated with polyethylene catheters (outer diameter = 0.9 mm ; Braun, Melsungen, Germany). For fluid maintenance during surgery, 0.9% NaCl (Baxter, Utrecht, The Netherlands) at a rate of $10 \text{ ml kg}^{-1} \text{ hour}^{-1}$ was administered. For liver resection, a 70% partial liver resection (PLR) was achieved by ligating branches of the hepatic artery and portal vein using 3/0 silk thread and resecting 2 lobes of the liver after a midline laparotomy. The left kidney was exposed, de-capsulated and immobilized in a Lucite kidney cup (K. Effenberger, Pfaffingen, Germany) via a 4 cm incision in the left flank. Renal vessels were carefully separated to preserve the nerves and adrenal gland. An ultrasonic flow probe was placed around the left renal artery (type 0.7 RB; Transonic Systems Inc., Ithaca, NY, USA) and connected to a flow meter (T206; Transonic Systems Inc.) to continuously measure renal blood flow (RBF). The left ureter was isolated, ligated and cannulated with a polyethylene catheter for urine collection.

After the surgical procedure (approximately 60 minutes), one optical fibre was placed above the de-capsulated kidney and another one above the renal vein to measure oxygenation using a phosphorescence lifetime technique (18). A small piece of aluminium foil was placed on the dorsal side of the renal vein to prevent the contribution of the underlying tissue toward the phosphorescence signal in the venous PO_2 measurement. Oxyphor G2 (a two-layer glutamate dendrimer of tetra-(4-carboxy-phenyl) benzoporphyrin; Oxygen Enterprises Ltd, Philadelphia, PA, USA) was subsequently infused (6 mg kg^{-1} IV over 5 min), followed by a 30-minute stabilization period. The surgical field was covered with a humidified gauze compress throughout the experiment to prevent drying of the exposed tissue.

Experimental protocol

After a stabilization period, the animals were bled from the left femoral artery catheter at a rate of 1 ml min^{-1} using a syringe pump (Harvard 33 syringe pump; Harvard apparatus, South Natick, MA) until reaching a MAP of 30 mmHg. This was maintained for 1 hour by re-infusing or withdrawing blood. Coagulation of the shed blood was prevented by adding 200 UI of heparin in the syringe. The animals were then randomized into a total of 12 groups: 4 groups for a 60-min fluid resuscitation process using RL, RA, RA-Glu/Mg or 0.9% NaCl (Saline) until a target MAP of 65 mmHg was reached, 2 hemorrhagic shock (HS) groups, as well as 2 control groups, both with and without PLR, were observed. The fluid infused was prepared in advance and blinded to the technician (B.E). However, only one technician performed the experiments therefore the blinding was only partial. Each group included six animals ($n = 6$). The resuscitation fluid was infused at a rate of 0.5 ml min^{-1} . Measurements were made at baseline (BL); 60 minutes after initiation of hemorrhagic shock (Shock); and the end of the experiment, which was 60 minutes after starting resuscitation (R60). The right kidney, the heart and the brain were harvested to determine their water content using the wet/dry weighing technique (held at 100°C for 24 h) and calculated as follows: $((\text{wet tissue weight} - \text{dry tissue weight}) / \text{wet tissue weight}) / 100$.

Blood gas measurements, acid-base balance, and osmolality

Arterial blood samples (0.2 ml) were taken at five separate time points. Arterial blood gas parameters were determined using a blood gas analyser (ABL505 Flex, Radiometer, Copenhagen, Denmark), and hemoglobin concentration (Hb), hemoglobin oxygen saturation, base excess (BE) and the concentrations of sodium and chloride were measured. Plasma creatinine, chloride, potassium content, aspartate transaminase (AST) and urine creatinine and urine Na^+ (U_{Na}) samples were measured using an automatic analyser (Roche Modular P800 automatic analyser, Roche Diagnostics, Basel, Switzerland) at the end of the experiment. The osmolality of the plasma was determined using the freezing point method with an osmotic pressure meter (OSMOSTATION, OM-6050; Arkray Europe, Amstelveen, The Netherlands) at the end of the experiment.

Supplementary Table 1. Physico-chemical properties of fluids used in the study compared to human plasma

	Plasma	Normal saline (9‰)	Ringer's Lactate (RL)	Ringer's Acetate (RA)	Plasma-Lyte (RA-Glu/Mg)
Sodium (mmol L ⁻¹)	142	154	131	130	140
Chloride (mmol L ⁻¹)	103	154	111	110	98
Potassium (mmol L ⁻¹)	4.5		5	4	5
Calcium (mmol L ⁻¹)	2.5		2	2	
Magnesium (mmol L ⁻¹)	1.25			1	1.5
Lactate (mmol L ⁻¹)	1.5		29		
Acetate (mmol L ⁻¹)				30	27
Gluconate (mmol L ⁻¹)					23
HCO ₃ (mmol L ⁻¹)	24				
Albumin	30-52				
Proteinate	20				
Effective Strong Ion Difference	24	0	29	27	50
Theoretical osmolarity (mosmol L ⁻¹)	291	308	276	277	294.5
Water content (%)	94	99.7	99.7	99.7	99.7
Theoretical osmolality (mosmol kg ⁻¹)	310	308	276	276	294.5
Osmotic coefficient	0.926	0.926	0.926	0.926	0.926
Actual osmolality (mosmol kg ⁻¹)	287	286	256	256	272.7

Measurement of renal microvascular and venous oxygenation

Renal microvascular PO₂ (μPO₂) and renal venous PO₂ (P_{rv} O₂) were measured by oxygen-dependent quenching of phosphorescence lifetimes of the systemically infused albumin-targeted (and therefore circulation-confined) phosphorescent dye Oxyphor G2 as described elsewhere (18). The saturation of renal venous blood (S_{rv} O₂) was determined by Hill's equation with an *n* coefficient of 2.3.

Calculation of oxygenation parameters and vascular resistance

Renal oxygen delivery was calculated as DO_{2ren} (ml minute⁻¹) = RBF×arterial oxygen content (1.31×hemoglobin×S_a O₂)+(0.003×P_a O₂), where S_a O₂ is the arterial oxygen saturation, and P_a O₂ is the arterial partial pressure of oxygen. Renal oxygen consumption was calculated as VO_{2ren} (ml minute⁻¹ g⁻¹) = RBF×(arterial–renal venous oxygen content difference). Renal venous oxygen content was calculated as (1.31×hemoglobin×S_{rv} O₂)+(0.003×P_{rv} O₂).

Assessment of kidney function

The glomerular filtration rate was estimated with the calculation of creatinine clearance (Cl_{clear}): Cl_{clear} = (U_{crea} × V)/P_{crea}, where U_{crea} is the concentration of creatinine in urine, V is the urine volume per unit time, and P_{crea} is the concentration of creatinine in plasma.

All urine samples were analysed for sodium concentration (Na^+). In addition, the fractional excretion of Na^+ (EFNa^+ (%)) was calculated and used as a marker of tubular function using the following formula: $\text{EFNa}^+ = (\text{U}_{\text{Na}} \times \text{P}_{\text{crea}}) / (\text{P}_{\text{Na}} \times \text{U}_{\text{crea}}) \times 100$, where U_{Na} is the (Na^+) in urine, and P_{Na} is the (Na^+) in plasma. Cl_{clear} and EFNa^+ were determined at all time points.

Measurements of lactate, gluconate and acetate in plasma and urine

The plasma and urine lactate concentrations were determined by test strips (EDGE™ Handheld Lactate Analyser, Red Med, Poland). The D-Gluconate/D-Glucono- δ -lactone assay kit (detection limit 0.5 mg/L) and acetic acid assay kit (detection limit 0.14 mg/L) (Megazyme International Ireland, Bray Business Park, Bray, Co. Wicklow, Ireland) were used to determine the plasma, urine gluconate and acetate concentrations. Briefly, this is based on an enzymatic UV (spectrophotometric at 340 nm) method using 2 enzymes, the gluconate kinase and the gluconate-6-phosphate dehydrogenase.

Statistical analysis

Statistical analysis was performed using GraphPad Prism version 6.1 for Windows (GraphPad Software, San Diego, CA). Values are reported as the mean \pm SD in the tables and are presented with box and whiskers (min – max). ANOVA for repeated measurements was used for intergroup and intragroup comparisons using *post hoc* analyses with the Bonferroni's post-test where $p < 0.01$. One-way variance analyses with parametric or non-parametric tests were used for the biochemical results, and *post hoc* analyses with Bonferroni's post-test were conducted when $p < 0.01$ was considered significant. We deliberately chose an alpha level of 0.01 to emphasize the significance of the results.

RESULTS

Systemic and renal hemodynamics (Table 1) and all the other parameters were similar in the PLR group and the control group at baseline (Table 2). The PLR procedure resulted in a significant increase in the liver AST enzyme compared to the control and HS groups ($p < 0.01$) even in the resuscitated groups (Supplementary Figure 1).

Hemorrhagic shock in both experiments (with and without PLR) induced significant decreases in MAP, RBF (Table 1), pH, base excess, HCO_3^- (Table 1), VO_2 , DO_2 , $\text{C}\mu\text{PO}_2$, and $\text{M}\mu\text{PO}_2$ (Supplementary Figure 2) ($p < 0.01$). Hemorrhage resulted in increased concentrations of lactate with a higher anion gap ($p < 0.01$) (Table 2, Figure 1). The level of lactate was similar at shock between the 2 experiments. During hemorrhage, all rats presented anuria.

Table 1. Systemic and renal hemodynamics during hemorrhagic shock with and without partial liver resection.

	Baseline	Shock	R60
MAP (mmHg)			
Control	101 ± 10	106 ± 8	89 ± 11
HS	103 ± 12	31 ± 1 *	27 ± 3 *
HS+RL	101 ± 11	30 ± 1 *	63 ± 7 **
HS+RA	106 ± 13	30 ± 1 *	66 ± 0 **
HS+RA-Glu/Mg	99 ± 9	31 ± 1 *	62 ± 4 *
HS+Saline	104 ± 17	30 ± 1 *	66 ± 1 **
PLR	91 ± 11	92 ± 10 *	71 ± 4 *
PLR+HS	98 ± 7	31 ± 1 *	30 ± 4 *
PLR+HS+RL	102 ± 6	31 ± 1 *	65 ± 1 **
PLR+HS+RA	99 ± 6	31 ± 1 *	65 ± 1 **
PLR+HS+RA-Glu/Mg	91 ± 8	30 ± 1 *	60 ± 5 **
PLR+HS+Saline	99 ± 10	30 ± 1 *	65 ± 1 **
RBF (mL min⁻¹)			
Control	5.5 ± 1.3	4.5 ± 1.0	4.3 ± 1.0
HS	6.2 ± 1.9	0.6 ± 0.5 *	0.3 ± 0.5 *
HS+RL	7.3 ± 1.4	0.0 ± 0.0 *	4.2 ± 1.2 +
HS+RA	6.9 ± 1.8	0.3 ± 0.6 *	4.4 ± 1.6 +
HS+RA-Glu/Mg	4.9 ± 2.2	0.2 ± 0.2 *	3.6 ± 2.2 +
HS+Saline	7.7 ± 1.4 *	0.0 ± 0.0 *	4.2 ± 0.8 +
PLR	5.7 ± 1.5	5.0 ± 1.5	3.7 ± 0.9
PLR+HS	6.5 ± 1.0	0.3 ± 0.4 *	0.6 ± 0.5 *
PLR+HS+RL	6.7 ± 1.3	0.1 ± 0.1 *	3.5 ± 1.2 +
PLR+HS+RA	5.6 ± 0.5	0.0 ± 0.0 *	4.5 ± 1.2 +
PLR+HS+RA-Glu/Mg	6.3 ± 1.3	0.1 ± 0.2 *	4.2 ± 2.2 +
PLR+HS+Saline	5.3 ± 0.9	0.0 ± 0.0 *	3.4 ± 1.4 +

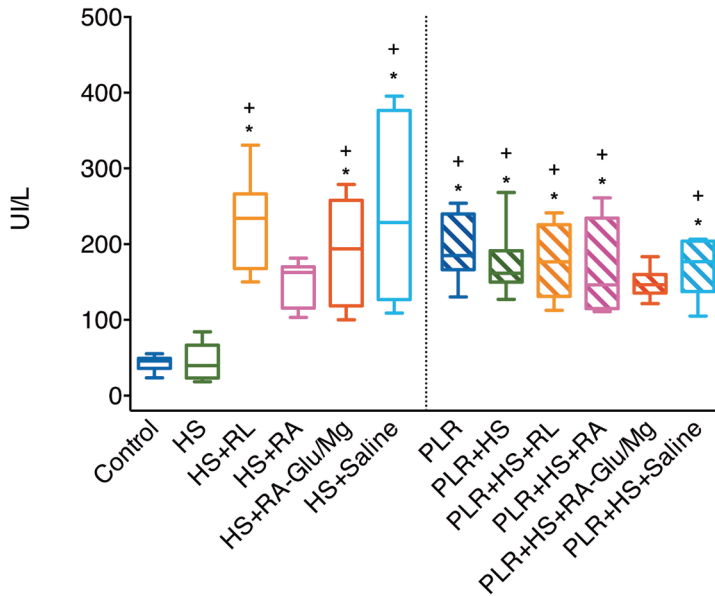
Values are represented as Mean ± SD, *p<0.01 vs. Control group; + p< 0.01 vs. HS group.

Abbreviations: MAP; mean arterial pressure, RBF; renal blood flow, HS; hemorrhagic shock, PLR; partial liver resection, RL; Ringer's lactate, RA; Ringer's Acetate, RA-Glu/Mg; PlasmaLyte.

The targeted MAP of 65 mmHg was achieved in both experiments after fluid resuscitation, regardless of the fluid used. The amounts of fluid required to achieve the targeted MAP were 28.5±5.9 ml for RL, 36.3±5.1 ml for RA, 44.7±10.4 ml for RA-Glu/Mg, and 28.0±8.8 ml for saline in the group without PLR. In the group with PLR, the amounts were 38.2±6.5 ml for RL, 45.9±9.3 ml for RA, 51.5±11.4 ml for RA-Glu/Mg, and 35±10.9 ml for saline. The volume of RA-Glu/Mg infused was significantly greater in both groups compared to the volumes of saline and RL (p<0.01).

Concentrations of bicarbonate precursors and acid-base status after fluid resuscitation

The lactate and gluconate concentrations in plasma at the end of both experiments are shown in Figure 1 and 2. The acetate level was not detectable in the plasma because the



Supplementary Figure 1. Plasma AST at the completion of the experiments. Data is presented in box and whiskers are (min-max), * $p < 0.01$ vs. Control group, + $p < 0.01$ vs. HS group.

level was below the threshold. Fluid resuscitation with either RA, RA-Glu/Mg or normal saline was effective in reducing lactate concentrations in experiment without PLR, but such a reduction was not achieved when RL was infused ($p < 0.01$). In the PLR experiment, the level of lactate in urine was higher in the RL group ($p < 0.01$) (Supplementary Figure 2). Gluconate was excreted in a similar manner in urine in the 2 experiments (Figure 2). However, plasma gluconate level was higher in the PLR group ($p = 0.03$). No significant change was observed in acetate excretion.

Acetate-based fluids resuscitation led to similar pH and bicarbonate concentrations to control group and increased bicarbonate concentrations more than RL or normal saline did in the PLR experiment ($p < 0.01$) (Table 2). Normal saline group in both experiments exhibited the worst acid-base status ($p < 0.01$). PaCO_2 did not change across experiments (Supplementary Table 2).

Renal oxygenation and function

CuPO_2 and $\text{M}\mu\text{PO}_2$ decreased during the hemorrhagic phase to ~ 2.7 and ~ 1.9 kPa (20 and ~ 14 mmHg), respectively. Overall, fluid resuscitation did not restore renal oxygenation to baseline ($p < 0.01$) (Supplementary Figure 3). $\text{DO}_{2\text{ren}}$ remained also significantly lower than the control group ($p < 0.01$) at the end of all experiments.

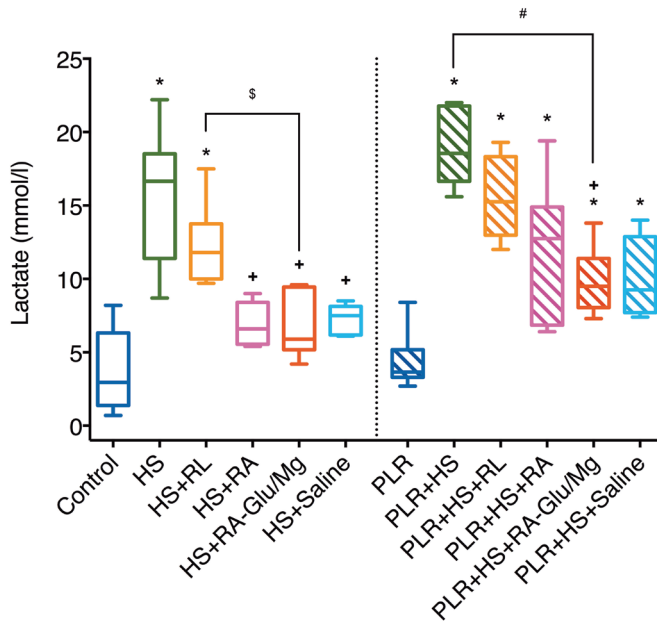


Figure 1. Concentrations of plasma lactate at the end of both experiments. Data is presented in box and whiskers are (min-max), * $p<0.01$ vs. Control group, + $p<0.01$ vs. HS group, § $p<0.01$ vs. HS+RA-Glu/Mg for resuscitation fluids within intact liver groups, # $p<0.01$ vs. PLR+HS+RA-Glu/Mg for resuscitation fluids within liver resection groups. HS; hemorrhagic shock, PLR; partial liver resection, RL; Ringer's lactate, RA; Ringer's Acetate, RA-Glu/Mg; PlasmaLyte.

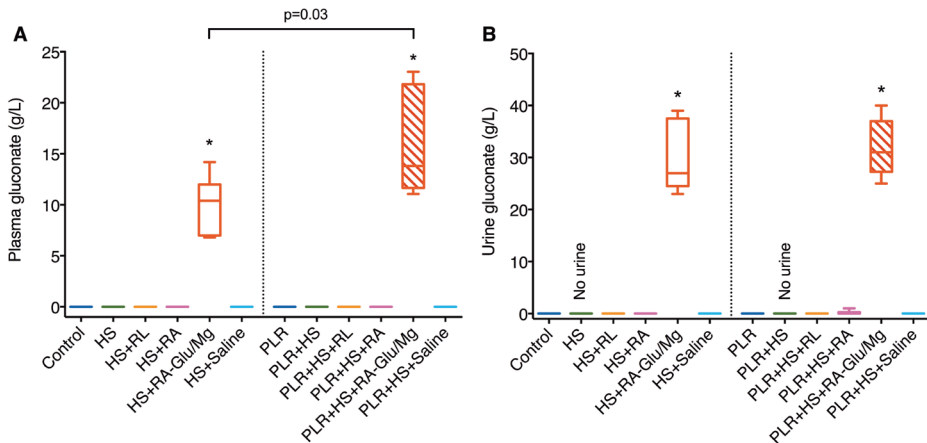
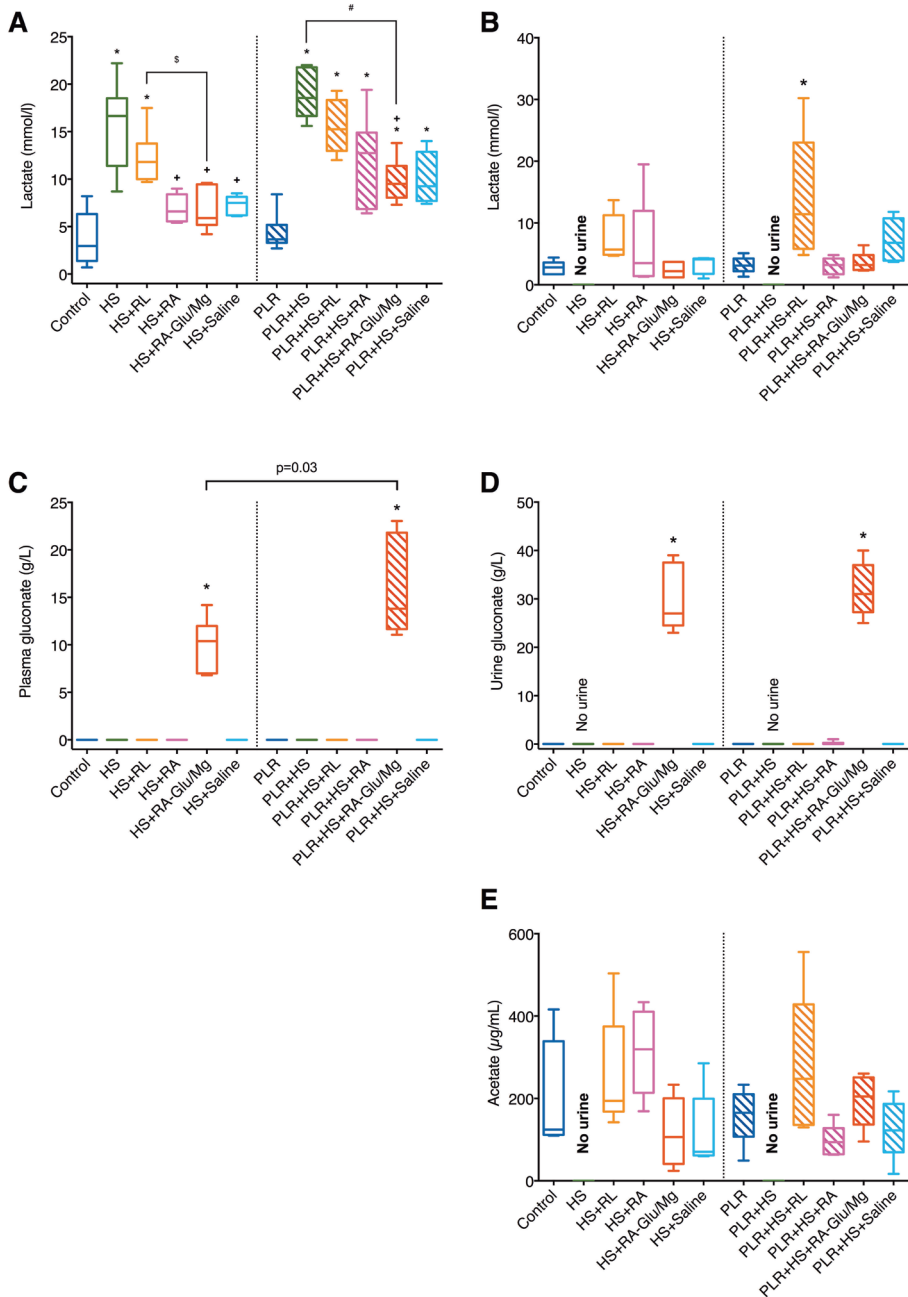


Figure 2. Concentrations of plasma (A) and urine (B) gluconate at the end of both experiments. Data is presented in box and whiskers are (min-max), * $p<0.01$ vs. Control group. HS; hemorrhagic shock, PLR; partial liver resection, RL; Ringer's lactate, RA; Ringer's Acetate, RA-Glu/Mg; PlasmaLyte.



Supplementary Figure 2. Concentrations of lactate, gluconate and acetate measured in plasma and urine. Acetate could not be detected in plasma. Data is presented in box and whiskers are (min-max), * p<0.01 vs. Control group, § p<0.01 vs. HS group, § p<0.01 vs. HS+RA-Glu/Mg for resuscitation fluids within intact liver groups, # p<0.01 vs. PLR+HS+RA-Glu/Mg for resuscitation fluids within liver resection groups.

Table 2. Acid-base status, anion gap, and chloride levels.

	Baseline	Shock	R60
pH			
Control	7.42 ± 0.02	7.36 ± 0.03	7.37 ± 0.04
HS	7.41 ± 0.02	7.12 ± 0.10 *	7.09 ± 0.09 *
HS+RL	7.39 ± 0.03	7.08 ± 0.09 *	7.25 ± 0.05 **
HS+RA	7.40 ± 0.04	7.06 ± 0.10 *	7.28 ± 0.03 **
HS+RA-Glu/Mg	7.39 ± 0.05	7.15 ± 0.09 *	7.31 ± 0.05 +
HS+Saline	7.40 ± 0.03	7.13 ± 0.29 *	7.18 ± 0.04 **\$
PLR	7.41 ± 0.03	7.34 ± 0.04	7.35 ± 0.05
PLR+HS	7.39 ± 0.04	7.11 ± 0.07 *	7.06 ± 0.07 *
PLR+HS+RL	7.40 ± 0.04	7.12 ± 0.05 *	7.22 ± 0.12 **
PLR+HS+RA	7.40 ± 0.02	7.12 ± 0.07 *	7.29 ± 0.09 +
PLR+HS+RA-Glu/Mg	7.40 ± 0.02	7.10 ± 0.06 *	7.30 ± 0.04 +
PLR+HS+Saline	7.40 ± 0.04	7.06 ± 0.10 *	7.14 ± 0.09 **
HCO₃⁻ (mmol L⁻¹)			
Control	19.6 ± 1.8	17.9 ± 1.9	16.3 ± 2.5
HS	19.6 ± 1.6	10.0 ± 2.0 *	8.6 ± 1.9*
HS+RL	20.3 ± 2.2	9.7 ± 1.9 *	14.6 ± 2.5+
HS+RA	19.6 ± 2.9	8.7 ± 2.1 *	15.0 ± 1.7+
HS+RA-Glu/Mg	20.1 ± 2.0	10.0 ± 1.1 *	15.9 ± 1.7+
HS+Saline	18.3 ± 1.1	9.2 ± 1.2 *	11.5 ± 1.1 **\$
PLR	20.3 ± 0.9	18.3 ± 1.3	17.2 ± 1.0
PLR+HS	19.9 ± 2.1	9.20 ± 1.8 *	9.00 ± 1.6*
PLR+HS+RL	20.0 ± 1.4	9.30 ± 1.5 *	13.40 ± 2.0**#
PLR+HS+RA	19.9 ± 1.8	10.10 ± 0.7 *	15.50 ± 1.1 +
PLR+HS+RA-Glu/Mg	20.6 ± 1.4	9.50 ± 2.2 *	16.40 ± 1.6 +
PLR+HS+Saline	19.7 ± 2.5	8.60 ± 1.8 *	11.50 ± 2.5 **#
Anion gap (K⁺) (mmol L⁻¹)			
Control	21.7 ± 2.4	24.5 ± 3.2	24.5 ± 4.0
HS	21.1 ± 2.7	30.4 ± 3.0*	33.8 ± 2.4 *
HS+RL	21.5 ± 2	31.6 ± 2.6*	26.0 ± 1.8 +
HS+RA	22.2 ± 3	34.3 ± 5.5*+	26.6 ± 3.7 +
HS+RA-Glu/Mg	20.4 ± 1.7	30.6 ± 3.1*	25.3 ± 1.9 +
HS+Saline	22.0 ± 2.1	33.0 ± 3.4*	28.1 ± 2.8 **\$
PLR	24.4 ± 1.8	27.4 ± 1.5*	28.8 ± 2.2 *
PLR+HS	21.8 ± 1.3	31.6 ± 2.3*	34.4 ± 1.8 *
PLR+HS+RL	21.9 ± 1.5	32.1 ± 2.2*	29.2 ± 2.2 **\$
PLR+HS+RA	22.0 ± 1.0	33.0 ± 2.6*	26.6 ± 1.0 +
PLR+HS+RA-Glu/Mg	21.3 ± 2.9	33.0 ± 1.5*	27.3 ± 1.6 +
PLR+HS+Saline	22.4 ± 0.7	34.7 ± 2.3*+	29.9 ± 1.3 **#
Cl⁻ (mmol L⁻¹)			
Control	107.5 ± 0.8	111.5 ± 2.3	115.0 ± 1.4
HS	108.2 ± 2.7	112.5 ± 4.2	114.5 ± 1.4
HS+RL	106.3 ± 1.0	110.0 ± 1.6	112.0 ± 0.9
HS+RA	107.5 ± 3.2	108.8 ± 3.7 +	111.0 ± 1.8 **

Table 2. Continued

	Baseline	Shock	R60
HS+RA-Glu/Mg	108.0 ± 2.5	112.5 ± 2.4	110 ± 2.28 **
HS+Saline	109.3 ± 2.6	111.5 ± 2.5	119.2 ± 2.3 **§
PLR	106.6 ± 0.6	110.0 ± 1.0	113.0 ± 1.0
PLR+HS	109.2 ± 1.8	114.2 ± 1.1	116.6 ± 2.0
PLR+HS+RL	108.0 ± 1.3	114.3 ± 1.4	112.3 ± 2.2 #
PLR+HS+RA	108.2 ± 2.8	115.2 ± 1.9 *	112.5 ± 1.8 #
PLR+HS+RA-Glu/Mg	109.5 ± 2.4	116.2 ± 1.8 **	108.7 ± 1.0 **
PLR+HS+Saline	108.3 ± 1.4	114.3 ± 1.2	118.7 ± 1.7 **#

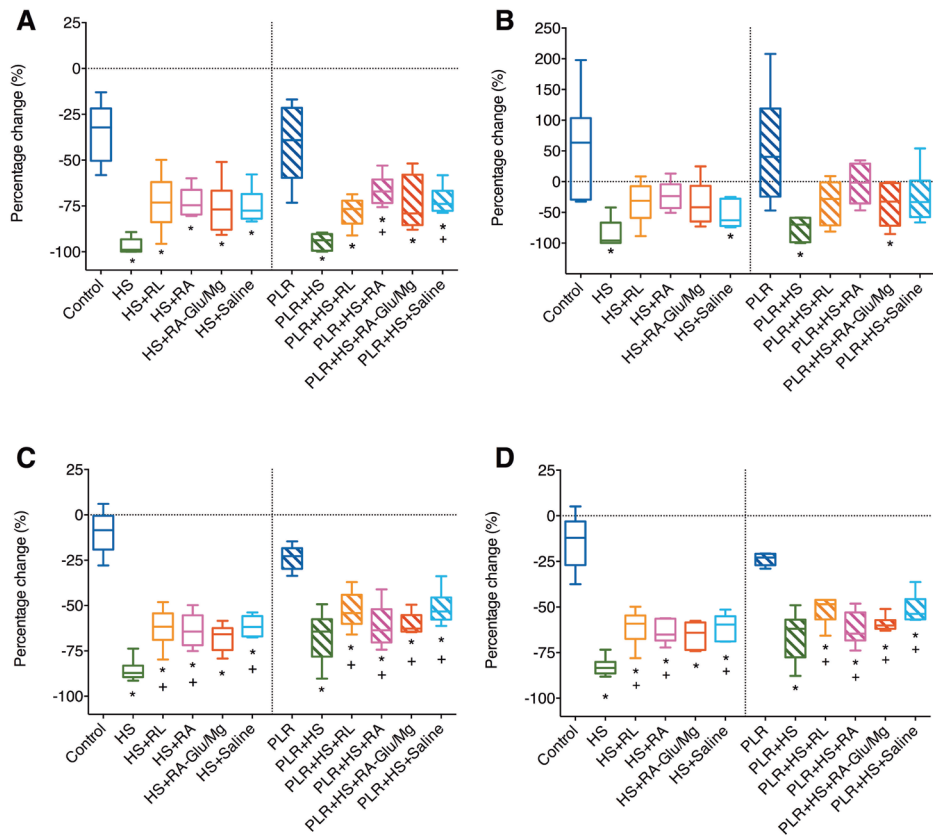
Values are presented as a Mean ± SD, *p<0.01 vs. Control group, # p< 0.01 vs. HS group, § p<0.01 vs. HS+RA-Glu/Mg, # p<0.01 vs. PLR+HS+RA-Glu/Mg group.

Abbreviations: HS; hemorrhagic shock, PLR; partial liver resection, RL; Ringer's lactate, RA; Ringer's Acetate, RA-Glu/Mg; PlasmaLyte.

Supplementary Table 2. Base excess and carbon dioxide partial pressure trends.

	Baseline	Shock	R60
PaCO₂ (mmHg)			
Control	4.3 ± 0.4	4.4 ± 0.3	3.9 ± 0.5
HS	4.3 ± 0.4	4.3 ± 0.8	3.9 ± 0.5
HS+RL	4.7 ± 0.4	4.4 ± 0.5	4.8 ± 0.4
HS+RA	4.4 ± 0.9	4.3 ± 0.9	4.4 ± 0.5
HS+RA-Glu/Mg	4.7 ± 1.1	4.1 ± 0.9	4.4 ± 0.4
HS+Saline	4.1 ± 0.3	4.8 ± 0.5	4.3 ± 0.3
PLR	4.4 ± 0.1	4.7 ± 0.5	4.4 ± 0.7
PLR+HS	4.5 ± 0.4	4 ± 0.5	4.4 ± 0.5
PLR+HS+RL	4.5 ± 0.3	3.9 ± 0.4	4.7 ± 1.7
PLR+HS+RA	4.4 ± 0.5	4.3 ± 0.4	4.5 ± 1.3
PLR+HS+RA-Glu/Mg	4.7 ± 0.3	4.3 ± 0.4	4.7 ± 0.7
PLR+HS+Saline	4.4 ± 0.4	4.1 ± 0.1	4.7 ± 0.7
Base excess (mmol L⁻¹)			
Control	-4.2 ± 1.8	-6.6 ± 2.1	-8.1 ± 2.7
HS	-4.3 ± 1.6	-17.5 ± 2.9*	-19.4 ± 2.9*
HS+RL	-3.9 ± 2.4	-18.3 ± 2.9*	-11.3 ± 3.0 *
HS+RA	-4.5 ± 2.5	-19.6 ± 2.9*	-10.5 ± 1.8 *
HS+RA-Glu/Mg	-4.1 ± 1.6	-17.3 ± 1.6*	-9.2 ± 2.1 *
HS+Saline	-5.7 ± 1.3	-19.4 ± 2.0*	-15.2 ± 1.5 **§
PLR	-3.6 ± 1.3	-6.3 ± 1.5	-7.3 ± 1.0
PLR+HS	-4.2 ± 2.3	-18.4 ± 2.6*	-19.3 ± 2.3 *
PLR+HS+RL	-4.0 ± 1.6	-18.2 ± 2.1*	-12.9 ± 3.0 **#
PLR+HS+RA	-4.1 ± 1.7	-17.3 ± 1.5*	-10.6 ± 2.5 *
PLR+HS+RA-Glu/Mg	-3.5 ± 1.6	-18.3 ± 3.0*	-8.8 ± 1.7 *
PLR+HS+Saline	-4.3 ± 2.8	-19.6 ± 2.8*	-15.7 ± 3.5 **#

Values are presented as a Mean±SD, *p<0.01 vs. Control group, # p< 0.01 vs. HS group, § p<0.01 vs. HS+RA-Glu/Mg for resuscitation fluids within intact liver groups, # p<0.01 vs. PLR+HS+RA-Glu/Mg for resuscitation fluids within liver resection groups.



Supplementary Figure 3. Percentage changes in cortical and medullary kidney oxygenation and renal oxygen delivery and consumption from baseline to the end of experiment (R60). (A) Cortical kidney micro PO_2 ($\text{C}\mu\text{PO}_2$), (B) medullary kidney micro PO_2 ($\text{M}\mu\text{PO}_2$), (C) renal oxygen delivery ($\text{DO}_{2\text{ren}}$), (D) renal oxygen consumption ($\text{VO}_{2\text{ren}}$). Data is presented in box and whiskers are (min-max), * $p < 0.01$ vs. Control group, + $p < 0.01$ vs HS group.

Renal function, as represented by EFNa^+ and creatinine clearance (Cl_{creat}), is shown in Table 3. There was no difference relative to the control group in the PLR experiment. FE_{Na} increased significantly in all groups after fluid resuscitation ($p < 0.01$) by the end of the experiment.

Fluid resuscitation resulted in increases in water content and tissue oedema in the kidney from $78.1 \pm 0.4\%$ for the control group to $81.1 \pm 0.6\%$, $81.1 \pm 1.2\%$, $82.1 \pm 0.6\%$, and $82.1 \pm 0.7\%$ for the RL, RA, RA-Glu/Mg, and saline groups, respectively, in the experiment without PLR ($p < 0.01$). The same was observed in rats with liver resection ($p < 0.01$). Finally, the plasma osmolality was higher only in the RA-Glu/Mg group with PLR ($p < 0.01$).

Table 3. Renal function according to different balanced fluid resuscitations in animals with and without partial liver resection. The shock time point was removed from the table because almost all animals presented anuria.

	Baseline	R60
Cl_{creat} (ml min⁻¹ g⁻¹)		
Control	0.14 ± 0.05	0.16 ± 0.09
HS	0.09 ± 0.08	/
HS+RL	0.16 ± 0.15	0.06 ± 0.05*
HS+RA	0.16 ± 0.04	0.07 ± 0.05
HS+RA-Glu/Mg	0.14 ± 0.03	0.09 ± 0.05
HS+Saline	0.11 ± 0.07	0.08 ± 0.04
PLR	0.10 ± 0.04	0.06 ± 0.04*
PLR+HS	0.09 ± 0.06	/
PLR+HS+RL	0.10 ± 0.04	0.16 ± 0.21
PLR+HS+RA	0.13 ± 0.05	0.13 ± 0.06
PLR+HS+RA-Glu/Mg	0.25 ± 0.37	0.14 ± 0.08
PLR+HS+Saline	0.09 ± 0.03	0.07 ± 0.02
EFNa⁺ (%)		
Control	2 ± 0.9	2.9 ± 2
HS	1.6 ± 0.9	/
HS+RL	2.7 ± 3.2	24 ± 8.9*
HS+RA	2.4 ± 1.6	32.5 ± 17.7*
HS+RA-Glu/Mg	2.1 ± 3.2	51 ± 15.6*
HS+Saline	4.6 ± 4.5	35.1 ± 18.8*
PLR	1.5 ± 1.4	2 ± 2
PLR+HS	1.6 ± 0.6	/
PLR+HS+RL	1.5 ± 1	32.9 ± 39*
PLR+HS+RA	1.3 ± 0.6	46 ± 36.3*
PLR+HS+RA-Glu/Mg	2 ± 1.3	45.2 ± 11*
PLR+HS+Saline	1.6 ± 1.5	58.1 ± 28.9*

Values are presented as a Mean ± SD, * p<0.05 vs. Control group.

Abbreviations: Cl_{creat}; creatinine clearance, EFNa⁺; fractional excretion of Na⁺, HS; hemorrhagic shock, PLR; partial liver resection, RL; Ringer's lactate, RA; Ringer's Acetate, RA-Glu/Mg; PlasmaLyte.

DISCUSSION AND CONCLUSION

The main results of our study were that acetate-balanced resuscitation fluids demonstrated a significant improved buffering capacity in the presence or absence of liver impairment. Ringer's lactate was also effective in correcting the acid-base status but to a lesser degree. Normal saline was the less effective fluid regarding acid-base control. Secondly, our study showed an increased plasma level of gluconate in the presence of liver failure (e.g., PLR), suggesting that this portion is actually metabolized by the liver while the other part potentially remains in the vascular system (19). In this respect, two recent studies have confirmed that gluconate is metabolized through gluconokinase in the human liver into 6-phosphogluconate, which could then be further degraded through the hexose

monophosphate shunt via the 6-phosphogluconate dehydrogenase (20,21). Although our results did not indicate an increase in gluconate excretion by the kidney after PLR, a large amount of gluconate was excreted in urine as previously observed (22,23). Two separate experimental studies showed no increase in the pH value after an infusion of gluconate (24,25). These suggest that gluconate is not relevant for the generation of bicarbonate. Therefore, the “anti-acidotic” effect of RA-Glu/Mg might not be due to gluconate, but rather attributed to acetate.

Acetate was metabolized effectively, regardless of liver failure and severe shock in this study. This confirms that acetate is metabolized elsewhere or that limited hepatic function is sufficient to support bicarbonate generation. Acetate can be metabolized in several extra-hepatic tissues, including the muscles, brain, myocardium, and renal cortex, because they all have the required enzymes (15,17). Therefore, acetate is subject to less accumulation in states of shock with impaired liver function. However, the literature provided inconsistent results regarding the buffering capacity of acetate-balanced fluids. In addition, an *in vitro* study revealed that the buffering capacity of these fluids was weak compared to human or animal plasma (26). Fluid resuscitation with RA-Glu/Mg yielded a similar buffering effect to RL but lower survival rate following fatal hemorrhage in swine (27). In a randomized clinical trial comparing RA-Glu/Mg versus RL during living donor right hepatectomy, a small improvement in base excess was noted without change in pH (28). Weinberg *et al.* observed less hyperchloremia and hyperlactatemia but also with no change in pH or base excess after infusion of RA-Glu/Mg compared to normal saline in patients with major liver resection (29). On the contrary, two studies, in trauma patients and in the perioperative setting, provided evidence of an improved acid-base status using RA-Glu/Mg (12,30).

As expected, lactate concentrations increased during hemorrhagic shock. Measured lactate concentrations were influenced by the additional lactate supplied by resuscitation with RL. In addition, PLR reduced the capacity of lactate to be metabolized as shown by the trend increase in urine lactate. It may have a negative impact on the acid-base balance when it accumulates. Nevertheless, RL was superior to normal saline in terms of correcting acid-base status even in the presence of liver failure. This result was consistent with the literature (31).

The issue about the choice of anions in resuscitation fluids has been central in the “Great fluid debate” and has mainly focused itself on the choice of chloride as the conventional anion in the routine use of 0.9% NaCl (13,32). The reason for the controversy has been the result of dilutional acidosis being caused by excessive amounts of chloride administration during fluid resuscitation. The effect of this procedure results in acidosis

not being corrected and possibly metabolic acidosis becoming dilutional acidosis causing confusion as to the origin of the acid base disturbance. On the other hand, acidosis in itself can have unwanted effects, such as renal vasoconstriction, and this can cause deleterious effects especially on the kidney. For these reasons balanced salt solutions such based on either acetate or lactate have been advocated also because these anions can function as bicarbonate precursors (9). Finally, the importance of the ability of clinicians to interpret the origin of acidosis as being metabolic in origin allows its use as a surrogate for tissue oxygenation and is an additional importance for understanding the contribution of various anions to acid base chemistry in a physiological setting such as we chose for this study.

All fluids improved systemic and renal hemodynamics after reaching the targeted MAP but failed to restore renal oxygenation as shown before (33). The ineffectiveness of the correction of renal oxygenation resides in the fact that these non-oxygen carrying fluids only marginally transport oxygen to the tissues (33,34). The differences between balanced solutions and normal saline for fluid were found to exist mainly in the acid-base imbalance. Because normal saline brought a large amount of chloride induced acid-base alteration, it could blunt the benefits of fluid resuscitation, as seen by its lack of efficacy at improving pH levels. While tissue oxygenation might be partially restored with efficient lactate clearance, the existence of a low pH and a low bicarbonate level may invite a further unrequired administration of fluid. This will contribute to increase the plasma level of chloride, prevent metabolic acidosis from being corrected, and increase the fluid load. However, in a large clinical trial including intensive care unit patients, Young *et al.* did not demonstrate beneficial outcomes of RA-Glu/Mg compared to normal saline, especially on the kidney (5).

Significantly more fluid was required to achieve a MAP of 65 mmHg when using acetate containing fluids. Acetate can cause vasodilation, which is presumably mediated by the release of adenosine from tissues (35,36), and these animals may require additional fluid. Moreover, magnesium present in RA-Glu/Mg may also induce vasodilation (37) and the combined action of both, acetate and magnesium, may decrease systemic resistance. However, it is unknown whether this amount of magnesium (3 mmol/L) can induce such a vasodilation, even though magnesium concentration is increased (29).

Regarding the limitations, we did not assess true liver function with an indocyanin green test. A 70% PLR might not be sufficient to induce a significant liver failure. However, in a pilot study, the animals did not survive in case of a larger resection. Although unlikely to have a clinical impact, we might have missed a change in plasma acetate concentrations, already low (0.06 to 0.2 mmol L⁻¹) (15), because it remained below the detection threshold

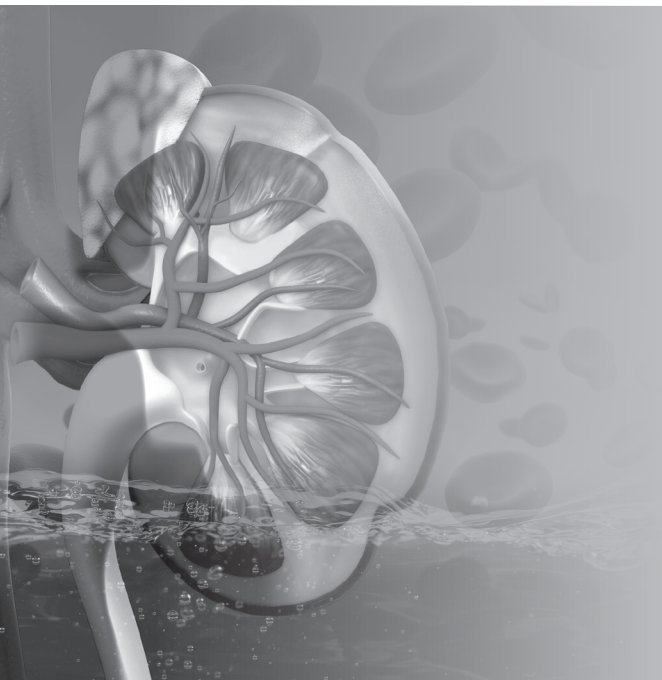
of our assay. We chose to administer 0.9% saline for fluid maintenance during liver surgery because we sought to evaluate the effect of anion buffers after PLR and HS and obtain same acid-base status at baseline (after PLR) in all animals. Although the experiment would have been purer, the infusion of normal saline was of similar amount in the different interventions in both experiments. By infusing the study fluid from the start of the surgery, baseline values recorded before hemorrhage might have differed significantly. Finally, although probably low, we cannot precisely state how much the gluconate accounted for the buffering effect during resuscitation.

In cases of hemorrhagic shock with liver failure, the subsequent accumulation of lactate dampened the buffering effect of RL. Acetate and the combination of acetate and gluconate appeared to be metabolized efficiently in this experimental study. Because of the large amount of gluconate excreted in an unchanged form, this anion may not contribute to the buffering effect. Normal saline seemed to be the most unsuitable fluid when compared to balanced fluids, even in cases of liver failure.

REFERENCES

1. Myburgh JA, Finfer S, Bellomo R, *et al.* Hydroxyethyl starch or saline for fluid resuscitation in intensive care. *N. Engl. J. Med.* 367: 1901–11, 2012.
2. Finfer S, Bellomo R, Boyce N, *et al.* A comparison of albumin and saline for fluid resuscitation in the intensive care unit. *N. Engl. J. Med.* 350: 2247–56, 2004.
3. Perner A, Haase N, Guttormsen AB, *et al.* Hydroxyethyl starch 130/0.42 versus Ringer's acetate in severe sepsis. *N. Engl. J. Med.* 367: 124–34, 2012.
4. Raghunathan K, Bonavia A, Nathanson BH, *et al.* Association between Initial Fluid Choice and Subsequent In-hospital Mortality during the Resuscitation of Adults with Septic Shock. *Anesthesiology* 123: 1385–93, 2015.
5. Young P, Bailey M, Beasley R, *et al.* Effect of a Buffered Crystalloid Solution vs Saline on Acute Kidney Injury Among Patients in the Intensive Care Unit: The SPLIT Randomized Clinical Trial. *JAMA* 314: 1–10, 2015.
6. Hammond NE, Taylor C, Saxena M, *et al.* Resuscitation fluid use in Australian and New Zealand Intensive Care Units between 2007 and 2013. *Intensive Care Med.* 41: 1611–9, 2015.
7. Cecconi M, Hofer C, Teboul J-L, *et al.* Fluid challenges in intensive care: the FENICE study: A global inception cohort study. *Intensive Care Med.* 41: 1529–37, 2015.
8. Boulain T, Boisrame-Helms J, Ehrmann S, *et al.* Volume expansion in the first 4 days of shock: a prospective multicentre study in 19 French intensive care units. *Intensive Care Med.* 41: 248–56, 2015.
9. Morgan TJ. The ideal crystalloid - what is 'balanced'? *Curr. Opin. Crit. Care* 19: 299–307, 2013.
10. Raghunathan K, Murray PT, Beattie WS, *et al.* Choice of fluid in acute illness: what should be given? An international consensus. *Br. J. Anaesth.* p. 772–83, 2014.
11. Rizoli S. PlasmaLyte. *J. Trauma* 70: S17–8, 2011.
12. Burdett E, Dushianthan A, Bennett-Guerrero E, *et al.* Perioperative buffered versus non-buffered fluid administration for surgery in adults. Burdett E, editor. *Cochrane Database Syst Rev.* Chichester, UK: John Wiley & Sons, Ltd; 12: CD004089, 2012.
13. Lobo DN, Awad S. Should chloride-rich crystalloids remain the mainstay of fluid resuscitation to prevent 'pre-renal' acute kidney injury?: con. *Kidney Int.* 86: 1096–105, 2014.
14. Morgan TJ, Power G, Venkatesh B, *et al.* Acid-base effects of a bicarbonate-balanced priming fluid during cardiopulmonary bypass: comparison with Plasma-Lyte 148. A randomised single-blinded study. *Anaesth. Intensive Care* 36: 822–9, 2008.
15. Ballard FJ. Supply and utilization of acetate in mammals. *Am. J. Clin. Nutr.* 25: 773–9, 1972.
16. Ewaschuk JB, Naylor JM, Zello GA. D-lactate in human and ruminant metabolism. *J. Nutr.* 135: 1619–25, 2005.
17. Knowles SE, Jarrett IG, Filsell OH, *et al.* Production and utilization of acetate in mammals. *Biochem. J.* 142:401–11, 1974.
18. Mik EG, Johannes T, Ince C. Monitoring of renal venous PO₂ and kidney oxygen consumption in rats by a near-infrared phosphorescence lifetime technique. *Am. J. Physiol. Renal Physiol.* 294: F676–81, 2008.
19. Diawoye, UNEPreport. Gluconic Acid and Its Derivatives. *OECD SIDS* 1–231, 2004.
20. Rolfsson Ó, Paglia G, Magnúsdóttir M, *et al.* Inferring the metabolism of human orphan metabolites from their metabolic network context affirms human gluconokinase activity. *Biochem. J.* 449: 427–35, 2013.
21. Rohatgi N, Nielsen TK, Bjørn SP, *et al.* Biochemical characterization of human gluconokinase and the proposed metabolic impact of gluconic acid as determined by constraint based metabolic network analysis. *PLoS ONE* 9: e98760, 2014.
22. Howard PJ, Wilde WS, Malvin RL. Localization of renal calcium transport; effect of calcium loads and of gluconate anion on water, sodium and potassium. *Am. J. Physiol.* 197: 337–41, 1959.
23. Stetten MR, Stetten D. The metabolism of gluconic acid. *J. Biol. Chem.* 187: 241–52, 1950.
24. Kirkendol PL, Starrs J, Gonzalez FM. The effects of acetate, lactate, succinate and gluconate on plasma pH and electrolytes in dogs. *Trans. Am. Soc. Artif. Intern. Organs* 26: 323–7, 1980.

25. Naylor JM, Forsyth GW. The alkalinizing effects of metabolizable bases in the healthy calf. *Can. J. Vet. Res.* 50: 509–16, 1986.
26. Traverso LW, Medina F, Bolin RB. The buffering capacity of crystalloid and colloid resuscitation solutions. *Resuscitation* 12: 265–70, 1985.
27. Traverso LW, Lee WP, Langford MJ. Fluid resuscitation after an otherwise fatal hemorrhage: I. Crystalloid solutions. *J. Trauma* 26: 168–75, 1986.
28. Shin W-J, Kim Y-K, Bang J-Y, *et al.* Lactate and liver function tests after living donor right hepatectomy: a comparison of solutions with and without lactate. *Acta. Anaesthesiol. Scand.* 55: 558–64, 2011.
29. Weinberg L, Pearce B, Sullivan R, *et al.* The effects of plasmalyte-148 vs. Hartmann's solution during major liver resection: a multicentre, double-blind, randomized controlled trial. *Minerva Anesthesiol.* 81: 1288–97, 2015.
30. Young JB, Utter GH, Schermer CR, *et al.* Saline versus Plasma-Lyte A in initial resuscitation of trauma patients: a randomized trial. *Ann. Surg.* 259: 255–62, 2014.
31. Orbegozo Cortés D, Rayo Bonor A, Vincent JL. Isotonic crystalloid solutions: a structured review of the literature. *Br. J. Anaesth.* 112: 968–81, 2014.
32. Ince C, Groeneveld ABJ. The case for 0.9% NaCl: is the undefendable, defensible? *Kidney Int.* 86: 1087–95, 2014.
33. Legrand M, Legrand M, Mik EG, *et al.* Fluid resuscitation does not improve renal oxygenation during hemorrhagic shock in rats. *Anesthesiology* 112: 119–27, 2010.
34. Johannes T, Mik EG, Nohé B, Unertl KE, *et al.* Acute decrease in renal microvascular PO₂ during acute normovolemic hemodilution. *Am. J. Physiol. Renal Physiol.* 292: F796–803, 2007.
35. Frohlich ED. Vascular Effects of the Krebs Intermediate Metabolites. *Am. J. Physiol.* 208: 149–53, 1965.
36. Nutting CW, Islam S, Ye MH, *et al.* The vasorelaxant effects of acetate: role of adenosine, glycolysis, lyotropism, and pHi and Cai²⁺. *Kidney Int.* 41: 166–74, 1992.
37. Teragawa H, Matsuura H, Chayama K, *et al.* Mechanisms responsible for vasodilation upon magnesium infusion in vivo: clinical evidence. *Magnes. Res.* 15: 241–6, 2002.



CHAPTER 12

The effect of anemia on intra-renal microcirculation in a pig model of acute normovolemic hemodilution

Bulent Ergin^{1,2}, Alex Lima¹, Tom van Rooij³, Yasin Ince^{1,2}, Patricia Specht⁴, Bert Mik⁴, Klazina Kooiman³, Nico de Jong^{3,5}, Can Ince^{1,2}.

¹ Department of Intensive Care Adults, Erasmus MC, Rotterdam, The Netherlands

² Department of Translational Physiology, Academic Medical Center, Amsterdam, The Netherlands

³ Department of Biomedical Engineering, Thorax Center, Erasmus MC, Rotterdam, The Netherlands

⁴ Laboratory of Experimental Anesthesiology, Department of Anesthesiology, Erasmus MC, Rotterdam, The Netherlands

⁵ Laboratory of Acoustical Wavefield Imaging, Department of Applied Sciences, Delft University of Technology, Delft, The Netherlands

ABSTRACT

Acute normovolemic hemodilution (ANH) is a technique used to reduce the requirement of allogeneic blood transfusions. However, reports have shown that ANH is associated with a reduction in renal oxygen delivery despite stable renal blood flow, suggesting that the kidney may be more vulnerable to hypoxic damage than the heart, brain, and spinal cord in ANH. Essential information is lacking of the influence of hemodilution on renal function and microvascular perfusion. The present study was designed to investigate the mechanisms underlying ANH-induced changes in intra-renal microcirculation and perfusion that subsequently cause acute kidney injury (AKI) and their relationship with macro-hemodynamic changes in pigs. Fully instrumented female Yorkshire pigs (27.2 ± 1.6 kg) were divided into two groups; those that underwent hemodilution (ANH, $n = 8$) and a control group (Ctr, $n = 7$). Hemodilution was performed by replacing blood with HES solution (6% Hydroxyethyl Starch 130/0.4, Voluven, Fresenius Kabi) till hematocrit levels reached 20% (T1), 15% (T2), and 10% (T3). Systemic hemodynamics and oxygenation were monitored, renal function and perfusion were visualized and quantified using contrast-enhanced ultrasound (CEUS) and laser speckle imaging (LSI), and the sublingual microcirculation was measured by means of Cytocam-IDF. Despite stable mean arterial pressure (MAP) during the entire study, we found that both HR ($p < 0.05$) and cardiac output (CO) ($p < 0.05$) were higher at hematocrit (Hct) 10%, while central venous pressure (CVP) ($p < 0.05$) and systemic vascular resistance (SVR) ($p < 0.05$) was significantly lower than the control group. No changes were found in oxygen delivery (DO_2) and oxygen consumption (VO_2). In parallel to the sublingual red blood cell (RBC) velocity results, CEUS parameters showed consistently that blood velocity was significantly higher in the kidney when Hct was decreased to 10% ($p < 0.05$). To conclude, together with systemic alterations, a reduced oxygen-carrying capacity and lower viscosity of the blood, higher intra-renal RBC velocity seems to be major contributors to renal hypoxia and finally AKI as a long-term consequence.

Keywords: pig, hemodilution, contrast-enhanced ultrasound, renal microcirculation.

INTRODUCTION

Hemodilution can occur as a result of fluid resuscitation in emergency situations (1), standard practice during cardiopulmonary bypass (2) or during elective surgery (3,4). For decades, there has been a debate concerning the efficiency of crystalloids or colloids in order to maintain the intravascular volume without causing the tissue edema, hyperchloremic acidosis, electrolytes imbalance, coagulopathy, allergic reaction, proinflammation and microcirculatory disturbance (5,6). Crystalloids are relatively insufficient as a plasma expander and need to be used larger amount to improve both intravascular volume and hemodynamic stability. However, colloids remain in vasculature for a longer time due to its oncotic effect and to be required 1:3 lesser amounts than crystalloids (7). Using the fluids can also lead to a decrease in the oxygen carrying capacity of the blood, which activates two compensatory mechanisms to meet the oxygen demands of organs: an increase in the cardiac output (CO) and an increase in oxygen extraction (ERO_2) (8). Although the tolerance of organ systems under conditions of decreased O_2 delivery (DO_2) varies, the compensatory system can balance O_2 delivery and consumption (VO_2) until oxygen delivery falls below the critical point (9). Practically, colloids might be more sufficient to prevent to decrease the oxygen delivery in this point. Moreover, hemodilution plays a central role in the disturbance of microcirculatory perfusion, which may lead to impaired tissue oxygenation, increased flow heterogeneity, and subsequent tissue injury (10).

Hemodilution has also been identified as an important risk factor in the development of acute kidney injury (AKI) among patients undergoing cardiopulmonary bypass (CPB) (11,12). It is well known that the kidney receives approximately one quarter of CO (13) and that DO_2 is in excess of the oxygen demand under normal conditions (9). Reports have shown that ANH is associated with a reduction in renal oxygen delivery despite stable renal blood flow, suggesting that the kidney may be more vulnerable to hypoxic damage than the heart, brain, and spinal cord in ANH (14). Findings from experimental studies have demonstrated that ANH with colloids reduces perfused vessel density (15), induces pro-inflammatory and procoagulant endothelial activation (16), but not impairs renal cortical and inner medullar oxygenation rather than crystalloids (7). Johannes *et al.* demonstrated that the oxygen supply to renal tissue is already critically altered in the early stage of colloid-mediated ANH in rats due to the combination of increased renal oxygen consumption, decreased renal oxygen delivery, and intra-renal O_2 shunting (17). However, there is limited information regarding the mechanisms underlying these intra-renal microcirculatory changes during colloid mediated ANH.

In the present study, we aimed to investigate the mechanism underlying the ANH with colloid-induced alteration in intra-renal microcirculation and perfusion, that can

subsequently cause AKI, and their relationship with macro-hemodynamic changes in pigs. For this purpose, the intra-renal and cortical microcirculation was assessed by contrast-enhanced ultrasound (CEUS) imaging and laser speckle imaging (LSI). Additionally, the assessment of sublingual microcirculation was used for the evaluation of remote tissue microcirculatory events.

MATERIALS AND METHODS

Experiments were conducted on 15 female pigs (crossbred Landrace \times Yorkshire, 3–4 months old) with permission of the local animal experimental committee (EMC3379 142-14-01) and in strict accordance with the National Guidelines for Animal Care and Handling. The animals were divided into two groups: with (ANH group, $n = 8$) or without ANH (control group, $n = 7$). The mean \pm standard deviation (SD) body weight of the animals was 27.2 ± 1.6 kg.

Animal preparation

After overnight fasting with free access to water, all animals were premedicated with an intramuscular injection of tiletamine (5 mg/kg), zolazepam (5 mg/kg) (Zoletil, Virbac Laboratories, Carros, France) and xylazine (2.25 mg/kg) (Sedazine \circledast 2%, AST Farma B.V. Oudewater, The Netherlands). Intravenous access was achieved by cannulation of an ear vein; anesthesia was maintained with intravenous infusion of midazolam (1.5 mg/kg/h, Actavis, New Jersey, USA), ketamine (5 mg/kg/h, Alfasan, Woerden, The Netherlands), and sufentanil (4 μ g/kg/h, Sufenta Forte, Janssen Pharmaceuticals Ltd. USA). Muscle relaxation was achieved with infusion of rocuronium bromide (4 mg/kg/h, Fresenius Kabi, Germany). All animals were intubated through a midline cervical tracheostomy using an endotracheal tube (7.0 Fr), which was placed in the trachea. Via this tube, the animal was ventilated in a pressure controlled mode (Servo 300, Siemens-Eléma, Solna, Sweden) with a fraction of inspired oxygen of 0.40, a frequency that achieves normocapnia and a positive end-expiratory pressure of 5 cm H₂O. Body temperature was monitored with a temperature probe in the nose and maintained at approximately 38–40°C with a heating pad. After establishing intravenous access of the auricular vein, anesthetics and maintenance fluid (10 mg/kg/h) (Sterofundin \circledast ISO, B. Braun Melsungen, Germany) were continuously infused throughout the experiment. The left femoral artery was cannulated with a 20-gauge catheter connected to a pressure transducer and used for sampling and continuous measurements of mean arterial blood pressure (MAP) and heart rate (HR). A catheter in the right femoral artery and femoral vein was used for the replacement of blood, HES-RA (Volulyte, Fresenius Kabi, Germany) was used to gradually induce hemodilution. After catheterization of the right external jugular vein, which was also

used to administer drugs and microbubbles, a Swan-Ganz catheter (Edwards Lifesciences, Irvine, CA, USA) was inserted via the introducer to measure central venous pressure (CVP), mean pulmonary arterial pressure (MPAP), stroke volume (SV) and thermodilution CO. A midline abdominal incision was made, and a cystostomy tube was inserted into the bladder with double purse-string sutures for the collection of urine samples. To evaluate renal cortical microvascular perfusion using LSI, the right kidney was exposed via an incision in the right flank. When all surgical procedures were completed, a perivascular ultrasonic transient time flow probe (Transonic Systems, Ithaca, NY, USA) was placed around the right renal artery and connected to a flow meter (model T206, Transonic Systems) for continuous measurement of renal blood flow (RBF).

Experimental protocol and hemodynamic measurements

After completing the surgical procedures, a 45- to 60-minute equilibration period was allowed, and baseline measurements were taken when the animal's hemodynamics had stabilized (MAP > 60 mmHg and HR < 110 bpm). After baseline measurements (T0), ANH was induced by the replacement of blood with HES-RA until the hematocrit value (Hct) reached 20% (T1), 15% (T2) and 10% (T3). Hemodynamic parameters were monitored continuously during the entire experiment. Arterial, venous blood and urine samples were taken at the end of the baseline period (BL) and at each hematocrit target. At these specific time points, we measured microvascular perfusion in two different tissues: renal microcirculation (measured using CEUS imaging and LSI) and sublingual microcirculation (measured using Cytocam-IDF). At the end of the experiment, the animals were euthanized with a bolus of potassium chloride.

Global oxygenation

Arterial oxygen content (CaO_2) was calculated by following equation; $(1.31 \times \text{hemoglobin} \times \text{S}_a\text{O}_2) + (0.003 \times \text{P}_a\text{O}_2)$, where S_aO_2 is arterial oxygen saturation and P_aO_2 is arterial partial pressure of oxygen. Central venous oxygen content (CvO_2) was calculated as $(1.31 \times \text{hemoglobin} \times \text{S}_v\text{O}_2) + (0.003 \times \text{P}_v\text{O}_2)$, where S_vO_2 is mix venous oxygen saturation and P_vO_2 is mix venous partial pressure of oxygen. Global oxygen delivery was calculated as $\text{DO}_2 (\text{L/min}) = \text{CO} \times \text{CaO}_2$. Global oxygen consumption was calculated as $\text{VO}_2 (\text{L/min}) = \text{CO} \times (\text{CaO}_2 - \text{CvO}_2)$.

Blood gases, electrolytes, lactate and creatinine measurements

Arterial blood samples (0.5 ml) were taken from the femoral artery at four time points of hematocrit levels. The samples were used for determination of blood gas values, as well as for determination of the hemoglobin concentration, hemoglobin oxygen saturation, lactate, sodium and potassium concentrations (ABL 800 flex blood

gas analyzer; Radiometer, Copenhagen, Denmark). The plasma samples were used for evaluation of plasma creatinine levels (Cobas 80000 c 502 Roche Diagnostic, IN, USA).

Renal Function

Creatinine clearance ($\text{Clear}_{\text{crea}}$ (mL/min)) was measured as an index of the glomerular filtration rate and calculated with the following formula: $\text{Clear}_{\text{crea}} = (U_{\text{crea}} \times V) / P_{\text{crea}}$, where U_{crea} was the concentration of creatinine in urine, V is the urine volume per unit time and P_{crea} was the concentration of creatinine in plasma.

Contrast-enhanced ultrasound imaging of the kidney

Contrast-enhanced ultrasound (CEUS) imaging was performed at BL and after each hematocrit target was achieved (Figure 1). At each time point, a 1-mL bolus of Definity® contrast agent (Lantheus Medical Imaging, North Billerica, MA, USA) was manually injected into the jugular vein followed by a 10-mL saline flush. Dipyridamole (Persantine®, Boehringer Ingelheim, Alkmaar, The Netherlands) was administered at a rate of 10 µg/kg/min 30 minutes before the first contrast bolus at baseline, and a few minutes before each injection of contrast agent a 0.5-mL bolus of sildenafil (Revatio, Pfizer, New York City, NY, USA) was administered to suppress contrast agent-induced pulmonary hypertension (18). Measurements were recorded using a Vevo® 2100 preclinical high-resolution ultrasound scanner (FUJIFILM VisualSonics Inc., Toronto, Ontario, Canada) equipped with a MS250 transducer using the wide beam-width setting to ensure a low, more uniform transmit pressure over depth (18 MHz transmit frequency, 10 frames per second, 10% power, mechanical index 0.1). Immediately after injection of the contrast agent into the catheter, ventilation of the animal was paused at an expiratory hold to minimize movement due to breathing. After 25-30 seconds, when the measurement was completed, ventilation was resumed. Cine loops of side-by-side B-mode and nonlinear contrast mode images were stored as lossless DICOM images for further offline analysis using MATLAB (The MathWorks, Natick, MA, USA).

CEUS data analysis

First, correction for tissue motion in the imaging plane were applied as described elsewhere (19, 20). Briefly, the motion pattern of tissue in the field of view (FOV) was extracted from the B-mode images and applied to the contrast mode images to correct for motion in the FOV. Next, regions of interest (ROI's) were chosen for every DICOM recording, including an ROI in the deeper cortex for evaluating arterioles (> 8 mm depth) and two ROI's in the cortex from just below the exposed surface of the kidney to a depth of 1.5 - 2.5 mm for evaluating microcirculation. The intensities of all pixels in the ROI's were summed and divided by the area of the ROI for every frame, resulting in a time-intensity curve (TIC) for each ROI.



Figure 1. An example of contrast enhanced ultrasound imaging after microbubble injection in kidney.

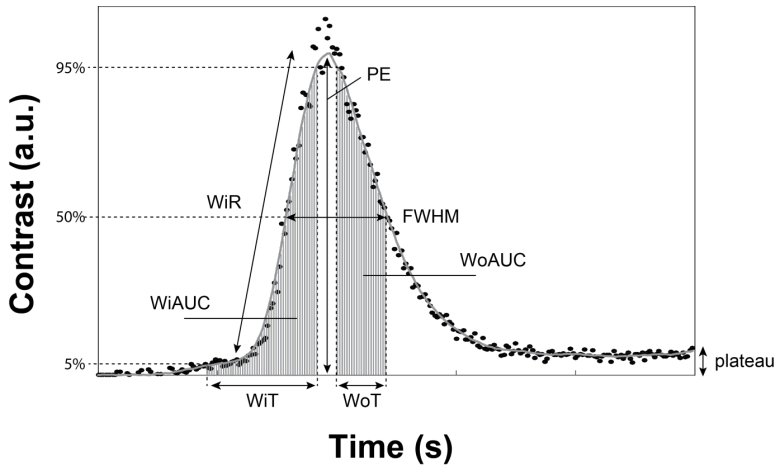


Figure 2. Semi-quantitative parameters are obtained from CEUS measurements.

The TIC's were filtered (15-point averaging filter) and the off-sets were subtracted. Next, the semi-quantitative parameters of interest were obtained from these filtered TIC's: slope, peak-enhancement (PE), full width at half maximum (FWHM), wash-in time (WiT), area under the curve (AUC) during wash-in (WiAUC) (Figure 2) (21, 22). In addition to these predefined parameters, we extracted another parameter which we previously defined as the intra-renal mean transit time (IRMTT) (23); the arrival time of microbubbles from the arterioles to the microcirculation, which may be used to determine the renal microvascular heterogeneity and distribution of perfusion at the different time points.

Laser Speckle Imaging of the kidney

LSI was used to visualize the spatiotemporal changes of renal cortical perfusion during ANH and control at the BL, Hct 20% (T1), Hct 15% (T2), and Hct 10% (T3) time points. For LSI measurements, a commercially available system was used (Moor Instruments, Devon, UK), in which a near-infrared laser source operating at 785 nm illuminated the renal cortex with a penetration depth of approximately 1 mm (24). LSI images were acquired using a 568×760 -pixel gray scale CCD camera containing a band-pass filter with a recording time constant of 1.0 s and a display rate of 25 Hz. A temporal acquisition window of 250 frames (10 s/frame) was selected. These images were converted to pseudo-color speckle contrast images in which perfusion was scaled using a flux value ranging from 0 to 2500 to obtain a complete distribution of all values. For LSI of the pig kidney, the FOV was set to 190×142 mm.

LSI data analysis

Histograms were generated from the LSI images for perfusion heterogeneity, which was calculated as the interquartile range of the perfusion values divided by the median perfusion value (25). Mean flux was analyzed and calculated as the mean \pm SD of renal microvascular perfusion.

Sublingual microcirculation

Sublingual microcirculation was measured using the Cytocam (Braedius Medical, Naarden, The Netherlands), which is based on video microscopy and IDF (26). To maximize the likelihood of a successful analysis of microvascular functionality, multiple videos were captured at each time point, varying the microscope's focal depth by steps of $4 \mu\text{m}$ around the depth with the optimal focus (judged by the operator). All captured videos had a fixed pre-set duration of 100 frames (i.e., 4 s, given the 25 Hz acquisition rate offered by the device). The operator aimed to image the same area throughout the experiment; this was crucial to achieve an optimal match among the FOVs at the subsequent time points and to minimize the influence of anatomical spatial heterogeneity in the sublingual microcirculation on the functional parameters evaluated during offline video-analysis. The Cytocam videos captured at each time point of ANH group with slightly different focal depths were carefully compared to identify the one offering the overall best quality as indicated by the Microcirculation Image Quality Score (27).

Data analysis Cytocam-IDF

Offline analysis (AVA 3.0 software; MicroVision Medical, Amsterdam, The Netherlands) involved quantitative assessment of the functional capillary density and the velocity of the erythrocytes flowing through the perfused microvessels (28,29). The microcirculatory

parameters were described as total vessel density (TVD), perfused vessel density (PVD), proportional perfused vessel density (PPD), microvascular flow index (MFI) and red blood cell velocity (RBCv). The RBCv was assessed using the space-time diagram method in specific perfused capillaries sampled at baseline and at successive time points. Evaluating the same area at different time points allowed us to identify and assign zero velocity to the capillaries without any erythrocytes, which were thus invisible in the FOV (29). Capillaries with zero velocity were not considered in the calculations of the average velocity changes at the four time points.

Statistical analysis

Data are expressed as the mean \pm SD. Repeated measures 2-way analysis of variance (ANOVA) (2 factors: time as a related sample factor and group as an independent sample factor) with *post hoc* Sidak's and Tukey's correction test for multiple analyses were used to determine inter- and/or intra-group differences of hemodynamic parameters, oxygenation, renal function, perfusion, biochemistry, CEUS derived parameters, and RBC velocity. Ordinary one-way ANOVA with Bonferroni's correction was used for the analysis of sublingual microcirculation. Statistical analysis was performed using GraphPad Prism version 7.0a for Mac (GraphPad Software, La Jolla, USA). A p-value < 0.05 was considered significant.

RESULTS

Systemic hemodynamics and lactate, electrolyte and blood gas levels

Data on the systemic macro-hemodynamic, electrolyte and blood gas variables are summarized in Table 1 and 2. MAP and MPAP were stable throughout the experiments. HR was significantly higher at Hct 10% in the hemodilution group compared to the control group at T3 ($p < 0.05$). CO was also higher in hemodilution group at Hct 10% than the control group at T3 ($p < 0.05$). Lastly, CVP and SVR were lower in the hemodilution group at Hct 10% in comparison to the control group at T3 ($p < 0.05$). No significant differences were observed in the plasma lactate, Na^+ , K^+ , pH, etCO_2 , PaO_2 and SvO_2 values among all time points between the control and hemodilution groups. However, low base excess was observed in the hemodilution group at Hct 10% with regard to the control group at T3 ($p < 0.05$).

Global oxygen delivery and consumption

Data on global oxygen delivery and consumption are summarized in Table 3. Both arterial oxygen content (CaO_2) and mixed venous oxygen content (CvO_2) in the control group were sustained throughout the entire procedure. CaO_2 gradually decreased over time in the hemodilution group at Hct 20%, 15% and 10% ($p < 0.05$) and it was found different

Table 1. Systemic hemodynamics.

	BL	T1 (Hct20%)	T2 (Hct15%)	T3 (Hct10%)
MAP (mmHg)				
Control	82.1±7.4	71.8±6.6	68.2±4.5[*]	65.8±5.4 [*]
Hemodilution	82.5±10.8	74.2±10.1	70.8±7.8[*]	67.7±5.9[*]
HR (bpm)				
Control	79.5±6.9	86.7±17.7	87.8±14.6	85.1±16.3
Hemodilution	80.5±11.5	79.7±7	86.6±10.1	106.3±18.1^{*,†,‡,§}
CVP (mmHg)				
Control	8±2.5	8.8±2.4	8.4±2.7	8.7±2.4
Hemodilution	5.7±1.7	6.1±1.5	6.5±1.1	5.8±1.4[§]
CO (L/min)				
Control	3.7±0.5	3.5±0.5	3.5±0.5	3.5±0.4
Hemodilution	4.1±0.6	3.9±0.6	4.6±0.9[§]	6.7±1.1^{*,†,‡,§}
MPAP (mmHg)				
Control	17.5±1.7	20.1±2.4 [§]	20.7±3.1	20.7±4.1
Hemodilution	16.7±2.6	16.2±3.3	17.3±2.4	17.6±2.3
SVR (dynes.sec.cm⁻⁵)				
Control	1630±159	1425±416	1287±213	1319±371
Hemodilution	1509±330	1383±262	1104±314[*]	704±128^{*,†,‡,§}

Values are presented as Mean±SD, *p<0.05 vs. BL, †p<0.05 vs. T1, ‡p<0.05 vs. T2 and §p<0.05 vs. Control group's same time point.

Abbreviations: MAP; mean arterial pressure, HR; heart rate, CVP; central venous pressure, CO; cardiac output, MPAP; pulmonary arterial pressure, SVR; systemic vascular resistance.

than the control group at T1, T2 and T3 (p<0.05). CvO₂ significantly decreased from BL to Hct 20%, Hct 15% and Hct 10% (p < 0.05) and was considerable lower than the control group at T2 and T3 (p<0.05). However, systemic DO₂ and VO₂ were stable in both control and hemodilution groups throughout experiments.

Renal function

Renal blood flow (RBF), creatinine clearance (CCr), urine output, and urine osmolality values are summarized in Table 4. Although creatinine clearances was stable entire hemodilution process compared to the control group, RBF and urine output were significantly increased in the hemodilution group at Hct 10% in comparison to the control group's T3 (p<0.05). Additionally, urine osmolality was lower in the hemodilution group at Hct 10% than the control group at T3 (p < 0.05).

Renal cortical microvascular perfusion

The cortical perfusion histogram, mean perfusion, and perfusion heterogeneity values are presented in Figure 3-4. Although hemodilution induced an increase in the perfusion (rightward shift in the histogram) and decreasing in perfusion heterogeneity at Hct 10%

Table 2. Plasma electrolyte and blood gas parameters.

	BL	T1 (Hct 20%)	T2 (Hct 15%)	T3 (Hct 10%)
SvO₂ (mmHg)				
Control	63.7 ± 8.9	60.1 ± 5.8	59.4 ± 7.2	61.4 ± 7.5
Hemodilution	61.3 ± 7.6	60.2 ± 6.9	58.2 ± 9.1	57.8 ± 8.4
PaO₂ (mmHg)				
Control	127 ± 30	106 ± 8	101 ± 6	126 ± 36
Hemodilution	112 ± 10	114 ± 10	112 ± 14	110 ± 17
Lactate (mmol/L)				
Control	1.5 ± 0.2	1.5 ± 0.9	0.9 ± 0.1	1.0 ± 0.2
Hemodilution	1.1 ± 0.3	1.1 ± 0.4	0.9 ± 0.3	0.9 ± 0.4
etCO₂ (kPa)				
Control	5.5 ± 0.2	5.3 ± 0.3	5.4 ± 0.3	5.3 ± 0.6
Hemodilution	5.2 ± 0.3	5.2 ± 0.3	5.1 ± 0.3	5.2 ± 0.2
pH				
Control	7.48 ± 0.02	7.49 ± 0.03	7.46 ± 0.04	7.44 ± 0.06
Hemodilution	7.47 ± 0.04	7.47 ± 0.03	7.47 ± 0.02	7.43 ± 0.03
Na⁺ (mmol/L)				
Control	142 ± 2	141 ± 2	142 ± 2	141 ± 3
Hemodilution	140 ± 2	141 ± 2	141 ± 3	141 ± 2
K⁺ (mmol/L)				
Control	3.8 ± 0.2	3.9 ± 0.1	3.9 ± 0.3	4.1 ± 0.3
Hemodilution	3.9 ± 0.3	3.9 ± 0.2	3.7 ± 0.3	3.7 ± 0.2
BE (mmol/L)				
Control	4.1 ± 1.7	4.2 ± 1	4.1 ± 1.4	3.8 ± 1.6
Hemodilution	4.2 ± 1.5	3.7 ± 0.6	3.1 ± 0.8	1.5 ± 1 ^{*,*,§}
Urea (mmol/L)				
Control	2.3 ± 0.4	2.9 ± 0.9	3.2 ± 0.8	3.4 ± 0.8
Hemodilution	2.6 ± 0.4	2.9 ± 0.6	3.1 ± 0.7	3.2 ± 0.8

Values are presented as the mean ± SD, * p < 0.05 vs. BL, † p < 0.05 vs. T1 and § p < 0.05 vs. Control group's same time point.

Abbreviations: SvO₂; central venous oxygen saturation, PaO₂; arterial oxygen partial pressure, etCO₂; end-tidal CO₂, BE; base excess.

(compared to T3 of control, p < 0.05), the mean perfusion values did not significantly change throughout the hemodilution process.

CEUS parameters

All the data obtained using CEUS imaging are presented in Figure 5. SL was steeper in the hemodilution group at Hct 10% than at BL, indicating a faster inflow of microbubbles, consistent with the FWHM that was significantly lower at Hct 10% than at BL and also at Hct 20% (p < 0.05). FWHM was also found to be lower in the hemodilution group than in the control group at T3 (p < 0.05). Both SL and FWHM showed that microbubble velocity and thus blood velocity in the chosen ROI in the microcirculation were higher

Table 3. Systemic oxygenation levels.

	BL	T1 (Hct 20%)	T2 (Hct 15%)	T3 (Hct1 0%)
CaO₂ (mL/dL)				
Control	626.3 ± 57.7	656.9 ± 67.8	658.8 ± 63.5	656.6 ± 32.8
Hemodilution	618.4 ± 40.8	524.6 ± 28.1^{*,§}	422.4 ± 47.4^{*,+§}	300.1 ± 30.3^{*,+§,§}
CvO₂ (mL/dL)				
Control	400.9 ± 79.7	397.8 ± 77.3	393.2 ± 69.2	404.8 ± 60.7
Hemodilution	381.6 ± 70.2	317.0 ± 49.4	247.6 ± 58.2^{*,§}	174 ± 35.8^{*,+§}
DO₂ (mL/min)				
Control	2373 ± 485	2317 ± 373	2338 ± 372	2344 ± 355
Hemodilution	2570 ± 519	2040 ± 340	1970 ± 464[*]	2028 ± 500
VO₂ (mL/min)				
Control	835 ± 172	920 ± 175	935 ± 145	910 ± 237
Hemodilution	969 ± 143	815 ± 186	798 ± 137	842 ± 218

Values are presented as the mean ± SD, ^{*}p < 0.05 vs. BL, [†]p < 0.05 vs. T1, [‡]p < 0.05 vs. T2 and [§]p < 0.05 vs. Control group's same time point.

Abbreviations: CaO₂; arterial oxygen content, CvO₂; venous oxygen content, DO₂; oxygen delivery, VO₂; oxygen consumption.

Table 4. Renal functional variables.

	BL	T1 (Hct 20%)	T2 (Hct 15%)	T3 (Hct 10%)
RBF (mL/min)				
Control	261 ± 52	218 ± 27	218 ± 24	209 ± 36
Hemodilution	255 ± 55	255 ± 70	272 ± 31	289 ± 46[§]
C_{cr} (mL/min)				
Control	1.55 ± 0.64	1.53 ± 0.54	1.45 ± 0.44	1.57 ± 0.7
Hemodilution	1.53 ± 0.36	1.49 ± 0.45	1.61 ± 0.24	1.43 ± 0.26
Urine output (mL/h)				
Control	22 ± 37	13.1 ± 3.7	13.1 ± 4.2	11.7 ± 5.2
Hemodilution	25.5 ± 13.2	21.7 ± 11.9	22.8 ± 8.3	26.6 ± 9.3[§]
Urine osmolality (mOsm/kg H₂O)				
Control	643 ± 136	753 ± 148	772 ± 177	806 ± 183
Hemodilution	572 ± 135	692 ± 192	697 ± 172	585 ± 92[§]

Values are presented as the mean ± SD, [§]p < 0.05 vs. Control group's same time points.

Abbreviations: RBF; renal blood flow, C_{cr}; creatinine clearances.

at Hct 10% than both BL and control T3. The WiT decreased, indicating faster inflow, especially at Hct 10% with respect to the other time points ($p < 0.05$) of hemodilution group as well as the control groups at T3 ($p < 0.05$). The constant PE, WiAUC throughout hemodilution confirmed that the concentration of microbubbles throughout the experiments remained constant. The IRMTT, the difference in arrival time of microbubbles between the renal artery to the ROI's in the microcirculation, was significantly lower at Hct 10% in the hemodilution group than at T3 in the control group ($p < 0.05$), confirming an increase in blood velocity.

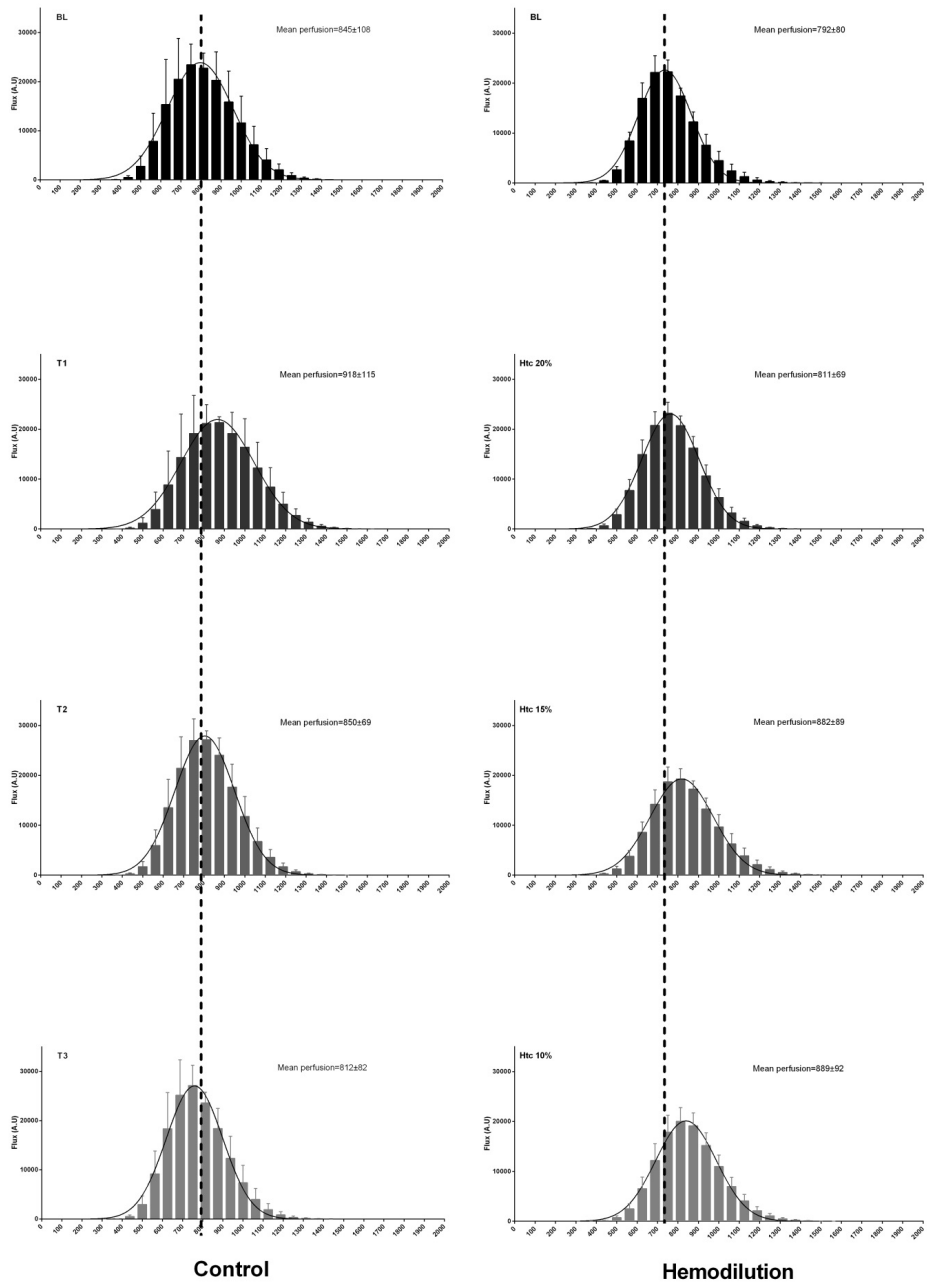


Figure 3. Renal microvascular perfusion histogram in the control and hemodilution groups.

Sublingual microcirculation

Data from the sublingual microcirculatory assessments and RBC velocity are reported in Figures 6 and 7. No significant differences were found in TVD, PVD, PPV, and MFI throughout the hemodilution process. However, the RBC velocity in the sublingual area was significantly elevated at Hct 20%, 15% and 10%.

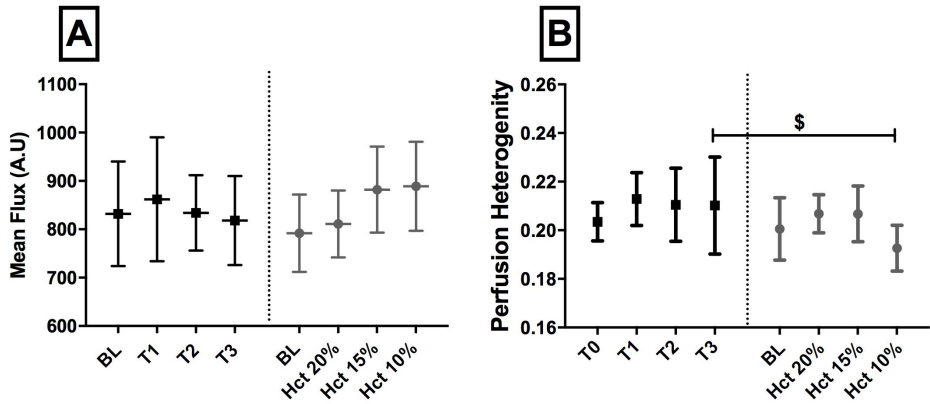


Figure 4. Renal microvascular perfusion (Panel A) and perfusion heterogeneity (Panel B). Values are presented as Mean \pm SD, $^{\$}$ p < 0.05 vs. Control group's same time points.

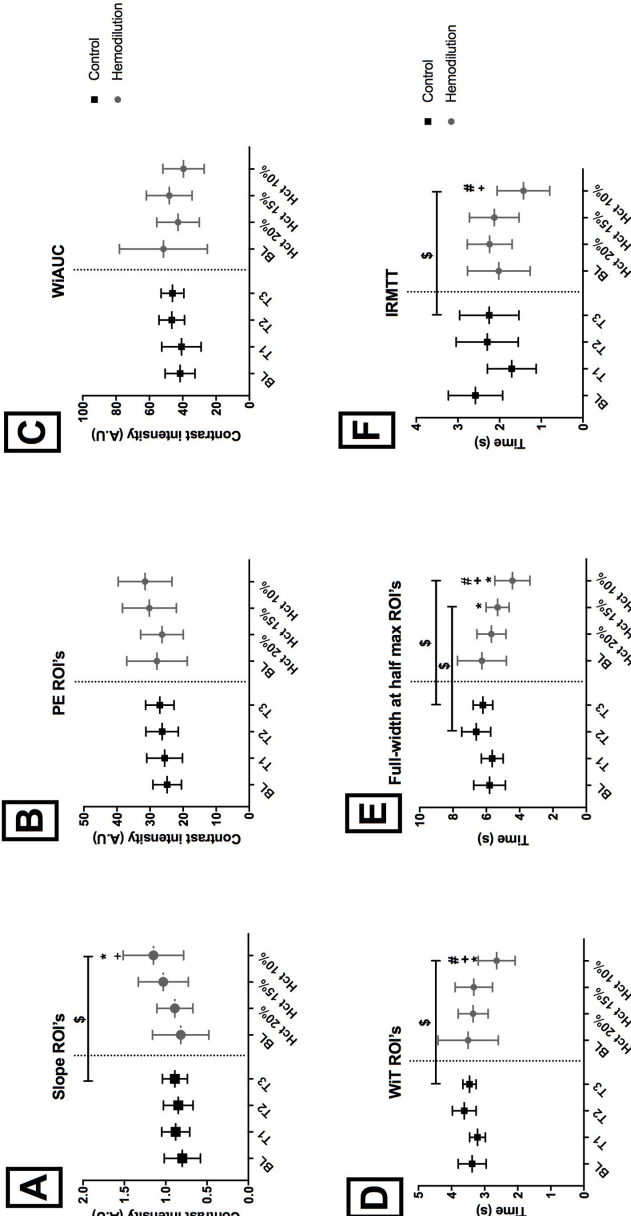


Figure 5. Results of the contrast-enhanced ultrasound analysis. ROI's; region of interest, WIT; wash in time, WIAUC; area under the wash in curve, PE; peak enhancement; IRMTT; intra-renal mean transit time. Values are presented as Mean \pm SD, $^{\$}$ $p < 0.05$ vs. BL, * $p < 0.05$ vs. Hct 20% (T1), $^{\#}$ $p < 0.05$ vs. Hct 15% (T2) and $^+$ $p < 0.05$ vs. Control group's same time points.

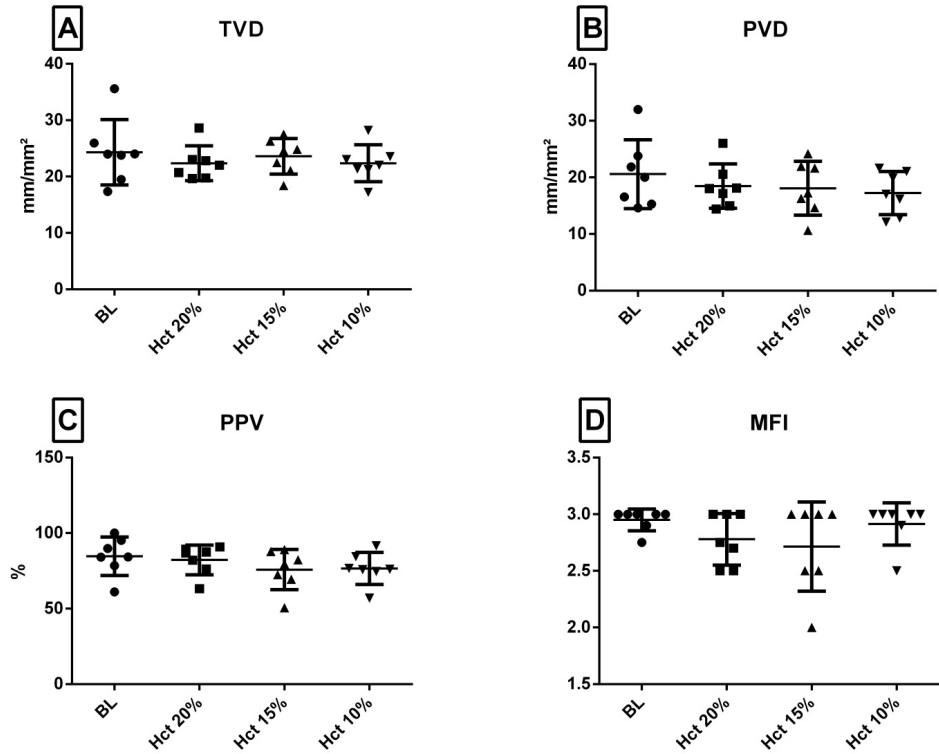


Figure 6. Sublingual microcirculatory parameters. TVD; total vessel density, PVD; perfused vessel density, PPV; proportional perfused vessel, MFI; mean flow index. Values are presented as Mean \pm SD.

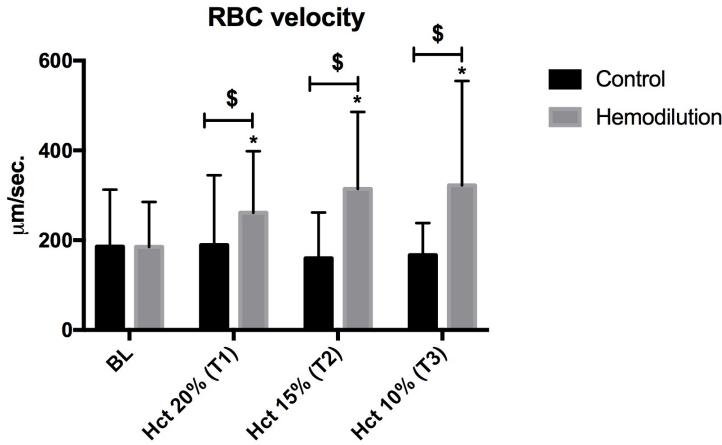


Figure 7. Results of red blood velocity in sublingual area. Values are presented as Mean \pm SD, * $p < 0.05$ vs. BL, $^{\$}p < 0.05$ vs Control group's same time points.

DISCUSSION AND CONCLUSION

In the present study, we found that despite stable MAP, MPAP, DO_2 and VO_2 , hemodilution with HES may induce an elevation of CO and HR, and reduction of CVP due to reduced systemic vascular resistance and oxygen-carrying capacity of arterial blood. In addition to hyperdynamic responses in the systemic circulation, short-term effects of HES on both the kidney and sublingual microcirculation were evaluated to verify the presence of coherence between the macro- and microcirculation. Together with systemic alterations, the reduced oxygen-carrying capacity, and lower viscosity of the blood, we found considerably higher renal inflow and intra-renal blood velocities that may be major contributors to renal hypoxia and finally AKI as a long-term consequence.

In this study, we confirmed in a pig model that moderate (Hct 20-10%) hemodilution did not affect any hemodynamic and oxygenation parameters, which has also been shown by Ghatanatti *et al.* in a prospective observational study conducted on 150 CPB patients (30). Previously, Crystal GJ found that ANH in dogs to Hct 10%, induced by 4% dextran, caused some hemodynamic alterations, such as in MAP and pulmonary capillary wedge pressure (PCWP), however these remained within acceptable limits (14). Additionally, although HR and the cardiac index (CI) were elevated, Crystal GJ demonstrated that this compensatory mechanism of oxygen supply resulted in a decrease in DO_2 level (without affecting VO_2) and an increase in the oxygen extraction level (14). In contrast, we demonstrated that the remarkably increased HR and CO, and a decreased SVR played an important role in maintaining oxygen delivery under conditions of a stable ERO_2 as a result of unchanged VO_2 . Although compensatory mechanisms preserve vital organ oxygenation over a wide range of hematocrit levels, ANH with HES might alter tissue oxygenation in critical organs due to long-term exposure to low viscosity and high velocity of the blood. Yuruk *et al.* reported that RBC transfusion in anemic patients increases blood viscosity and the RBC aggregation index, which is associated with high perfused vessel density, thus showing the influence of RBCs on blood viscosity and microcirculation (31). A study of solute extraction from individual capillaries showed that oxygen extraction is less effective at high flow rates because erythrocytes pass through the microvasculature at transit times that are too short to permit complete extraction of their oxygen load; this process is called functional shunting (32,33). Presson *et al.* reported measurements of the entire transit time distribution for RBCs crossing single subpleural capillary networks in canine lungs using *in vivo* fluorescence videomicroscopy and reported a decrease in transit times with increased CO (34). In the present study, both the sublingual microcirculatory and the CEUS data demonstrated that ANH accelerated RBC velocity due to lower viscosity of the blood caused by loss of RBCs; moreover, this process was associated with high CO regardless of microcirculatory parameters (TVD,

PVD and MFI, etc.) or RBC recruitment. Therefore, we conclude that hemodynamic coherence may exist, it means that the systemic hemodynamic variables are able to support microcirculation and maintain an optimized oxygen supply to the parenchymal cells, thereby maintaining their ability to support organ function (35).

It is well known that the kidney is one of the most sensitive organs to hemodynamic instability and hypoxia due to the complexity of renal microvasculature, functional discrepancy of different regions and workload (1/4 of CO). Johannes *et al.* demonstrated that Hct 10% in rats might induce a reduction of renal cortical PO_2 , medullar PO_2 , DO_{2ren} and VO_{2ren} and an elevation of renal ERO_2 with sustained renal and systemic hemodynamics. These results were explained by the presence of renal oxygen shunting in the kidney (17). A study conducted by Ghatanatti *et al.* demonstrated that although Hct < 21% correlated with a greater risk of AKI than Hct > 21% in CPB patients due to a significant reduction of GFR and C_{Cr} , only 4% of patients required dialysis (30). However, Konrad *et al.* demonstrated that ANH with HES preserved the renal cortical and inner medullar oxygenation in comparison to crystalloid at Hct 15% (7). In the present study creatinine clearance was stable during the entire hemodilution process, even at Hct 10%, with the exception of elevated RBF and urine output. Johannes *et al.* also demonstrated that ANH with HES may induce a reduction of colloidal osmotic pressure and elevation of plasma osmolality in rats (17). In contrast to ANH with colloids, Konrad *et al.* showed that the use of crystalloids leads to perturbation of systemic hemodynamics as well as renal microvascular oxygenation and function in pigs (7). Thus, the type of fluid used for hemodilution appears to be important to prevent AKI. Moreover, our systemic and renal functional results indicate that using HES for ANH is safe for the kidney.

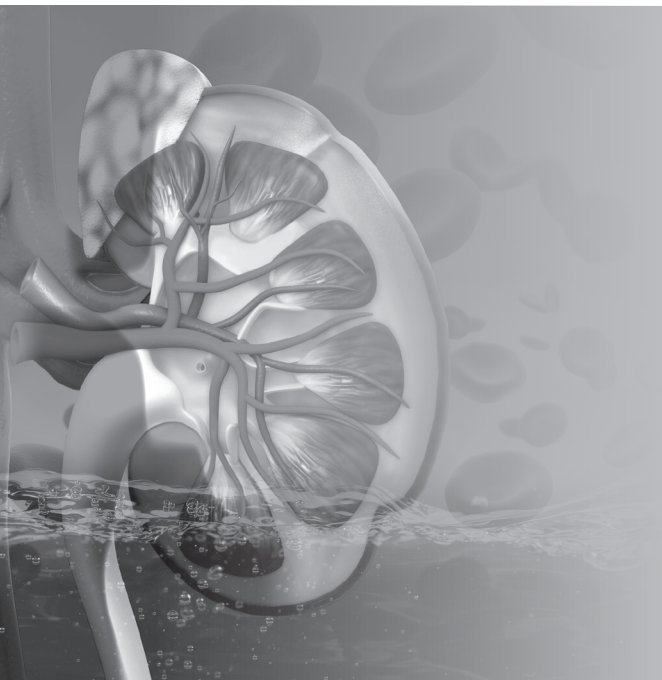
Although LSI showed that renal cortical microvascular perfusion was unaltered, perfusion heterogeneity tended to decrease during hemodilution. In accordance with this finding, CEUS imaging clearly showed a progressive increment of blood velocity in the renal microcirculation (increase in SL, decrease in FWHM and WiT) and a decrease of IRMTT. Indeed, the CEUS findings are in agreement with the LSI findings, as unaltered PE and WiAUC at Hct 10% clearly indicated that intra-renal blood volume in the microcirculation was sustained by HES even at the lowest hematocrit levels in this study. Additionally, IRMTT as an indicator of macro- to microcirculatory flow transition, showed substantially faster intra-renal blood velocity as also systemically confirmed by sublingual RBC velocity. In our previous study, we demonstrated a presence of plugged vessel in sublingual microcirculation confirmed by prolonged contrast enhancement in intra-renal microcirculation, and even worsened during normalization of systemic hemodynamic through crystalloid resuscitation in septic pigs (23). However, in present study, we have not detected any plugged vessel or slow flow as the reason of HES related coagulopathy in both sublingual and renal microcirculation.

To conclude, we clearly demonstrated that ANH with HES is associated with alterations of systemic and renal hemodynamics, resulting in increased blood velocity due to lower viscosity and SVR in the kidneys and peripheral tissues. We showed that oxygen deliver, utilization or demand is not influenced by short-term hemodilution. These results confirmed that the reduced oxygen-carrying capacity of blood under certain situations (Hct 10%) may not impair systemic oxygenation and renal function because of compensation by high cardiac output and a reduced systemic vascular resistance. Therefore, we showed evidence supporting the presence of coherence between macro- and microcirculation by using different methods for the assessment of microcirculation during the hemodilution process. However, this coherence between macro and microcirculation seems to have a further overwhelming potential due to functional shunting of oxygen in the kidney. Despite a maintained stable intravascular volume during hemodilution process in kidney, an increased renal blood flow and urine output may showed a depletion of water reabsorption indicating an impairment of oxygen utilization and energy efficiency. However, increased inflow and intra-renal of RBC velocity in the kidney might be a major contributor to acute kidney injury due to functional shunting, which reduces the efficiency of oxygen extraction as a result of a shorter transit time for the erythrocytes to release adequate oxygen to tissue. These alterations were found most likely relevant with the imbalance between the systemic hemodynamic, blood composition and microcirculatory regulation, but not HES alone.

REFERENCES

1. Beards SC, Watt T, Edwards JD, *et al.* Comparison of the hemodynamic and oxygen transport responses to modified fluid gelatin and hetastarch in critically ill patients: a prospective, randomized trial. *Crit. Care Med.* 22:600–605, 1994.
2. Ranucci M, Romitti F, Isgrò G, *et al.* Oxygen delivery during cardiopulmonary bypass and acute renal failure after coronary operations. *Ann. Thorac. Surg.* 80:2213–2220, 2005.
3. Licker M, Ellenberger C, Sierra J, *et al.* Cardioprotective effects of acute normovolemic hemodilution in patients undergoing coronary artery bypass surgery. *Chest* 128:838–847, 2005.
4. Jones SB, Whitten CW, Monk TG. Influence of crystalloid and colloid replacement solutions on hemodynamic variables during acute normovolemic hemodilution. *J. Clin. Anesth.* 16:11–17, 2004.
5. Ince C, Groeneveld ABJ. The case for 0.9% NaCl: is the undefendable, defensible? *Kidney Int.* 86:1087–1095, 2014.
6. He H, Liu D, Ince C. Colloids and the Microcirculation. *Anesth. Analg.* 126:1747–1754, 2018.
7. Konrad FM, Mik EG, Bodmer SIA, *et al.* Acute normovolemic hemodilution in the pig is associated with renal tissue edema, impaired renal microvascular oxygenation, and functional loss. *Anesthesiology* 119:256–269, 2013.
8. Crystal GJ, Kim SJ, Salem MR. Right and left ventricular O₂ uptake during hemodilution and beta-adrenergic stimulation. *Am. J. Physiol.* 265:H1769–1777, 1993.
9. Crystal GJ, Salem MR. Beta-adrenergic stimulation restores oxygen extraction reserve during acute normovolemic hemodilution. *Anesth. Analg.* 95:851–857, 2002.
10. Koning NJ, de Lange F, Vonk ABA, *et al.* Impaired microcirculatory perfusion in a rat model of cardiopulmonary bypass: the role of hemodilution. *Am. J. Physiol. Heart Circ. Physiol.* 310:H550–558, 2016.
11. Habib RH, Zacharias A, Schwann TA, *et al.* Role of hemodilutional anemia and transfusion during cardiopulmonary bypass in renal injury after coronary revascularization: implications on operative outcome. *Crit. Care Med.* 33:1749–1756, 2005.
12. Karkouti K, Beattie WS, Wijeyesundera DN, *et al.* Hemodilution during cardiopulmonary bypass is an independent risk factor for acute renal failure in adult cardiac surgery. *J. Thorac. Cardiovasc Surg.* 129:391–400, 2005.
13. Brezis M, Rosen S. Hypoxia of the renal medulla--its implications for disease. *N. Engl. J. Med.* 332:647–655, 1995.
14. Crystal GJ. Regional tolerance to acute normovolemic hemodilution: evidence that the kidney may be at greatest risk. *J. Cardiothorac. Vasc. Anesth.* 29:320–327, 2015.
15. Cabrales P, Tsai AG, Frangos JA, *et al.* Oxygen delivery and consumption in the microcirculation after extreme hemodilution with perfluorocarbons. *Am. J. Physiol. Heart Circ. Physiol.* 287:H320–330, 2004.
16. Morariu AM, Maathuis M-HJ, Asgeirsdottir SA, *et al.* Acute isovolemic hemodilution triggers proinflammatory and procoagulatory endothelial activation in vital organs: role of erythrocyte aggregation. *Microcirculation* 13:397–409, 2006.
17. Johannes T, Mik EG, Nohé B, *et al.* Acute decrease in renal microvascular PO₂ during acute normovolemic hemodilution. *Am. J. Physiol. Renal Physiol.* 292:F796–803, 2007.
18. Grauer SE, Pantely GA, Xu J, *et al.* Myocardial imaging with a new transpulmonary lipid-fluorocarbon echo contrast agent: experimental studies in pigs. *Am. Heart J.* 132:938–945, 1996.
19. Daeichin V, Akkus Z, Skachkov I, *et al.* Quantification of bound microbubbles in ultrasound molecular imaging. *IEEE Trans. Ultrason. Ferroelectr. Freq. Control* 62:1190–1200, 2015.
20. Hoogi A, Akkus Z, van den Oord SCH, *et al.* Quantitative analysis of ultrasound contrast flow behavior in carotid plaque neovasculature. *Ultrasound Med. Biol.* 38:2072–2083, 2012.
21. Dietrich CF, Averkiou MA, Correas J-M, *et al.* An EFSUMB introduction into Dynamic Contrast-Enhanced Ultrasound (DCE-US) for quantification of tumour perfusion. *Ultraschall. Med.* 33:344–351, 2012.
22. Needles A, Arditi M, Rognin NG, *et al.* Nonlinear contrast imaging with an array-based micro-ultrasound system. *Ultrasound Med Biol.* 36:2097–2106, 2010.

23. Lima A, van Rooij T, Ergin B, *et al.* Dynamic Contrast-Enhanced Ultrasound Identifies Microcirculatory Alterations in Sepsis-Induced Acute Kidney Injury. *Crit. Care Med.* 2018.
24. Draijer M, Hondebrink E, van Leeuwen T, *et al.* Review of laser speckle contrast techniques for visualizing tissue perfusion. *Lasers Med. Sci.* 24:639–651, 2009.
25. Bezemer R, Legrand M, Klijn E, *et al.* Real-time assessment of renal cortical microvascular perfusion heterogeneities using near-infrared laser speckle imaging. *Opt. Express.* 18:15054–15061, 2010.
26. Hutchings S, Watts S, Kirkman E. The Cytocam video microscope. A new method for visualising the microcirculation using Incident Dark Field technology. *Clin. Hemorheol. Microcirc.* 62:261–271, 2016.
27. Massey MJ, Larochelle E, Najarro G, *et al.* The microcirculation image quality score: development and preliminary evaluation of a proposed approach to grading quality of image acquisition for bedside videomicroscopy. *J. Crit. Care* 28:913–917, 2013.
28. De Backer D, Hollenberg S, Boerma C, *et al.* How to evaluate the microcirculation: report of a round table conference. *Crit. Care* 11:R101, 2007.
29. Sorelli M, Bocchi L, Ince C. Monitoring the microcirculation at the bedside using hand-held imaging microscopes: Automatic tracking of erythrocytes. *Conf. Proc. IEEE Eng. Med. Biol. Soc.* 2015:7378–7381, 2015.
30. Ghatanatti R, Teli A, Narayan P, *et al.* Ideal Hematocrit to Minimize Renal Injury on Cardiopulmonary Bypass. *Innovations (Phila)* 10:420–424, 2015.
31. Yürük K, Milstein DMJ, Bezemer R, *et al.* Transfusion of banked red blood cells and the effects on hemorrheology and microvascular hemodynamics in anemic hematology outpatients. *Transfusion* 53:1346–1352, 2013.
32. Østergaard L, Granfeldt A, Secher N, *et al.* Microcirculatory dysfunction and tissue oxygenation in critical illness. *Acta. Anaesthesiol. Scand.* 59:1246–1259, 2015.
33. Renkin EM: B. W. Zweifach Award lecture. Regulation of the microcirculation. *Microvasc. Res.* 30:251–263, 1985.
34. Presson RG, Graham JA, Hanger CC, *et al.* Distribution of pulmonary capillary red blood cell transit times. *J. Appl. Physiol.* 79:382–388, 1995.
35. Ince C, Ertmer C. Hemodynamic coherence: Its meaning in perioperative and intensive care medicine. *Best Pract. Res. Clin. Anaesthesiol.* 30:395–397, 2016.



CHAPTER 13

General discussion and future directions

In this thesis, we investigated the influence of common therapeutic approaches on the renal microcirculation and oxygenation following acute kidney injury (AKI) in different states of shock and resuscitation, and tested whether or not microcirculatory-targeted therapies may improve the outcome parameters related to AKI in term of renal oxygenation, function, tubular damage and oxidative stress. In this general discussion we summarize our main findings and consider the implications of these findings with respect to clinical practice and future investigations.

Ischemia-reperfusion (I/R) injury following release of an aortic cross clamp is not limited to the lower extremities, but also causes damage to remote organs and tissues such as lungs, kidneys, heart, and liver (1,2). After removal of the aortic clamp, reperfusion leads to the generation of oxygen-derived free radicals leading to damage proteins, lipids, mitochondria, and DNA (3,4), release of systemic vasoconstrictors, activation of neutrophils (5), and inflammation resulting in disturbed microvascular function and consequent tissue hypoxia (6-7). In this thesis, we demonstrated that I/R injury results in a fall in systemic, renal hemodynamics and oxygenation parameters (PO_2 , DO_2 and VO_2), and significantly increases the expression of biomarkers of kidney injury (e.g. NGAL and L-FABP), oxidative damage (MDA), high plasma creatinine, lactate levels and inflammatory mediators indicating the presence of AKI. In thesis, we showed that use of anti-oxidant (such as ascorbic acid and tempol (**Chapter 3, 4**), immunosuppression (mycophenolate mofetil (**Chapter 5**) and anti-inflammatory therapies with hypertonic saline (**Chapter 6**), or recombinant activated protein C (recap) (**Chapter 9**) can result in an improvement in renal microcirculation, oxygenation and function regardless of macro-hemodynamic alterations.

Sepsis is a condition characterized by a massive increase in inflammatory mediators and activated leukocytes, which together cause severe microcirculatory dysfunction and disrupt oxygen homeostasis, leading to oxidative stress and hypoxemia in organs resulting in progressive systemic hemodynamic deterioration (8). One of the most serious complications for septic patients is AKI characterized by a rapid failure of the kidneys to adequately filter the blood, regulate ion and water balance, and generate urine (9). Fluid resuscitation is considered a cornerstone therapy to preserve an adequate intravascular volume thought to achieve microvascular perfusion and tissue oxygenation needed for organ function (10). In this thesis, we found that fluid therapy, irrespective of the buffer or composition of fluids used, was ineffective in correcting sepsis-induced acidosis or sepsis-induced microcirculatory alterations, or sepsis induced renal microcirculatory hypoxemia and function (**Chapter 7**). However, we showed that sepsis related disturbance of renal oxygenation, function and tissue damage might be resolved if compounds targeting inflammation such as recAP (**Chapter 8**) or oxidative stress such as

N-Acetylcysteine (**Chapter 9**) were added to fluids. These results led us to test the idea that enhancement of the oxygen carrying capacity of the circulation by administering blood transfusion may be beneficial on renal tissue oxygenation, function and tissue integrity in sepsis-induced AKI (**Chapter 10**). In this study (**Chapter 10**) we found that in comparison to fluid resuscitation, blood transfusion significantly improved renal function following sepsis in part by the improvements in renal microvascular oxygenation and endothelial cell dysfunction. .

Current evidence suggests that the type of fluid used for resuscitation, particularly colloids, may lead to unfavorable outcomes or have no effect compared to normal saline (11,12). Cecconi *et al.* have demonstrated that balanced fluids are commonly used for volume expansion of critically ill patients (13). This has led to increased interest on the role of crystalloids and the effects of their different compositions on the permeance of AKI during fluid therapy. In the last two studies of this thesis (**Chapter 11-12**), we aimed to determine to identify a best resuscitation fluid in term of composition and buffering capacity on the occurrence of AKI in compromised blood oxygen carrying capacity such as occurs in hemorrhage or hemodilution.

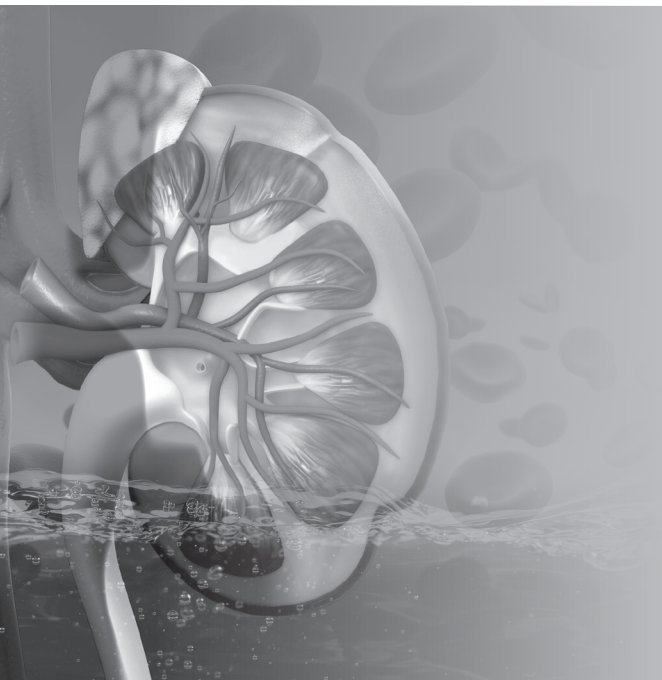
In summary our studies show that therapy targeting systemic hemodynamic together with microcirculatory dysfunction have the most favorable effect on averting the impairment of renal perfusion, oxygenation and function, and cell survival and thereby AKI.

FUTURE RESEARCH PERSPECTIVE

In this thesis we clearly showed that hemodynamic targeted or fluid replacement therapies alone are not sufficient for providing adequate intravascular volume and oxygenation to supply oxygen needed to support kidney function. Therefore, microcirculatory targeted therapies may provide a more effective approach to resolve AKI or failure of other organs seen in states of critical illness. In considering future perspectives, of course depending on the precise nature of the condition, more focus on correcting microcirculatory failure in addition to macrocirculatory alterations should be considered. This would have to take the pathogenesis of microcirculatory alterations in states of critical illness into account and require new types of therapies and targets. Such therapies more focused on resolving microcirculatory alteration could include anti-oxidant and anti-inflammatory drugs, peripheral vasodilators, glycocalyx protector agents, blood transfusions (taking transfusion related lesions into account) or even hemoglobin based oxygen carrier (HBOC). Such novel therapeutic strategies protect the vital organs better than conventional strategies and possibly reduce mortality in critical illness (14).

REFERENCES

1. Parrino PE, Laubach VE, Gaughen JR, *et al.* Inhibition of inducible nitric oxide synthase after myocardial ischemia increases coronary flow. *Ann. Thorac. Surg.* 66:733, 1998.
2. Koksel O, Ozdulger A, Aytacoglu B, *et al.* The influence of iloprost on acute lung injury induced by hind limb ischemia-reperfusion in rats. *Pulm. Pharmacol. Ther.* 18(4):235-41, 2005.
3. Noiri E, Nakao A, Uchida K, *et al.* Oxidative and nitrosative stress in acute renal ischemia. *Am. J. Physiol. Renal Physiol.* 281:F948, 2001.
4. Versteilen AM, Di Maggio F, Leemreis JR, *et al.* Molecular mechanisms of acute renal failure following ischemia/reperfusion. *Int. J. Artif. Organs* 27: 1019, 2004.
5. Grace PA. Ischemia-reperfusion injury. *Br. J. Surg.* 81:637, 1994.
6. Lum H, Roebuck KA. Oxidant stress and endothelial cell dysfunction. *Am. J. Physiol. Cell Physiol.* 280:C719, 2001.
7. Legrand M, Ince C, Mik E, *et al.* Renal hypoxia and dysoxia following reperfusion of the ischemic kidney. *Mol. Med.* 14: 502–516, 2008.
8. Wan L, Bagshaw SM, Langenberg C, *et al.* Pathophysiology of septic acute kidney injury: what do we really know? *Crit Care Med.* 36(4): S198- S203, 2008.
9. Zarjou A, Agarwal A. Sepsis and acute kidney injury. *J. Am. Soc. Nephro.* 22: 999-1006, 2011.
10. Vincent JL, De Backer D: Circulatory shock. *N. Engl. J. Med.* 369(18):1726-34, 2013 .
11. Myburgh JA, Finfer S, Bellomo R, *et al.* Hydroxyethyl starch or saline for fluid resuscitation in intensive care. *N. Engl. J. Med.* 367: 1901–11, 2012.
12. Finfer S, Bellomo R, Boyce N, *et al.* A comparison of albumin and saline for fluid resuscitation in the intensive care unit. *N. Engl. J. Med.* 350: 2247–56, 2004.
13. Cecconi M, Hofer C, Teboul J-L, *et al.* Fluid challenges in intensive care: the FENICE study: A global inception cohort study. *Intensive Care Med.* 41: 1529–37, 2015.
14. Legrand M, Ait Oufella H, Ince C. Could resuscitation be based on microcirculation data? *Intensive Care Med.* 8 May 7. doi: 10.1007/s00134-018-5121-0, 2018.



CHAPTER 14

Summary and conclusion

It is currently known that microcirculatory oxygenation is a crucial factor for maintaining organ integrity and function, especially in sepsis, I/R, hemorrhagic shock and hemodilution, during which macro- and microcirculatory imbalances are prevalent. Moreover, in this thesis, we simulated clinical scenarios and translated these scenarios into renal pathological and physiological concepts to aid the development of new therapeutic approaches based on microcirculatory oxygenation and to further our insight and knowledge on the underlying mechanisms of acute kidney injury under these pathological or traumatic conditions.

First, we demonstrated that acute ischemia/reperfusion leads to impairment of kidney cortical and medullar oxygenation. These microcirculatory alterations are associated with decreases in renal oxygen supply and oxygen consumption and increases in renal vascular resistance. Simultaneously, these changes also correlated with some degree of systemic hypotension, tissue damage, inflammatory activation and oxidative stress. Treatment with ascorbic acid resulted in improved renal cortical and medulla oxygenation and partially enhanced renal oxygen delivery and consumption due to a decreased amount of oxygen used for reactive oxygen species production. We demonstrated that ascorbic acid administration was able to completely prevent an increase in oxidative stress, inflammation and renal injury. Moreover, SOD-mimicking TEMPOL administration had a protective effect on AKI by reducing renal damage, inflammation, and iNOS production. The beneficial effects of TEMPOL on renal hemodynamics and oxygenation were limited, however, as they improved only the level of RVR and pO_2 but not MAP, RBF, DO_{2ren} , VO_{2ren} , and $ERO_{2ren}\%$.

The MMF study confirmed that administration of MMF as an immunosuppressant effectively improved renal microcirculatory oxygenation, renal oxygen delivery and renal hemodynamics, including a reduction in the degree of inflammation and injury in lower body I/R-induced AKI. We also showed that in addition to positive effects of hypertonic saline (HSal) administration on systemic hemodynamics, anti-inflammation and renal function, HSal also improved renal oxygenation, possibly as a result of reduced tubular Na^+ reabsorption and increased excretion fraction of Na^+ due to high Na^+ load in the plasma. Our results also demonstrated that despite these renal hemodynamic and inflammatory improvements, HSal did not ameliorate AKI and even worsened renal epithelial and tubular damage following ischemia/reperfusion.

In the first study concerning sepsis-induced AKI, we investigated whether the composition of fluids had a beneficial effect on the known pathogenic factors involved in sepsis-induced acute kidney injury. To this end, we showed that the composition of the fluids alone, whether they were balanced or unbalanced or a colloid or crystalloid,

was ineffective in supporting renal function during endotoxic shock despite administration of adequate volumes. These findings suggest that additional compounds to control inflammation and promote oxygen transport to the parenchymal cells are required for fluids to be effective in resolving renal failure under conditions of endotoxic shock.

RecAP, as an LPS-neutralizing agent, was used to treat both I/R-induced sterile inflammation and sepsis-associated AKI. We found that recAP promoted renal oxygenation and hemodynamics immediately following lower body I/R-induced AKI but did not influence these parameters during endotoxemia-induced AKI. However, RecAP did exert a clear renal protective, anti-inflammatory effect in both models.

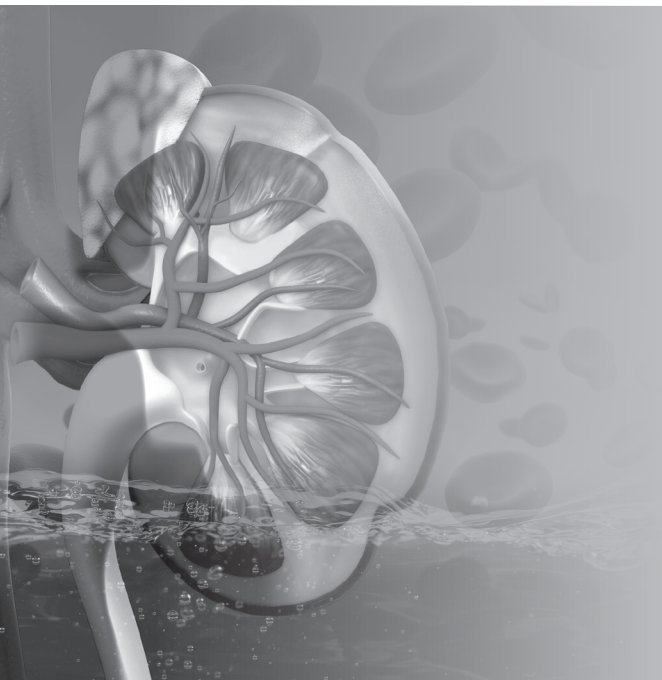
In another study, we found that fluid supplemented with NAC improved cortical renal oxygenation, oxygen delivery, and oxygen consumption compared to the LPS group. Fluid resuscitation alone partially ameliorated kidney hypoxia compared to the LPS group, but the difference was not statistically significant. It suggested that NAC has a specific effect on microvascular oxygenation independent of renal macrovascular perfusion.

Finally, we showed an improvement in microcirculatory recruitment by infusing fresh blood; renal microcirculatory oxygenation and, by extension, kidney function were restored in a rat model of endotoxemia. Sepsis-induced eNOS deficiency and renal damage were also corrected by blood transfusion (BT) but not by fluid resuscitation alone.

We also aimed to determine the efficiency of the different fluids and the role of the liver in their metabolism during hemorrhagic shock. To accomplish this, an ~70% partial liver resection (PLR) was performed to reduce the capacity of the liver to metabolize these precursors. The primary results of this study demonstrated that acetate-balanced resuscitation fluids significantly improved the buffering capacity in the presence or absence of liver impairment.

Lastly, we clearly demonstrated that ANH is associated with alteration of systemic and renal hemodynamics and results in an increase in blood velocity due to lower blood viscosity and SVR in the kidneys and peripheral tissues. However, increased red blood cell velocity in the kidney might be a major contributor to acute kidney injury due to functional shunting, which reduces the efficiency of oxygen extraction as a result of shorter erythrocyte transit time.

To conclude, acute kidney injury is defined as a complex multifactorial event including the systemic and renal perfusion defects, impairment of intra-renal organization of microcirculatory vessels and oxygenation, inactivation or over-activation of systemic and intra-renal regulatory pathways, diminished oxygen utilization, renal tubular damage caused by reactive oxygen and nitrogen species and pro and anti-inflammatory mechanisms. To conclude, in therapeutic strategies for the treatment of acute kidney injury we suggest that in addition to monitoring systemic hemodynamics, there should be an inclusion of the treatment of renal microcirculation by targeting restriction of pro-inflammation, or ROS and RNS production, regulation of sufficient and effective oxygen utilization, proper and adequate intravascular volume expansion and oxygen carriers with fluids or blood, and treatment of renal energy requirement needed for function.



CHAPTER 15

Samenvatting en conclusie

Het is nu bekend dat de microcirculatoire oxygenatie een cruciale factor is om de integriteit en functie van het orgaan te behouden, in het bijzonder bij sepsis, I / R, hemorragische shock en hemodilutie waarbij storing in de macro- en microcirculatie diepgaand wordt waargenomen. Bovendien wilden we in dit proefschrift klinische scenario's produceren en deze scenario's vertalen in nierpathologisch en fysiologisch concept om nieuwe therapeutische benaderingen te ontwikkelen op basis van microcirculatoire oxygenatie, en om een nieuw inzicht en kennis in de literatuur toe te voegen over het onderliggende mechanisme van acute nierschade in deze pathologische of traumatische omstandigheden.

Allereerst hebben we aangetoond dat acute ischemie / reperfusie een verslechtering van de niercorticale en medullaire oxygenatie veroorzaakt. Deze veranderingen in de microcirculatie hangen samen met afname van de zuurstofvoorziening en zuurstofconsumptie door de nier en toename van de weerstand van de niervaten. Tegelijkertijd waren deze veranderingen ook gecorreleerd met enige mate van systemische hypotensie, weefselschade, inflammatoire activering en oxidatieve stress. De behandeling van ascorbinezuur resulteerde in verbetering van de renale corticale en medulla-oxygenatie en gedeeltelijk verbeterd in de afgifte en consumptie van zuurstof door de nier als een gevolg van een verminderde hoeveelheid zuurstof voor de productie van reactieve zuurstofverbindingen. We toonden aan dat toediening van ascorbinezuur de uitbarsting in oxidatieve stress, ontsteking en nierbeschadiging volledig kon voorkomen. SOD-nabootsing van TEMPOL-toediening verleende echter een beschermend effect op AKI in termen van nierbeschadiging, ontsteking en iNOS-productie. De gunstige effecten van TEMPOL op de hemodynamiek en oxygenatie waren beperkt, maar manifesteerden zich alleen op het niveau van RVR en μPO_2 , maar niet MAP, RBF, $\text{DO}_{2\text{ren}}$, $\text{VO}_{2\text{ren}}$ en $\text{ERO}_{2\text{ren}}$.

MMF-onderzoek bevestigde dat de toediening van MMF als een immunosuppressivum effectief de renale microcirculatoire oxygenatie, de zuurstofafgifte door de nier en de hemodynamica van de nier verbeterde, waaronder een verminderde ontstekingsgraad en letsel bij I / R-geïnduceerde AKI in het onderlichaam. We toonden ook aan dat naast positieve effecten van hypertonische zoutoplossingtoediening (HSal) op systemische hemodynamische, ontstekingsremmende en nierfunctie, HSal ook de nieroxygenatie verbeterde, waarschijnlijk als gevolg van verminderde tubulaire Na^+ -reabsorptie en verhoogde excretiefractie van Na^+ als gevolg van hoge Na^+ -lading in plasma. Onze resultaten toonden ook aan dat ondanks deze renale hemodynamische en inflammatoire verbeteringen, HSal geen AKI herstelde en zelfs verslechterd renale epitheliale en tubulaire schade na ischemie / reperfusie.

In de eerste studie met betrekking tot sepsis induceren AKI waarbij we hebben onderzocht of de samenstelling van vloeistoffen al dan niet een gunstig effect had op de bekende pathogene factoren die betrokken zijn bij sepsis-geïnduceerde acute nierschade. Hiertoe toonden we aan dat de samenstelling van de vloeistoffen, in de zin van hetzij gebalanceerd of ongebalanceerd, hetzij een colloïde of een kristalloïde, ondanks de toediening van voldoende volumes, op zichzelf niet effectief was in het ondersteunen van de nierfunctie tijdens endotoxische shock. De bevindingen suggereren dat voor vloeistoffen om effectief te zijn in het oplossen van nierfalen onder dergelijke omstandigheden, extra verbindingen nodig zijn die effectiever zijn in de beheersing van ontsteking en de bevordering van zuurstoftransport naar de parenchymcellen.

Om dit te doen, gebruikten we een recAP als een LPS neutraliserend middel op zowel I / R-induceer steriele ontsteking en sepsis zelf-geassocieerde AKI. We vonden dat recAP nieroxygenatie en hemodynamica stimuleerde onmiddellijk na I / R-geïnduceerde AKI onder het lichaam, maar deze niet beïnvloedde tijdens door endotoxemie geïnduceerde AKI. RecAP had in beide modellen een duidelijk renaal beschermend anti-inflammatoir effect.

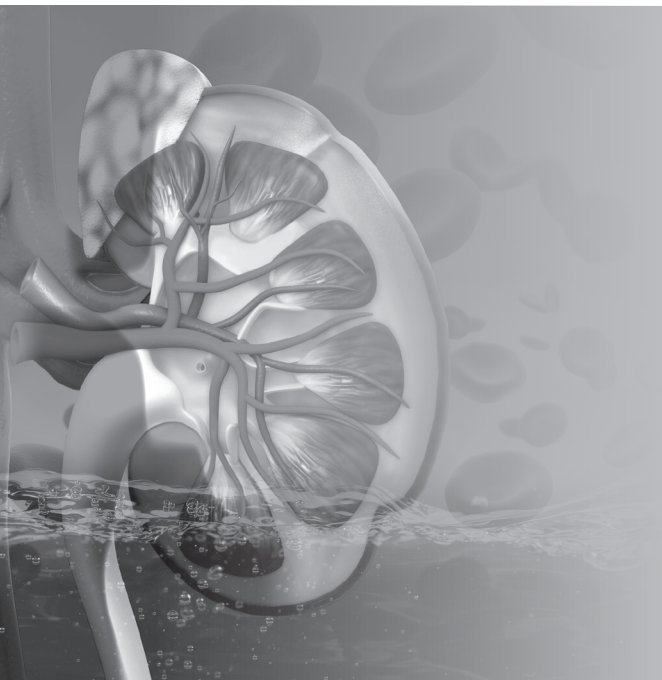
In andere studies vonden we dat vloeistof aangevuld met NAC verbeterde corticale nieroxygenatie, zuurstofafgifte en zuurstofconsumptie vergeleken met de LPS-groep. Vloeistofreanimatie alleen was gedeeltelijk effectief bij het corrigeren van nierhypoxie maar bereikte geen significant niveau in vergelijking met de LPS-groep. Er is gesuggereerd dat een specifiek effect van NAC op microvasculaire oxygenatie onafhankelijk van de macrovasculaire perfusie van de nieren bestaat.

Ten slotte toonden we de verbetering van de rekrutering van microcirculatie door gegeven vers bloed herstelde microcirculatoire oxygenatie van de nier en, bij uitbreiding, de nierfunctie in een ratmodel van endotoxemie. Sepsis-geïnduceerde eNOS-deficiëntie en nierbeschadiging werden ook gecorrigeerd door BT, maar niet door alleen vloeistofreanimatie.

Bij hemorrhagische shock probeerden we de efficiëntie van de verschillende vloeistoffen en de rol van de lever in hun metabolisme te bepalen. Om dit te bereiken, werd een partiële leverresectie (PLR) van 70% uitgevoerd om het vermogen van de lever om deze precursors te metaboliseren te verminderen. De belangrijkste resultaten van deze studie waren dat acetaat-gebalanceerde reanimatievloeistoffen een significant verbeterd buffercapaciteit vertoonden in aanwezigheid of afwezigheid van leverfunctiestoornissen.

Als laatste toonden we duidelijk aan dat ANH geassocieerd met verandering van de systemische en renale hemodynamica resulteert in een verhoogde bloedsnelheid als gevolg van lage viscositeit en SVR in nier- en perifere weefsels. Een verhoogde rode bloedcelsnelheid in de nieren kan echter een belangrijke oorzaak zijn voor de acuut nierbeschadiging door functioneel rangeren dat een efficiëntie van zuurstofextractie vermindert als gevolg van een korte doorlooptijd van de erythrocyten om voldoende zuurstof af te geven.

Concluderend wordt acuut nierletsel gedefinieerd als een complex multifactoriaal voorval, inclusief de systemische en renale perfusiedefecten, verminderde intra-renale organisatie van microcirculatoire vaten en oxygenatie, inactivatie of over-activatie van systemische en intra-renale regulatorische routes, verminderd zuurstofgebruik, renale tubulaire schade veroorzaakt door reactieve zuurstof- en stikstofspecies en pro- en ontstekingsremmende mechanismen. Als conclusie van dit proefschrift suggereerden we dat naast systemische hemodynamica, in therapeutische strategieën voor de behandeling van acuut nierletsel, ook de behandeling van renale microcirculatie moet worden opgenomen door beperking van pro-ontsteking, of ROS- en RNS-productie, regulatie van voldoende en effectief zuurstofgebruik, juiste en adequate intravasculaire volume-expansie en zuurstofdragers met vloeistoffen of bloed, en behandeling van renale energiebehoefte die nodig is voor de functie.



APPENDICES

Dankwoord

List of publications and presentations

PhD portfolio

Curriculum vitae

DANKWOORD

I would like to thank all the people who contributed and supported me in enabling the creation and completion of this thesis.

Firstly, I wish to express my sincere gratitude to my supervisor and mentor, Can Ince, for the amazing opportunities, enthusiasm, motivation and patience he has shown during my PhD study and research. He has provided me with thoughtful discussion, important suggestions and the supportive advice regarding my research. Can Ince has played a major role in making me a real scientist and physiologist. I wish to thank Prof. Dr. Cihan Demirci-Tansel who was my first supervisor for my MSc. and PhD program in Istanbul University.

I feel myself very fortunate to have worked with so many wonderful people with high levels of skill, bright minds and full of love during the creation of this thesis. I would like to especially show my gratitude to my lovely colleagues and friends, Albert van Wijk, Dr. Otto Erberk, Dr. Willeke M.C Jong, Dr. Emre Almac, Dr. Koray Yuruk, Dr. Rick Bezemer, Dr. Dan Milstein, Dr. Michal Heger, Dr. Zuhre Uz, Dr. Göksel Güven, Yasin Ince and Yilmaz Ince for all the methodological and motivational support they have provided me during those challenging years.

As the last, I would like to thank my wife, Semra Ergin for her unconditional support and love I deeply appreciate that she stood by my side during all the difficult years and has given me the most important persons in my life, my son Ruzgar Batu and my daughter Larin fulfilling even more meaning to my life. I am also deeply thankful to my mother Ipek and my father Nuri for their constant love and support throughout my life. Thanks to my brothers Nihat and Murat, and my sisters, Cigdem and Melek who have always been at my side.

LIST OF PUBLICATIONS

- 1- Lima A, van Rooij T, **Ergin B**, Sorelli M, Ince Y, Specht PAC, Mik EG, Bocchi L, Kooiman K, de Jong N, Ince C. Dynamic Contrast-Enhanced Ultrasound Identifies Microcirculatory Alterations in Sepsis-Induced Acute Kidney Injury. *Crit. Care Med.* 2018 May 15.
- 2- Uz Z, van Gulik TM, Aydemirli MD, Guerci P, Ince Y, Cuppen DV, **Ergin B**, Aksu U, de Mol BA, Ince C. Identification and quantification of human microcirculatory leukocytes using handheld video microscopes at the bedside. *J. Appl. Physiol.* (1985). 2018 Mar 8. doi: 10.1152/jappphysiol.00962.2017. [Epub ahead of print]
- 3- **Ergin B**, Zuurbier CJ, Kapucu A, Ince C. Divergent Effects of Hypertonic Fluid Resuscitation on Renal Pathophysiological and Structural Parameters in Rat Model of Lower Body Ischemia/Reperfusion-Induced Sterile Inflammation. *Shock.* 2017 Dec 27. doi: 10.1097/SHK.0000000000001096. [Epub ahead of print]
- 4- Guerci P, **Ergin B**, Ince C. The macro- and microcirculation of the kidney. *Best. Pract. Res. Clin Anaesthesiol.* 2017 Sep;31(3):315-329. doi: 10.1016/j.bpa.2017.10.002. Epub 2017 Nov 2. Review.
- 5- Hilty MP, Pichler J, **Ergin B**, Hefti U, Merz TM, Ince C, Maggiorini M. Assessment of endothelial cell function and physiological microcirculatory reserve by video microscopy using a topical acetylcholine and nitroglycerin challenge. *Intensive Care Med. Exp.* 2017 Dec;5(1):26. doi: 10.1186/s40635-017-0139-0. Epub 2017 May 18.
- 6- Zafrani L, **Ergin B**, Kapucu A, Ince C. Blood transfusion improves renal oxygenation and renal function in sepsis-induced acute kidney injury in rats. *Crit. Care.* 2016 Dec 20;20(1):406.
- 7- **Ergin B**, Heger M, Kandil A, Demirci-Tansel C, Ince C. Mycophenolate mofetil improves renal hemodynamics, microvascular oxygenation, and inflammation in a rat model of supra-renal aortic clamping-mediated renal ischemia reperfusion injury. *Clin. Exp. Pharmacol. Physiol.* 2016 Oct 25. doi: 10.1111/1440-1681.12687.
- 8- Peters E, **Ergin B**, Kandil A, Gurel-Gurevin E, van Elsas A, Masereeuw R, Pickkers P, Ince C. Effects of a human recombinant alkaline phosphatase on renal hemodynamics, oxygenation and inflammation in two models of acute kidney injury. *Toxicol. Appl. Pharmacol.* 2016 Dec 15;313:88-96. doi: 10.1016/j.taap.2016.10.015.

- 9- **Ergin B**, Guerçi P, Zafrani L, Nocken F, Kandil A, Gurel-Gurevin E, Demirci-Tansel C, Ince C. Effects of N-acetylcysteine (NAC) supplementation in resuscitation fluids on renal microcirculatory oxygenation, inflammation, and function in a rat model of endotoxemia. *Intensive Care Med. Exp.* 2016 Dec;4(1):29.
- 10- Guerçi P, Ince Y, Heeman P, Faber DJ, **Ergin B**, Ince C. A LED-based phosphorimeter for measurement of microcirculatory oxygen pressure. *J. Appl. Physiol.* (1985). 2016, Dec 8:jap.00316.2016. doi: 10.1152/japphysiol.00316.2016.
- 11- Varya Daeichin, Tom van Rooij, Ilya Skachkov, **Bulent Ergin**, Patricia A.C. Specht, Alexandre Lima, Can Ince, Johan G. Bosch, Antonius F.W. van der Steen, Nico de Jong, and Klazina Kooiman. Microbubble composition and preparation for high-frequency contrast-enhanced ultrasound imaging: in vitro and in vivo evaluation. *IEEE Transactions on Ultrasonics Ferroelectrics and Frequency Control*. January 2017 DOI: 10.1109/TUFFC.2016.2640342
- 12- **Ergin B**, Kapucu A, Guerçi P, Ince C. The role of bicarbonate precursors in balanced fluids during haemorrhagic shock with and without compromised liver function. *Br. J. Anaesth.* 117 (4): 521–8 (2016).
- 13- **Ergin B**, Zafrani L, Kandil A, Baasner S, Lupp C, Demirci C, Westphal M, Ince C. Fully Balanced Fluids do not Improve Microvascular Oxygenation, Acidosis and Renal Function in a Rat Model of Endotoxemia. *Shock*. 2016 Jul;46(1):83-91.
- 14- **Ergin B**, Zuurbier CJ, Bezemer R, Kandil A, Almac E, Demirci C, Ince C. Ascorbic acid improves renal microcirculatory oxygenation in a rat model of renal I/R injury. *J. Transl. Internal. Med.* 2015 Sep; 3-3.
- 15- **Ergin B**, Bezemer R, Kandil A, Demirci-Tansel C, Ince C. TEMPOL has limited protective effects on renal oxygenation and hemodynamics but reduces kidney damage and inflammation in a rat model of renal ischemia/reperfusion by aortic clamping. *J. Clin. Transl. Res.* 2015; 1(2): 116-128.
- 16- **Ergin B**, Kapucu A, Demirci-Tansel C, Ince C. The renal microcirculation in sepsis. *Nephrol. Dial. Transplant.* 2015 Feb;30(2):169-77. Review.
- 17- Aksu U, **Ergin B**, Bezemer R, Kandil A, Milstein DM, Demirci-Tansel C, Ince C. Scavenging reactive oxygen species using tempol in the acute phase of renal ischemia/reperfusion and its effects on kidney oxygenation and nitric oxide levels. *Intensive Care Med. Exp.* 2015 Dec;3(1):57.

18- Yildirim FI, Kizilay D, **Ergin B**, Ekmekçi Ö, Topal G, Kucur M, Demirci Tansel C, Uydeş Doğan BS. Barnidipine ameliorates the vascular and renal injury in L-NAME-induced hypertensive rats. *Eur. J. Pharmacol.* 2015 Oct 5;764:433-42.

19- Gurel E, Ustunova S, **Ergin B**, Tan N, Caner M, Tortum O, Demirci-Tansel C. Herbal haemorrhoidal cream for haemorrhoids. *Chin. J. Physiol.* 2013 Oct 31;56(5):253-62.

20- Topal G, Koç E, Karaca C, Altuğ T, **Ergin B**, Demirci C, Melikoğlu G, Meriçli AH, Kucur M, Ozdemir O, Uydeş Doğan BS. Effects of Crataegus microphylla on vascular dysfunction in streptozotocin-induced diabetic rats. *Phytother. Res.* 2013 Mar;27(3):330-7.

21- Oztay F, **Ergin B**, Ustunova S, Balci H, Kapucu A, Caner M, Demirci C. Effects of Coenzyme Q10 on the Heart Ultrastructure and Nitric Oxide Synthase During Hyperthyroidism. *Chin. J. Physiol.* 2007 Oct 31;50(5):217-24.

22- Gezerler F, Takir S, Alp FI, **Ergin B**, Demirci C, Ozdemir O, Uydes-Dogan BS. Retina Derived Relaxations are maintained in Carotid and Mesenteric Arteries of L-NAME-Induced Hypertensive Rats. *Journal of Vascular Research.* 46:151-151.(Conference paper), 2009.

BOOK CHAPTERS

1- P. Guerci, **B. Ergin**, C. Ince. Acute Kidney Injury and Microcirculatory Shock. *Annual Update in Intensive Care and Emergency Medicine* 2018 pp 293-307.

LIST OF POSTER AND ORAL PRESENTATION

1- **Ergin B.**, Guerci P, Uz Z., Ince Y., Yasin C., Ince C. Influence of the different fluids on the vascular endothelial barrier permeability and glycocalyx layer in a rats model of the acute normovolemic hemodilution. European Society of Intensive Care Medicine, Vienna, 2017.

2- **Ergin B.**, Guerci P, Uz Z., Ince C., Heger M., Ince C. Glycocalyx degradation is independent of vascular barrier dysfunction in non-traumatic hemorrhagic shock. International Symposium of Turkish Association of Intensive Care, 12-13 May 2017, Istanbul, Turkey.

- 3- **Ergin B.**, Lima A, van Rooij T, Sorelli M., Ince Y., Specht P, Mik G.E., Bocchi L., Kooiman K., de Jong N., Ince C. Dynamic contrast-enhanced ultrasound identifies microcirculatory alterations in sepsis-induced acute kidney injury. International Symposium of Turkish Association of Intensive Care, 12-13 May 2017, Istanbul, Turkey.
- 4- Akin S., Duran S., Soliman O., Guven G., **Ergin B.**, Lima A., Ince C. Pulmonary hypertension early after successful resuscitation in different shock states. International Symposium of Turkish Association of Intensive Care, 12-13 May 2017, Istanbul, Turkey.
- 5- Guven G., **Ergin B.**, Akin S., Lima A., Ince C. The response of renal blood flow to fluid resuscitation in experimental pig models. International Symposium of Turkish Association of Intensive Care, 12-13 May 2017, Istanbul, Turkey.
- 6- **B. Ergin.**, P. Guerçi., P.A.C. Specht., Y. Ince., C. Ince. HES (130/0.4) has no negative effect on kidney function and microvascular perfusion in severe acute normovolemic hemodilution in pigs. European Society of Intensive Care Medicine, Milan, 2016.
- 7- P. Guerçi., Y. Ince., P. Heeman., **B. Ergin.**, C. Ince. A novel led-based phosphorimeter for measurement of microcirculatory oxygen concentrations in vivo in the kidney. Intensive Care European Society of Intensive Care Medicine, Milan, 2016.
- 8- **Ergin B** and C Ince. Hypertonic saline improves renal oxygenation, renal function and inflammation following ischemia/reperfusion-induced acute kidney injury. European Society of Intensive Care Medicine, Barcelona, 2015.
- 9- **Ergin B.**, A. Kandil., S. Baasner., C. Lupp., M. Wespthal., C. Demirci-Tansel., C. Ince. Effects of supplementing resuscitation fluid with N-acetylcystein (NAC) on renal hemodynamics, microcirculatory oxygenation, inflammation, oxidative stress, and renal function in a rat model of septic shock. 4th International Fluid Academy Days, Antwerpen, Nov 2014.
- 10- **Ergin B.**, Üstünova S., Kandil A., Gürel Gürevin E., Büyük U., Dedeakayoğulları H., *et al.*, "Aktif Protein C ve COX Enzimlerinin Septik Sıçan Kortikal Böbrek Perfüzyonu ve Glukoz Taşıyıcıları Üzerine Etkileri", Türk Fizyolojik Bilimler Derneği 39. Ulusal Kongresi, Ankara, Türkiye, 1-4 Eylül 2013, ss.74-74
- 11- **Ergin B.**, Kapucu A., Demirci Tansel C., Ince C., "Hemorajik Şok Yapılan Sıçanlarda Böbrek Fonksiyonları Üzerine Sıvı Terapisinin Etkileri", 40. Ulusal Fizyoloji Kongresi 2014, Kayseri, Türkiye, 2-6 Eylül 2013, ss.142-142

12- **Ergin B.**, Bezemer R. , Kandil A., Almac E., Demirci Tansel C., İnce C., “Ascorbic Acid Protects Renal Oxygenation And Oxidative Stress After Ischemia/Reperfusion Injury”, European Society of Intensive Care Medicine, Lisbon, 2012.

13- **Ergin B.**, Bezemer R., Kandil A., Almac E., Demirci Tansel C., Ince C., “Mycophenolate Mofetil Reduced Renal Inflammation And Protected Renal Cortical Oxygenation After Ischemia/ Reperfusion Injury”. European Society of Intensive Care Medicine, Lisbon, 2012.

14- Kandil A., **Ergin B.**, Bezemer R. , İnce C., Demirci Tansel C., “The Role of MMF In The Renal Ischemia-Reperfusion of Rat”, 14th International Congress of Histochemistry and Cytochemistry (IHC 2012), Kyoto, Japan, 1-4 August 2012, pp.125-125

15- **Ergin B.**, Kandil A., Gezerler F., Uydeş Doğan B.S., Demirci Tansel C., “Deneyisel hipertansiyonda karotid arter ve retina”, 20. Ulusal Elektronik Mikroskopi Kongresi, Antalya, Türkiye, 25-28 Ekim 2011, ss.158-158

16- Gezerler F, Takir S., Alp F, **Ergin B.**, Demirci Tansel C., Özdemir O., *et al.*, “Retina derived relaxations are maintained in carotid and mesenteric arteries of L-NAME-induced hypertensive rats.”, 10th International Symposium on Mechanisms of Vasodilatation, Miyagi, Japan, 1-4 Dec 2009, pp.151-151

17- Balci H., Hürdağ C., Uyaner İ., Gürel Gürevin E., Kandil A., **Ergin B.**, *et al.*,”Hipertiroidili Sıçan Tiroidinde a-Lipoik Asit-Nitrik Oksit İlişkisi”, 19. Ulusal Biyoloji Kongresi, Trabzon, Türkiye, 23-27 Haziran 2008, ss.550-550

18- Gürel E., Kapucu A., Kandil A., Üstünova S., **Ergin B.**, Akgün Dar K., *et al.*,”Diyabetik Sıçan Pankreasında Leptinin Etkileri Ve Nitrik Oksit İle Olan İlişkisi”, Türk Fizyolojik Bilimler Derneği 33. Ulusal Kongresi, Girne, Kuzey Kıbrıs Türk Cum., 15-19 Ekim 2007, ss.118-118

19- Gürevin E, Kapucu A, Kandil A, Üstünova S, **Ergin B**, Akgün Dar K “Diyabetik sıçan pankreasında leptinin etkileri ve nitrik oksit ile olan ilişkisi.”, Türk Fizyolojik Bilimler Derneği 33. Ulusal Kongresi (Uluslararası Katılımlı), Girne, Kuzey Kıbrıs Türk Cum., 15-19 Ekim 2007, ss.118-118

20- Oztay F, **Ergin B.**, Ustunova S., Balci H., Kapucu A., Caner M., Demirci C. Coenzyme Q10 Effects on The Heart Ultrastructure and Nitric Oxide Synthase During Hyperthyroidism, 11. Annual of the European Council for Cardiovascular Research, Nice, France, 29 September-1 October 2006.

21- Hurdag C., Uyaner I., Kapucu A., **Ergin B.**, Hatipoğlu I. The Effects of Alfa -Lipoic Asid and Streptozotocine on the Testis of Diabetic Induced Rats the Distribution of Nitric Oxide Synthase.12.International Congress of Endocrinology, Lizbon, August 31-September 4, 2004

22- A. Kandil, A. Kapucu, S. Üstünoğlu, E. Gürel, H. Balci, İ. Uyaner, **B. Ergin**, K. Akgündar, C. Demirci, "Relationship of Nitric oxide and Leptin in Diabetic Rats Adipose Tissue". Association of Turkish Physiological Sciences XXXII. International Congress, September 18-22, 2006, Denizli/Turkey

23- C. Hurdag, H. Balci, İ. Uyaner, E. Gürel, A. Kandil, **B. Ergin**, C. Demirci, Relationship Alpha -Lipoic Acide And Nitric Oxide in Hyperthyroid Rat's Thyroid. National Biology Congress XXIX. June 23-27 2008, Trabzon/Turkey

24- **Ergin B** and C. Demirci. Relationship Nitric oxide and leptin on kortical blood flow in diabetic rat's brain. Association of Turkish Physiological Sciences XXXIV. International Congress, October 6-10, 2008, Erzurum/Turkey


PHD PORTFOLIO

	Year	Workload
1. PhD TRAINING		
General academic courses		
Course of Molecular Endocrinology	2008	2
Advanced Histology	2008	3
Antioxidants and Detoxification in Biological System	2008	3
Physiology of Membrans	2008	3
Molecular Mechanism of Cell Cycle	2008	3
Cell and Tissue Pathology	2009	3
Aging in Animal Tissue	2009	3
Selected Topic in Cell Biology II	2009	2
Endocrinology of Reproduction	2009	2
In-depth courses		
Course of Laboratory Animal Science	2011	3
Mass Spectrometry, Proteomic and Protein Research	2012	1
DNA Technology	2013	1
Conferences-participation and presentation		
European Society of Intensive Care Medicine, Vienna <i>Oral presentation</i>	2017	1
Turkish Association of Intensive Care, Istanbul, <i>Two poster presentations</i>	2017	1
European Society of Intensive Care Medicine, Milan <i>Poster presentation</i>	2016	1
European Society of Intensive Care Medicine, Barcelona <i>Poster presentation</i>	2015	1
4th International Fluid Academy Days, Antwerpen <i>Poster presentation</i>	2013	1
4th International Fluid Academy Days, Antwerpen, <i>Poster presentation</i>	2014	1
European Society of Intensive Care Medicine, Lisbon, <i>Oral presentation and poster presentation</i>	2012	1
Association of Turkish Physiological Sciences XXXIV International Congress, Erzurum <i>Poster presentation</i>	2008	1

	Year	Workload
Association of Turkish Physiological Sciences XXXII International Congress, Denizli <i>Poster presentation</i>	2006	1
2. TEACHING ACTIVITIES		
Supervising, training and teaching of Lara Zafrani	2014-2015	2
Supervising, training and teaching of Aysegul Kapucu	2015-2016	2
Supervising, training and teaching of Philippe Guerci	2016-2017	2
Supervising, training and teaching of Matthias Hilty	2018-	2
	Total	46

CURRICULUM VITAE

The author of this thesis, Bülent Ergin, was born in Istanbul, Turkey at 1978. He graduated from University of Istanbul, with bachelor degree of Biology in 2004. He completed his master at 2008 and obtained PhD degree at 2013 at Zoology Division of Istanbul University. He is a physiologist and experienced regarding small or large animal surgery, anesthesiology, histology, electron microscopy, immunohistochemistry and biochemical analysis in a model of sepsis, hemorrhagic shock, hemodilution, ischemia/reperfusion, diabetes and liver failure. At the 2011, he started working with the Prof. dr. Can Ince at the Department of Translational Physiology in Academic Medical Center in Amsterdam. He is married with Semra Ergin. They have a son, Batu, and a daughter, Larin.



The Renal Microcirculation as a Target for the Treatment
of Acute Kidney Injury in Models of Critical Illness

© Bülent Ergin, 2018